# Institute of Energy and Climate Research
# IEK-6: Nuclear Waste Management
# Report 2013 / 2014

## *Material Science for Nuclear Waste Management*

S. Neumeier, M. Klinkenberg, D. Bosbach (Editors)




Member of the Helmholtz Association

**Energie & Umwelt / Energy & Environment**
**Band / Volume 327**
**ISBN 978-3-95806-155-2**

JÜLICH
FORSCHUNGSZENTRUM

Schriften des Forschungszentrums Jülich
Reihe Energie & Umwelt / Energy & Environment Band / Volume 327

Forschungszentrum Jülich GmbH
Institut für Energie- und Klimaforschung
Nukleare Entsorgung und Reaktorsicherheit (IEK-6)

# Institute of Energy and Climate Research IEK-6: Nuclear Waste Management Report 2013 / 2014

## *Material Science for Nuclear Waste Management*

S. Neumeier, M. Klinkenberg, D. Bosbach (Editors)

Schriften des Forschungszentrums Jülich
Reihe Energie & Umwelt / Energy & Environment Band / Volume 327

ISSN 1866-1793 ISBN 978-3-95806-155-2

Bibliographic information published by the Deutsche Nationalbibliothek.
The Deutsche Nationalbibliothek lists this publication in the Deutsche
Nationalbibliografie; detailed bibliographic data are available in the
Internet at http://dnb.d-nb.de.

| | |
|---|---|
| Publisher and Distributor: | Forschungszentrum Jülich GmbH<br>Zentralbibliothek<br>52425 Jülich<br>Tel: +49 2461 61-5368<br>Fax: +49 2461 61-6103<br>Email: zb-publikation@fz-juelich.de<br>www.fz-juelich.de/zb |
| Cover Design: | Grafische Medien, Forschungszentrum Jülich GmbH |
| Printer: | Grafische Medien, Forschungszentrum Jülich GmbH |
| Copyright: | Forschungszentrum Jülich 2016 |

Schriften des Forschungszentrums Jülich
Reihe Energie & Umwelt / Energy & Environment, Band / Volume 327

ISSN 1866-1793
ISBN 978-3-95806-155-2

The complete volume is freely available on the Internet on the Jülicher Open Access Server (JuSER)
at www.fz-juelich.de/zb/openaccess.

**TABLE OF CONTENTS**

# 1 Preface

## Research for the safe management of nuclear waste

This is the third bi-annual report of the **Nuclear Waste Management section of the Institute of Energy and Climate Research (IEK-6) at Forschungszentrum Jülich** since 2009 – almost a tradition. Our institute has seen two more years with exciting scientific work, but also major changes regarding nuclear energy in Germany and beyond. After the reactor accident in Fukushima (Japan) in 2011, it was decided in Germany to phase out electricity production by nuclear energy by 2022. It seems clear, that the decommissioning of the nuclear power plants will take several decades. The German nuclear waste repository Konrad for radioactive waste with negligible heat generation (all low level and some of the intermediate level radioactive waste) will start operation in the next decade. The new site selection act from 2013 re-defines the selection procedure for the German high level nuclear waste repository. Independently of the decision to stop electricity production by nuclear energy, Germany has to manage and ultimately dispose of its nuclear waste in a safe way.

Our basic and applied research for the safe management of nuclear waste is focused on radiochemistry and materials chemistry aspects – it is focused on the behaviour of radionuclides and radioactive waste materials within the back-end of the nuclear fuel cycle. It is organized in four areas: (1) research supporting the scientific basis of the safety case of a deep geological repository for high level nuclear waste, (2) fundamental structure research of radionuclide containing (waste) materials (3) R & D for waste management concepts for special nuclear wastes and (4) international safeguards.

A number of excellent scientific results have been published in more than 80 papers in international peer-reviewed scientific journals in 2013 - 2014. Here, I would like to mention four selected scientific highlights – more can be found in this report:

(1) The retention of radionuclides within a nuclear waste repository system by secondary phases for the long-term safety assessment is one of the major research topics in the institute. The fundamental understanding of a long-standing open issue regarding the thermodynamics of radium-barium-sulfate **solid solutions** and its applicability in long-term safety assessments for nuclear waste disposal could be resolved. This was achieved by a novel approach combining atomistic simulations, radiochemical batch-type laboratory experiments and modern analytical techniques supported by thermodynamic modelling allowing a reliable description of Ra solubility control by a $(Ba,Ra)SO_4$ solid solution. This research is supported by the Swedish waste management agency SKB.

(2) A major step forward was achieved regarding the prediction of actinide- and lanthanide-bearing materials properties by **atomistic simulations**. Performance tests of the DFT+U method for calculations of f-element-bearing systems (the Hubbard U parameter derived from first principle methods) showed that this method, in contrast to standard DFT, results in exceptionally good predictions of the formation and reaction enthalpies as well as the structures of lanthanide- and actinide-bearing materials.

(3) The **actinide solid state chemistry** group has been very active in recent years to unravel the crystal structure of actinide containing oxo-salts. From the 1101 new crystal structure entries in the ICSD crystal structure database between 2005 and 2012, Prof. Evgeny Alekseev has contributed to 98 entries (almost 10%).

(4) A new **nondestructive neutron interrogation technique** based on Prompt and Delayed Gamma Neutron Activation Analysis (P&DGNAA) called MEDINA was developed in recent years. In the last two years we have demonstrated its capability to characterize radioactive waste packages with respect to the acceptance criteria for the German Konrad repository regarding chemotoxic and reactive elements. The MEDINA technology has also been successfully applied for analysing conventional waste with respect to its recycling potential and for quality control of industrial products and raw materials.

The **safeguards group** in the institute, headed by Dr. Irmgard Niemeyer, has been very successful in coordinating the German contribution to IAEAs support programme. Furthermore, the scientific collaboration with IAEAs safeguards laboratories in Seibersdorf (Austria) has evolved very well, with currently two doctoral students involved. Scientifically, we are focusing on the production and characterisation of actinide-bearing reference particles, which will be used in nuclear forensic applications. Dr. Irmgard Niemeyer became the German representative in the **IAEA "Standing Advisory Group on Safeguards Implementation"** (SAGSI), which is advising IAEA's director general Yukiya Amano.

In general, our research is contributing to the **research program NUSAFE (Nuclear Waste Management, Safety and Radiation Research) of the Helmholtz Association**. One of the successes during the last two years was without a doubt the very positive outcome of the POF-3 international evaluation in January 2014, which concluded that NUSAFE is one of the best research programs within the Helmholtz Association. Furthermore Prof. Evgeny Alekseev's Helmholtz Young Investigator Group "Solid-state Actinide Chemistry" was evaluated in late 2014 with an extremely positive result.

The institute was very successful in obtaining **third party funded projects** and has received substantial funding for a number of national, European and international projects. Collaborative projects funded by BMWi (Federal Ministry of Economic Affairs) and BMBF (Federal Ministry of Education and Science) included the projects VESPA, ImmoRad, f-Kom, Neutron Imaging, Conditioning (Ceramic Waste Forms) and PGAA-Actinide. On a European level the institute has been participating in various collaborative projects, namely SKIN, FIRST NUCLIDES, ASGARD, and SACSESS.

The institute celebrated its **50 years anniversary** in 2014 with a seminar at RWTH Aachen, which was open to the public (with more than 100 participants) with presentations covering the scientific-technical as well as the social science aspects of nuclear waste management. A scientific Kolloquium at Forschungszentrum Jülich with presentations from industry and research concluded this very successful event. All former directors of the institute, namely Prof. E. Merz (founding director), Dr. H. Brücher and Prof. R. Odoj participated. In recent years, many young scientists joined the institute forming a stable basis now for the future of the institute – more than 60% of the IEK-6 staff is younger than 35 years. This fortunate situation will ensure that we will be able to keep the competence in research for the safe management of nuclear waste.

The scientific staff of IEK-6 Nuclear Waste Management is committed to support universities in Aachen, Bonn and Freiberg in educating and training students in topics related to nuclear waste management. Currently 12 graduate students are working on their PhD projects. In 2013 and 2014 seven graduate students have finished their dissertation – most of them at RWTH Aachen University: **Stephan Schneider**, „Numerische Simulation von Abfallgebinden aus der Wiederaufbereitung von Kernbrennstoffen" (2013) RWTH Aachen University, **Sarah Finkeldei**, "Pyrochlore as nuclear waste form: actinide uptake and chemical stability" (2014) RWTH Aachen University, **Andreas Havenith**, "Stoffliche Charakterisierung radioaktiver Abfallprodukte durch ein Multi-Element-Analyseverfahren basieren auf der instrumentellen

Neutronen-Aktivierungs-Analyse – MEDINA" (2014) RWTH Aachen University, **Thomas Krings**, "SGSreco – Radiologische Charakterisierung von Abfallfässern durch Segmentierte y-Scan Messungen" (2014) RWTH Aachen University, **Sabrina Labs**, "Secondary Phases of Spent Nuclear Fuel - Coffinite, $USiO_4$, and Studtite, $UO_4*4H_2O$ - Synthesis, Characterization and Investigations Regarding Phase Stability" (2014) RWTH Aachen University, **Clemens Listner**, "Änderungsdetektion digitaler Fernerkundungsdaten mittels objekt-basierter Bildanalyse" (2014), TU Bergakademie Freiberg and **Michal Sypula**, "Innovative SANEX process for trivalent actinides separation from PUREX raffinate" (2014) RWTH Aachen University.

**Dr. Sarah Finkeldei** finished her dissertation in November 2014 and received the Promotionspreis (prize for the best doctoral thesis) by the Nuclear Chemistry Division of the Gesellschaft Deutscher Chemiker (GDCh - German chemical society). **Dr. Giuseppe Modolo** finished his Habilitation at RWTH Aachen University in the field "Chemistry and Technology of Nuclear Waste Management".

The "HITEC – communicator award 2014" of the HITEC graduate school (Helmholtz Interdisciplinary Doctoral Training in Energy and Climate Research) at Forschungszentrum Jülich went to Sarah Finkeldei for her excellent presentation on ceramic based nuclear waste forms. The graduate school also organizes a science slam, which was won by Yulia Arinicheva with a presentation also on ceramic waste forms in 2014. Two examples demonstrating, that our young scientists and students are not only able to present the complexity of the science for the safe management of nuclear waste to experts in the field, but also to the general public.

In recent years the institute has established numerous collaborations within Forschungszentrum Jülich, with partners in industry, at universities and beyond in Germany, in Europe and beyond. I would quite like to take the opportunity to thank all of them.

Dirk Bosbach

# 2 Institute's Profile

Forschungszentrum Jülich pursues cutting-edge interdisciplinary research on pressing issues facing society today. With its competence in materials science and simulation, and its expertise in physics, nanotechnology, and information technology, as well as in the biosciences and brain research, Jülich is developing the basis for the key technologies of tomorrow. In this way, Forschungszentrum Jülich helps to solve the grand challenges facing society in the fields of energy and the environment as well as information and the brain. Forschungszentrum Jülich is also breaking new ground in the form of strategic partnerships with universities, research institutions, and industry in Germany and abroad. With more than 5,500 employees, Jülich – a member of the Helmholtz Association – is one of the large interdisciplinary research centres in Europe.

The Nuclear Waste Management section of the Institute of Energy and Climate Research (IEK-6) focusses on scientific topics relevant to safety aspects of nuclear waste management considering the process of the *"Energiewende*", the German energy transition. It performs fundamental as well as applied research and development for the safe management of nuclear waste, covering issues from the atomic scale to the macroscopic scale of actual waste packages, waste compounds / materials and the engineered barrier system in a deep geological nuclear waste repository.

Research at IEK-6 with respect to the **long-term safety of nuclear waste disposal** includes work on spent nuclear fuel corrosion, the formation of secondary phases, and radionuclide retention processes – the radio(geo)chemistry of the deep geological repository nearfield, thus contributing to the scientific basis of the safety case. In order to study **innovative waste management strategies,** IEK-6 research groups are focusing on partitioning of actinides from reprocessing wastes and the development of ceramic waste forms for special nuclear waste streams, such as separated plutonium unsuitable for further use, or separated minor actinides. The research programme is supported by a strong **"structure research"** group covering the fields of solid state chemistry and physics, crystallography and supercomputing-aided atomistic modelling. Application oriented waste management concepts for special categories of problematic radioactive wastes (e.g. irradiated nuclear graphite or radioactively contaminated heavy metals) are developed by integrating the development of **non-destructive essay techniques**, for which IEK-6 is well known for decades, and **waste treatment procedures**. The nuclear safeguards group in IEK-6 investigates and develops **nuclear safeguards** methods and techniques, and is responsible for the scientific coordination of the German **IAEA safeguards support programme**.

The research programme of IEK-6 is focused on radiochemical and nuclear chemical aspects with a special focus on solid state / material science issues relevant for the safe management of nuclear wastes. IEK-6 operates radiochemistry laboratories equipped with state-of-the-art analytical facilities to study atomic scale ordering phenomena and the microstructure on different scales – sub-nanometre to micrometre. Recent instrumental upgrades / installations (last 5 years) include two Raman spectrometers, powder & single crystal XRD and FIB for TEM studies. A central hot cell facility (GHZ) is operated in Jülich, in which IEK-6 uses two hot cells for spent nuclear fuel corrosion studies. One of the hot cells is equipped for in-situ Raman measurements. The atomistic modelling group and the reactive transport modelling group use the superior supercomputing resources located at Forschungszentrum Jülich and RWTH Aachen University, including the powerful Blue Gene/Q machine JUQUEEN, which are available through **the Jülich-Aachen Research Alliance in High Performance Computing (JARA-HPC)** initiative, in which IEK-6 is an active member.

Complementary to the scientific activities the IEK-6 places particular emphasis on promotion of earlier-carrier scientists to maintain and expand competence and know-how in all fields of nuclear waste management. Senior scientists of the institute are involved in lecturing and teaching mainly at RWTH Aachen University as well as at other universities in Germany and abroad.

## “Material science for the safe management of nuclear waste”

## 2.1. Staff

85 staff members (Dec. 2014)

| | | |
|---|---|---|
| 37 scientists | 18 PhD students | 10 graduands |
| 10 engineers & technicians | 6 laboratory assistants | 4 administration |

## 2.2. Organization chart

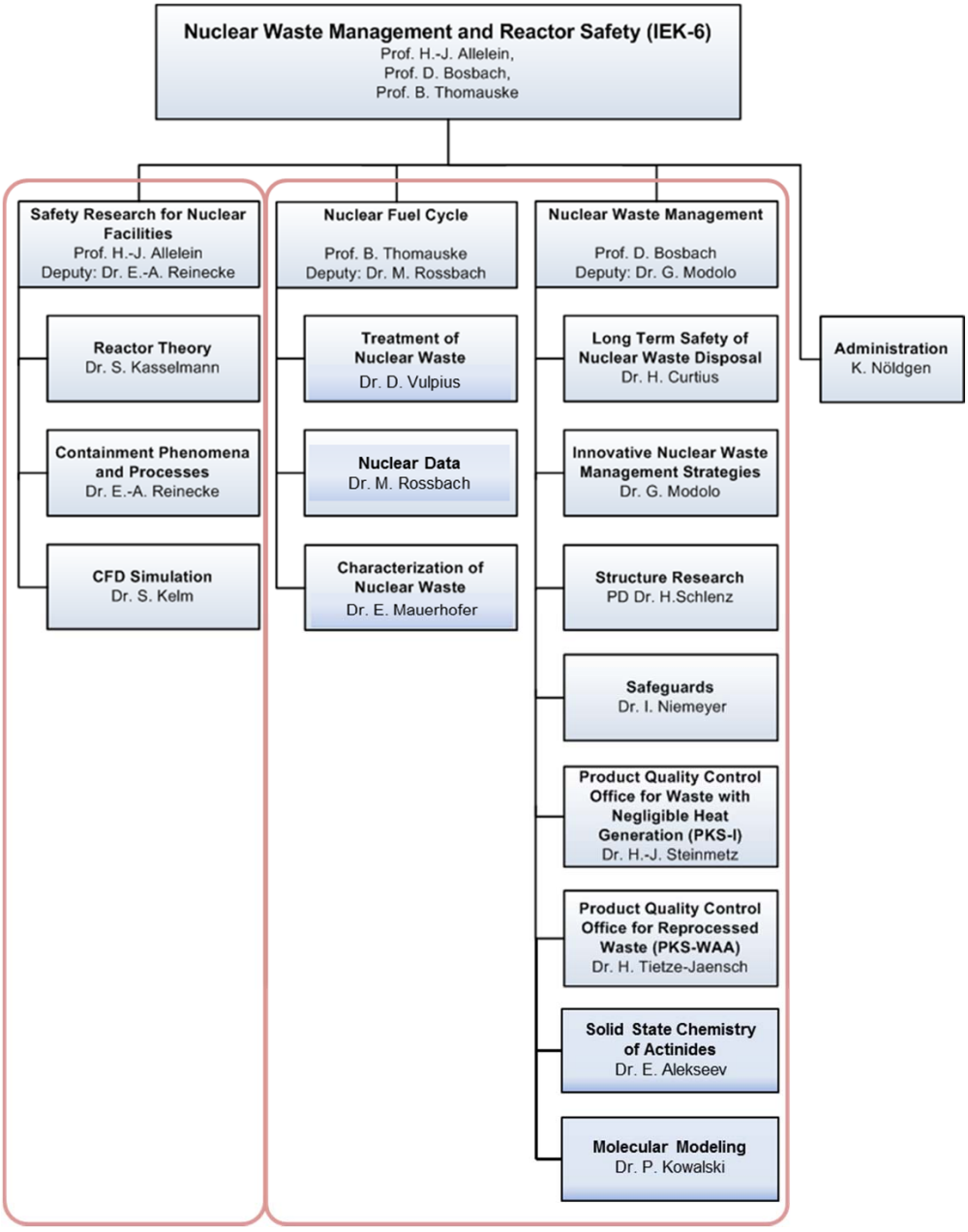


**Fig. 1: Organization chart of the Institute of Energy and Climate Research (IEK-6), Nuclear Waste Management and Reactor Safety devision.**

## 2.3. Budget

### 2013

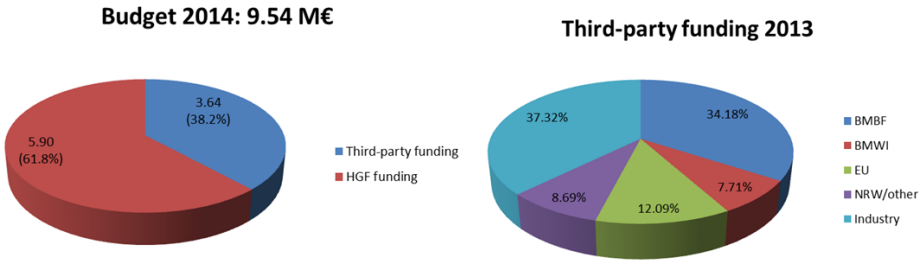


### 2014

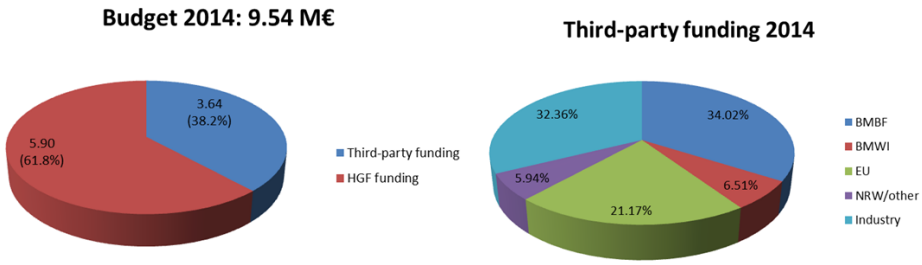

# 3 Key Research Topics

## 3.1. Long Term Safety of Nuclear Waste Disposal

The disposal of high-level nuclear waste in deep geological formations poses major scientific and social challenges to be met in the next decades. One of the key issues is related to the long term safety of a waste repository system over extended periods of time - typically time frames of up to a million years are taken into account when designing waste repositories, due to the long half-live of some of the radionuclides. There is a consensus in the scientific community that deep geological disposal offers the largest long term isolation potential - it relies on the passive safety of the geological formation. There seems also to be a consensus in the scientific community that the long-term safety of a repository system cannot be demonstrated by technical means only. With respect to the expected repository evolution, relevant scenarios for disposal concepts integrated the presence of water and its contact to the waste forms. Water interaction with the waste forms is the prerequisite for any radionuclide release from the repository. A key issue within this context is the provision of a detailed insight in processes and mechanisms that control the corrosion behaviour of waste forms and to evaluate the radionuclide release rates.

**Fig. 2: Hot cell line 1 (HZ1) located in the hot cell facility (GHZ) at the research center Jülich.**

Furthermore, a molecular-level process understanding can help improving the confidence in available data on radionuclide behaviour in the geosphere beyond a simple phenomenological description.
The research at IEK-6 is focusing on the interaction of ground water with nuclear waste forms, particularly with spent nuclear fuels. These investigations are performed by IEK-6 in the hot cell facility (operation since 1969; including a control area of 3576 $m^2$) within the hot cell line 1 (Fig. 2).
As mentioned before, radionuclides may be released from the spent fuel matrix upon interaction with ground water after container failure. It should be noted, that the release of radionuclides is a time dependent process. In contact to groundwater radionuclide are released instantaneously (the so-called instant release fraction (IRF)). The determination of this volatile fast/instant radionuclide release fraction is integrated within the European project FIRST NUCLIDES (end 31.12.2015). The long-term process describes the release of embedded radionuclides due to the oxidative dissolution of the fuel matrix itself. Corrosion of the fuel matrix, of waste containers, of other near field materials leads to the formation of secondary phases. Dissolved radionuclides may bind to these secondary phases by one or more distinct sorption reactions. The immobilisation of radionuclides by isostructural incorporation (irreversible process) in secondary phases, hence the formation of solid solutions is investigated at IEK-6 in detail. The research with respect to these solid solutions including the formation of solid solutions from decay products, is related to: a.) derive structural models, b.) investigate physical-chemical properties under repository relevant-conditions and 3.) obtain thermodynamic data. The work is integrated in three projects (SKIN, ImmoRAD, VESPA).

Contact: Dr. Hildegard Curtius
h.curtius@fz-juelich.de

## 3.2. Innovative Nuclear Waste Management Strategies

The R&D programme dedicated to “Innovative nuclear waste management strategies” focuses on the separation of long-lived radionuclides (minor actinides, $^{129}I$, $^{99}Tc$ etc.) from high active waste solution and subsequent conversion into new ceramic waste forms.

**Fig. 3: Separation of Minor Actinides using mixer-settler units.**

**Separation of long-lived radionuclides**

Research on the separation of radionuclides from nuclear waste solutions is based on highly selective hydrometallurgical separation processes. For a successful separation of specific waste components, a fundamental understanding of the principles of the complexation of radionuclides in aqueous and organic extractant solution is a crucial issue. Research covers the fields of thermodynamics, hydrodynamics and kinetics of liquid-liquid extraction as well as the long-term operation of the solvent (hydrolysis and radiolysis). This includes also recycling and cleaning of the solvent and the management of secondary waste.

Highly sophisticated analytical techniques (e.g. X-ray diffraction, laser spectrometry, NMR, EXAFS) are used to understand the complexation and extraction mechanisms. This is being undertaken in close cooperation with European partners under the on-going European Union project SACSESS (duration 2013-2016) and in the current project F-KOM (duration 2012-2015) funded by the German Federal Ministry of Education and Research (BMBF). This knowledge is important to develop multi-scale models to be used in a simulation code, which is an indispensable tool to operate such processes in a safe manner. The flow-sheets are tested and evaluated by comparing them with model predictions.

**New ceramic waste forms**

Ceramic waste forms for the immobilisation of long-lived radionuclides have been investigated extensively in the last few decades since they seem to exhibit certain advantages over other waste forms (incl. borosilicate glasses and spent fuel). Most on-going nuclear waste management strategies do not include ceramic waste forms. However, it still seems important to study this option, e.g. with respect to specific waste streams and certain constraints regarding deep geological disposal. Research focuses on single-phase ceramics such as Monazite and zirconium-oxide-based materials and includes:

- synthesis (sol-gel route, hydrothermal synthesis and co-precipitation),
- structural and microstructural characterisation using state-of-the-art spectroscopic/diffraction (Raman, XRD, TRLFS, EXAFS) and microscopic techniques (SEM, FIB/TEM),
- thermodynamic stability and reactivity under conditions relevant for nuclear disposal, in particular with respect to leaching/corrosion in aqueous environments as well as
- studies on radiation damage.

Finally, a fundamental understanding of these aspects will help to improve long-term safety assessments of deep geological disposal concepts using these materials.

This work is part of a German joint research project “Conditioning” funded by BMBF (2012-2015).

Contact: PD Dr. Giuseppe Modolo
g.modolo@fz-juelich.de

## 3.3. Structure Research

The chemical and physical properties of a material are determined by its chemical composition, chemical bonds and particularly by its structure, no matter if crystalline or amorphous materials (glasses) are investigated. According to nuclear waste management mainly ceramics and glasses are considered for the immobilization of actinides. For the purpose of understanding material properties and for the development of such new materials, knowing the structure is an indispensable prerequisite. As an example the crystal structure of the mineral monazite is determined as a function of varying amounts of Uranium (U) and Thorium (Th) using x-ray powder diffraction, in order to detect structural changes due to varying chemical composition and possible radiation damage caused by the radioactive decay of U and Th. Further candidate phases for the immobilization of actinides are e.g. pyrochlore, Ce-, U- and Th-oxides, as well as U- and Th-silicates.

At the IEK-6 structure research is performed using diffraction, spectroscopic analysis and computer simulations. X-ray synchrotron diffraction and spectroscopy experiments are performed at large research facilities like ANKA (Karlsruhe), HASYLAB (Hamburg) or ESRF (Grenoble). Neutron diffraction experiments are performed in cooperation with the RWTH Aachen, e.g. at the nuclear research reactor FRM II (Garching). To be able to examine further structural details complementary analytical methods like Raman spectroscopy (Fig. 4) and IR spectroscopy are applied. Irradiation experiments are performed using e.g. heavy ions like $Kr^{+}$ in a Transmission Electron Microscope (TEM) at dedicated facilities in Saclay and Orsay (France). Finally, structure models are generated by computer simulations (Reverse Monte Carlo) and the radiation damage of a solid can be simulated using advanced Monte Carlo algorithms.

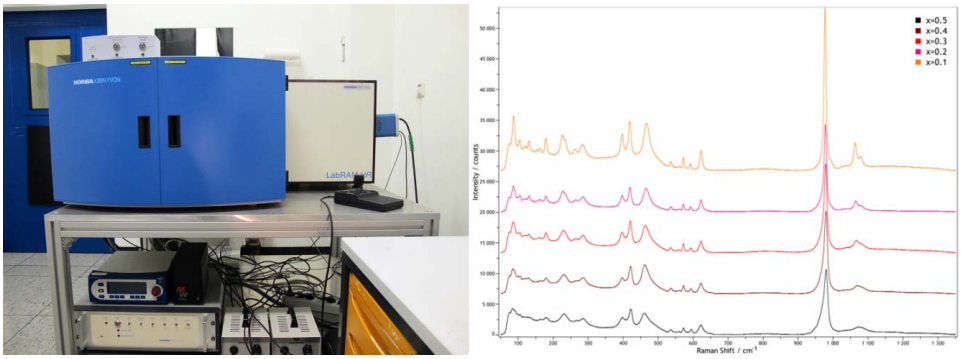


**Fig. 4: Raman spectrometer (Horiba LabRAM HR) and Raman spectra of synthetic monazite-type phases with composition $Nd_{1-x}Ca_{0.5x}Th_{0.5x}PO_4$.**

Contact: PD Dr. Hartmut Schlenz
h.schlenz@fz-juelich.de

## 3.4. Solid State Chemistry of Actinides (Helmholtz Young Investigator Group)

The actinide elements are of particular concern due to their long half-life and their high radiotoxicity. Knowledge of the stability and the reactivity of actinide compounds under conditions relevant for a waste repository system require a sound understanding of their solid state chemistry. From a solid state chemistry perspective, the actinides with their characteristic 5f electrons, exhibit an extremely complex redox and binding behaviour in particular in the solid state. The relationship between structure of actinide based materials and their properties is one of the most important questions of fundamental actinide science. The research of the proposed “Solid State Chemistry of Actinides” groups is oriented on understanding fundamental properties of actinide based solid compounds. The research includes an understanding of formation of complex phases and their structure, thermodynamic and material’s properties. The priority in research is given to the inorganic phases based on oxo-anions due to their importance for safety assessment in final disposal sites for nuclear waste. State-of-the art techniques are used for structure characterization and thermodynamic characterization of synthesized phases. The work is mostly focused on U and Th but some experiments have been carried out with transuranic elements (Np, Pu) in cooperation with group of Prof. Albrecht-Schmitt (FSU, USA). The formation of materials is studied under normal and extreme conditions (high-temperature/high-pressure; s. Fig. 5). Stability of materials has been characterized with various methods including high-temperature powder X-ray diffraction in cooperation with Prof. Thorsten Gesing (University of Bremen, Germany).

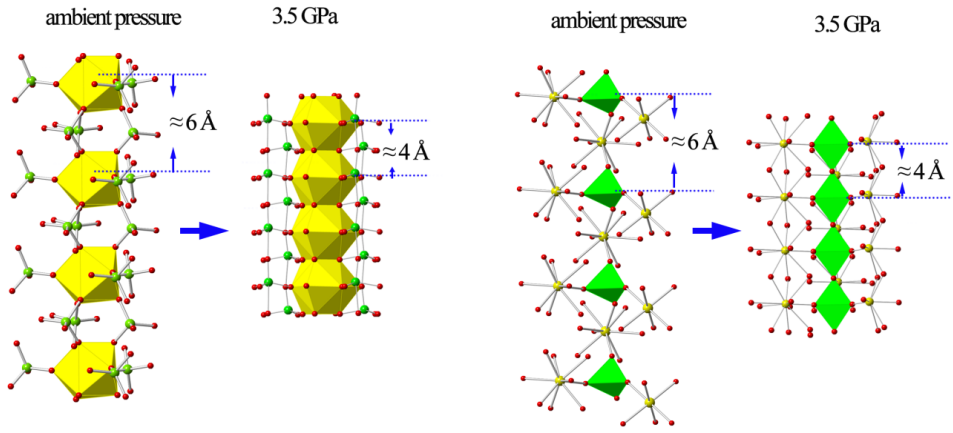


**Fig. 5: The nature of high-temperature/high-pressure phase transition in $ThMo_2O_8$. (a, b) Th and Mo polyhedral geometries change dramatically among the implementation of high-pressure (3.5 GPa). Th is shown in yellow, Mo in green, oxygen atoms are in blue.**

Contact: Dr. Evgeny Alekseev
e.alekseev@fz-juelich.de

## 3.5. Jülich Young Investigator Group: Atomistic Modeling

Safe Management of radioactive waste is a challenging process that involves in-depth understanding of the long-term behavior and stability of different radionuclide-bearing materials. One of the main reasons for the encountered difficulties is the limited understanding of the atomic-scale processes that governs the interaction of radionuclides with different materials. The lack of knowledge is in large part caused by the limitations of the experimental techniques which are often restricted to the specific laboratory conditions. Experiments on active samples are in general also problematic. This results in limited availability of materials that could be used for long term immobilization of radionuclides and safe disposal of nuclear waste. On the other hand the continuous improvement of computers performance allows for simulations of even complex materials using first principles (*ab initio*) methods. Such studies can provide valuable information on the chemical and physical properties of radionuclide-bearing materials which is often difficult to obtain by experimental techniques. The aim of our atomistic modeling studies is to use the world-class supercomputing resources located at Forschungszentum Jülich and allied institutions and the state-of-the-art quantum chemistry and materials science software to perform virtual experiments that reveal crucial information on the atomic-scale mechanisms governing the interactions of radionuclides with various materials, including these constituting the storage and disposal environments (Fig. 6).

**Fig. 6: Left: one of the electronic orbitals responsible for bonding between U atom (grey) and neighbouring O atoms (red) in $Ba_2(UO_2)_3(PO_4)_2$ borophosphate. Interaction between Uranium f orbital and Oxygen p orbitals is clearly visible. An atomic scale analysis of charge distribution provides information on the bonding environment. Right: Computer cluster at RWTH Aachen used in the investigation within Jülich-Aachen Research Alliance (JARA-HPC).**

In order to perform meaningful research we develop computational methodologies that allow for reliable and feasible simulations of nuclear materials. The new computational techniques are used for computer simulations of various structural and thermodynamic properties of novel waste forms, prediction of the formation of new radionuclide-bearing crystalline-solids

(secondary phases), simulation of radiation damage cascades and defects formation in materials, to name but a few. The derived information helps in the assessment of the stability of the novel nuclear waste forms. Our ultimate goal however, is to complement the ongoing experimental work in order to obtain good understanding of radionuclide-bearing materials. The long-term goal of such a joined modeling and experimental studies aims at the development and characterization of new, advanced materials for safe management of nuclear waste. These materials could be used to permanently immobilize dangerous radionuclides in a deep geological disposal, providing a reliable barrier against potential leaks of dangerous elements into environment.

Contact: Dr. Piotr Kowalski
p.kowalski@fz-juelich.de

## 3.6. Characterization of Nuclear Waste

The Waste Characterization group at IEK-6 develops innovative passive and active non-destructive analytical techniques (Fig. 7) for the accurate and reliable characterization of radioactive waste and other materials. R&D activities focus on neutron interrogation techniques for the determination of chemotoxic elements using Prompt and Delayed Gamma Neutron Activation Analysis (P&DGNAA) and for the localization of large shielding structures by fast neutron imaging in 200 L waste packages. Simulation tools such as MCNP and GEANT4 are applied for system design and optimization.
In the field of technology transfer industrial applications of P&DGNAA for recycling of conventional waste and for quality control of products and raw materials are also investigated.

P&DGNAA - MEDINA Facility

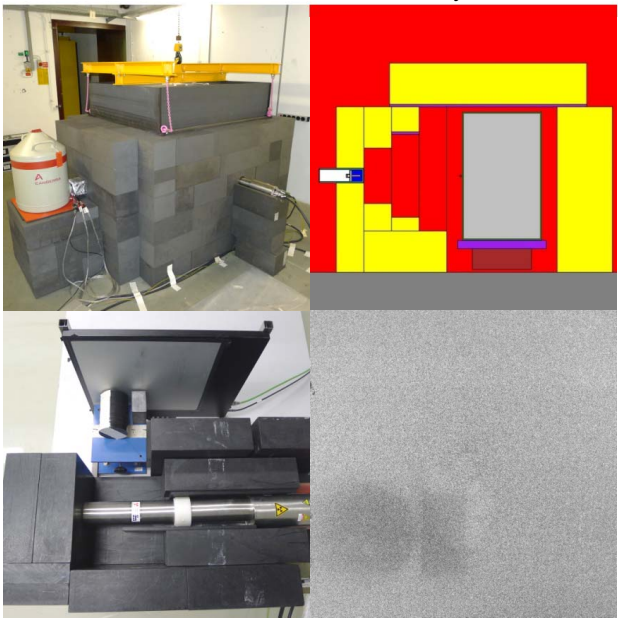

Fast Neutron Imaging

**Fig. 7: Non-destructive analytical techniques: MEDINA (Multi-Element-Detection based on Instrumental Activation Analysis) and Fast Neutron Imaging.**

Contact: Dr. Eric Mauerhofer
e.mauerhofer@fz-juelich.de

## 3.7. Nuclear Data for Waste Characterisation

In cooperation with the PGAA group at the FRM II and funded by a BMBF contract (**02 S 9052A) "**Bestimmung und Validierung nuklearer Daten von Actiniden zur zerstörungsfreien Spaltstoffanalyse in Abfallproben durch prompt Gamma Neutronenaktivierungsanalyse (PGAA-Actinide)" the instrument FaNGaS has been designed and constructed at the Institute of Energy and Climate Research, IEK-6, Nuclear Waste Management and Reactor Safety of the Forschungszentrum Jülich GmbH. It has been installed and tested at the SR10 channel of the FRM II Research reactor of the TUM at Garching. Complimentary to cold neutron PGAA we intend to explore inelastic scattering reactions induced by fission neutrons in elements and radio-isotopes, e.g. actinides. This information is particularly important when hazardous materials need to be investigated non-destructively, such as in safeguards applications, in nuclear waste processing or for storage purposes.
The fission neutron beam created at a 30 by 25 cm large 95% enriched $^{235}U$ converter plate inside the heavy water cooling tank of the reactor delivers fission neutrons of 2.3 E8 $cm^{-2}s^{-1}$ to a bunker where the new FaNGaS instrument is located (see Fig. 8). Two adjacent collimators in the beam channel confine the beam to 5 cm diameter and irradiate elemental or isotopic samples in front of a heavily shielded 50% eff. HPGe detector. The shielding consists of 15 cm of lead, 1 cm of boron carbide and 40 cm of poly-ethylene to reduce scattered fast neutrons and gamma rays from producing background in the detector.


**Fig. 8: Fast Neutron Gamma Spectroscopy (FaNGaS) instrument installed at the FRM II.**

Contact: Dr. Matthias Rossbach
m.rossbach@fz-juelich.de

## 3.8. Nuclear Waste Treatment

Development of strategy for waste treatment is required nowadays for every facility, be it industrial plant or research institute. This process becomes much more complex when radionuclides come into play. The application of radionuclides in science, health care and industry generates radioactive wastes divers in their chemical behaviour and having different half-lives. Therefore radioactive wastes have to be collected and treated for further reuse or safe disposal.

The group of Nuclear Waste Treatment at IEK-6 focuses its research activity on fundamental understanding of the structure and properties of different waste forms. This information enables selection of the efficient methods for the waste treatment and provides the boundary conditions for theoretical modelling of waste stability in the long-term. One of the actual research topics is the treatment of nuclear graphite – highly heterogeneous material containing activation products (e.g. $^{14}C$, $^{3}H$, $^{36}Cl$) and products of nuclear fission (e.g. $^{137}Cs$, $^{90}Sr$). Modern analytical techniques, like SEM, XPS, SIMS, HPLC, GC-MS, autoradiography etc., are used for radionuclide identification, quantification, localisation and speciation in nuclear graphite. Besides the high analytical performance, these methods enable different spatial resolution, which is of high importance for the analysis of uneven distributed radionuclides (Fig. 9). Application of theoretical tools is essential in many cases, given the extremely low radionuclide concentration (e.g. tenths of ppm for $^{36}Cl$), difficult to detect with conventional analytical tools. Different experimental setups are used for investigation of radionuclide release from nuclear graphite, e.g. selective separation of $^{14}C$ by thermal treatment, $^{14}C$ speciation in the gas and liquid phase on repository relevant conditions, etc. Such comprehensive analysis helps to understand the radionuclides' chemical behaviour in the graphite wastes and to develop options for graphite waste minimization, which is an essential step, providing a safe and economic solution to the worldwide problem of nuclear waste accumulation.

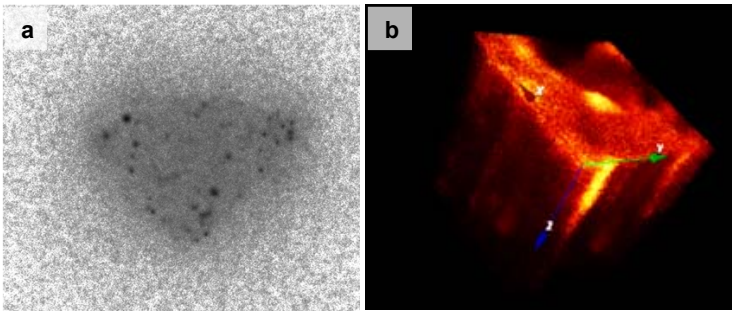


**Fig. 9 Autoradiography (a) and SIMS imaging of Cl spatial distribution (b) demonstrating inhomogeneous distribution of radionuclides in nuclear graphite.**

Contact: Dr. Natalia Shcherbina
n.shcherbina@fz-juelich.de

## 3.9. International Safeguards

Safeguards are activities by which the International Atomic Energy Agency (IAEA), in accordance with the Nuclear Non-Proliferation Treaty (NPT), can verify that a State is in compliance with its international commitments not to use nuclear programmes for nuclear-weapons purposes. The NPT requires the Member States to cooperate with the IAEA in order to facilitate the application of safeguards in these States. On this basis, the IAEA and the German Government have agreed upon the “Joint Programme on the Technical Development and Further Improvement of IAEA Safeguards” in 1978. Since summer 1985, the Forschungszentrum Jülich has coordinated the programme implementation in close cooperation with the German Government, represented by the Federal Ministry of Economics and Technology (BMWi). Since May 2009, IEK-6 has been in charge of coordinating the German Support Programme (GER SP) to the IAEA within Forschungszentrum Jülich.

Recent tasks of the GER SP (about 27 in late 2014) have focused on the implementation of containment and surveillance systems (NGSS, EOSS), and the development and implementation of measurement methods and techniques for non-destructive assay (DMCA, HM-5). Other tasks have enhanced geophysical methods and techniques (seismics, underground radar) for detecting unauthorized activities at geological repositories, as well as satellite imagery processing and geospatial information tools in support of inspection planning and the evaluation of site declarations. Using mathematical models, procedures for estimating optimal inspection strategies as well as for backing the IAEA’s State level concept (acquisition path analysis) have been developed.

Besides scientific management of the GER SP, the group has carried out R&D in three areas: Safeguards analytical techniques, acquisition path analysis, and satellite imagery processing.

Firstly, IEK-6 has cooperated with the IAEA Safeguards Analytical Services (SGAS) on the production and characterisation of particles for quality assurance and quality control. As the availability of monodisperse uranium- and plutonium-containing particles with well-defined properties such as size, density, elemental and/or isotopic composition is limited so far, the project intends to assist the IAEA in acquiring particle reference materials.

In February 2013, the German Federal Ministry of Economics and Technology nominated Forschungszentrum Jülich as a candidate laboratory for the IAEA’s Network of Analytical Laboratories (NWAL). In line with the above mentioned research, the IAEA requested Forschungszentrum Jülich to join the NWAL as a laboratory for provision of particle reference materials.

Secondly, tools for better implementing State-level safeguards have been developed. One important tool is the acquisition path analysis (APA), which has been improved with regard to standardization, automation and visualization. By analyzing all plausible paths that a State could consider in order to acquire weapons usable material, APA is expected to help allocating safeguards measures and inspectorate’s resources for the particular State.

Thirdly, the use of remote sensing in support of nuclear non-proliferation and arms control regimes has been investigated. Particular attention has been given to the development of object-based and non-coherent approaches for detecting and classifying changes in very high resolution optical and high resolution SAR satellite imagery respectively. IEK-6 has been a partner to the European Copernicus initiative, aimed at establishing an European capacity for Earth Observation.

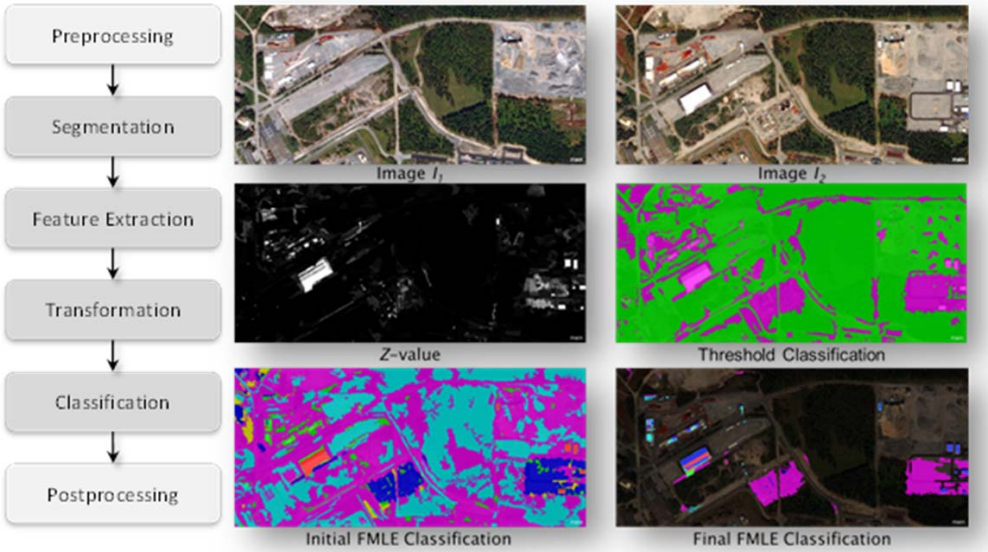


**Fig. 10: Left: Schema of optical change detection procedure using very high resolution satellite imagery. Right: Input satellite imagery and products from optical change detection procedure.**

Contact: Dr. Irmgard Niemeyer
i.niemeyer@fz-juelich.de

# 4 Facilities

The institute operates several radiochemical laboratories (750 $m^2$) for experimental work with radioactive material including alpha emitters (actinides). About 500 $m^2$ are licensed according to the German Atomic Energy Act which permits the handling of nuclear fuels. One part of the controlled area is used for the development of non-destructive characterisation methods for radioactive waste applying neutron sources. In addition to the radiochemical laboratory equipment, the controlled area provides glove boxes which enable the handling of radioactive materials. Furthermore, analytical instruments, such as α-, β-, and γ-spectrometry, as well as x-ray diffraction, Raman spectroscopy and electron microscopy are available.

## 4.1. Solution Calvet Type calorimeter Setaram C80

This machine was installed in mid-2013 in the frame of Helmholtz Young Investigator Group leading by Evgeny V. Alekseev. This equipment constructed for determination of the heat of dissolution of crystalline and amorphous materials. Especially for the solid state chemistry of actinides group, the vessels were made from Teflon to be used with highly aggressive dissolvents such as HF, conc. $HNO_3$ and $H_2SO_4$. It is due to the high stability of solid state actinide phases in normal dissolvents, especially for An(IV). The calorimeter allows using of very small amount of studying materials with about 2 mg. Such, we can use this machine for study not only Th and U bearing materials but also Np and Pu containing phases. Using standard methods of calorimetry we can determinate enthalpy of formation of studied materials. Combining with thermophysical measurements of third low heat capacity we can archive Gibbs free energy for the actinide based solid state materials. These data are absolute necessary for processes modeling with actinides.


**Fig. 11: Setaram C80 calorimeter.**

## 4.2. Combined piston cylinder / Multi anvil press

In November 2013 the new high pressure/high temperature facility was established at IEK-6. The aim of the new device is to investigate the physical and chemical behavior and properties of actinide materials under elevated pressures and temperatures. The apparatus is used for the synthesis of new actinide materials and hydrostatic sintering of new ceramic compounds.

The combined piston cylinder / multi anvil press (Voggenreiter LP 1000 – 540/50) is a tool for producing high hydrostatic pressure and high temperature simultaneously with relatively large sample volumes compared to a diamond anvil cell which usually has sample sizes in µg range. The advantage of the device is that two well established high pressure / high temperature methods (piston cylinder apparatus and walker type multi anvil press) can be used in one instrument (Fig. 12). The high-pressure modules can be replaced within a few minutes. Both technologies have different advantages that complement each other perfectly. The piston cylinder module has a relatively simple sample structure setup with a significantly increased sample volume and a very precise control of the pressure-temperature conditions. In addition, it has very short operating times between the experiments (30-60 minutes per cycle). The multi anvil module offers an ability to generate very high pressures up to 24 giga pascal (240 000 bar) and also a very precise control of the pressure-temperature conditions.


**Fig. 12: Combined piston cylinder / multi anvil press. In this picture the piston cylinder module is installed under the main cylinder. On the left workbench side of the device the walker-type multi anvil module is visible.**

For the piston cylinder module 2 different setups are available:

- ¾ ´´: $p_{min}$ = 0.3 GPa, $p_{max}$ = 2.5 GPa, $T_{max}$: 1500 °C, sample volume up to 800 mg;
- ½ ´´: $p_{min}$ = 0.5 GPa, $p_{max}$ = 4.5 GPa, $T_{max}$: 1800 °C, sample volume up to 125 mg.

For the multi anvil module 3 different setups are available:

- 18/11: $p_{min}$ = 3 GPa, $p_{max}$ = 10 GPa, sample volume up to 15 mg;
- 14/8: $p_{min}$ = 8 GPa, $p_{max}$ = 15 GPa, sample volume up to 10 mg;
- 10/4: $p_{min}$ = 15 GPa, $p_{max}$ = 24 GPa, sample volume up to 5 mg;

$T_{max}$ for all setups is approx. 2300 °C.

It is noticeable that the different setups of the combined piston cylinder/multi anvil press have overlapping pressure ranges. This helps to avoid experimental and methodical errors.
Performing experiments under high pressure / high temperature conditions will allow a deeper insight in the chemistry of actinides as well as actinide bearing compounds and ceramics like the change of coordination or the change of electron configuration (especially of *5f* electrons). It will help us to get a better understanding of An behavior in solid state materials at different conditions.

## 4.3. Microparticle production facility

There is great need for uranium microparticle materials as (certified) reference materials [(C)RM's] for nuclear safeguards applications. Therefore, a microparticle generator has been constructed at IEK-6 which is used for the preparation of such materials with accurately characterized isotopic compositions and elemental contents. The production is based on the preparation of an uranyl containing aerosol using a so-called vibrating orifice aerosol generator. A liquid jet consisting of an uranyl nitrate solution is prepared and by applying an oscillating frequency to the jet, the liquid jet is broken up into monodisperse aerosol droplets. The aerosol droplets with a diameter of approximately 40 μm are dried and calcined to obtain solid uranium oxide microparticles with diameters of about 1 μm.

Uranyl nitrate solutions prepared by dilution of certified reference materials with certified isotopic compositions are used as liquid feed. As no alteration of the isotopic composition is expected, the isotopic composition of the produced microparticles should be comparable to the isotopic composition of the reference material. A major advantage of the system at IEK-6 in comparison to other methods is the production of monodisperse microparticles. Since the aerosol volume can be calculated as the liquid feed rate divided by the oscillating frequency and the uranium content of the liquid feed can be accurately determined by ICP-MS, the amount of uranium per particle can be calculated.

First microparticles consisting of depleted uranium have been produced using IRMM-183 as liquid feed. The particles are characterized by SEM/EDX to obtain information on the particle size distribution, morphology, and the chemical composition. Measurement by SIMS and ICP-MS confirmed the isotopic composition of the produced microparticles. Installation of a new optical particle sizer allows the online measurement of the particle size distribution as additional quality control measure during production.

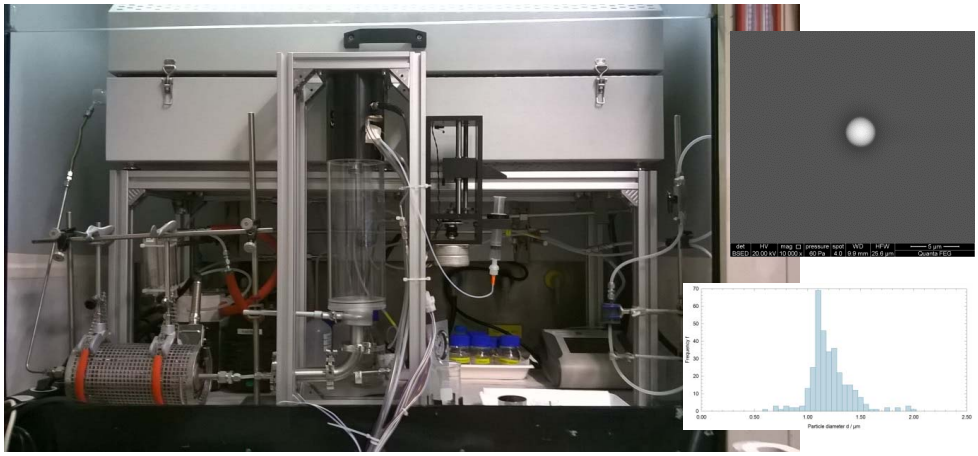

**Fig. 13: Microparticle generator (left) and SEM micrograph of single particle (right-top) with particle size distribution (right-bottom).**

## 4.4. FaNGaS, a new Instrument for Fast Neutron Gamma Spectroscopy installed at FRM II in Garching

A new instrument to study fission neutron inelastic scattering reactions in elements and actinides has been designed, constructed and tested at the SR10 channel of the Forschungsneutronen-quelle Heinz Maier-Leibnitz, MLZ in Garching. Together with the local support team of the FRM II the Nuclear Data and Waste Characterization groups of the IEK-6 have developed the innovative facility to apply PGAA techniques for (n,n'$\gamma$) and other nuclear reaction channels to explore possible analytical benefits for actinide and heavy metal characterization. First results obtained with FaNGaS indicate that e.g. strong neutron absorbers such as Cd, Gd (and possibly other lanthanides) can be more accurately determined using fast compare to thermal neutrons. This effect might be helpful in detecting clandestine materials or hidden sources in strong shielding structures. Additionally, some of the reactions will produce radioactive isotopes that can be measured with high sensitivity after irradiation at a close-to-detector position to extract production probabilities and other nuclear-physical properties.

The fission neutron beam created at a 93 % enriched $^{235}$U converter plate of 15 x 15 cm² effective area in immediate vicinity of the tip of the beam tube delivers unmoderated fission neutrons of 2.3·108 $cm^{-2}s^{-1}$ (with 6 cm PB filter) to the MEDAPP experimental bunker where the new FaNGaS instrument is located. Two adjacent collimators in the beam channel confine the beam to 5 cm diameter and irradiate elemental or isotopic samples in front of a heavily shielded 50 % eff. HPGe detector. The shielding consists of 15 cm of lead, 1 cm of boron carbide and 40 cm of polyethylene to reduce scattered fast neutrons and gamma rays producing background in the detector. The present system allows taking spectra with sufficient sensitivity to determine systematically prompt gamma signals from (n,n'γ), and delayed gamma signatures of (n,p), (n,$\alpha$) and in some cases also (n,2n) reactions.

FaNGaS has been set-up under a BMBF contract (02 S 9052A) "Bestimmung und Validierung nuklearer Daten von Actiniden zur zerstörungsfreien Spaltstoffanalyse in Abfallproben durch prompte Gamma Neutronenaktivierungsanalyse (PGAA-Actinide)" in close cooperation with the PGAA, MEDAPP and NECTAR groups of the FRM II.

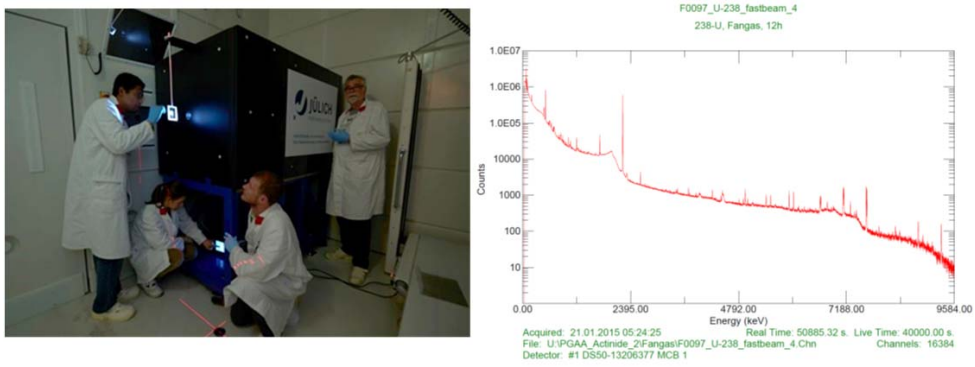


**Fig. 14: Left: The FaNGaS instrument at work, right: $^{238}$U prompt gamma spectrum, 12 h irradiation with fission neutrons**

## 4.5. Hot Cell Facility, GHZ

Interaction of ground water with nuclear waste forms, particularly with spent nuclear fuels, are performed by IEK-6 in the hot cell facility (operation since 1969; including a control area of 3576 $m^2$) within the hot cell line 1 (HZ1).
HZ1 consists of 5 working cells and 5 attached cells. The hot cell area varies from 3 x 3 m to 10.7 x 3 m and allows handling of different spent fuel geometries. In the used hot cells, the handling of radioactive material (i.e. spent $UO_2$ fuel (enriched in $^{235}U$ up to 93.2%) containing 1.37 kg of $^{235}U$) is possible. The ventilation system has an output of 96.000 $m^3$ per hour. Each hot cell is equipped with (a) Master-Slave manipulators, (b) a manual driven manipulator and (c) a crane (3 t). To bring in/out radioactive materials glove boxes and Padirac coupling systems are equipped to the hot cells. For external transportation of radioactive material a truck sewer port and a hall, hosting a crane (30 t), is available.

On 17th September 2012 the IEK-6 started a corrosion experiment with spent research reactor fuel samples (dispersed $U_3Si_2$ Al fuel) in the hot cell 601.
Raman spectroscopy is used to identify the secondary phases formed due to corrosion processes of the fuel sample. For that reason the Raman instrument is attached to fibre-optics connected to Raman sensors which are located in the hot-cell. With one Raman sensor in-situ measurements of the fuel corrosion process can be directly performed.
On 12th January 2015 another experiment started in the hot cell 505. Spent $UO_2$ fuel developed for prototype VHTR reactor is used. The used fuel samples (TRISO coated particles) are miniature fuel elements with a diameter of 1 mm. To work in a hot cell with this material a high-resolution camera was installed. In Fig. 15 TRISO coated particles and the camera are shown. The hot cell 505 possesses three windows equipped with six Master-slave manipulators. Due to this equipment, three experiments will be performed with this fuel material: (a) isolation from the graphite matrix, (b) isolation of the spent $UO_2$ fuel kernel from the coatings and (c) determination of the volatile/instant radionuclide release fraction.

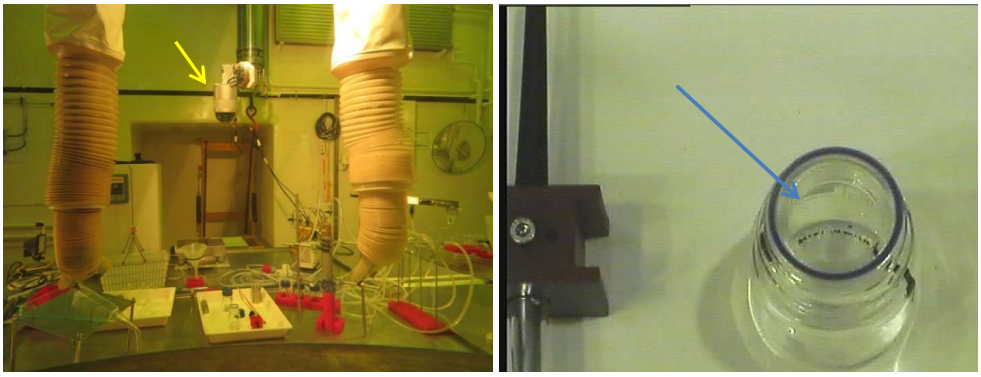

**Fig. 15: Left: Installed camera (yellow arrow), Right: Glass bottle containing one mm sized TRISO coated particles (blue arrow) within the hot cell 505.**

## 4.6. Single Pass Flow Through Experiments (SPFT)

Single-pass flow through experiments (SPFT) are the most commonly applied dynamic type of experiments to determine dissolution rates of nuclear waste. The SPFT set up prevents the progressive accumulation of reaction products which may affect the element release rate. During the experiment, a continuous flow of fresh influent solution keeps up constant, well defined chemical conditions within the flow-through reactor.
Two different types of SPFT experiments were set up, (1) SPFT for the temperature range between room temperature and 90 °C and (2) a pressurized SPFT setup for temperatures above 100 °C. Around 20 SPFT experiments which mainly consist of PFA and Teflon parts are now simultaneously run in order to systematically explore the dissolution kinetics of phosphate and zirconia based ceramic waste forms.
In addition, a titanium and PEEK based setup is used to carry out experiments above 100 °C. The setup consists of a pressurized titanium mixed-flow reactor, a high-performance pressure HPLC pump ($p_{max}$ = 60 bar) and a computer controlled high precision outlet valve which is automatically opened and closed according to a set pressure within the titanium reactor. Thus, a constant fluid flow can be guaranteed although the solution flowing into the reactor is at room temperature and the solution flowing out of the reactor may well be above 200 °C. During the experiments, the pressure can be adjusted to keep the water below the boiling point, ensuring a well-defined contact between the aqueous solution and the nuclear waste form.

## 4.7. X-ray Diffraction Analysis

In principle all kinds of analysis can be performed by the structure research group according to x-ray diffraction: qualitative and quantitative phase analysis, cell constant determination, structure analysis, structure refinement (Rietveld) and the determination of radial distribution functions are possible.

- **Single-crystal X-ray diffractometer:** is equipped with the state-of-the-art SuperNova system. It has a multi-layer X-ray optics ($CuK_\alpha$ and $MoK_\alpha$). The SuperNova combines high intensity Nova X-ray micro-source with the 165 mm fast, high performance Eos™ CCD detector. Mounted on a 4-circle goniometer, the copper radiation Nova X-ray source provides up to 3x the intensity of a 5 kW rotating anode generator with optics and the data quality of a micro-focus rotating anode. Additionally, the SuperNova goniometer has been designed to accept all major open flow cryogenic sample cooling device, including CryojetJet (Oxford Instruments) liquid nitrogen device (90 – 500 K). With this equipment we are able to provide a full structural characterization of radioactive single crystals including very small objects (up to 10-15 µm) in wide temperature range.
- **Bruker x-ray powder diffractometer D8:** is equipped with a copper tube (Cu $K_\alpha$), a molybdenum tube (Mo $K_\alpha$) and two suitable detector systems (scintillation counter and Si semiconductor detector), in order to perform X-ray diffraction analysis on crystalline, semi-crystalline and amorphous samples. Radioactive and non-radioactive powder samples can be measured. Additionally, a climate chamber is available on request that enables *in situ* measurements at different atmospheres and humidities and at temperatures up to 250°C.

- **Bruker x-ray powder diffractometer D4:** is equipped with a copper tube (Cu Kα) and a multi-sample stage (66 samples) as well as with a fast LynXEye detector, appropriate for high throughput measurements. The D4 can also be used for any kind of analysis, with the exception of radial distribution function determination and *in situ* measurements using the climate chamber.

## 4.8. Electron Microscopy

- **ESEM (Environmental Scanning Electron Microscope)**
  - Quanta 200 F from FEI: high resolution field emission SEM
  - High/low vacuum, and ESEM: up to 2700 Pa: Investigation of wet samples at ESEM-mode
  - Detectors: Everhart Thornley SE-detector (high vac.), Gaseous large field SE-detector (low vac.), BSE-detector (high/low vac.), Gaseous analytical detector (GAD) BSE-detector (low vac.), Gaseous secondary electron detector (GSED) (ESEM)
  - EDX: Apollo X Silicon Drift Detector (SDD) from EDAX
  - WDX: TEXS LambdaSpec from EDAX

- **FIB (Focused Ion Beam)**
  - NVision 40 Cross Beam Workstation from Zeiss
  - High resolution field emission GEMINI SEM
  - High performance SIINT zeta FIB column
  - Gas injection system
  - Detectors: In-column: EsB detector with filtering grid for BSE detection; In-lense: SE detector; chamber: Everhardt Thornley SE detector, 4Q BSE detector, GEMINI® multimode BF/DF STEM (Scanning Transmission Electron Microscopy) detector.
  - EDX: INCA energy dispersive x-ray spectroscopy from Oxford Instruments
  - EBSD: Nordlys II Electron Backscattered Diffraction detector from Oxford Instruments.

## 4.9. Non-destructive Assay Testing

**Segmented Gamma-Scanner GERNOD II.**

The Segmented Gamma-Scanner GERNOD II is used for the characterization of 200-L or 400-L drums radioactive waste with wide range of matrices and isotopic compositions. The Gamma-Scanner consists of a mechanical part, a control unit, a detection system and a system unit and operator interface. The mechanical system consists basically of a turntable to accommodate different waste drums (max. weight 6000 kg) and a platform for the vertical movement of the gamma detection and collimation unit. The driving units comprise stepping motors with superior positioning capabilities. The positioning of the drum and detector is handled by a SPS control unit. This offers superior positioning capabilities together with highly reliable performance and control of the system status. Scanning programs are performed either continuously (fast measurements) or in a step by step mode (long time measurements). The detection of gamma emitting nuclides is performed by an HPGe detector connected to a digital spectrometer for signal processing and data acquisition. The

detector can be used together with different collimators depending on the type of application. A dose rate meter is attached to the detector to record the dose rate at the surface of the drum over the whole assay period. All routine operator interactions are carried out via a PC-based control system using the software SCANNER32 developed in cooperation with a professional software engineering company for ease operations and reliable data handling.

**Transmission and Emission Tomography System**

The Transmission and Emission Tomography System developed at IEK-6 is an advanced tool for the characterization of 200-L radioactive waste drums. The radiation emitted from a $^{60}Co$ transmission source (200 GBq in DU shielding) is collimated in the direction of 4 fast scintillation detectors located in the detector collimation shielding bank to perform 4 transmission measurements at the same time. Meanwhile, the 3 HPGe-detectors are used for the emission measurements of the waste drum. An irradiation of these detectors by the transmission source is avoided by the source and detector collimation. Two stepping motors move the drum horizontally and rotate it between two measurement steps respectively. On the data collected for each measurement a pulse height analysis is performed. This leads to the basic data sets for the algorithms used for Transmission Computer Tomography, Emission Computer Tomography and Digital Radiography.

**MEDINA**

MEDINA (Multi-Element Detection based on Instrumental Neutron Activation) is an innovative analytical technique based on prompt and delayed gamma neutron activation analysis for non destructive assay of 200-L waste packages.

## 4.10. Radiochemical Analytics

- **LSC (Liquid Scintillation Counter):**
  - Analysis of aqueous and organic samples
  - Quantulus (PerkinElmer), Autosampler, Ultra low activity determination, determination of environmental activity ($^{14}C$), α,β discrimination
  - TRI-CARB 2020 (PerkinElmer) Autosampler > 100 samples

- **α-spectrometry:**
  - Qualitative and quantitative analysis of α-emitter, Si-detector, low level detection

- **γ-spectrometry:**
  - HP Ge-detector ($N_2$-cooled), NaI-detector, LaBr-detecor, Radionuclide detection with low γ-energy ($^{55}Fe$: $E_\gamma$ < 5.9 kEV), low level detection, borehole detector

## 4.11. Miscellaneous

- ICP-MS ELAN 6100 DRC (PerkinElmer SCIEX )
- STA 449C Netzsch
- FTIR-spectrometer: Equinox 55 (Bruker), KBr-pellets, ATR (attenuated total reflection), TGA
- Horiba raman spectrometer LabRAM HR Vis (400 – 1100 nm), currently equipped with a He-Ne laser (wavelength λ = 633 nm, visible red light), a Diode laser (wave length λ = 785 nm, NIR), an edge filter, two gratings (600 and 1800), focus length 800 mm, a peltier cooled solid state detector, five objectives (x10, x50, x100, x50 NIR, x100 NIR), a safety energy supply system, a safety box for the microscope and a video camera for sample observation using reflected or transmitted visible light.
- Dilatometer DIL 402C (Netzsch)
- Induction furnace (Linn High Therm GmbH), max. temperature 2500 °C, mass spectrometer for analysis of combustion gases
- High temperature furnace HTK 8 (GERO GmbH), max. temperature 2200 °C
- BET AUTOSORB-1 (Quantachrome Instruments)
- Spectral photometer CADAS 100
- Granulometer CILAS 920
- Autoclaves
- Gas chromatography (Siemens AG)
- Gas chromatography PerkinElmer Clarus 580 devices
- Vacuum hot press HP W 5 (FCT Systeme), max. temperature 2200 °C, press capacity max. 50 kN, 5 x $10^{-2}$ mbar

# 5 Scientific and Technical Reports 2013/2014

## 5.1. Instant release fraction and microstructure evolution of spent $UO_2$ TRISO coated particles

H. Curtius*, G. Kaiser, N. Lieck, M. Güngör, M. Klinkenberg, D. Bosbach

* Corresponding author: h.curtius@fz-juelich.de

**Abstract**

The impact of burn-up on the instant release fraction (IRF) from spent fuel was studied using very high burn-up $UO_2$ fuel (~100 GWd/t) developed for the prototype VHTR (**V**ery **H**igh **T**emperature **R**eactor). Within the spherical fuel element, TRISO (TRi-structural-ISO-tropic) particles are embedded. The particles contain $UO_2$ fuel kernels (500 µm diameter) coated by three tight layers.

After cracking of the coatings $^{85}Kr$ and $^{14}C$ as $^{14}CO_2$ were detected in the gas fraction. Xe was not detected in the gas fraction, although ESEM (Environmental Scanning Electron Microscope) investigations revealed an accumulation in the buffer. $UO_2$ fuel kernels were exposed to synthetic groundwater under oxic and anoxic/reducing conditions. U concentration in the leachate was below the detection limit, indicating an extremely low matrix dissolution. Within the leach period of 276 days Sr and Cs fractions located at grain boundaries were released and contribution to IRF up to max. 0.2 % respectively 8 %. Depending on the environmental conditions, different release functions were observed. Second relevant release steps occurred in air after ~ 120 days, indicating the formation of new accessible leaching sites. ESEM investigations were performed to study the impact of leaching on the microstructure. In oxic environment, numerous intragranular open pores acting as new accessible leaching sites were formed and white spherical spots containing Mo and Zr were identified. Under anoxic/reducing conditions numerous metallic precipitates (Mo, Tc and Ru) filling the intragranular pores and white spherical spots containing Mo and Zr, were detected. In conclusion, leaching in different geochemical environments influenced the speciation of radionuclides and in consequence the stability of neoformed phases, which has an impact on IRF.

**Introduction**

The reference inventory of high-level nuclear wastes designated for geological disposal in Germany as used within the preliminary safety assessment for a geological repository in the Gorleben salt dome (“vorläufige Sicherheitsanalyse Gorleben”, vSG) includes various types of spent nuclear fuels from research and prototype reactors, besides LWR spent fuels and vitrified high-level wastes [1]. At the IEK-6 (Research Center Jülich) investigations concentrate on $UO_2$ based fuel elements developed for the prototype VHTR reactor. Compared to $UO_2$ LWR fuel, the VHTR fuel is very different in design and in applied irradiation conditions. A fuel pebble consists of up to 10000 small $UO_2$ fuel kernels with diameters of about 500 µm, embedded in a moulded graphite sphere with a diameter of about 60 mm (Fig. 16). The outer shell (5 mm thick) of such a fuel pebble represents a fuel free zone. Each TRISO coated particle (Fig. 16) possesses an $UO_2$ kernel which is coated

with four layers (porous carbon buffer, inner dense pyrocarbon layer (IPyC), silicon carbide (SiC) and outer dense pyrocarbon layer (oPyC)), represents a miniature fuel element of about 1 mm in diameter. Safety assessment of spent nuclear fuel disposal in a deep geological formation requires information about the release of radionuclides from the fuel after groundwater breaches the container and contacts the fuel. The fraction of the total inventory of a given radionuclide in the spent fuel available for instant release (instant release fraction, IRF) is used as source term in safety assessment models and contribute to the long-term safety analysis. Within the European project FIRST NUCLIDES the impact of burn-up on the instant radionuclide release fraction from spent $UO_2$ fuel was investigated. For $UO_2$ LWR fuel, many papers were published and experimentally determined fuel dissolution and radionuclide release rates were given for oxidizing and reducing conditions [2, 3, 4]. Results from leaching experiments using HTR pebbles lead to the conclusion, that these fuel pebbles are well designed for direct disposal [5, 6]. The design of the moulded graphite pebble in which the coated fuel kernels are embedded represents a functional multi-barrier system. As long as the coatings are intact, no large fractions of radionuclides will be released. Within this work extremely high burn-up spent $UO_2$ fuel kernels were selected as sample material. Details towards fuel and irradiation conditions are given in [7]. The contributions to IRF of radionuclides present in gaseous form, as water soluble salts, as metallic inclusions and the effects of leaching on the microstructure are presented.

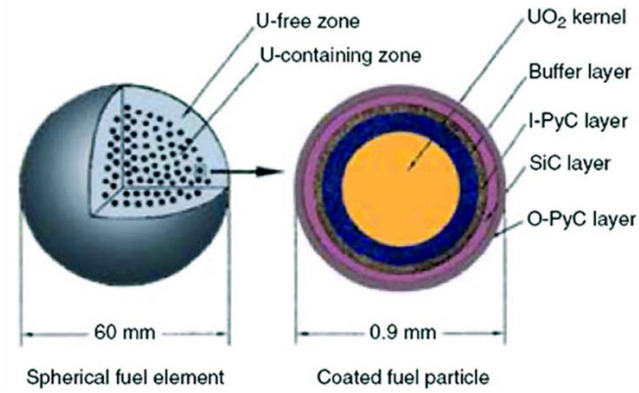


**Fig. 16: Design of a fuel element and a TRISO coated fuel particle**

**Radionuclide distribution within fuel/coatings after irradiation**

Calculated and measured values for the activities of $^{134/137}Cs$, $^{154/155}Eu$, $^{144}Ce$, $^{106}Ru$, $^{125}Sb$, $^{144}Pr$ and $^{241}Am$ present in a coated particle (CP) were compared. The determined activities agree with the calculated values. By cracking the fuel kernel and the coatings were separated and treated with the Thorex reagent. The radioisotopes are quantitatively located within the fuel kernel, but Cs is an exception. Up to 95 % of the inventory of Cs was present in the coatings. A high accumulation of Cs within the buffer was confirmed by ESEM investigations. An excellent work performed by Barrachin et al. [8] summarized results from fission product behaviour in irradiated TRISO coated particles. A high Cs release was confirmed by electron probe microscopy analyses (EPMA) and calculations with MFRR code (module for fission product-release). The significant Cs release can be explained by the strong reduction of kernel oxygen potential. Under the performed irradiation conditions one can consider carbon oxidation leading to a strong decrease of fuel-kernel oxygen potential.

Under this low oxygen potential (-650 kJ/mol) ternary Cs compounds are not stable and Cs-atom diffusion by U vacancies and subsequent release is considered. This low oxygen potential is the key point in Cs behaviour in $UO_2$TRISO particles, very different to $UO_2$ LWR fuel. In LWR irradiation conditions, uranium and plutonium fissions are described as oxidizing because oxygen liberated from fission is only partially associated with fission products and an amount of "free" oxygen is created corresponding to an increase of the oxygen/metal ratio and of the oxygen potential. Even for LWR fuel with comparable irradiation characteristics (10 % FIMA, 1273 K) the oxygen potential determined was around -310 kJ/mol [9]. This clearly indicates that the main contribution of the reduction of the oxygen potential comes from carbon oxidation. As was mentioned before, ESEM investigations revealed an accumulation of the released Cs within the buffer. Within the buffer, the formation of intercalation compounds of $CsC_n$ can be assumed [10].

**Gas release**

Radionuclides insoluble in the $UO_2$ matrix and present in gaseous form contribute to the IRF. Especially the irradiation conditions of the HTR fuel (high temperature, high fission rates) favour gas release by diffusion towards grain boundaries where it is released. More over gas resolution from gas bubbles occur [11]. This gas fraction also diffuses to grain boundaries where it is released. Due to the high temperature, the thermal diffusivity is high. Compared to LWR fuel [12] (fission gas release: around 2 % for average burn-up of 48 GWd/t; around 8 % for average burn-up of 75 GWd/t) the fission gas release from HTR fuel is expected to be significantly higher.

Within this study He, tritium and Xe were not detected in any gas sample. However ESEM investigations revealed an accumulation of Xe within the buffer region. We assumed that Xe is significantly released from the fuel kernel, hence from the fuel matrix and therefore Xe contributes significantly to the IRF. Further investigations will focus on verifying the Xe location within the coatings. An identical observation for the Xe accumulation within the buffer was already reported by Minato et al. [10]. Under the irradiation conditions, Xe remained in atomic form and diffused to grain boundaries. Calculations performed with the MFRR code [8] assume that the Xe fraction released is in the range of 70 %, indicating that the fission gas release in HTR fuel is much higher than that of irradiated $UO_2$ LWR fuels. It is thought that the release mechanism for Xe and Cs are similar. As mentioned before, 95 % of the inventory of Cs was detected in the coatings after irradiation. Considering carbon oxidation and consequently the formation of an extremely low oxygen potential, Cs is present in atomic form like Xe. A high diffusivity by U-vacancies toward grain boundaries and subsequent release for Cs and Xe is assumed. In all gas samples high amounts of the fission gas $^{85}Kr$ were detected. Compared to the calculated inventory approximately 35% of $^{85}Kr$ was released instantaneously. In conclusion, Xe and Kr are significantly released from the fuel kernel and highly contribute to the IRF. In all gas samples, $^{14}C$, present in the chemical form as $^{14}CO_2$ was identified and an activity of 15 ± 5 Bq was measured for this activation product. $^{14}C$ mainly is produced by neutron capture reactions involving nitrogen $^{14}N$ (n, p) and carbon $^{13}C$ (n, $\gamma$). Both are present as impurities in fuel. The formation of $CO_2$ can be explained by carbon oxidation, a reaction which is known to consume oxygen and hence contribute to the low oxygen potential as mentioned before. Like Xe or Kr also $^{14}C$ preferentially segregate from the fuel matrix and contributes to the IRF.

**Leaching**

Leaching experiments were performed under anoxic/reducing (96 % of $Ar/H_2$ type 4.8 and 4 % of $H_2$ type 3.0) and oxic (air) conditions using a low molar salt solution containing 19 mM NaCl and 1 mM $NaHCO_3$ (pH value of this solution was 7.4 ± 0.1). The Fraction of Inventory of an element i released in the Aqueous Phase (FIAP) was calculated according to:

$$FIAP_i = m_{i,\,aq} / m_{i,\,SNF} \quad (1)$$

where $m_{i,aq}$ is the mass of the element i in the aqueous phase (g) and $m_{i,SNF}$ is the mass of the element in the SNF sample (g). The Instant Release Fraction of an element i ($IRF_i$) is the Fraction of Inventory of the element i in the Aqueous Phase ($FIAP_i$) reduced by FIAP of uranium. For the reported time period no uranium was detected in solution, hence the $FIAP_i$ of the elements represent the $IRF_i$. It has to be stated, that this is an assumption, because there is U in solution, but within the detection limit the U concentration cannot be specified.
In the leachate the radioisotopes $^{234/235/236}U$ (detection limit: 0.73 Bq/mL, respectively 0.72 Bq/mL respectively 0.58 Bq/mL), $^{237}Np$( detection limit: 0.88 Bq/mL), $^{238/239/240}Pu$ (detection limit: 1.08 Bq/mL respectively 0.96 Bq/mL respectively 0.96 Bq/mL)), $^{241}Am$ (detection limit: 1.05 Bq/mL), $^{244}Cm$ (detection limit: 0.09 Bq/mL), $^{90}Sr$(detection limit: 0.1 Bq/mL) and $^{134/137}Cs$ (detection limit:0.1 Bq/mL ) were analysed.
Independent on geochemical redox states, U, Np, Pu, Am and Cm were not detected in solution in the time frame of investigation (276 days), hence these radioisotopes do not contribute significantly to the IRF. Especially, the low oxidative dissolution rate of the matrix under oxic conditions can be related to the very high burn-up. This high burn-up cause an extensive doping of the fuel matrix, which makes the oxidative dissolution of the matrix difficult. Also, the low oxygen potential of this fuel (oxygen is consumed by carbon oxidation) create a low oxygen concentration in solution which delayed the oxidative dissolution of the fuel matrix.
Within the fuel matrix, Sr is present as SrO and it also can be present in the perovskite phase ($Ba(Sr)ZrO_3$). However, up to now no significant amounts of a perovskite phase were detected [8]. As SrO, Sr is highly soluble within the $UO_2$ matrix and low release values are expected. For both environmental conditions the contributions of Sr to the IRF were low (max 0.2 %) and comparable to $UO_2$ LWR fuel [13]. It can be assumed that this Sr release fraction indicates the Sr inventory of fines (located at the periphery of the fuel kernels) and accessible grain boundaries. Unexpected, a lower Sr release occurred at (air) conditions within the first 100 days and might be due to the high doping of the fuel matrix and/or to the formation of a protective layer, which lead to a passivation of the grain boundaries. This however needs to be clarified in future with intensive Raman investigations. The contribution of Cs to IRF was significant. Within the first 5 days of leaching a value of 8 % was determined in ($Ar/H_2$) and no further contribution was observed (time frame of 270 days). In (air) the release of Cs within the first 100 days reached a value of 5 % and increased in the next 100 days to the steady state cumulative IRF of 7 %. In conclusion, the determined values or the IRF reflect the labile Cs fraction located at accessible grain boundaries. Compared to $UO_2$ LWR fuel (60 GWd/t) these values are one order of magnitude higher [13], due to the higher oxygen potential in LWR fuel which trapped Cs in separated phases (stable ternary Cs compounds ($CsUO_4$, $Cs_2MoO_4$)).

**Microstructure evolution**

The influence of leaching on the microstructure is clearly visible and was studied with ESEM/EDX technique. Independently of redox conditions, first, leaching seemed to clean up the surface and the grain boundaries (Fig. 17 c), d), e) and f)). This mainly can be attributed to the removal of graphite fines steaming from the carbon buffer after the crack process. Under oxic conditions (Fig. 17 c) and d)), white spherical spots containing the elements Mo (52.02 wt%) and Zr (47.98 wt%) are visible, but the hexagonal platelets seem to be dissolved and Tc could not be detected (Apollo X Drift detector: detection limit: 0.1 wt%). Instead, numerous open pores were formed accounting for new assessable leaching sites. Under anoxic/reducing conditions (Fig. 17 e) and f)) the pores are filled with platelets hosting the metallic phases (Mo (59.17 wt%), Ru (21.57 wt%) and Tc (18.96 wt%)) and white spots containing Mo (22.51 wt%) and Zr (77.49 wt%) were detected. The unexpected association of Zr within the metallic precipitates will be investigated in future in detail. However, this observation underlines the former findings [8], that the expected perovskite phases are not that significant for this fuel type under this irradiation conditions. In general, the metallic particles influence the oxidative matrix dissolution by hydrogen activation and the observed instability of metallic particles in dependency of environmental leaching conditions must be studied in more detail in future.

**Conclusion**

To provide knowledge of the fast/instantly released radionuclides from high burn-up spent $UO_2$ fuel, spent TRISO coated particles were used as extremely high burn-up (10.2 % FIMA) samples.

By cracking of the coatings an instant gas fraction released. $^{14}C$ as $^{14}CO_2$ and $^{85}Kr$ (up to 35 % of the inventory) were identified as gas components. Xe was not detected in the gas fraction but an accumulation within the buffer/iPyC layer was confirmed by ESEM investigations. The observed high fission gas release from the $UO_2$ matrix is different to $UO_2$ LWR spent fuel. The used TRISO particles were irradiated under conditions which enabled re-solution of fission gas from bubbles and like the amount of fission gas present in atomic form within the fuel matrix to diffuse (high thermal diffusivity) to grain boundaries, where it is released. Under the irradiation conditions a low oxygen potential is created by carbon oxidation (CO and $CO_2$ formation) and explain the presence of $^{14}CO_2$.

In a time frame of 276 days leaching experiments have been performed in order to determine the instant radionuclide release fractions under different geochemical environments. U was not detected in solution, indicating insignificant matrix dissolution effects. The contribution of $^{90}Sr$ to the IRF (represents the inventory of $^{90}Sr$ located at grain boundaries) was max.0.2 % and comparable to LWR fuel. The behaviour of Cs was found to be very different to LWR fuel. After irradiation 95 % of Cs is located within the coatings. Under the as mentioned low oxygen potential of the fuel, ternary Cs compounds are instable. It is assumed that Cs in atomic form released similar to Xe. Within the first five days of leaching under anoxic/reducing conditions, the maximum contribution to the IRF of $^{134/137}Cs$ (8 %) was reached, representing the Cs inventory located at the grain boundaries. Compared to LWR spent fuel (60 GWd/t) these values are one order of magnitude higher.

Strongly, the release behaviour of Cs and Sr depend on environmental conditions. Only in oxic environment second relevant release steps occurred after ~100 days, indicating the formation of new accessible leaching sites.

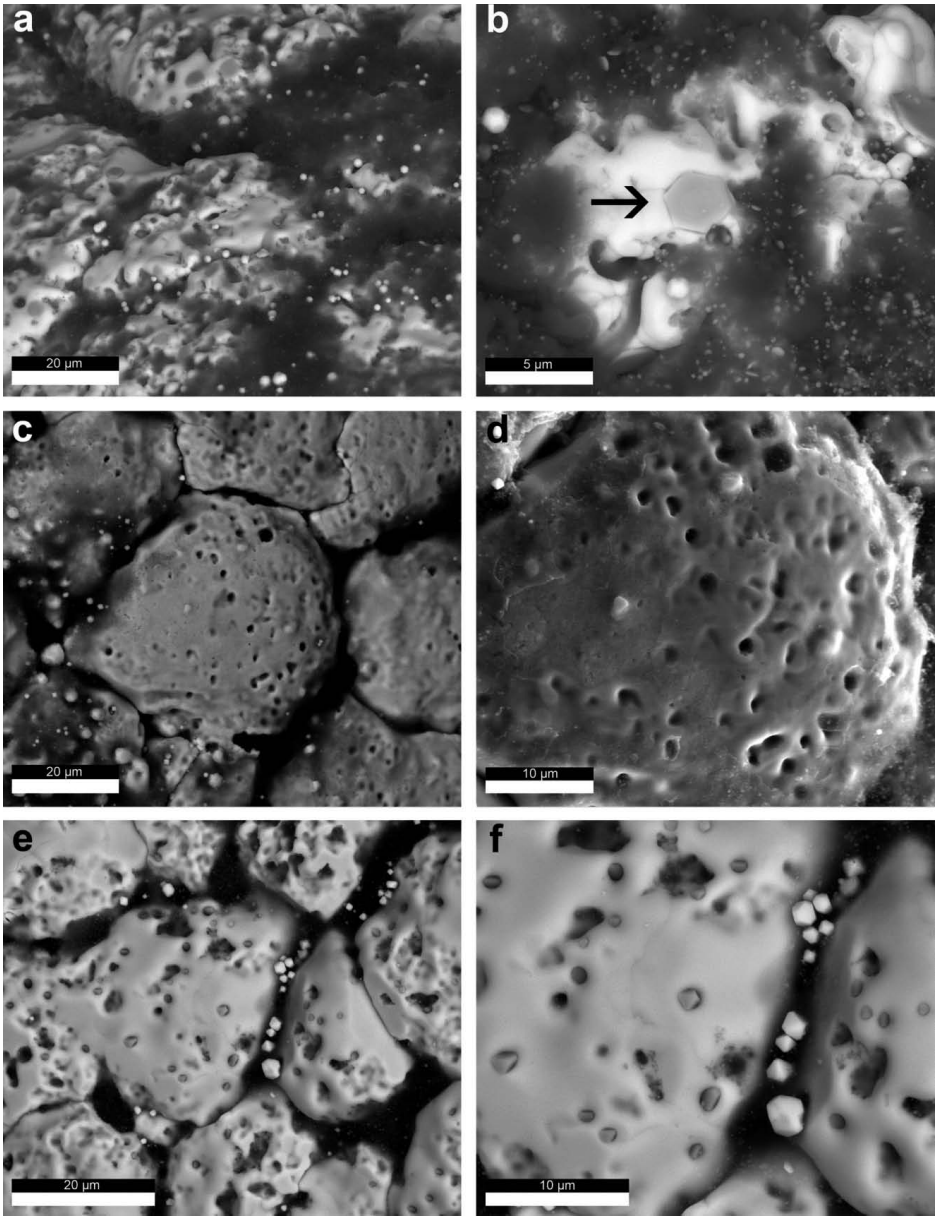


**Fig. 17: (a) Periphery of the irradiated $UO_2$ fuel kernel before leaching, (b) with hexagonal platelets (arrow) and white spots, (c) and (d) periphery of the irradiated $UO_2$ fuel kernel after leaching under oxic conditions with grain boundaries, white spots and numerous open intragranular pores, (e) and (f) periphery of the irradiated $UO_2$ fuel kernel after leaching under anoxic/reducing conditions with grain boundaries, white spots and numerous intragranular pores filled with metallic precipitates.**

SEM investigations revealed the influence of leaching on the microstructure. In oxic environment, Tc could not be detected anymore within the white spots (containing Mo and Zr), but the formation of numerous intragranular open pores was observed. Open pores represent new accessible sites for solution attack and might explain the second relevant release steps observed for Cs and Sr. Under anoxic/reducing conditions white spherical spots (containing Mo and Zr) and numerous metallic precipitates (Mo, Tc and Ru) filling the intragranular pores were detected. It can be stated, that leaching in different geochemical environments influenced the speciation of radionuclides which affects the evolution of the microstructure and this directly had an impact on the IRF of radionuclides. However, the observed high dissolution rate of Tc under oxic conditions and the association of Zr within the metallic phases are not completely understood and these topics will be investigated in future.

**Acknowledgement**

Special thanks to Sander de Groot and Ralph Hania from Nuclear Research and Consultancy Group in Petten for the TRISO Coated Particles and for their kind support. The research leading to these results has received funding from the European Union's European Atomic Energy Community's (Euratom) Seventh Framework Programme FP7/2007-2011 under grant agreement n° 295722 (FIRST-Nuclides project).

**References**

[1] Kienzler, B. et al.: Radionuclide source term for irradiated fuel from prototype, research and education reactors, for waste forms with negligible heat generation and for uranium tails. KIT Scientific Reports 7365 (2013).[2] Johnson, L.H., Shoesmith, D.H.: Radioactive waste forms for the future, Elsevier Science Publishers B.V. Ed. Lutze and Ewing, 635 (1988).

[2] Johnson, L. et al.: Rapid aqueous release of fission products from high burn-up LWR fuel: Experimental reults and correlations with fission gas release, Journal of Nuclear Materials 420, 54-62 (2012).

[3] Johnson, L.H., Tait, J.C.:Release of segregated nuclides from spent fuel, SKB technical report 97-18 (1997).

[4] Rainer, H., Fachinger, J.: Studies on the long-term behaviour of HTR fuel elements in highly concentrated repository-relevant brines, Radiochimica Acta 80, 139-145 (1998).

[5] Fachinger, J. et al.: Nuclear Engineering and Design 236, 543-554 (2006).

[6] Fütterer, M.A. et al.: Results of AVR fuel pebble irradiation at increased temperature and burn-up in the HFR Petten, Nuclear Engineering and Design 238, 2877-2885 (2008).

[7] Curtius, H. et al.: Spent $UO_2$ TRISO coated particles – instant release fraction and microstructure evolutionRadiochimica Acta. ISSN (Online) 2193-3405, ISSN (Print) 0033-8230, DOI: 10.1515/ract-2014-2354, January 2015.

[8] Barrachin, M. et al.: Fission-product behaviour in irradiated TRISO-coated particles: Results of the HFR-EU-1bis experiment and their interpretation, Journal of Nuclear Materials **415,** 104-116 (2011).

[9] Walker, C.T. et al.: On the oxidation state of $UO_2$ nuclear fuel at a burn-up of around 100 MWd/kg HM, Journal of Nuclear Materials 345, (2005) 192-205.

[10] Minato, K. et al.: Journal of Nuclear Materials **20**, 266-281 (1994).

[11] Barrachin, M. et al.: Progress in understanding fission-product behaviour in coated uranium-dioxide fuel particles, Journal of Nuclear Materials **385**, 372-386 (2009).

[12] Johnson, L.H., Mc Ginnes, D.F.: Partitioning of Radionuclides in Swiss power reactor fuels, NAGRA Technical Report 02-07 (2002).

[13] Roudil, D. et al.: Journal of Nuclear Materials,**362**, 411-415 (2007).

[14] Moriyama, K., Furuya, H.: Thermochemical Prediction of chemical form distribution of fission products in LWR oxide fuels irradiated to high burnup, Journal of Nuclear Science and Technology **34**, 900-908 (1997).

## 5.2. Secondary Phases/Solid Solutions

E. Alekseev, B. Xiao, H. Curtius, S. Labs, K. Rozov, D. Bosbach

* Corresponding author: h.curtius@fz-juelich.de

Secondary phases form by corrosion of nuclear waste forms, waste containers and by alteration of other near-field materials. These neoformed phases can retain radionuclide species by different mechanisms and thereby significantly affect the migration of various radionuclides into the environment. Especially the formation of solid solutions as a result of structural incorporation of a radionuclide species into the matrix material, offers the possibility of long term immobilization. The development of (a) a molecular-level process understanding will improve the understanding of radionuclide behavior in the geosphere and (b) the development of a thermodynamic data base will lead to a more reliable long-term prediction with respect to the geochemical evolution of the repository system. Investigations at IEK-6 are mainly focusing on retention of radionuclides by structural incorporation in (a) Layered Double Hydroxides (LDHs), in (b) uranium silicates and (c) in thorium selenite/selenate systems.

### Layered double hydroxides (LDHs)

#### Introduction

The disposal of radioactive waste in geological environments calls for the development of materials which will prevent the migration of radionuclides to biosphere for long-enough time. Layered double hydroxide phases (LDHs) or “hydrotalcite-like solids” with general formula $[M^{II}_{(1-x)}M^{III}_{(x)}(OH)_2]^{x+}[A^{y-}_{x/y}\cdot nH_2O]^{x-}$ are of interest to these studies due their ability to retain wide range of different cations and especially due to anion-exchange properties. Thus, LDHs are considered as potential buffers for retention of radioactive anions [1]. However, at the present time, the understanding of the retention properties of LDHs and applying them for geochemical modeling are hampered by scarce data on their thermodynamic properties. Particularly, there is the important problem to retrieve thermodynamic data and to predict the stability properties of LDHs where various types of cations are incorporated into the structure. This work focused on the synthesis, characterization of chloride-bearing LDHs with incorporated Zr(IV), Fe(II), Co(II) or Ni(II) cations. The primary objective was to explore the isostructural incorporation of Fe(II), Co(II), Ni(II) or Zr(IV) into the LDH. The second objective was to investigate the effect of incorporation of these cations on stability properties (i.e., the standard Gibbs free energies of formation) of LDHs with the help of thermodynamic modeling [2].

#### Results and conclusion

Fe(II)-, Co(II)-, Ni(II)- and Zr(IV)-containing LDHs have been prepared by co-precipitation method. PXRD measurements demonstrated that: (1) pure Mg-Al-Fe(II) LDHs are existing in the range of the mole fraction of iron $x_{Fe}$ = Fe/(Mg+Fe) between 0 and 0.13 [3]. Unit-cell parameters ($a_o$=$b_o$) as a function of $x_{Fe}$ follow Vegard’s law corroborating the existence of a solid solution when $x_{Fe}$ = 0 - 0.13. Products of syntheses with $x_{Fe} \geq 0.13$ contain detectable amounts (≥ 1-2 wt%) of additional phases (like, magnetite, maghemite, lepidocrocite); (2) pure $Ni^{2+}$- and $Co^{2+}$-containing LDHs (mole fractions of Ni and Co were equal to 0.1) have

been synthesized successfully [4]; (3) Mg-Al-Zr(IV) precipitates with mole fraction of zirconium $x_{Zr}$ = Zr/(Zr+Al) = 0.0 - 0.5 show PXRD patterns attributed to pure LDHs and the variation of lattice parameters $a_o$=$b_o$ as a function of $x_{Zr}$ is in agreement with Vegard's law demonstrating the presence of solid solution in this compositional range [5]. In contrast, PXRD analyses of precipitates with $x_{Zr}$ ≥ 0.5 have shown the presence of additional X-ray reflexes typical for brucite. The stoichiometry of LDHs has been established by ICP-OES and SEM-EDX analyses and reveals that (Mg+Fe)/Al, (Mg+Co)/Al and (Mg+Ni)/Al ratios in $Fe^{2+}$-, $Co^{2+}$- and $Ni^{2+}$- containing solids are remarkably close to desired 3:1 for the whole range of solid compositions. However, in Mg-Al-Zr(IV) LDHs the increase of $x_{Zr}$ in co-precipitating synthesis solutions leads to the formation of solids with significantly reduced Mg/(Al+Zr) ratios. This fact and results of thermodynamic calculations with GEM-Selektor software [2] indicate that the incorporation of Zr into the LDH structure increases significantly the aqueous solubility (Fig. 18a) of LDHs partial localization of $Zr(OH)_5^-$-ligands in the interlayer space of brucite-like layers. On the other hand estimates of molar Gibbs free energies shown that the substitution of $Fe^{2+}$, $Co^{2+}$ and $Ni^{2+}$ into the LDHs does not affect so significantly on the stability of LDHs (Fig. 18b) indicating that these cations are situated in brucite-like layers.

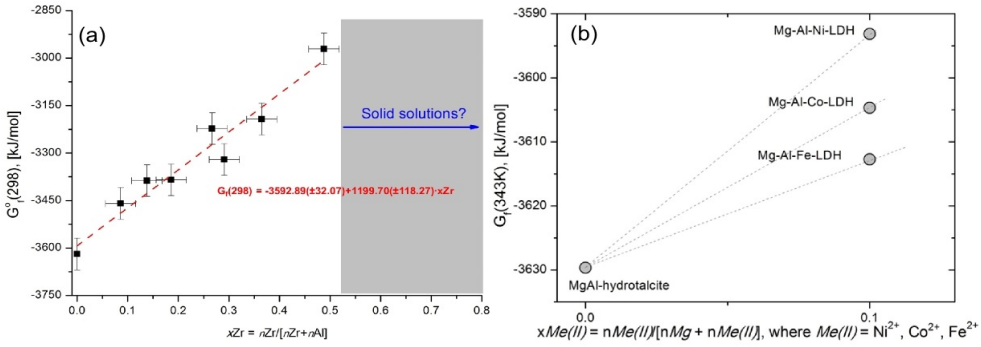


**Fig. 18: Gibbs free energies of formation of (a) Zr(IV)-containing and (b) Fe(II)-, Co(II), Ni(II)-containing LDH solids.**

Finally, reliable estimate of standard Gibbs free energy of formation for pure Mg-Al hydrotalcite composition (-3619.04 ± 15.27 kJ/mol) has been provided. For the first time, by applying Calvet-type solution calorimetry values of standard enthalpy (-4013.89 ± 13.27 kJ/mol) and absolute molar entropy (254.63 ± 25.34 J/mol·K) of pure Mg-Al-Cl LDH have been determined.

**Acknowledgement**
Financial support from BMWi, Germany (Vespa project; grant 02E10780) and BMBF, Germany (ImmoRad project; grant 02NUK019C) is gratefully acknowledged.

## Uranium/Thorium silicates

### Introduction

Coffinite, $USiO_4$, is widely considered to be an important alteration mineral of uraninite. [6, 7] Under reducing conditions as in the repository system, the uranium solubility in aqueous solutions is extremely low and typically derived from the solubility product of $UO_2$. Stable U(IV) minerals, which could form as secondary phases, would impart lower uranium solubility to such systems. Thus knowledge of coffinite thermodynamics would be highly useful for a more realistic safety assessment in a final repository for spent nuclear fuel. One way to achieve this goal is by synthesizing pure $USiO_4$ and measuring dissolution enthalpy and entropy (via heat capacity measurements) directly. The synthesis however proves rather challenging. Coffinite, $USiO_4$, like thorite, $ThSiO_4$, under ambient conditions crystallizes in the zircon-type structure, spacegroup $I\,4_1/amd$. Hence the route via formation of solid solutions with the comparably easy to synthesize $ThSiO_4$ is used. This way the $ThSiO_4$ – $USiO_4$ system can be studied in detail and from the observed tendencies conclusions towards preparation and properties of the uranium end member may be drawn.

### Results

Samples of $U_xTh_{(1-x)}SiO_4$, x = 0 – 1, solid solutions were prepared via a hydrothermal route and thoroughly investigated. [8] Lattice parameters and unit cell volume derived from Le Bail fit of the x-ray data are in considerably good accordance to Vegard's Law, cf. Fig. 19.

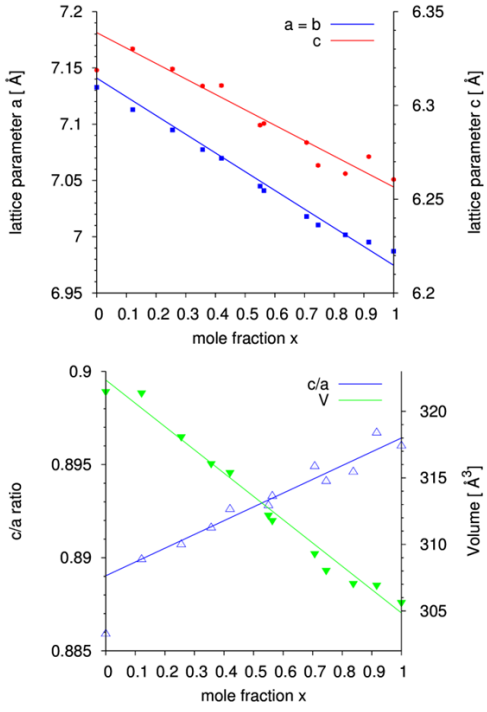


**Fig. 19: Lattice parameters, unit cell volume and c/a-ratio of the $U_xTh_{(1-x)}SiO_4$ uranothorite solid solutions as derived from Le Bail fit of the powder diffraction data.**

It appears that complete miscibility can be achieved between thorite, $ThSiO_4$, and coffinite, $USiO_4$. An overview of the obtained compositions and lattice parameters can be found in [8]. All synthesized samples show small lentil shaped particles in the SEM imaging. The composition was confirmed through EDS measurements employing the ThL and UL edge. While it appears that the longest axis shortens with increasing uranium mole fraction, the particles establish a considerably symmetric shape in those samples close to equimolar Th/U - ratios. It is notable that the change in the particles' habitus correlates with the change in the c/a-ratio; as x decreases, the c/a-ratio also decreases. Yet, the particle morphology and particle size should not be mixed up with the crystallite size and changes of the unit cell as observed from x-ray data.
Subsequent IR spectrometry on the uranothorite samples reveals that all samples show characteristic $SiO_4^{4-}$ tetrahedron bending- and stretching modes in the range 400–1100 $cm^{-1}$ as well as signals for water in the spectra. Neither spectrum establishes a band ~ 530 $cm^{-1}$, specific for $UO_2$, nor at ~ 920 $cm^{-1}$ characteristic for $UO_2^{2+}$. It can therefore be concluded that the prepared samples do not contain any other uranium oxides of type $MO_2$ (M = U, Th) or that significant oxidation of U(IV) → U(VI) has taken place. While all other bands remain constant within the experimental resolution throughout the whole composition of the solid solution, the $B_{1g}$ – mode at 459 $cm^{-1}$ decreases with increasing uranium content down to 444 $cm^{-1}$. For the $ThSiO_4$ – $ZrSiO_4$ and $ThSiO_4$ – $HfSiO_4$ systems recently investigated in our group, the energy of the $B_{1g}$ – mode increases with decreasing thorium content while all other modes however shift to lower wavenumbers.
Very promising $USiO_4$ samples and some of the solid solutions after investigation were provided to the group of Prof. Alexandra Navrotsky, University of California Davis, Davis, CA, USA for high-temperature drop-solution calorimetry.

**Conclusion**

From the x-ray diffraction data it appears that complete and ideal miscibility can be established in the $USiO_4$ – $ThSiO_4$ system. Following the analysis of composition and short range order, it can be concluded that no further uranium containing phases are present in the prepared samples and a reproducible synthesis route for $USiO_4$ has been established. Comprehensive data has been collected on the uranothorite solid solutions as well as the end members, including investigations towards the behaviour under elevated pressures. [9] The reproducible synthesis procedure will serve as a good basis for production of more sample mass and successional dissolution and/or leaching experiments on this topic.
Just recently obtained calorimetric data confirm the thermodynamic metastability of coffinite with respect to uraninite plus quartz but in turn show that it can form from silica - rich aqueous solutions in contact with dissolved uranium species in a reducing environment. [10] These insights support that coffinitization in uranium deposits and spent nuclear fuel may occur through dissolution of $UO_2$ (often forming hexavalent uranium intermediates) followed by reaction with silica rich fluids. [6, 7, 11–13]

**Acknowledgement**

Financial support by the Bundesministerium für Bildung und Forschung through BMBF grant 02NUK019C is gratefully acknowledged.

## Thorium selenites and selenates

### Introduction

Thorium, unlike most of the early actinides possessing various oxidation states, is practically solely stable in tetravalent state Th(IV). In aqueous solution, Th(IV) tends to hydrolyze and to construct a wide diversity of $Th(OH)_n^{4-n}$ hydroxide complexes, the olation or oxolation of which can further result in the formation of polynuclear compounds [14,15]. These polynuclear compounds, in conjunction with the aggregates and colloids of actinides, have already gathered extensive attention due to the role of transporting and migrating of radionuclides to the environment. $^{79}Se$ is one of the prominent long-lived fission products that forms within the nuclear fuel cycle. The detailed knowledge of crystallographic features of the actinide compounds is the essential precondition for establishing a structure-property relationship in order to model complex processes in the nuclear waste disposal sites. This is a scientific basis for a safe handling of nuclear waste. Going along this line, we started a systematical exploration on the reaction of Th(IV) salts with selenium oxide under the mild hydrothermal and low-temperature (180-220 ˚C) flux conditions, and such efforts resulted in the isolation of four new compounds with selenium in different valence states: ***α*-$Th(Se^{4+}O_3)_2$**, ***β*-$Th(Se^{4+}O_3)_2$**, **$Th(Se^{4+}{}_2O_5)_2$** and **$Th_3Se^{6+}{}_3O_{14}(OH)_2$**.

### Results

#### *α*-$Th(SeO_3)_2$ and *β*-$Th(SeO_3)_2$

The isolation of ***α*- and *β*-$Th(SeO_3)_2$** from hydrothermal conditions is very likely to be driven by stoichiometry. The reagent ratio of the starting materials controls the formation of these two compounds. ***α*-$Th(SeO_3)_2$** is more favored at a low Th: Se ratio and ***β*-$Th(SeO_3)_2$** can be present when increasing the amount of Se. A major difference between these two structures is the interior of the apparently empty voids between adjacent $ThO_8$ polyhedra chains, where the lone pairs of selenite groups ($SeO_3^{2-}$) are present. Fig. 20 shows the channels accommodated with the selenite polyhedra. For the ***α***-polymorph, the lone pairs of both Se(1) and Se(2) sites are oriented vertically to the chain direction. For the ***β***-polymorph, however, these lone pairs are directing parallel and vertical to the chain direction for Se(1) and Se(2), respectively.

#### $Th(Se_2O_5)_2$

Compared to ***α*- and *β*-$Th(SeO_3)_2$**, **$Th(Se_2O_5)_2$** obtained using the boric acid as the flux is characterized by a very high Th/Se ratio. This method has been proven to be an effective way to synthesize novel actinide borates in the past few years. The borate acid which does not include into the structure of **$Th(Se_2O_5)_2$** serves as the role of reaction medium, its presence, however, without a doubt plays an important role in the process of crystallization. The symmetry of **$Th(Se_2O_5)_2$** is orthorhombic with space group *Pbca*. Each $SeO_3^{2-}$ trigonal pyramid shares two corners with two Th polyhedra and the third one with another selenite polyhedron to yield a $Se_2O_5^{2-}$ dimer. The $ThO_8$ polyhedra are corner-linked to $Se_2O_5^{2-}$ dimers, thus completing the 3D framework.

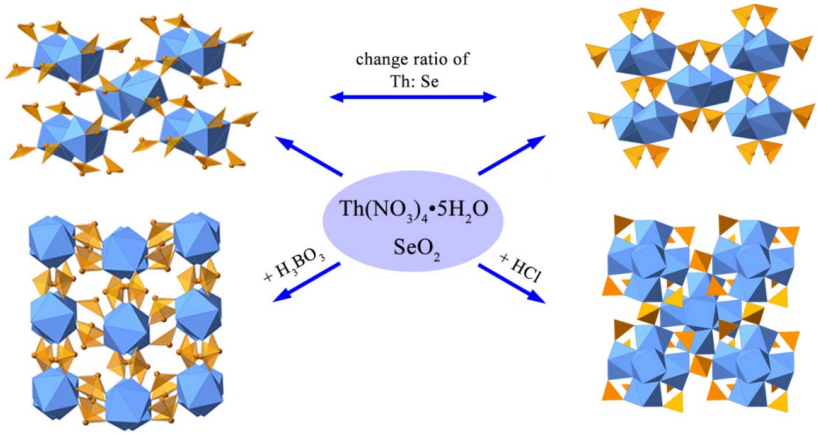


**Fig. 20: Study of phase formation in Th selenium system under solvothermal conditions was undertaken. Ratios change in the system resulted in *α*- and *β*-$Th(SeO_3)_2$ polymorphs formation. The compositions of reactions products can be changed via variation of reaction media or pH as it was shown for $Th(Se_2O_5)_2$ and $Th_3O_2(OH)_2(SeO_4)_3$, respectively. The structures of obtained phases were investigated using X-ray and spectroscopic methods.**

**$Th_3O_2(OH)_2(SeO_4)_3$**

Up to now, most of the thorium polynuclear complexes are synthesized *via* slow precipitation method with organic acids as reaction media. To the best of our knowledge, **$Th_3O_2(OH)_2(SeO_4)_3$** is the first inorganic hexanuclear thorium material prepared under hydrothermal conditions. The 3D framework structure adopts a tetragonal system with space group *I4/m*, consisting of $[Th_6(\mu_3\text{-}O)_4(\mu_3\text{-}OH)_4]^{12+}$ clusters put together by six Th(IV) atoms. Comparing already isolated hexanuclear thorium clusters, no incorporated water was found in the crystal structure of **$Th_3O_2(OH)_2(SeO_4)_3$**. The fact that similar plutonium clusters $[Pu_6(OH)_4O_4]^{12+}$ have been found recently underlines the possibility for using such structures to understand the hydrolysis trends in actinide chemistry [16].

**Conclusion**

The compounds discussed here, containing $SeO_4^{2-}$, $SeO_3^{2-}$ and $Se_2O_5^{2-}$ units, display an outstanding diversity regarding the coordination geometry of selenium cations. ***α*-** and ***β*-$Th(SeO_3)_2$** are based on similar structural skeletons but differ mainly with respect to the orientation of $SeO_3^{2-}$ trigonal pyramids. It is clear that due to a lack of oxygen connections between neighboring $ThO_8$ polyhedra in **$Th(Se_2O_5)_2$**, all $ThO_8$ polyhedra are thoroughly isolated from each other by neighboring $Se_2O_5^{2-}$ units. **$Th_3O_2(OH)_2(SeO_4)_3$** is by far the first inorganic compound containing hexanuclear thorium clusters. The Raman spectra show the typical vibrational modes for selenites and selenates in studied phases with local features respected their symmetry. These four new thorium selenium compounds, together with another previously published $Th(SeO_3)(SeO_4)$ compound become a cornerstone for studying other actinide complexation, such as $Np^{IV}$ and $Pu^{IV}$, in oxo-selenium systems. It is clear that the introduction of counter cations, such as alkali or alkaline earth metals, will generate more chemically and structurally complex phases in studied systems.

**Acknowledgement**
We are grateful to the Helmholtz Association for funding within the VH-NG-815 grant.

## References

[1] NAGRA TECHNICAL REPORT 02-05: Project Opalinus Clay. Demonstration of disposal feasibility for spent fuel, vitrified high-level waste and long-lived intermediate-level waste (Entsorgungsnachweis), NAGRA: Wettingen 2002.
[2] D.A.Kulik, et al. (2013) GEM-Selektor geochemical modeling package: revised algorithm and GEMS3K numerical kernel for coupled simulation codes. Comput. Geosci. 17, 1-24.
[3] K.Rozov et al. Synthesis, characterization and stability properties of Cl-bearing hydrotalcite-pyroaurite solids. Radiochimica Acta. 101(2), 101-110 (2013).
[4] H. Curtius et al. Preparation and characterization of Fe-, Co-, and Ni- containing MgAl-layered double hydroxides, Clays and Clay minerals, 61, 424-439 (2013).
[5] K.Rozov et al. Preparation, characterization and thermodynamic properties of Zr-containing Cl-bearing layered double hydroxides (LDHs). Radiochimica Acta. doi:10.1515/ract-2014-2326 (in press)
[6] Janeczek J. and Ewing R. C., Coffinization – a mechanism for the alteration of uranium dioxide under reducing conditions. Mater. Res. Soc. Symp. Proc. 257, 1991, 494.
[7] Janeczek J. and Ewing R. C., Dissolution and alteration of uraninite under reducing conditions. J. Nucl. Mater. 190 1992, 157-173.
[8] Labs S., et al. Synthesis of coffinite, $USiO_4$, and structural investigations of $U_xTh_{(1-x)}SiO_4$ solid solutions. Environ. Sci. Technol. 48(1) 2014, 854-860.
[9] Bauer J. D. et al. High-Pressure Phase Transition of coffinite, $USiO_4$, J. Phys. Chem. C 118(43) 2014, 25141–25149.
[10] Guo X. et al. Thermodynamics of Formation of Coffinite, $USiO_4$. PNAS 2015 in press.
[11] Deditius A. P. et al. The chemical stability of coffinite, $USiO_4 \cdot nH2O$; $0 < n < 2$, associated with organic matter: A case study from Grants uranium region, New Mexico, USA. Chem. Geol. 251(1-4) 2008, 33-49.
[12] Speer J. A., the actinide orthosilicates. Rev. Mineral. 5(1) 1980, 113-135.
[13] Förster H.-J. Composition and origin of intermediate solid solutions in the system thorite-xenotime-zircon-coffinite. Lithos 88(1-4) 2006, 35-55.
[14] Fanghänel, T.; Neck, V., Pure Appl. Chem. 2002, 74, 1895-1907.
[15] Neck, V.; Kim, J., Radiochim. Acta 2001, 89, 1-16.
[16] Knope, K. E.; Soderholm, L., Inorg. Chem. 2013, 52, 6770-6772

## 5.3. Radium uptake via formation of a $(Ba,Ra)SO_4$ solid solution

F. Brandt, M. Klinkenberg, V.L. Vinograd, U. Breuer[1], K. Rozov, J. Weber, D. Bosbach

[1]ZCH Central Division of Analytical Chemistry, Research Centre Jülich GmbH, Jülich, Germany,

Corresponding author: f.brandt@fz-juelich.de

**Introduction**

Demonstrating the long-term safety of a deep geological waste repository for spent nuclear fuel is one of the aspects which are in the focus of current discussions – time scales of several hundred thousands of years have to be considered. The safety for such time scales cannot be demonstrated by technical means only. There seems to be a consensus in the scientific community that long-term predictions regarding the geochemical evolution of a waste repository system should be guided by equilibrium thermodynamics and geochemical insights. A molecular-level process understanding is essential to improve the confidence in available data on radionuclide behavior in the geosphere beyond a simple phenomenological description.

The future geochemical evolution of a repository system cannot be predicted in the sense of a weather forecast. However, possible future developments can be assessed in the sense "what is expected to happen in the future" based on fundamental scientific principles and arguments. Ultimately, the safety of all conceivable scenarios needs to be demonstrated. In some scenarios for the disposal of spent fuel, radium dominates the radiological impact to the environment associated with the potential release of radionuclides from the repository in the future (Fig. 21).

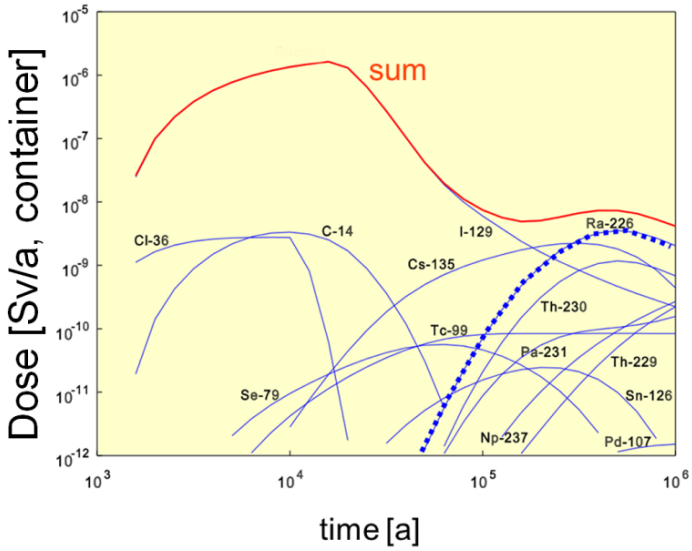


**Fig. 21: Evolution of dose vs. time in a deep geological waste repository in crystalline rock from a Swedish scenario (Norrby et al. 1997).**

The migration of radionuclides in the geosphere is to a large extent controlled by sorption processes onto minerals and colloids. On a molecular level, sorption phenomena involve surface complexation, ion exchange as well as formation of solid solutions. Solid solution formation leads to the structural incorporation of radionuclides in a host structure. Such solid solutions are ubiquitous in nature – on the atomic scale most minerals are mixtures of many chemically distinct components. In many cases the formation of solid solutions leads to a thermodynamically more stable phase compared to the formation of pure compounds. Deriving a thermodynamic model for a solid solution requires a molecular level concept including information such as the actual substitution mechanism, crystallographic site occupancies and related chemical ordering phenomena.

Within the long-term safety assessment, the maximum concentration of a radionuclide is in many cases assumed to be controlled by the solubility of a pure compound, e.g. radium sulfate. However, the solubility of radium controlled by $(Ba,Ra)SO_4$ solid solutions is currently not considered, although this could reduce the radium solubility by several orders of magnitude. One reason is related to the fact that so far only a limited number of rather simple solid solution systems have been studied to a sufficient level.

**Aims** - The aim of the project is to derive a solid solution model allowing for a description of a solid solution - aqueous solution equilibrium under conditions relevant for a nuclear waste repository. Since the classical work of Marie Curie, Henry Alfred Doerner & W.M.Hoskins [1], and Otto Hahn in the early decades of the previous century, the structural incorporation of radium into barium sulfate has not received much attention. It is well established that radium has a high affinity for barium sulfate. However, thermodynamic mixing data were either absent or inaccurate, leading to a high degree of uncertainty. Furthermore, it was unclear whether a radium-containing aqueous solution in contact with pure barium sulfate will completely re-equilibrate thus forming a homogeneous radium-containing barium sulfate (radiobarite) solid solution or only partial equilibration will occur.

The scientific questions described above were solved by an interdisciplinary approach. Modern atomistic simulation tools were combined with state-of-the-art macroscopic as well as microscopic experimental and analytical techniques. This combination was complemented with a comprehensive thermodynamic modeling of the solid solution – aqueous solution system. Long-term experiments - covering time scales beyond three years so far - were carried out to unravel the barite – radiobarite transformation. With respect to thermodynamic modelling, data for the relevant aqueous species as well as the solubility products of the end-members $RaSO_4$ and $BaSO_4$ were already available. However, it was not known whether the mixing between $BaSO_4$ and $RaSO_4$ is ideal or if a significant excess enthalpy exists. Also it was not clear whether radium and barium are randomly distributed within the mixed solid or locally ordered. Consequently, the key thermodynamic mixing data were missing.

**Experimental & analytical studies on radiobarite** - In general, Ra-uptake experiments can be carried out as co-precipitation experiments or as recrystallization experiments. Co-precipitation experiments, which were performed in the majority of previous studies [1,2,3,4] of the $(Ba,Ra)SO_4$ system, have a general disadvantage: The thermodynamic information cannot be accurately obtained due to kinetic effects. The alternative setup adopted here was based on the recrystallization approach [5,6] and permits to directly address the following two questions, which are highly relevant to the safe disposal of spent fuel: Will radium be taken up into barite at close to equilibrium conditions and will this uptake follow laws of thermodynamic equilibrium?

Based on thermodynamic modeling, an experimental window was carefully selected (solid/liquid ratio, grain size and specific surface area etc.) in order to follow the uptake of Ra into pure barite during recrystallization. For the first time, both the composition of the solid and the element concentrations in the aqueous solution were analyzed. Sufficiently high radium concentrations within the experiments enabled the direct microanalyses and detection of the spatial distribution of radium within the solid phase. Based on thermodynamic modeling, the initial concentration of radium was chosen below the solubility limit of pure $RaSO_4$, so that a decrease in its concentration is expected to be only due to adsorption or formation of a $(Ba,Ra)SO_4$ solid solution. Long-term experiments of up to 1000 days were carried out using two commercially available barites (Sachtleben (SL) and Aldrich (AL)) to follow the evolution of the system until a steady state could be observed.

Within the experiments a decrease of the aqueous radium concentration by up to three orders of magnitude was observed indicating a very efficient mechanism of radium uptake. A reproducible final concentration plateau was reached after about 600 to 800 days, suggesting the approach of the thermodynamic equilibrium between the solid and the aqueous phase (Fig. 22).

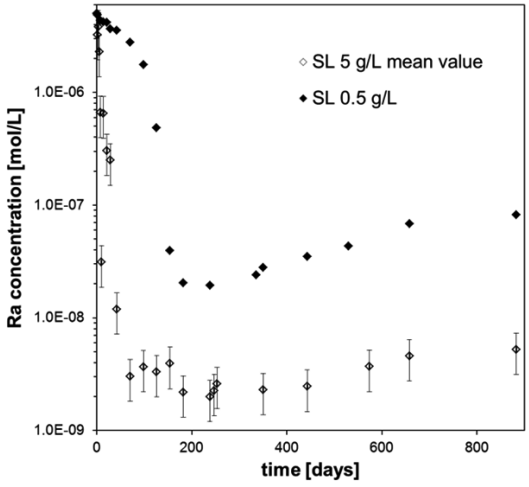


**Fig. 22: Temporal evolution of the aqueous radium concentration within experiments with SL barite at solid/liquid ratios of 5 g/L and 0.5 g/L.**

A combined microscopic and micro analytical approach was applied to monitor the changes in the barite during the uptake experiment using direct microanalysis (Time-of-Flight – Secondary Ion Mass Spectrometry, ToF-SIMS) and detailed electron microscopy (SEM) observations. The SEM observations indicate only minor changes in grain size and shape which is typical for replacement reactions. However, small changes in the grain size distribution (Ostwald ripening) and the accretion of grains (Fig. 23) could be clearly attributed to the presence of radium and could be distinguished from parallel radium-free experiments.

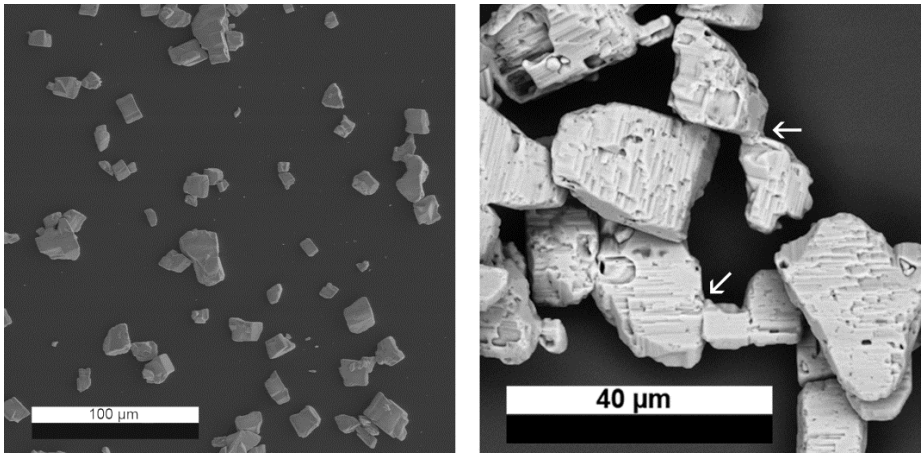


**Fig. 23: SL barite at the beginning of the re-crystallization experiment (left) and at the end (right). Grains are grown together (marked with arrows).**

Complementary to the decrease of the Ra concentration in solution an uptake not only on the surface but in the entire recrystallized solid was observed with ToF-SIMS. On the scale of ToF-SIMS resolution (µm) radium is distributed mostly homogeneously within the recrystallized solid (Fig. 24). For the first time, direct evidence is available that the radium uptake into barite leads to the formation of a homogenous solid solution due to recrystallization. Thus, the micro analytical information provides the basis and justification for applying the thermodynamic modeling.

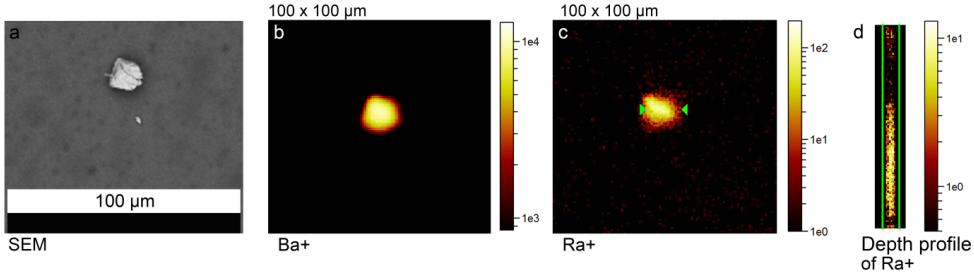


**Fig. 24: a) SEM image of barite particle before ToF-SIMS analysis, b) integrated intensity of the barium signal, c) integrated intensity of the radium signal, d) depth profile of the integrated Ra signal.**

**Atomistic simulation** – In order to be able to apply a thermodynamic model for the system $BaSO_4$ - $RaSO_4$, knowledge gaps about the ideality or non-ideality of this system had to be filled. Instead of a traditional series of co-precipitation experiments covering the complete range of compositions between the end-members, state-of-the-art atomistic simulations were used to independently compute the Guggenheim interaction parameter $a_0$, which determines the equilibrium composition of the radiobarite solid solution. The method of calculation of $a_0$ is based on the recent progress in first principles simulations of periodic systems. Using the software package CASTEP, which is based on Density Functional Theory, we could compute the excess enthalpy of a 2 x 2 x 2 supercell of $BaSO_4$ due to insertion of a single substitutional defect of Ra. When the size of the supercell is large, the excess enthalpy is equal to $a_0$/RT, with R = universal gas constant and T = temperature in Kelvin. The challenge of the study was to compute the enthalpy change in the reaction $Ba_{31}Ra(SO_4)_{32}$ = 31 $BaSO_4$ + $RaSO_4$ with a precision of better than ~0.01 eV. A variety of means was used to decrease the computational noise and to consider every possible source of uncertainty. The error due to the limited size of the supercell and due to the associated unwanted interaction of a radium defect with its periodic images was estimated by computing the excess energies of Ra-Ra defect pairs in a 2 x 2 x 2 supercell and by investigating their conversion with the distance between the defects (Fig. 25). The sensitivity of the computed excess energy (and of the interaction parameter) to the difference in the radii of the exchangeable cations was additionally investigated for $BaSO_4$ - $SrSO_4$ and $SrSO_4$ - $RaSO_4$ systems and for a range of analogous binary systems of orthorhombic carbonates.

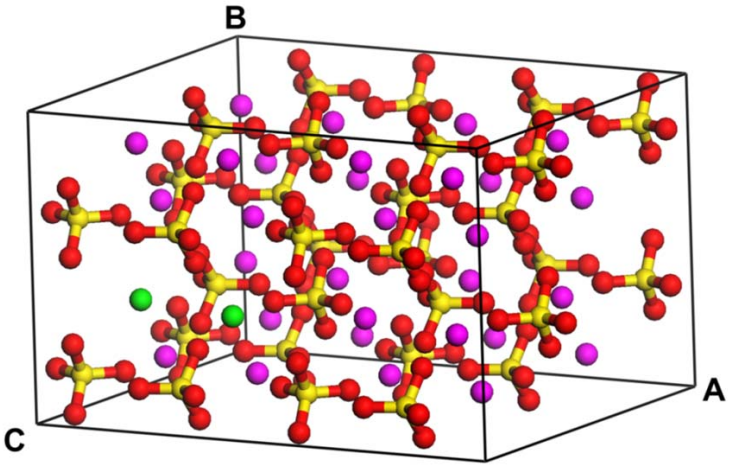


**Fig. 25: 2 x 2 x 2 supercell of barite; red = O, yellow = S, magenta = Ba, green = Ra-defect.**

A solid solution can be characterized with a single interaction parameter only when the mixing is not affected by chemical ordering. In the $BaSO_4$ - $RaSO_4$ system the tendency to ordering is determined by the enthalpies of the exchange reactions BaBa + RaRa = 2 BaRa at all cation-cation distances. The enthalpies of these reactions were computed from first principles and their combined effect was investigated with the aid of a Monte Carlo method. Our simulations have shown that in the temperature range of 300 ± 100 K the ordering tendency is insignificant.

**Thermodynamic modelling** – The interaction parameter and known thermodynamic properties of the endmembers were combined to provide a complete thermodynamic model for the $(Ba,Ra)SO_4$ solid solution. The behavior of this system in aqueous media has been modeled successfully by applying the Gibbs free energy minimization approach as implemented in the GEMS-PSI code [7]. The combination with these two methods and the thermodynamic approach allowed a verification of the degree of non-ideality expressed by the newly derived interaction parameter for a regular solid solution in the $(Ba,Ra)SO_4$ system by comparison of model results with experimental results (Fig. 26). Ultimately, thermodynamic modelling provides the bridge between fundamental laboratory scale results and the final application, the safety assessment of a deep geological repository for nuclear waste.

Thus, based on the achieved agreement between the experimental and the atomistic simulations and the thermodynamic modeling we could conclude that the $(Ba,Ra)SO_4$ solid solution system behaves as a regular mixture and can be accurately described with the single Guggenheim parameter $a_{0,BaRa}$ of 1.00 ± 0.40.

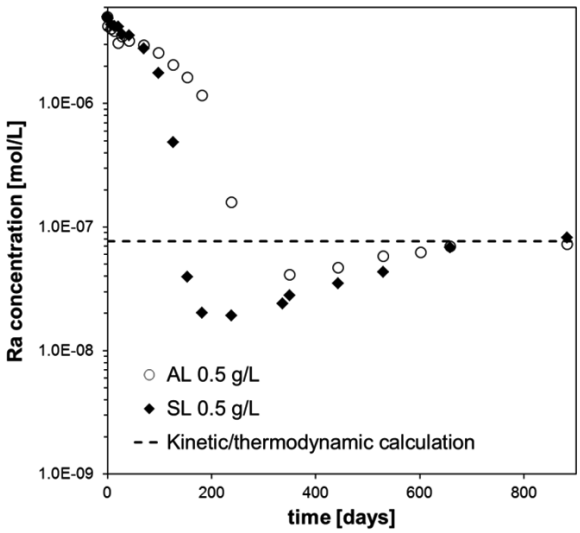


**Fig. 26: Comparison of the radium concentration at the end of AL and SL 0.5 g/L experiments and the equilibrium from thermodynamic calculations using $a_0 = 1$ and log $K_s^0(RaSO_4) = -10.41$.**

## Conclusion and Applications

In summary, it could be shown that a radium-containing aqueous solution equilibrates with solid barium sulfate - controlled by thermodynamics. The transformation occurs in a relatively short time of a few years compared to the time scales considered in safety assessments for nuclear waste disposal. The second important outcome is a fundamental understanding of the thermodynamics of mixing in the $(Ba,Ra)SO_4$ solid solution system. This refined thermodynamic model will set the basis for future long-term safety assessments for nuclear waste disposal regarding radium solubility under the conditions foreseen for deep geological nuclear waste repositories.

In conclusion, the reduction of uncertainties of solid solution – aqueous solution systems helps to improve the confidence in the long-term safety of deep geological disposal and the associated safety margins. It will encourage waste management agencies, licensing authorities and ultimately the critical public to include radionuclide solubility controlled by a solid solution – aqueous solution equilibrium even in systems that are more complex than radium – barium – sulfate – water system.

**Acknowledgements**

The work has been partially funded by the European FP 7 project SKIN ("Slow processes in close-to-equilibrium conditions for radionuclides in water/solid systems of relevance to nuclear waste management") as well as by the national BMBF funded cooperative project ImmoRad ("Basic investigations on the immobilization of long-lived radionuclides by interaction with secondary mineral phases") and by the Deutsche Forschungsgemeinschaft ("Thermodynamics of mixing from defect calculations: Applications to geochemically and petrologically important solid solutions").

**References**

[1] Doerner, H. A. and Hoskins, W. M. (1925) Co-precipitation of radium and barium sulfates Journal of the American Chemical Society, 47, 662-675.

[2] Rosenberg Y. O., Metz V. and Ganor J. (2011a) Co-precipitation of radium in high ionic strength systems: 1. Thermodynamic properties of the Na-Ra-Cl-$SO_4$-$H_2O$ system - Estimating Pitzer parameters for $RaCl_2$. Geochim. Cosmochim. Acta 75, 5389–5402.

[3] Rosenberg Y. O., Metz V., Oren Y., Volkman Y. and Ganor J. (2011b) Co-precipitation of radium in high ionic strength systems: 2. Kinetic and ionic strength effects. Geochim. Cosmochim. Acta 75, 5403–5422.

[4] Rosenberg Y. O., Sadeh Y., Metz V., Pina C. M. and Ganor J. (2014) Nucleation and growth kinetics of $Ra_xBa_{1-x}SO_4$ solid solution in NaCl aqueous solutions. Geochim. Cosmochim. Acta 125, 290–307.

[5] Bosbach, D.; Böttle, M. & Metz, V. (2010) Experimental study on $Ra^{2+}$ uptake by barite ($BaSO_4$), SKB Technical Report TR-10-43 Waste Management, Svensk Kärnbränslehantering AB.

[6] Curti, E.; Fujiwara, K.; Iijima, K.; Tits, J.; Cuesta, C.; Kitamura, A.; Glaus, M. & Müller, W. (2010) Radium uptake during barite recrystallization at 23±2°C as a function of solution composition: An experimental $^{133}Ba$ and $^{226}Ra$ tracer study Geochimica et Cosmochimica Acta, 74, 3553-3570.

[7] Kulik, D.; Wagner, T.; Dmytrieva, S.; Kosakowski, G.; Hingerl, F.; Chudnenko, K. & Berner, U. (2013) GEM-Selektor geochemical modeling package: Numerical kernel GEMS3K for coupled simulation codes. Computational Geosciences, 17, 1-24.

## 5.4. Complex Structure of An and Ln Complexes with Modified Diglycolamides in Solution and Solid State using Different Speciation Techniques

A. Wilden[1], G. Modolo[1], S. Lange[1], F. Sadowski[1], D. Kardhashi[1], Y. Li[1], P. Kowalski[1], B. Beele[2,3], A. Skerencak-Frech[2], P. Panak[2,3], A. Geist[2], J. Rothe[2], K. Dardenne[2], S. Schäfer[4], A. T. Wagner[4], P. W. Roesky[4], W. Verboom[5]

[1]Forschungszentrum Jülich GmbH, Institut für Energie- und Klimaforschung, Nukleare Entsorgung und Reaktorsicherheit (IEK-6), 52428 Jülich, Germany

[2]Karlsruher Institut für Technologie, Institut für Nukleare Entsorgung (INE), 76021 Karlsruhe, Germany

[3]Ruprecht-Karls-Universität Heidelberg, Physikalisch Chemisches Institut (PCI), 69120 Heidelberg, Germany

[4]Karlsruher Institut für Technologie, Institut für Anorganische Chemie, 76131 Karlsruhe, Germany

[5]University of Twente, MESA+ Institute for Nanotechnology, P.O. Box 217, 7500 AE Enschede, The Netherlands

Corresponding author: a.wilden@fz-juelich.de

**Introduction**

The diglycolamide class of extracting ligands is one of the most important ligand classes currently investigated in the treatment of used nuclear fuel solutions for minor actinide separation, especially for the extraction of trivalent actinides An(III) together with the trivalent lanthanides Ln(III). TODGA (*N,N,N',N'*-tetraoctyl-diglycolamide) resembles the most prominent ligand, although a large number of modifications, mainly on the amide side groups, have been studied.[1]

Recently, modified diglycolamides were synthesized and tested for An(III)/Ln(III) extraction with a focus on modifying the ligand backbone.[2] Fig. 27 shows the chemical structures of TODGA and the substituted analogues Me-TODGA and $Me_2$-TODGA, which have been tested in solvent extraction studies (R = octyl). It was found that the extraction efficiency of the investigated metal ions were reduced drastically with introduction of additional methyl groups into the ligand backbone structure.[2] It was found that the distribution ratios followed the order TODGA > Me-TODGA > $Me_2$-TODGA for all studied An(III) and Ln(III) cations.

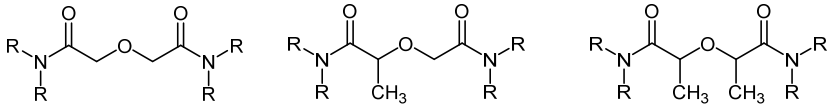

**R=$C_8H_{17}$: TODGA**
**R=$C_2H_5$: TEDGA**
**R=$CH_3$: TMDGA**

**R=$C_8H_{17}$: Me-TODGA**
**R=$C_2H_5$: Me-TEDGA**
**R=$CH_3$: Me-TMDGA**

**R=$C_8H_{17}$: $Me_2$-TODGA**
**R=$C_2H_5$: $Me_2$-TEDGA**
**R=$CH_3$: $Me_2$-TMDGA**

**Fig. 27: Chemical structures of the ligands used in this study.**

Conditional stability constants were measured by Time-Resolved Laser Fluorescence Spectroscopy (TRLFS) and showed the same trend. Solvent extraction slope analysis suggested the formation of 1:3 (metal:ligand) complexes in an aliphatic diluent, which was

supported by TRLFS investigations. In monophasic TRLFS experiments using an alcoholic diluent the formation of 1:1 complexes was observed additionally.[3]

No information of EXAFS investigations in solution with aliphatic diluents using TODGA for complexation of trivalent metal ions has been found. Yaita et al. reported on EXAFS measurements of a *N*,*N'*-dimethyl-*N*,*N'*-diphenyldiglycolamide complex with Er(III) and Cm(III), however in ethanol solution, where different coordination modes of the two investigated metal ions were described.[4] Antonio et al. recently reported on EXAFS measurements of a solid TODGA complex with Eu: $[Eu(TODGA)_3][BiCl_4]_3$.[5] In this study the formation of 1:3 complexes was described. Nine oxygen atoms at an average distance of 2.40(1) Å, six carbon atoms at 3.34(3) Å, and another six carbon atoms at 3.55(2) Å gave the best fit to the experimental data.

More information was available on single crystal structure analysis with short-chain diglycolamide ligands, as the lipophilic long-chain ligands did not yield crystalline solids. The short-chain analogues are soluble in water and alcohols. Thus, crystallization experiments were frequently conducted in water/alcohol mixtures.

Kannan et al. studied La(III) and U(VI) complexes of (*i*-$Pr_4$)DGA and (*i*-$Bu_4$)DGA. La(III) formed 1:3 complexes with the ligands in a tridentate complexation mode resulting in a nine-coordinated La center, while U(VI) only formed a 1:1 complex $[UO_2(NO_3)_2L]$ with the ligand in the equatorial plane together with two bidentate nitrate ions.[6] Tian et al. studied Np(V) complexes with TMDGA (Fig. 27). Here, they found the neptunyl-ion $NpO_2$ coordinated by two tridentate ligands arranged in the equatorial plane. However, they didn't crystallize in the presence of nitrate ions, but used a perchlorate salt.[7] Reilly et al. described the Pu(IV) complexation with TMDGA, finding 1:3 complexes with three tridentate ligands in the first coordination shell and non-coordinating nitrate ions for charge compensation in the outer shell.[8] An extensive systematic investigation of crystal structures of Ln(III) (Ln = La, Ce, Pr, Nd, Sm, Eu, and Gd) with TEDGA (Fig. 27) was recently published by Kawasaki et al.[9] They reported 1:3 complexes of all metal ions co-crystalized with $[Ln(NO_3)_6)]^{3-}$ anions and found the same nine-fold coordination for all lanthanides. The Ln-$O_{ether}$ and Ln-$O_{carbonyl}$ bond lengths decreased with increasing atomic number.

In this paper the combination of different speciation techniques in solid and liquid phase together with DFT-based ab-initio calculations for the analysis of metal-diglycolamide complexes is presented.

**Experimental**

The organic ligands TODGA, Me-TODGA, $Me_2$-TODGA, TEDGA, Me-TEDGA, and $Me_2$-TEDGA (Fig. 27) were purchased from Technocomm Ltd., United Kingdom. Single crystals were grown by diffusion of diethyl ether into a methanolic solution of metal nitrate containing solution and a 2-3 fold excess of the shorter chain ligand. Alternatively, single crystals were obtained by slow solvent evaporation of a solution of metal nitrate and the ligand in a water/alcohol mixture. Samples for EXAFS measurements were prepared by solvent extraction of the desired metal ion from nitric acid solution with solutions of the desired ligand in kerosene. Afterwards, the phases were separated and the organic phases were directly measured at the INE-beamline of the ANKA synchrotron in Karlsruhe, Germany.[10] EXAFS data reduction and analysis was performed using the Athena and Artemis software together with FEFF6 included in the Demeter software package.[11]

**Results and Discussion**

Based on the previously published results[3] further studies of the complexation of trivalent metal ions with diglycolamides were conducted.

Single crystals suitable for X-ray single crystal structure analysis were obtained by the ether diffusion method or the solvent evaporation method. Suitable crystals were obtained for $[Ln(TEDGA)_3]$ (Ln = La, Sm, Eu, Yb) and $[Ln(TMDGA)_3]$ (Ln = La, Sm, Eu). All investigated complexes showed the same structure of the central metal ion coordinated by three tridentate ligand molecules, resulting in a nine-fold coordination of the ligand oxygen atoms. The complexes are isostructural with the previously published complexes of trivalent Ln and Pu(IV).[6, 8-9] Fig. 28 shows the ORTEP view of a $[Eu(TEDGA)_3]$ complex as a representative.

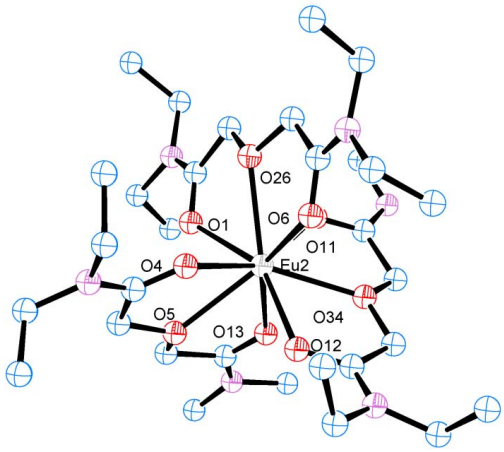


**Fig. 28: ORTEP view of the $[Eu(TEDGA)_3]$ complex structure with 50% thermal ellipsoid probability level. H atoms, $NO_3^-$ counter anions and water molecules are omitted for clarity. Grey = Eu, Red = O, Blue = C, Purple = N.**

In contrast to previous investigations, EXAFS measurements were conducted under realistic conditions for solvent extraction experiments, as the samples were prepared by actually extracting the desired metal ions from aqueous nitric acid solution into a kerosene phase containing the ligand. Therefore, the formation of identical complexes as in solvent extraction is achieved and can be compared to complexes formed in other diluents or even different aggregate states.

Exemplary, Eu measurements using the TODGA ligand are presented here. The primary $k^3\chi(k)$ Eu EXAFS data and Fourier transform of the $k^3\chi(k)$ Eu EXAFS data and fit are shown in Fig. 29 (left).

The structure model used for the fitting was derived from the measured crystal structure data of the $[Eu(TEDGA)_3]$ complex (Fig. 28). The best fit was achieved by applying the same structural motif as observed in the solid state. Six oxygen atoms in a first coordination shell (carbonyl O) and three additional oxygen atoms (ether O) in a second coordination shell were fitted to 2.40(4) and 2.50(3) Å, respectively. These distances are only slightly larger than those observed in the crystal structure (2.38(1) and 2.49(3) Å). Both oxygen sites are reflected by the large peak at 1.93 Å in the Fourier transform of the $k^3\chi(k)$ Eu EXAFS data (Fig. 29 (right), not phase corrected). The next two distinct peaks in Fig. 29 (right) at 2.65 and

3.10 Å correspond to the bridging carbon atoms in the ligand backbone. The fitted distances in EXAFS are 3.26(3) and 3.47(5) Å, which correspond well to the measured distances of 3.27(3) and 3.44(4) Å in the crystal structure. A scattering path for six nitrogen atoms was also included into the fit, which improved the fit slightly at larger distances. The fitted distance for the nitrogen atoms was 4.7(2) Å, which is slightly larger than the measured distance of 4.52(3) Å in the crystal structure. However, the contribution of nitrogen scattering to the EXAFS signal was very low and the uncertainty of the fitted distance is relatively large.

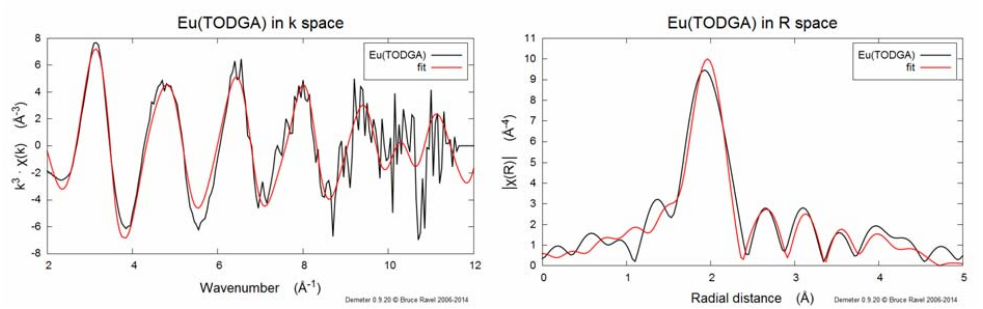


**Fig. 29: Left: Primary $k^3\chi(k)$ Eu EXAFS data and fit. Right: Fourier transform of the $k^3\chi(k)$ Eu EXAFS data and fit.**

TMDGA and the related methylated derivatives (complexes with La(III), Eu(III), and Am(III)) were calculated using density functional theory (DFT). The calculations were performed with plane wave Quantum-ESPRESSO code.[12] The optimized geometries of the $ML_3$ complexes are shown in Fig. 30 and the calculated formation energies of the complexes are shown in Tab. 1. The formation energies were computed as energy differences between the $ML_3$ complexes and isolated metal cations and ligands. The trend in formation energies is consistent with the reported extraction efficiencies.[3] The modified TMDGA complexes have lower formation energies, which are reflected by the lower extraction efficiencies. Additionally, for a given ligand the intensities of affinity to different metal ions are also reflected consistently both in calculation and experiment.

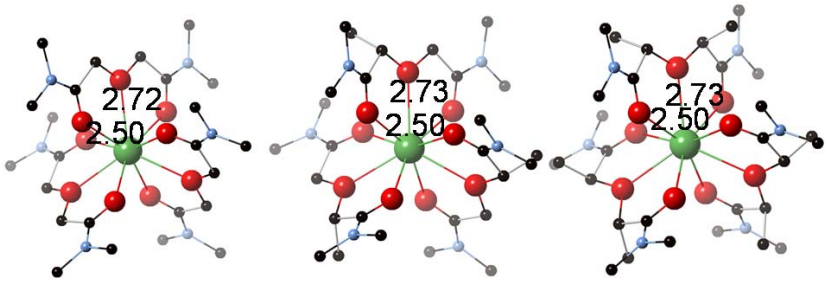


**Fig. 30: Optimized geometries of the $ML_3$ complexes. Bond lengths for M=La are given in Å.**

**Tab. 1 Calculated formation energies (kJ/mol) of the complexes bearing different elements and ligands.**

| | $La^{3+}$ | $Eu^{3+}$ | $Am^{3+}$ | |
|---|---|---|---|---|
| | | | PBE | PBE+U |
| TMDGA | -2750.6 | -2970.5 | -2888.8 | -2808.8 |
| Me-TMDGA | -2704.9 | -2923.9 | -2842.5 | -2762.4 |
| $Me_2$-TMDGA | -2700.7 | -2918.4 | -2837.3 | -2757.1 |

## Conclusions

The structure of metal ion complexes with TODGA and methylated derivatives was studied using different speciation techniques. Solvent extraction slope analysis, TRLFS, solid state single crystal structure analysis, and EXAFS measurements in organic liquid phase showed the formation of 1:3 complexes with all investigated metal ions. Bond lengths and angles were determined and conditional stability constants were measured and compared for the different ligands and metal ions. It was found that the complex stability decreased in the order TODGA>Me-TODGA>$Me_2$-TODGA. The central metal ions were nine-fold coordinated by oxygen with two different metal-oxygen bond lengths, corresponding to the different oxygen moieties in the ligands. In EXAFS investigations, two different carbon scattering sites were found corresponding to the two carbon atoms of the ligand backbone structure. The same complex structure was found in solid state using shorter chain analogues of the investigated ligands by single crystal X-Ray diffraction analysis.

## Acknowledgements

Financial support for this research was provided by the European Commission (project SACSESS—Contract No. FP7-FISSION-2012-323282) and the German Federal Ministry of Education and Research (Contract No. 02NUK020A, 02NUK020B, 02NUK020D, and 02NUK020E).

## References

[1] Ansari, S.A. et al. (2012): Chem. Rev. Vol. 112 (3), 1751-1772.
[2] Iqbal, M. et al. (2010): Supramol. Chem. Vol. 22 (11), 827-837.
[3] Wilden, A. et al. (2014): Solvent Extr. Ion Exch. Vol. 32 (2), 119-137.
[4] Yaita, T. et al. (1999): Proceedings of Evaluation of Speciation Technology, Workshop Proceedings 1999, Tokai-mura, Ibaraki, Japan, 26-28 October 1999, pp 273-280.
[5] Antonio, M.R. et al. (2015): Dalton Trans. Vol. 44 (2), 515-521.
[6] Kannan, S. et al. (2008): Inorg. Chem. Vol. 47 (11), 4691-4695.
[7] Tian, G. et al. (2005): Angew. Chem. Int. Ed. Vol. 44 (38), 6200-6203.
[8] Reilly, S.D. et al. (2012): Chem. Comm. Vol. 48 (78), 9732-9734.
[9] Kawasaki, T. et al. (2014): Bull. Chem. Soc. Japan Vol. 87 (2), 294-300.
[10] Rothe, J. et al. (2012): Rev. Sci. Instrum. Vol. 83 (4), 043105.
[11] Ravel, B. et al. (2005): J. Synchrotron Rad. Vol. 12 (4), 537-541.
[12] Giannozzi, P. et al. (2009): J. Phys.-Condes. Matter Vol. 21 (39), 19.

## 5.5. Development of innovative Minor Actinide partitioning and co-conversion processes

G. Modolo, P. Kaufholz, H. Schmidt, F. Sadowski, C. Schreinemachers, S. Lange, A. Wilden
Corresponding author: g.modolo@fz-juelich.de

**Introduction**

The final disposal of high active waste (spent fuel, vitrified high active waste) in a deep underground repository is a complex issue mainly related to the fact that these wastes contain long-lived radionuclides with high radiotoxicity which remains the case for a very long period of time, i.e. thousand to million years.

A possible solution to this problem is to separate these long-lived radionuclides (i.e. plutonium and the minor actinides) and to convert them into shorter lived or stable nuclides by nuclear reactions. This is the so-called Partitioning & Transmutation strategy (P&T) under study in several countries.[1-3] The benefits of "advanced fuel cycle" schemes including P&T in terms of waste management can be summarised as follows:[3]

- reducing the capacity needs for geological repositories by reducing volume and heat generation of waste to be disposed of;
- reducing the repository long term-risk by reducing long-term radiotoxic inventories;
- reducing uncertainties in repository performance, especially for disruptive scenarios (e.g. human intrusion);
- possibly improving public acceptance of geological disposal.

Up to now, hydrometallurgical (i.e. solvent extraction) processes have been the reference technology for nuclear fuel processing at commercial scale for more than 60 years and the reasons for this are numerous. Solvent extraction processes are able to provide extremely high separation yields, considering both recovery and purification yield, without generating excessive amounts of secondary waste, which is very important in the nuclear industry.

Plutonium, the main contributor to radiotoxicity, can already be recovered today by the PUREX process, which with some modifications can also recover neptunium (advanced PUREX), whilst the fission products and minor actinides (MA) Np, Am, and Cm are vitrified in nuclear glass.

The separation of trivalent actinides from the HAR (i.e. the aqueous raffinate or concentrate from the PUREX process) is challenging due to the presence of nitric acid, fission products (one third of them being lanthanides) and corrosion/activation products which can interfere with actinide extraction. Significant scientific and technical progress has been made in European collaborative research over the last two decades, i.e. in the NEWPART, PARTNEW, EUROPART programmes. It has resulted in the development of multi-cycle processes [e.g. DIAMEX (DIAMide EXtraction) + SANEX (Selective ActiNide EXtraction)] and recently within the FP7 project ACSEPT[4] the development of innovative processes with reduced number of cycles (innovative-SANEX, 1-cycle SANEX) has also been envisaged. In the new FP-7 project SACSESS (Safety of Actinide Separation Processes, Start March 2013) an alternative process to those already developed was studied, allowing the partitioning of americium alone, reducing the hazards related to the handling of curium in fuel for enhanced safety.

The Jülich laboratory (IEK-6) as partner within previous and current European contracts (NEWPART, PARTNEW, EUROPART, ACSEPT, SACSESS), belongs to one of the leading

laboratories in the process development of innovative hydrometallurgical partitioning processes. The research covers also the design, synthesis and assessment of new organic extracting molecules and new diluents. A fundamental understanding of the principles of complexation, including thermodynamics and kinetics, is crucial. Hence, the present paper summarizes the recent achievements within the development of new partitioning processes and on fundamental solvent extraction studies. The conversion of separated Minor Actinides (e.g. Americium) from solution to suitable pre-cursors for fuel fabrication forms an essential link between partitioning and transmutation. One of the objectives of work carried out within the European ASGARD project is to study the sol-gel processes for actinide co-conversion. Here we present the latest achievements on internal gelation studies.

**Innovative-SANEX process demonstration**

Within the European collaborative project ACSEPT the development of innovative processes with reduced number of cycles was envisaged. Therefore, the so-called innovative-SANEX process was developed. In the innovative-SANEX process the selective separation of An(III) from a simulated PUREX raffinate was achieved using a tailored strategy of extraction and back-extraction of trivalent metal ions. First, trivalent actinides and lanthanides were extracted together using the diglycolamide extractant TODGA (*N,N,N',N'*-tetraoctyldiglycolamide, Fig. 31), thus separating those elements from other fission and corrosion products. Zirconium and palladium were masked using the masking agent CDTA (trans-1,2-diaminocyclohexane-*N,N,N',N'*-tetraacetic acid, Fig. 31), developed for this purpose at IEK-6.[5] Then, An(III) were selectively back-extracted from the loaded organic phase using the hydrophilic complexing agent $SO_3$-Ph-BTP ((2,6-bis-(5,6-di(sulfophenyl)-1,2,4-triazin-3-yl)-pyridine, Fig. 31 ).[6]

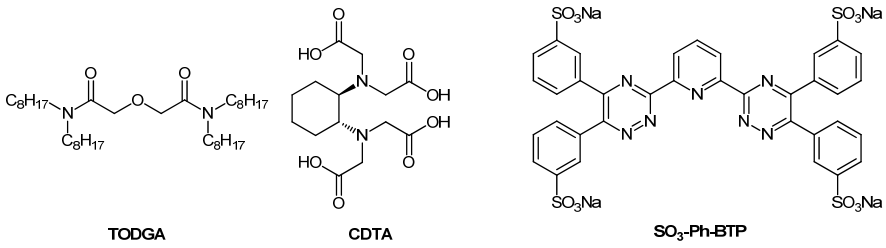


**Fig. 31: Chemical structures of TODGA, CDTA and $SO_3$-Ph-BTP.**

A flow-sheet was developed based on batch equilibrium experiments as well as single centrifugal contactor kinetics experiments.[7-9] The flow-sheet shown in Fig. 32 comprised several extraction, scrubbing and stripping sections with different compositions of aqueous and organic phases shown in the figure. A counter-current centrifugal contactor demonstration test using simulated PUREX raffinate was run in the centrifugal contactor battery installed at IEK-6 using the flow rates also shown in Fig. 32.[10-11] The results (Fig. 32) demonstrate that the innovative-SANEX process showed an excellent performance. An(III) were recovered with ≥99.7% and an excellent separation from Ln(III) due to the high selectivity of $SO_3$-Ph-BTP, which is an improvement over the formerly used buffered polyaminocarboxylic acid solutions.[10]

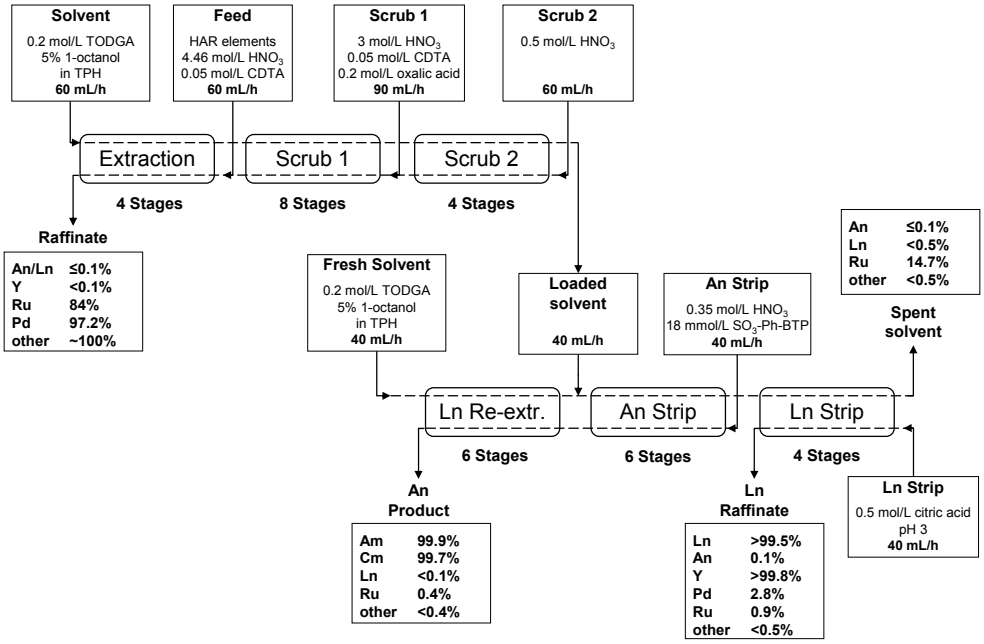


**Fig. 32: Flow-sheet and results of the innovative SANEX demonstration process.**

### Selective Separation of Americium from Highly Active Raffinates

Current partitioning processes strive for a selective separation of americium from curium and the fission products together within a single process.[12-13] In cooperation with international partners the IEK-6 investigates liquid-liquid separation processes for the selective separation of Am(III) from highly radioactive PUREX raffinates in the frame of the European commission (FP 7-fission) SACSESS project.

Based on the i-SANEX process, a selective back extraction of only Am would lead to an Am selective process. Therefore, novel Am(III) selective back extraction complexants are necessary. The hydrophilic TS-BTPhen developed at University of Reading (UK) is a promising candidate for selective Am(III) separation in combination with TODGA. The basic concept is shown in Fig. 33.[14-16]

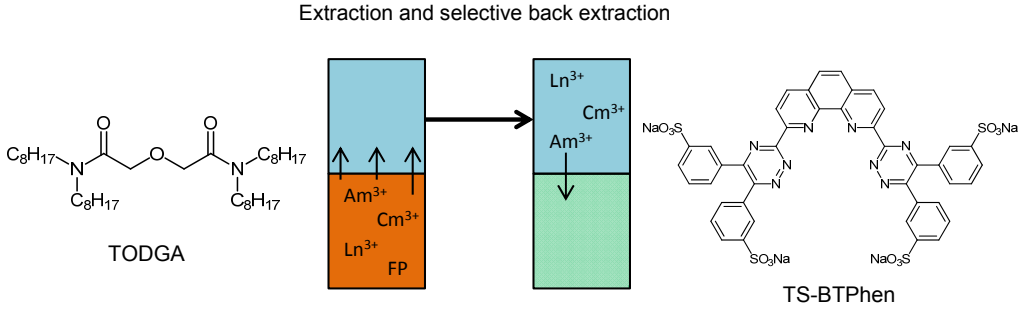


**Fig. 33: Schematic concept of the Am selective separation process investigated at IEK-6.**

To analyse the performance of the novel complexant TS-BTPhen, it was tested for its selectivity related to minor actinides and Eu as representative lanthanide from a TODGA containing organic phase in radiotracer tests. Fig. 34 shows the distribution ratios of Am(III), Cm(III) and Eu(III) for a TODGA based organic phase as a function of the nitric acid concentration. The distribution ratios D were calculated as the quotient of the concentration/activity of the metal ion in the organic phase over the concentration/activity of the metal ion in the aqueous phase ($D=c_{M(org)}/c_{M(aq)}$).
The separation between two metal ions is expressed using the separation factor, being the quotient of the distribution ratios of two metal ions ($SF=D_{M1}/D_{M2}$). Open symbols depict the distribution ratios for TODGA alone as a function of the nitric acid concentration; the filled symbols depict the distribution ratios for TODGA with addition of 10 mmol/L TS-BTPhen as a function of the nitric acid concentration.
The figure shows that the distribution ratios for Am, Cm and Eu were significantly reduced, but stronger for the An(III), leading to an increased selectivity between An(III) and Eu(III). Furthermore, the separation between Am(III) and Cm(III) was increased from 1.6 for TODGA alone to 3.6 applying TS-BTPhen while Eu(III) stays preferentially in the organic phase. Under these conditions an Am(III) selective separation process seems to be possible in a multi-stage counter current separation process.

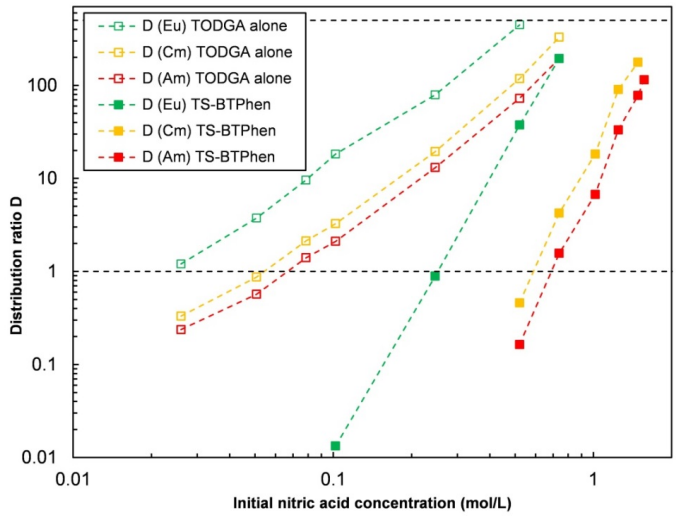


**Fig. 34: The effect of TS-BTPhen on the distribution ratios of Am(III), Cm(III) and Eu(III). Organic phase: 0.2 mol/L TODGA in TPH + 5 vol.-% 1-octanol Aqueous phase: diff. $c_{(HNO_3)}$ with and without addition of 10 mmol/L TS-BTPhen.**

**Radiolysis studies**

For the development of selective extraction processes on an industrial scale, one main issue to consider is the detailed knowledge of radiolytic stability of the chemicals used since a solvent would be in contact for longer times with highly radioactive process streams. Degradation of the solvent may lead to the production of interfering degradation products, decreases in ligand concentration and changes in solvent viscosity as well as changes in phase separation parameters.[17]

This degradation may result in losses in selectivity and affinity for target metal extraction. Radiolytic degradation of the BTBP ligand family was investigated previously.[18-20] A variety of different BTBP molecules was developed, such as C5-BTBP *(6,6'-bis(5,6-dipentyl-[1,2,4]triazin-3-yl)-[2,2']bipyridine)* or the annulated MF2-BTBP *(4-tert-butyl-6,6'-bis-(5,5,8,8-tetramethyl-5,6,7,8-tetrahydro-benzo[1,2,4]triazin-3-yl[2,2']-bipyridine)* and tested for their process performance.[21]
Since it was proven that annulated BTBPs are much more stable towards radiolytic degradation than the tetra alkyl substituted BTBPs, those annulated systems were further investigated. Finally, the $CyMe_4BTBP$ (*6,6'-bis(5,5,8,8-tetramethyl-5,6,7,8-tetrahydro-benzo[1,2,4]-triazin-3-yl)-[2,2']-bipyridine*, Fig. 35) system was chosen as reference system in European research, resulting in the above mentioned SANEX process.

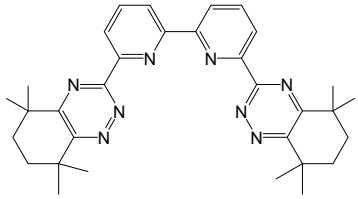

**$CyMe_4BTBP$**

**Fig. 35: Chemical structure of $CyMe_4BTBP$**

The gamma radiolysis studies were performed using a $^{60}Co$ source at the CHALMERS University of Technology, Gothenburg, Sweden. Organic solutions of the ligand (10 mmol/L) in 1-octanol were irradiated with or without contact to nitric acid up to an absorbed dose of 300 kGy. Subsequently, liquid-liquid extraction experiments as well as mass spectrometric investigations were conducted.
A protection of $CyMe_4BTBP$ against radiolytic degradation was found for solutions irradiated in contact with nitric acid. In contrast to irradiation experiments without contact to nitric acid solutions, no decrease in $^{241}Am$ and $^{152}Eu$ distribution ratios was observed.[22] But even then, the concentration of the ligand molecules after irradiation decreased, as observed for experiments without nitric acid.
In mass spectroscopy we could find many different degradation products for samples irradiated without contact to an aqueous phase. However, whit addition of nitric acid to the system, an addition product of one 1-octanol molecule to the ligand was found exclusively, even for the highest dose applied (300 kGy). As nitric acid is commonly used in partitioning processes for trivalent actinide separation, this protective effect plays a crucial role for the long-term performance of the used solvents.
As a next step, it is planned to perform high resolution mass spectroscopy to further identify the radiolysis products and to clarify the structure of the found 1-octanol adducts to $CyMe_4BTBP$. Afterwards, synthesis and testing of those adducts within the current European SACSESS project is planned. Additionally, the $CyMe_4BTBP$ molecule, which is the current reference molecule in European research, will be compared to the very promising molecule $CyMe_4BTPhen$, where the bipyridine moiety is replaced by a phenanthroline functionality to fix the molecule in the cis-conformation resulting in a thermodynamically more favoured metal-ligand complexation.

**Internal gelation studies**

Conversion of dissolved actinide compounds after partitioning to suitable pre-cursors for fuel fabrication forms an essential link between partitioning (P) and transmutation (T). In the ASGARD project the conversion issue has been addressed coherently, focussing on dust-free methods. The main challenge here is the treatment of (trivalent) Minor Actinides (MA) as compared to (tetravalent) U or Pu. Fabrication of such fuels containing MA has high demands due to radiotoxicity and contamination issues. A procedure minimising the connected risks is highly beneficial.

Different wet co-conversion concepts are today conceivable, based on co-precipitation operations, sol-gel transition and matrix infiltration[23]. A quite innovative context for the future systems is the more required handling of actinide mixtures, either in solution or in the solid phase. Therefore, sol-gel methods are still interesting due to the need to prevent the formation of dust containing minor actinides. These wet chemical routes transform an aqueous sol into a solid gel. Common sol-gel routes are water extraction, as well as the internal and external gelation. Advantages of these techniques are a possible co-processing of different actinides (trivalent, tetravalent), a wide range of sphere sizes can be fabricated (suitable for *Sphere-pac* fuel[24]) and the technique is capable for non-oxide ceramics (nitride, carbide) [25].

The studies presented in this work were done with $Nd^{3+}$, which acts as a surrogate for trivalent actinides like $Am^{3+}$. The internal gelation study is based on the process developed by KEMA[26], which has been modified at Forschungszentrum Jülich by Förthmann[27]. The process has been slightly changed and altered to include Nd. The sol-gel route via internal gelation was applied to prepare oxidic microspheres containing uranium and neodymium. During the synthesis, hexamethylenetetramine (HMTA) is used as gelification agent and urea as complexing agent. Acid deficient uranyl nitrate (ADUN[28]) and neodymium nitrate solutions were used as precursors to fabricate microspheres containing defined mixtures of Nd and U.

A detailed description of the U / Nd particle synthesis and characterisation (SEM/EDX) is published in [29], the Nd mole fraction was varied from 0 % to 43 % with an increment of 5 %. Fig. 36 shows a photograph of the products. The thermal behaviour of the particles was studied by applying TG-DSC technique (Netzsch, STA 449 C Jupiter, artificial air, maximum temperature: 1300 °C). Finally, a thermal treatment was carried out at different maximum temperatures (1300 °C and 1600 °C) under reducing conditions. The treated particles were characterized by scanning electron microscopy SEM (FEI, Quanta 200F) and X-ray powder diffraction (Bruker, D8 Advance).

For the particles treated at 1300 °C (2 h) in a reducing $H_2$:Ar (4:96) atmosphere one cubic phase was found for compositions containing up to 30 % Nd. Mixtures containing more neodymium consist of two cubic phases. The particles treated at 1600 °C (10 h) under reducing conditions ($H_2$:Ar) consist of one $UO_2/Nd_2O_3$ solid solution, only.

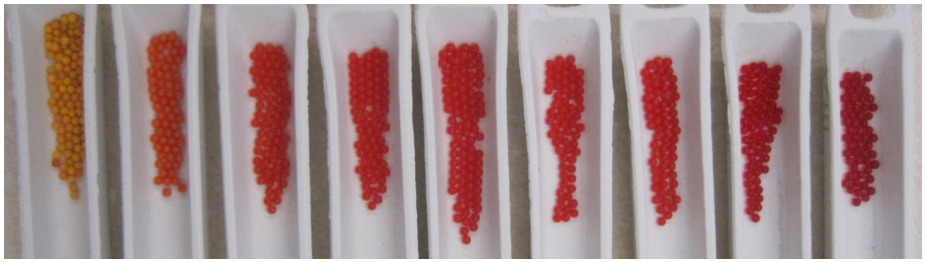

**Fig. 36: Photograph of U microspheres (left) and particles with U/Nd compositions after drying at air (right: max. Nd content).**

The lattice parameter *a* of the cubic $U_yNd_{1-y}O_{2-0.5y}$ lattice was calculated using the Nelson-Riley method[30]. Up to a Nd content of approximately 30 % the lattice parameter depend linearly on the molar fraction of neodymium, according to Vegard's law. The particles containing more Nd are showing an unexpected behaviour. Lattice parameters of all compositions treated at both temperatures are plotted in Fig. 37. The results of this study show that the synthesis of single phase $U_yNd_{1-y}O_{2-0.5y}$ solid solutions is possible by the internal gelation synthesis route with Nd contents up to 42.63 %.

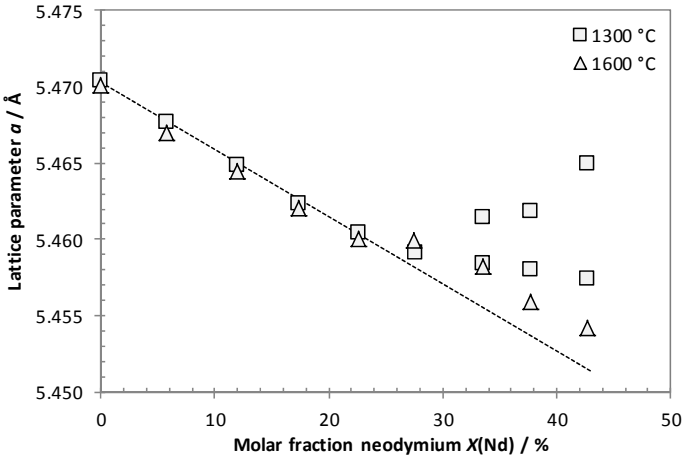


**Fig. 37: Lattice parameter *a* as function of the Nd content. Particles treated under reducing conditions ($H_2$:Ar) at 1300 °C (squares) and 1600 °C (triangles).**

## Conclusions

The separation processes described in this study are based on solvent extraction studies which benefit from the experience gained over the last 20 years in European international collaborative projects. As shown, the scientific feasibility of these processes involving new extracting or complexing organic molecules and new diluents was demonstrated recently, such as in the innovative SANEX process. The concept of separating solely Am(III) from all the FP and Cm(III) in a single process is the focus of the current work at Jülich. It is important to improve the mechanistic understanding of the chemical and physical reactions involved in

the solvent extraction processes (thermodynamics and kinetics) and the diverse safety issues involved in the chemical processes.
Last but not least, the long term operation of the solvent accounting for degradation by hydrolysis and radiolysis reactions must be demonstrated before industrial deployment can be considered. Here, in close collaboration with different international partners we are studying the most promising extraction systems, developed in Europe.

Actinide co-conversion processes can ensure the closing of the actinide co-partitioning steps. At the same time mixed-actinide solid compounds are formed and can be used as starting materials for the fabrication of innovative nuclear fuels. Co-precipitation and sol-gel concepts were studied at Jülich within former European collaborative projects (Europart, ACSEPT). The current work is located within the European ASGARD project and especially internal gelation synthesis pathways are studied. This includes the fabrication process as well as the post processing steps. Furthermore, solid state characteristics of the $UO_2$ - $Nd_2O_3$ solid solution system were investigated.

**Acknowledgements**
Financial support for this research was provided by the European Atomic Energy Community's 7th Framework programme projects SACSESS – grant agreement No. FP7-Fission-2012-323-282 and ASGARD – grant agreement No. 295825, as well as the German Federal Ministry of Education and Research (Contract No. 02NUK020E). KIT, Heidelberg University, the Universities Twente and Reading are acknowledged for the collaboration in this research.

**References**
[1] OECD-NEA (1999): P&T report
[2] OECD-NEA (2006): NEA No. 5990;
[3] OECD-NEA (2011): NEA No. 6894;
[4] Bourg, S. et al. (2011): Nuclear Engineering and Design Vol. 241 (9), 3427-3435.
[5] Sypula, M. et al. (2012): Solvent Extr. Ion Exch. Vol. 30 (7), 748-764.
[6] Geist, A. et al. (2012): Solvent Extr. Ion Exch. Vol. 30 (5), 433-444.
[7] Magnusson, D. et al. (2013): Chem. Eng. Sci. Vol. 99, 292-297.
[8] Magnusson, D. et al. (2012): Proc. Chem. Vol. 7, 245-250.
[9] Magnusson, D. et al. (2012): Solvent Extr. Ion Exch. Vol. 30 (2), 115-126.
[10] Wilden, A. et al. (2015): Solvent Extr. Ion Exch. Vol. 33 (2), 91-108.
[11] Modolo, G. et al. (2014): Progr. Nucl. Energ. Vol. 72, 107-114.
[12] Poinssot, C. et al. (2012): Procedia Chem. Vol. 7, 358-366.
[13] Taylor, R. et al. (2015): Nucl. Future Vol. 11 (4), 38-43.
[14] Lewis, F.W. et al. (2012): Proc. Chem. Vol. 7, 231-238.
[15] Lewis, F.W. et al. (2015): Chemical Science Vol. 6 (8), 4812-4821.
[16] Šťastná, K. et al. (2015): J. Radioanal. Nucl. Chem. Vol. 304 (1), 349-355.
[17] Mincher, B.J. (2010): ACS Symp. Ser. Vol. 1046 (Nuclear Energy and the Environment), 181-192.
[18] Hill, C. et al. (2005): Proceedings of GLOBAL 2005 2005, Tsukuba, Japan, 9-13 October, p 283.
[19] Retegan, T. et al. (2007): Radiochim. Acta Vol. 95 (11), 637-642.
[20] Fermvik, A. et al. (2009): Dalton Trans.(32), 6421-6430.
[21] Fermvik, A. et al. (2009): Radiochim. Acta Vol. 97 (6), 319-324.
[22] Schmidt, H. et al. (2015): Nukleonika, accepted.
[23] OECD/NEA (2005): NEA No. 5419.
[24] Pouchon, M.A. et al. (2012): Chap. 11 in Comprehensive Nuclear Materials, Vol. 3: Advanced Fuels/Fuel Cladding/Nuclear Fuel Performance Modeling and Simulation, Konings, R.J.M., et al., Elsevier: pp 275-312.
[25] Vaidya, V.N. (2008): Journal of Sol-Gel Science and Technology Vol. 46 (3), 369-381.
[26] Van Der Brugghen, F.W. et al. (1968) Technical report, Keuring van Electrotechnische Materialen, NV, Arnhem (Netherlands).

[27] Förthmann, R. (1973): Technical report, KFA Jülich.
[28] Haas, P.A. (1972): ORNL-TM-3817,
[29] Schreinemachers, C. et al. (2014): Progress in Nuclear Energy Vol. 72 (0), 17-21.
[30] Nelson, J.B. et al. (1945): Proceedings of the Physical Society Vol. 57 (3), 160-160.

## 5.6. Monazite-type ceramic waste forms

S. Neumeier, Y. Arinicheva, J. Heuser, F. Brandt, A. Bukaemskiy, G. Deissmann, G. Modolo, D. Bosbach

Corresponding author: s.neumeier@fz-juelich.de

### Introduction

In the last decades, various ceramic materials have been proposed as potential waste forms for the immobilization of special nuclear waste streams, such as separated plutonium from civilian or military sources unsuitable for further use. Among them, monazite-type orthophosphates ($Ln$PO$_4$; $Ln$ = La – Gd) appear as promising candidates due to their specific physico-chemical properties including high structural flexibility, high chemical durability, and high radiation resistance[1-3].

These outstanding properties have been demonstrated by natural analogues being exposed to geological events for several hundred millions of years. They can contain up to 27 wt.% natural radioelements, such as tetravalent Th and U without suffering from amorphization due to radiation damages[4] and show significant modifications only due to mechanical abrasion but not due to chemical alteration by weathering[5].

In order to obtain tailored materials, the understanding of incorporation of radionuclides into the monazite structure is the key factor developing the material properties.

At IEK-6, a research program has been developed in order to investigate systematically the correlation between structure and properties of ceramic waste forms focusing in particular on the long-term behavior of the materials under repository relevant conditions. This program includes and links

- the development and optimization of wet chemical synthesis methods suitable for the immobilization of radionuclides in ceramic waste forms such as co-precipitation and hydrothermal synthesis as well as sintering methods in order to fabricate dense ceramic waste forms with well-defined microstructure,
- structural and microstructural characterization using state-of-the-art diffraction (powder and single crystal XRD), spectroscopic (Raman, TRLFS, EXAFS) and microscopic (SEM, FIB/TEM) methods,
- the determination of mechanical and thermal properties as well as thermodynamic data,
- the investigation of reactivity under conditions relevant to geological disposal, in particular with respect to dissolution/corrosion in aqueous environments,
- investigations of radiation damages utilizing heavy ion irradiation,
- the development of synergies between experimental investigations and atomistic simulations (e.g. regarding structure, physical properties and radiation damages).

### Structure and chemical flexibility

The $ABO_4$ monazite-type structure (monoclinic, space group P2$_1$/n, Fig. 38) offers a remarkable opportunity for incorporating a wide range of elements regarding size and charge which is correlated to the low symmetry of $Ln$O$_9$ polyhedron. The actinides are mainly observed in phosphate and silicate compounds as can be seen by natural analogues, e.g. $Ln$PO$_4$ monazite and associated cheralite $Ln_{1-2x}M_xAn_xPO_4$ and huttonite ($ThSiO_4$)[3].

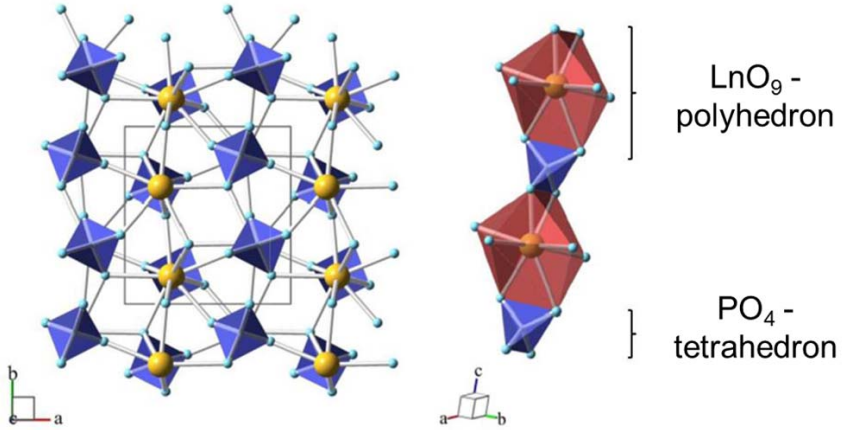


**Fig. 38: Representation of monazite structure and *Ln*$O_9$ polyhedron connection.**

Within this period of reporting several solid solution series with monazite structure have been synthesized by direct substitution of trivalent lanthanides (e.g. $La_{1-x}Ln_xPO_4$, *Ln* = Nd, Eu, Gd and Tb). As expected, the incorporation of *Ln* = Nd, Eu, Gd results in the formation of single phase solid solutions since all pure end-members are known to crystallize in the monazite structure[6].

Additionally, the flexibility of the monazite structure has been investigated by the incorporation of Tb. The pure $TbPO_4$ end-member forms a tetragonal xenotime structure (space group: $I4_1/amd$) due to the smaller cationic size of Tb. It was shown that Tb up to 75 mol% can be incorporated into the monazite structure before a separate xenotime phase was observed. These experiments prove the chemical flexibility of the monazite structure[7].

### Synthesis and sintering

Various wet-chemical methods such as co-precipitation and hydrothermal synthesis have been developed for the preparation of pure and single phase monazite solid solutions. In dependence of the synthesis parameters and methods the shape and structure of the precursor material (either rhabdophane ($LnPO_4 \cdot 0.667H_2O$, monoclinic structure)[8] or monazite or a mixture of both) and therefore also the final microstructure of the ceramic waste forms can be tuned by the way of synthesis. For instance a hydrothermal synthesis in basic (pH 10; HTS-10) and acidic (pH 1; HTS-1) media yield nano-sized spherical (Fig. 39,a) and up to 2 µm long needle-like (Fig. 39,b) particles of the precursor after synthesis, respectively.

SEM measurements have been performed in order to investigate the influence of the precursor particle shape on the microstructure of sintered $La_{0.5}Eu_{0.5}PO_4$ pellets[9]. The microstructure of the ceramics differs significantly. The HTS-10 pellet (left micrograph, Fig. 2, c) shows an inhomogeneous microstructure of a coarse and a fine fraction of grains. In the coarse fraction, large aggregates can be observed which consist of submicron grains with an average diameter of ~ 0.5 µm (Inset, Fig. 39,c). The bulk porosity is mainly dominated by intergranular pores at triple junctions. In contrary, in the SEM micrograph of the HTS-1 pellet (Fig. 39,d) a more homogeneous and dense microstructure is evident with an intragranular porosity (Inset, Fig. 39,d). Therefore, the needle-like precursor might be most promising for

the fabrication of a monazite-type ceramic waste form since the intragranular porosity might serve as cavities to compensate He built-up due to α-decay of the immobilized actinides and hence reduce swelling and crack formation[9].

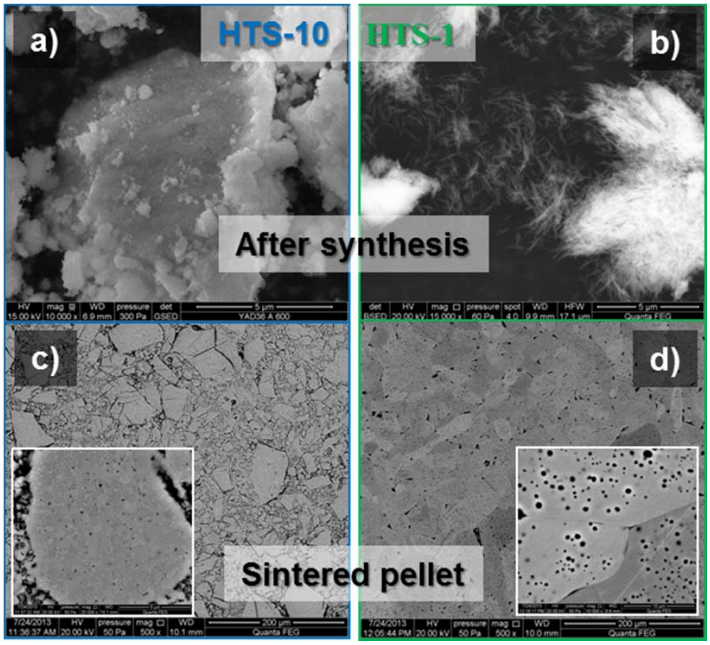


**Fig. 39: SEM micrographs of $La_{0.5}Eu_{0.5}PO_4$ precursors after synthesis by hydrothermal precipitation at pH 10 (a, spheres) and pH 1 (b, needles) and microstructure after sintering at 1450°C for 5 h (c&d). The insets show a magnification of c&d.**

Besides the microstructure evolution, the final crystallization and formation of monazite solid solution takes place during sintering. These processes have been investigated by means of thermogravimetry and XRD measurements. Fig. 40, left shows a typical thermogram of a (La,Eu)$PO_4$ precursor. A mass loss of ~ 5% has been measured up to 400°C due to desorption of adsorbed water[10] and the complete dehydration of rhabdophane[8]. Between 600°C and 1050°C an exothermic effect is observed that can be assigned to the rhabdophane-monazite phase transition and is in very good agreement with the literature[6].
The phase transition has been confirmed by XRD measurements that have been performed after thermal treatment at temperatures based on the results of TG-DSC measurements (Fig. 40, right). The XRD of pristine powder and the samples heated up to 600°C show characteristic reflexes of the rhabdophane phase (15° and 20° *2Θ*). After thermal treatment at 800°C the characteristic XRD pattern of a monazite structure was obtained. An additional thermal treatment at 1450°C results in XRD patterns with sharp reflexes indicating the formation of a pure single phase monazite solid solution of high crystallinity.

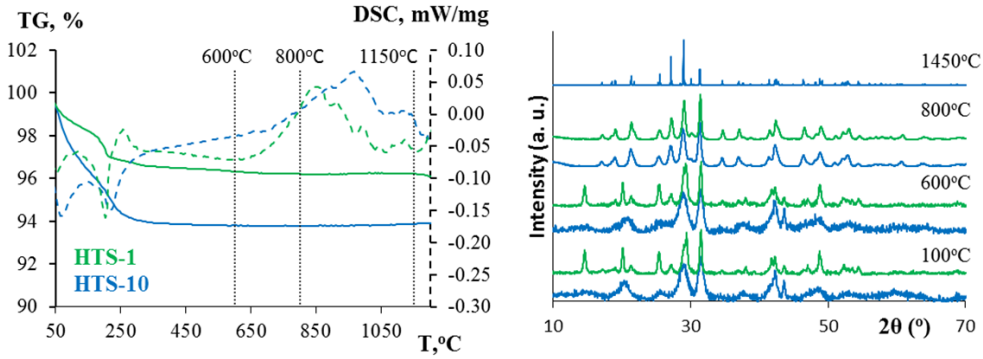


**Fig. 40: Left graph: TG (solid lines) and DSC (dashed lines) of $La_{0.5}Eu_{0.5}PO_4$ powders after synthesis by hydrothermal precipitation at pH 1 (green lines) and pH 10 (blue lines) and the corresponding XRD patterns after thermal treatment at selected temperatures (right graph).**

### Physical properties

The knowledge of physical properties of ceramic waste forms is essentially needed to understand the behavior of ceramic materials (pellets) exposed to conditions that might deform or crack the waste form. Crack formations may occur due to external pressure and more likely due to swelling processes caused by He formation. These cracks increase the reactive surface area of the waste form which significantly affects the dissolution behavior.

Physical properties such as fracture toughness and Young's modulus have been determined in dependence of the composition of $La_{1-x}Eu_xPO_4$ solid solution series and a structure / property correlation was clearly observed (Fig. 41). The lattice parameters derived from XRD measurements (Fig. 41, left) as well as the fracture toughness and Young's modulus (Fig. 41, right) show linear trends in dependence of the Eu content[6,11]. Obviously these properties are directly connected to the lattice contraction due to the increasing content of smaller $Eu^{3+}$-ions in the solid solution. The Young's modulus data are in very good agreement with calculations performed by the Atomistic Modelling group (Dr. P. Kowalski)[12].

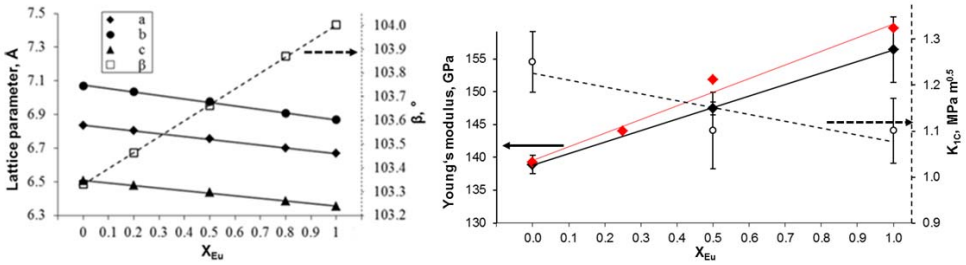


**Fig. 41: Linear correlation of crystallographic data (left; solid lines: lattice parameter; dashed line. lattice angle) and physical properties (fracture toughness (dashed line), Young's modulus (solid lines; black line corresponds to experimental, red line to simulated data) in dependence of the Eu content in a $La_{1-x}Eu_xPO_4$ solid solution series.**

**Chemical durability**

Regarding the long-term behavior of a ceramic waste form the chemical durability is of particular interest with respect to the radionuclide release from the waste matrix if it comes into contact with ground water.

Dynamic dissolution experiments have been performed at 90°C and c(HCl) = 0.1 M[13]. The steady state dissolution rates of $La_{1-x}Eu_xPO_4$ solid solutions in dependence of the Eu content are plotted in Fig. 42. It turns out that the normalized steady state dissolution rates depend on the Eu content of the solid solution series and show a non-linear behavior, in contrast to the physical properties. At higher Eu content a systematic increase of the dissolution rate is observed which is consistent with the higher dissolution rate of pure $EuPO_4$ compared to $LaPO_4$[13]. In contrary, at a mole fraction of 20 mol% Eu a minimum of the dissolution rate is evident. This effect most likely can be attributed to lattice contraction due to the incorporation of the smaller Eu-ion.

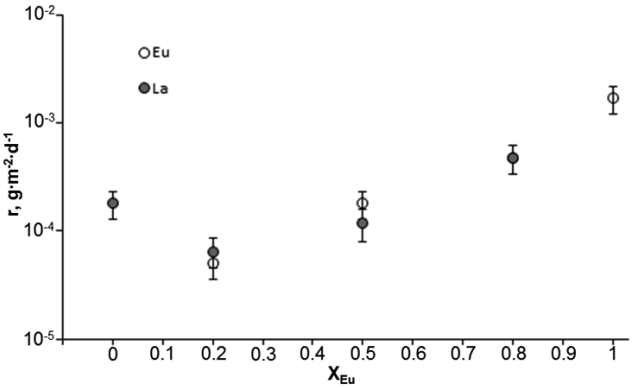


**Fig. 42: Normalized steady state dissolution rates of La and Eu of a $La_{1-x}Eu_xPO_4$ solid solution series at 90°C and pH 1 show a minimum of 20 mol% of Eu.**

**Radiation damages**

The α-decay of actinide elements (e.g. U, Np, Pu, Am, and Cm) produces α-particles with an energy of 4.5 to 6 MeV, recoil nuclei (70 to 160 keV), and some γ-rays. Despite of the higher energy compared to the recoil nuclei the α -particles induce 100 – 200 atomic displacements mainly due to ionization while the recoil nuclei produce 1000 - 2000 atomic displacements due to ballistic effects and therefore mainly contribute to radiation damages in crystalline ceramic materials. A refined understanding of the consequences of radiation effects on structure and properties and hence on the macroscopic stability of the ceramic material is of significant importance in order to derive a reliable description of the long-term stability of the waste form.

At IEK-6 the investigations on radiation damages have been started using heavy ion irradiation (*emir*-network within the *JANNuS*-platform, Saclay, Paris). Fig. 43, left shows a FIB lamella (area: 20 µm x 15 µm; thickness ~ 600 nm) of $SmPO_4$ that has been prepared at IEK-6 to be irradiated with an $Au^{n+}$-ion beam with energies up to 7 MeV and total fluence from $6 \cdot 10^{12}$ to $5 \cdot 10^{14}$ ions/cm$^2$. Accompanying SRIM calculations revealed that the total thickness of the FIB lamella is irradiated by the applied experimental conditions[7].

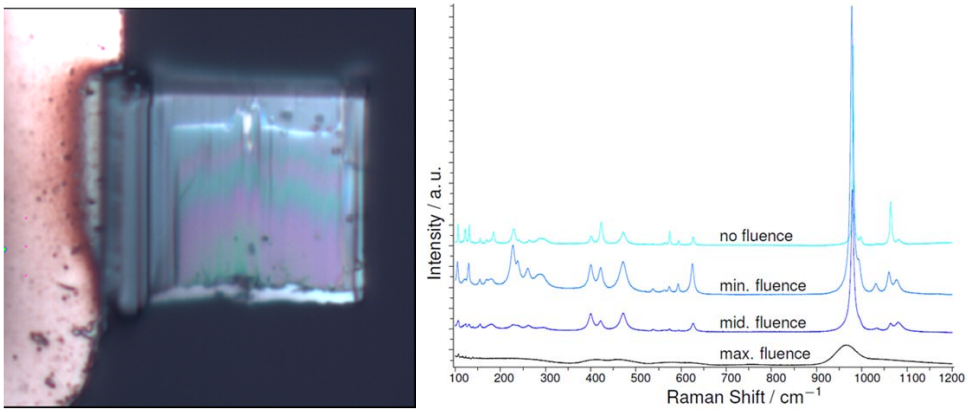


**Fig. 43: Left: Photomicrograph of a $SmPO_4$ FIB-lamella (20 µm x 15 µm area; ~600 nm thickness); Right: Raman spectra of $SmPO_4$ before and after irradiation with different fluences[7].**

In Fig. 43, right the Raman spectra of $SmPO_4$ before and after irradiation with different fluences are plotted. It turns out that the maximum fluence leads to an amorphization of $SmPO_4$. Since these measurements have been performed at room temperature recrystallization effects were not observed because the critical temperature of $SmPO_4$ is around 200°C [14].

## Conclusions

At IEK-6, systematic fundamental studies on monazite-type waste forms are performed covering several aspects, such as synthesis and sintering, structure research, physical properties, dissolution behavior and radiation damages. From XRD measurements a linear dependency of the lattice parameter from the *Ln*-content was observed indicating a single phase solid solution formation for monazite-type $La_{1-x}Ln_xPO_4$, *Ln* = Nd, Eu and Gd. The chemical flexibility of the monazite structure was demonstrated by the incorporation of significant amounts (up to 75 mol%) of smaller $Tb^{3+}$ ions that usually tends to form the xenotime structure. The microstructure of a monazite waste form can be tailored by the synthesis parameters and methods. A strong correlation in terms of linear trends between structure and physical properties (fracture toughness and Young's modulus) was observed. It seems that the properties are directly linked to the increase of density due to lattice contraction. These results finally make the behavior of monazite-type ceramics predictable with respect to these properties. In contrast the dissolution behavior does not follow this trend. A minimum of dissolution rate at 20 mol% Eu content was evident indicating a significant influence of lattice contraction on the dissolution rate. The investigation of amorphization behavior of a $SmPO_4$ due to radiation effects on the monazite structure has been successfully started by Au-ion irradiation experiments.

## Acknowledgements

This work was financially supported by the German Federal Ministry of Education and Research (BMBF); grant no.: 02NUK021 and the German Research Foundation (DFG); grant-no.: SCHL 495/3-1.

## References


[1] Lumpkin, G.R. 2006, Elements 2, 365–372.
[2] Ewing, R.C. and Wang, L.M. 2002, Rev. Min. Geochem. 48, 673–699.
[3] Dacheux, N. et al. 2014, Am. Min. 98, 833–847.
[4] Boatner, L.A., 2002, Rev. Min. Geochem. 48, 87-120.
[5] Montel, J.M. et al. 2011, Eur. J. Mineral. 23, 745-757.
[6] Arinicheva, Y. et al. 2014, Prog. Nucl. Energy 72, 144-148.
[7] Heuser, J. 2015, PhD thesis, RWTH Aachen University.
[8] Mesbah, A. et al. 2014, Cryst. Growth Des. 14(10), 5090-5098.
[9] Neumeier et al. 2016, Prog. Nucl. Energy, accepted.
[10] Feick, G. and Hainer, R.M. 1954, J. Am. Chem. Soc. 76(22), 5860–5863.
[11] Thust, A. et al. 2015, J. Am. Ceram. Soc. 98(12), 4016-4021.
[12] Kowalski, P. et al. 2015, J. Nucl. Mater. 464, 147-154.
[13] Brandt, F. et al. 2014, Prog. Nucl. Energy 72, 140–143.
[14] Meldrum, A. et al. 1997, Phys. Rev. B, 56(21), 13805-13814.

## 5.7. Pyrochlores as tailor-made waste forms for specific high level nuclear waste

S. Finkeldei, F. Brandt, M. Klinkenberg, A. Bukaemskiy, D. Bosbach
Corresponding author: s.finkeldei@fz-juelich.de

### Introduction

The direct disposal of spent fuel and the vitrification of separated waste streams are well-established strategies for the safe disposal of high level nuclear waste (HLW) in a deep geological repository. Among the high level nuclear waste, the minor actinides (MA = Am, Cm, Np) contribute a high share of the long-term radiotoxicity even though they only account for a small share of the nuclear waste from a volumetric point of view (0.1% [1]). Moreover, significant amounts of excess Pu either from the reprocessing of civil Pu (e.g. 123 tons in Great Britain [2]) or from dismantled nuclear weapons are stored in different countries and need to be safely disposed. For these specific waste streams or separated elements, ceramics are considered as an alternative nuclear waste form. In order to include ceramic waste forms into a safety assessment for a deep geological nuclear waste repository, a process understanding of these outstanding properties is required. For the safe disposal of HLW, the properties of a nuclear waste form are considered as part of the engineered barrier of the deep geological repository.

A high aqueous durability, a high radiation tolerance as well as the structural uptake of the radionuclides make ceramic systems attractive potential nuclear waste forms. The most important advantage of such ceramics compared to glasses is their crystallinity which leads to a retention of the radionuclides on defined lattice sites inside a chemically and physically very stable host phase [3]. Beside rare earth phosphates like monazites, in particular titanate based ceramics such as brannerite, zirconolite, perovskite and pyrochlore are examined as potential nuclear waste forms [4]. These need to exhibit some porosity to avoid cracking of the matrix due to fission gas release and α-decay, which can be adjusted by choosing an appropriate synthesis route. Natural analogues have been identified for many of these ceramics, indicating the structural retention of natural radionuclides for more than 40 million years [3]. These natural analogues prove a high chemical stability, a high durability and a distinct tolerance towards radiation damage of certain ceramic waste forms.

A major concern for a crystalline waste form is the change and potential loss of its beneficial properties. Several $TiO_2$-based ceramic systems are known to transform to amorphous phases due to radiation damage [5] whereas $ZrO_2$ based ceramics typically undergo a structural order/disorder transition but remain crystalline [6]. From technical applications, $ZrO_2$ based ceramics are known to be extremely corrosion resistant. $ZrO_2$ based ceramics with the pyrochlore structure are of particular interest due to their high radiation tolerance [7] ensuring a high long-term durability. Here, the properties of $ZrO_2$ based pyrochlores with respect to their radionuclide uptake and chemical stability were investigated. Qualitatively, $ZrO_2$ based pyrochlores were already well known for their high radiation tolerance and chemical stability [7]. However, there is a lack of quantitative details concerning the rate of dissolution at repository relevant conditions, the phase stability field of $ZrO_2$ based

pyrochlores and the uptake of radionuclides and these aspects have therefore been in the focus of this study.

**Aims**

The key aspects which qualify pyrochlore as a potential nuclear waste form are summarized in Fig. 44. Here, we report recent findings about the aspects of (1) the chemical flexibility, (2) the radionuclide uptake and (3) the chemical stability.

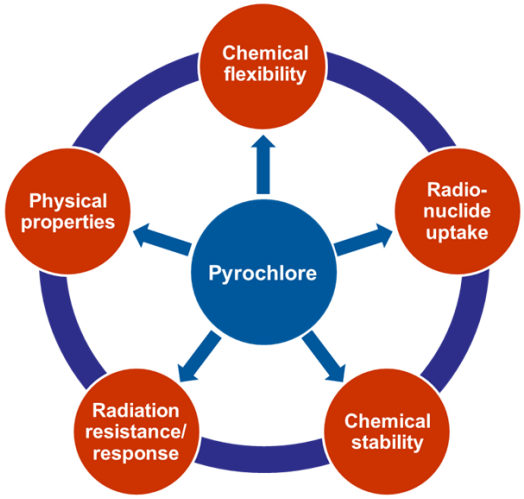


**Fig. 44: Key aspects of pyrochlore as a potential nuclear waste form.**

As soon as pyrochlores are considered as potential nuclear waste forms, stoichiometric $A_2B_2O_7$ pyrochlores are the exception. The radionuclide uptake will lead to the formation of non-stoichiometric pyrochlores, which exhibit mixed A or B positions as a consequence of radionuclide embedding at one of these sites. Moreover, the order/disorder transition as a consequence of self-irradiation is expected for $ZrO_2$-based pyrochlores. To follow the chemical flexibility (1) and structural evolution of these non-stoichiometric compositions a complete series of various compositions was synthesized and the structural evolution including the structural order/disorder pyrochlore/defective fluorite transition was followed by XRD and TEM.

In order to probe if actinide dopants are structurally taken up (2), Cm doped $ZrO_2$-based pyrochlores were synthesized and their structural site was determined by luminescence spectroscopy. Approaching a more real waste form with a realistic actinide content, $^{239}$Pu-pyrochlore ceramics with 5 and 10 mol% Pu contents were synthesized via a wet-chemical route.

The scenario of water intrusion into a deep geological repository and the performance of a pyrochlore in terms of its chemical stability (3) are mimicked by dissolution studies. To go beyond the macroscopic quantification of dissolution rates of pyrochlores, microscopic dissolution studies have been carried out. Dissolution of pyrochlores was followed by SEM and VSI to deconvolute the macroscopic dissolution rate into various microscopic contributors.

**(1) Chemical flexibility –** The structural uptake of radionuclides will lead to the formation of non-stoichiometric pyrochlores. As consequence of self-irradiation of these non-stoichiometric pyrochlores doped with radionuclides, $ZrO_2$-based pyrochlores are expected to undergo an order/disorder transition from the pyrochlore to the less ordered defective fluorite structure. In order to keep the system simple non-stoichiometric pyrochlores were prepared by partial substitution of the A site cation with an excess of Zr which is the B site cation leading to $(Nd,Zr)_2Zr_2O_{7+x}$compositions. A series of samples with different chemical compositions in the range of $Nd_2Zr_2O_7$ to $Nd_{0.94}Zr_{2.53}O_{6.47}$ was prepared via a wet-chemical coprecipitation route with subsequent sintering at 1600 °C. Powder X-ray diffraction patterns allowed to study the crystal structure of these materials and to determine the lattice parameter *a* of each phase. The $Nd_2Zr_2O_7$ composition crystallized in the pyrochlore structure. The subsequent substitution of the A site cation up to a pyrochlore content of 20 mol% $Nd_2O_3$ led to a single pyrochlore phase with a linear decreasing lattice parameter. Further replacement of Nd by Zr led to the coexistence of the pyrochlore and defective fluorite structure. This miscibility gap could be localized as a rather narrow region between 18 – 20 mol% $Nd_2O_3$ by XRD. Further replacement of neodymium by zirconium is stabilized via the formation of a defective fluorite crystal structure (Fig. 45). The linear decrease of the lattice parameter *a* in the pyrochlore (blue) and defective fluorite (yellow) region with the decrease of the Nd content indicates a solid solution formation in both cases.

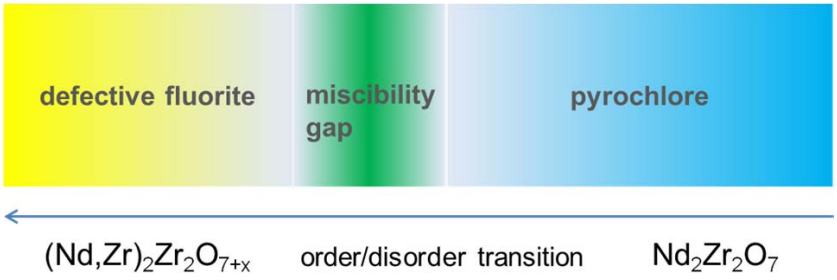


**Fig. 45: Sketch of the structural order/disorder transition from a stoichiometric pyrochlore $Nd_2Zr_2O_7$ to the defective fluorite structure by partial substitution of the A site cation Nd with the B site cation Zr.**

To follow the order/disorder transition along different crystallographic directions, TEM measurements were recorded for three selected samples. A stoichiometric pyrochlore, a pyrochlore sample with a content of 25 mol% $Nd_2O_3$ and a defective fluorite sample with 15.6 mol% $Nd_2O_3$. For each sample TEM pattern along three different zone axes [110], [112] and [100] were collected and are indexed by the defective fluorite structure in Fig. 46. The stoichiometric pyrochlore sample shows typical electron diffraction pattern for a pyrochlore structure along the [110] direction. Moreover, a diffraction spot at GF ± ½ (002)F is present which neither belongs to the pyrochlore nor the defective fluorite structure. This spot may be originated by a break of symmetry in the pyrochlore structure caused by anionic or cationic disorder in the structure. The possibility of anionic disorder namely the swap of an oxygen with an oxygen vacancy seems to be more likely due to lower defect formation energies for an oxygen vacancy formation than for a swap of cations. The second sample Py-Nd showed in the XRD pattern still the pyrochlore crystal structure. The TEM patterns of this sample (Fig. 46d-f) show along all directions the same diffraction spots as a stoichiometric pyrochlore.

However, partial decrease of the superstructure reflex intensity is observed. The partial replacement of Nd by Zr on the A site can provide an explanation for the observed change in the intensity compared to a stoichiometric pyrochlore, because Nd and Zr have different scattering factors which are part of the structure factor. The patterns of a defective fluorite sample (Fig. 46g-i) along the [110] and [112] zone axes still contain pyrochlore superstructure reflexes however with a highly reduced intensity. Along the [100] direction all superstructure reflexes are absent (Fig. 46i). The remaining superstructure reflexes could be an indication of partial retention of the cationic order even for the defective fluorite structure.

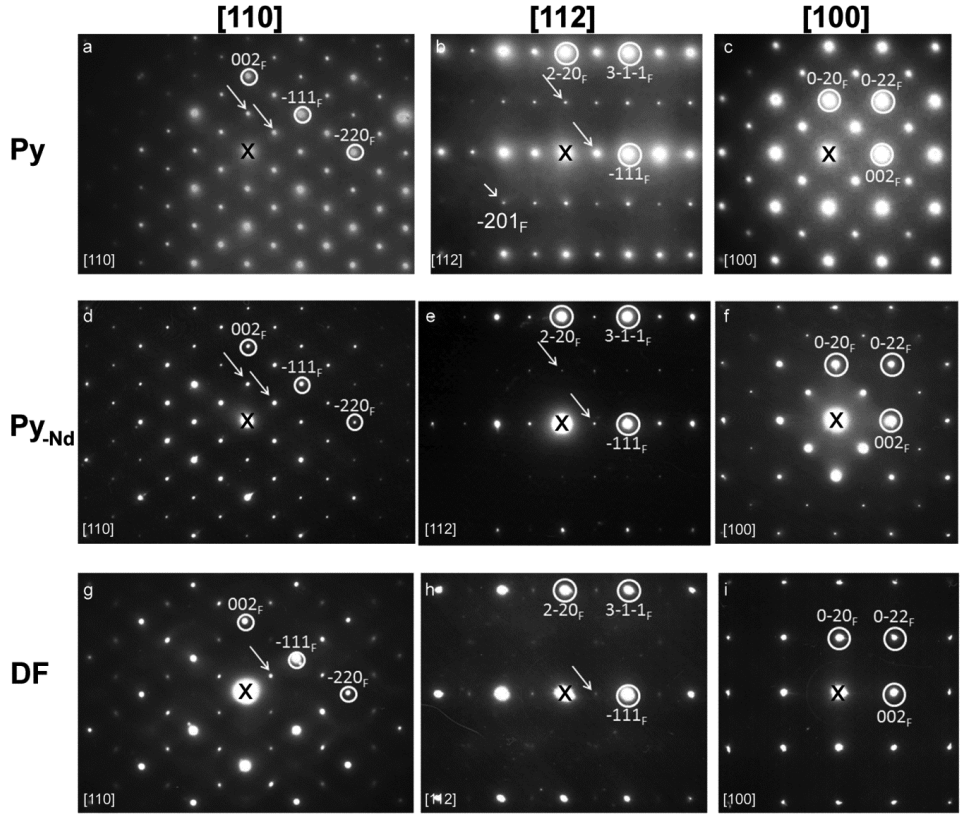


**Fig. 46: Transmission electron diffraction patterns of a stoichiometric pyrochlore (a-c), a 25 mol% $Nd_2O_3$ pyrochlore composition (d-f) and a 15.6 mol% $Nd_2O_3$ defective fluorite sample (g-i). The zone axis along which the patterns are recorded is indicated on top of the figure. Taken from Finkeldei 2014 [8].**

On the basis of the XRD and TEM patterns for a series in the $Nd_2O_3 – ZrO_2$ system the structural order/disorder transition from the pyrochlore to the defective fluorite structure was found to proceed non-uniformly along different zone axis with a miscibility gap at the order/disorder transition. The non-uniform transition can most likely be described by the retention of partial order during the order/disorder transition.

**(2) Actinide uptake by the pyrochlore crystal structure -** Time resolved laser fluorescence spectroscopy (TRLFS) is a highly sensitive technique to study the local structure of crystalline materials. To identify which cationic site of a pyrochlore is adopted by e.g. an actinide, TRLFS is an ideal method, because the emission spectra give information of the direct environment of the probed dopant. Here, Cm and Eu as actinide surrogate were doped in trace amounts into the $La_2Zr_2O_7$ system.
In a first attempt UV emission spectra were recorded after excitation with a pulsed excimer pumped dye laser. Such spectrum allows the identification whether one or more different environments of a dopant are present, which are referred to as different species. The emission spectra of a Cm doped pyrochlore showed more than a single peak for the relaxation from the excited state to the ground state, which indicated the presence of more than a single species. Via direct excitation each species can be excited individually. This allows the unraveling of the direct environment of the probed species, here Cm. The emission spectrum of the major species in a Cm doped pyrochlore sample showed a triplet (Fig. 47, black spectrum). The splitting of the emission spectrum into the triplet confirmed the replacement of $La^{3+}$ by $Cm^{3+}$ on the A site in the pyrochlore crystal structure, because a splitting of the $^8S_{7/2}$ ground state which is less than fourfold can only be caused by the presence of isocentric symmetry [9] as it is the case for the A site in the pyrochlore.

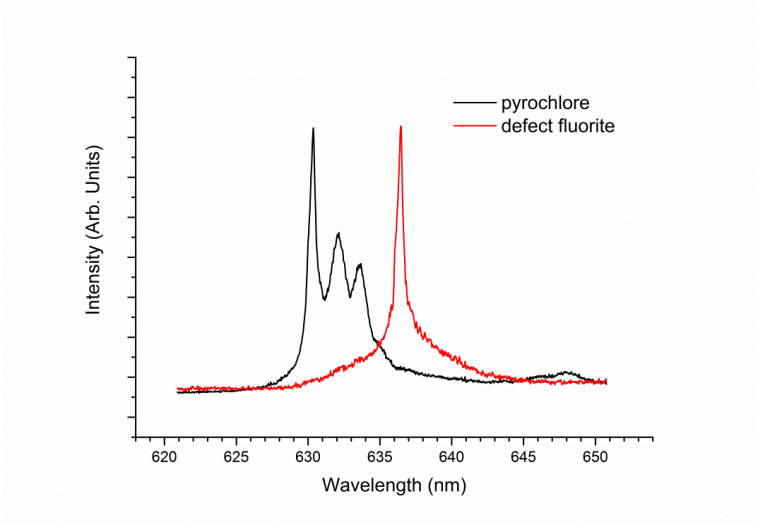


**Fig. 47: Emission spectra after direct excitation of a Cm doped $La_2Zr_2O_7$ sample with the pyrochlore (black) and the defective fluorite (red) crystal structure.**

Similarly to the pyrochlore, UV excitation spectra of a Cm doped defective fluorite sample indicated the presence of more than one Cm species, with the more abundant species resulting in a rather broad peak. A direct excitation of the more abundant Cm species at 636.5 nm led to a single peak (Fig. 47, red spectrum). Within a defective fluorite structure the cationic site is on average sevenfold coordinated, whereas the oxygen vacancies are randomly distributed in the structure. Therefore, various similar cationic positions exist in a defective fluorite structure, which are very likely to cause a multitude of similar single peaks, resulting in a broad peak in the UV excitation spectra.
Besides the two above described major species in the pyrochlore and the defective fluorite structure, in both crystal structures a second, minor species was present. Within a Cm doped pyrochlore the major part of the Cm species is located on the A site within a pyrochlore structure environment, whereas a minor part of the Cm retains in a defective fluorite structure environment. The same case was true for the defective fluorite samples, whereas the major portion of the Cm shows a defective fluorite environment, but a minor Cm part is already located in a pyrochlore type environment.
Additional measurements were carried out for Eu doped pyrochlore and defective fluorite samples, which confirmed the findings of the Cm doped ceramics.
$ZrO_2$ based pyrochlores are expected to undergo a phase transition to a defective fluorite structure as a consequence of radiation damage. Due to the possibility to distinguish between the species in the two different crystal structures, TRLFS could be applied to quantify radiation damage for these pyrochlores with a high sensitivity.
All discussed TRLFS results are published in Holliday, Finkeldei et al. (2013) [10].

Plutonium-pyrochlores

In order to approach a more realistic waste form zirconate based pyrochlore ceramics $(Nd,Pu)_2Zr_2O_7$ with a content of 5 and 10 mol% Pu were synthesized. With respect to the stability range of the pyrochlore structure concerning the ionic radii for the A and B site cations [7] we were aiming to fabricate a pyrochlore with Pu(III) located at the A site. The complete synthesis route was carried out in a glove box line, partially under argon atmosphere. The wet chemical coprecipitation route of the Nd/Zr pyrochlores took place in liquid ammonia and was enhanced for the plutonium-pyrochlore fabrication.
A fresh stock solution of plutoniumnitrate in 1 M nitric acid was prepared for the precipitation reactions. In a first attempt a 10 mol% Pu pyrochlore was synthesized and the plutonium hydroxide was precipitated prior to the neodymium- and zirconiumhydroxides to study its formation separately. In order to fabricate a homogeneous 5mol% Pu doped pyrochlore within a second approach all hydroxides were coprecipitated simultaneously according to the scheme in Fig. 48. A calcination step under reducing atmosphere was followed by a thorough grinding step and cold pressing of the calcined powders for the pellet fabrication. Afterwards a sintering step took place under reducing atmosphere at 1450 °C for 80 h.
The plutonium stock solution was assumed to result in a plutonium(IV) solution, which was expected to have no critical influence on the oxidation state in the pyrochlore ceramic, because sintering took place under reducing conditions. To prevent the plutonium polymer formation all stock solutions were acidified and for each synthesis fresh stock solutions were prepared and directly used. Particularly for the simultaneous coprecipitation of all hydroxides this step was important.

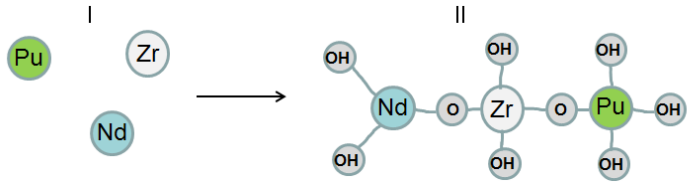


**Fig. 48: Scheme of the hydroxide precipitates for the coprecipitation of Pu-, Nd- and Zr-hydroxides. Taken from Finkeldei 2015 [8].**

The fabricated plutonium pyrochlores were characterized by XRD, SEM and EDX measurements to probe their crystal structure as well as their chemical homogeneity. XRD measurements confirmed the pyrochlore crystal structure formation in both cases and no additional phase could be identified. SEM measurements revealed the formation of a homogeneous pellet. EDX measurements at different locations of the pellet showed a homogeneous distribution of Zr, Nd as well as Pu. All applied characterization techniques led to the conclusion of a structural plutonium uptake by the pyrochlore crystal structure.
Further structural insight as well as insight about the Pu oxidation state will be gained by EXAFAS and XANES analysis.

**Chemical stability –** To characterize the response of a potential nuclear waste form to water intrusion into a deep geological repository dissolution kinetics of potential waste forms are studied. Macroscopic dissolution studies are commonly applied to determine dissolution rates which allow the derivation of dissolution rates at repository relevant conditions. Temperature as well as pH dependent dissolution studies of pyrochlore ceramics have resulted in low dissolution rates [11] which allow these ceramics to be considered as potential nuclear waste forms. However, macroscopic dissolution studies only allow to determine an overall dissolution rate, regardless of the presence of various rate contributors. Here, we have studied the dissolution kinetics of $Nd_2Zr_2O_7$ pyrochlore ceramics by a microscopic approach with vertical scanning interferometry (VSI). The advantage of VSI is the highly variable field of view. VSI is a complementary technique to SEM.
Extreme acidic conditions and a temperature of 90 °C were applied for the microscopic batch dissolution study of a pyrochlore ceramic pellet to make the dissolution observable within a relatively short period. Microscopic dissolution studies with SEM showed a preferential dissolution at the grain boundaries and triple junctions. Moreover, at various areas of the pellet a grain pull-out was observed by SEM. An identical batch dissolution experiment was set-up to study the dissolution process by VSI. Prior to the experiment a thin gold layer was deposited at half of the pellet to act as a height reference. Fig. 49a shows a VSI image after 40 h of dissolution. The green areas have a size of approximately 1 µm and correspond to the dissolution of grains of the pyrochlore monolith. The grain retreat proceeded around 20 nm (Fig. 49c) during the first 40 h of dissolution and continues to a depth of up to 90 nm for several grains after 336 h of dissolution. The VSI image after 336 h of dissolution (Fig. 49b) shows the grain retreat to continue. With increasing dissolution time the number of grains which have started to dissolve has significantly increased. VSI images with a larger field of view probed the magnification shown in Fig. 49 to be representative for the complete pyrochlore monolith surface. A detailed analysis of the VSI data including materials flux maps of the pyrochlore monolith dissolution is ongoing and will allow the identification of the various rate contributors.

The microscopic study of the dissolution kinetics showed a heterogeneous reactivity of the polycrystalline pyrochlore pellet. A SEM study of the pyrochlore monolith prior and after the dissolution experiment revealed the dissolution at the reactive grain boundaries. The mechanism of individual grain dissolution was observed by VSI. The time dependent activation of grains for dissolution is most likely caused by different crystallographic orientations of the grains of the pyrochlore monolith. Future dissolution experiments will include the characterization by EBSD to study the impact of grain orientation on the dissolution.

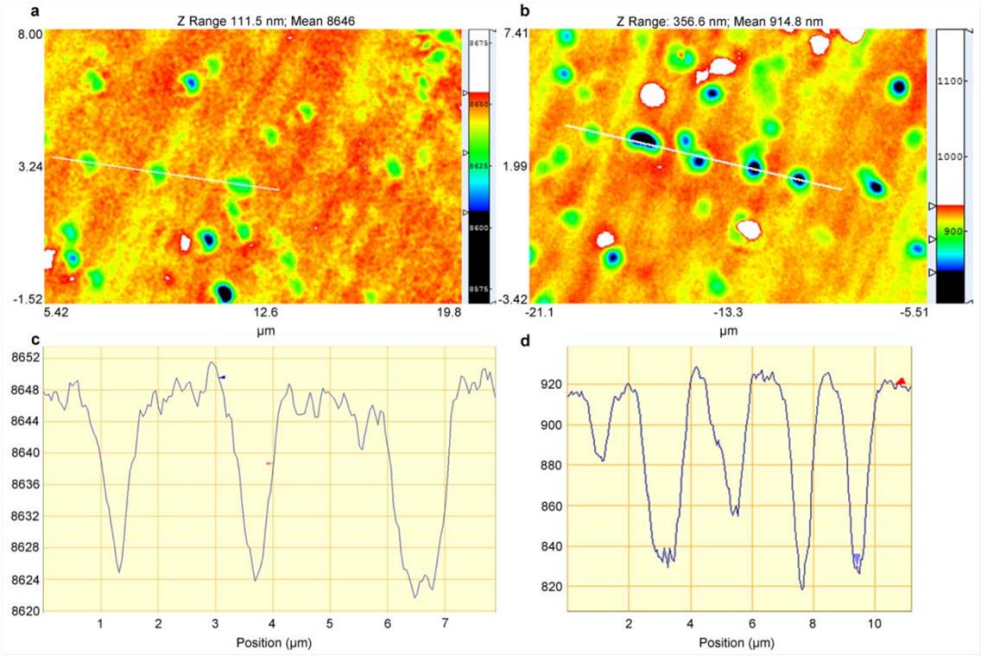


**Fig. 49: VSI images of a pyrochlore monolith after (a) 40 h and (b) 336 h of dissolution. The corresponding depth profiles to the white line in images (a) and (b) are shown in (c) and (d) respectively. Taken from Finkeldei 2015 [8].**

**Conclusion and applications**

Here, we have summarized aspects concerning the chemical flexibility, the radionuclide uptake as well as the chemical flexibility of $ZrO_2$ based pyrochlores which are key aspects of a potential nuclear waste form.

We have followed the order/disorder transition of a pyrochlore ceramic by XRD and TEM and have identified the transition to the defective fluorite structure to proceed non-uniformly along different directions. Moreover, the TEM images indicated a partial retention of the superstructure order of a pyrochlore for a defective fluorite structure. The structural uptake of actinides by a pyrochlore ceramic was proven by TRLFS. A high actinide content of up to 10 mol% plutonium could be successfully immobilized within the pyrochlore structure. Previous macroscopic dissolution studies have identified pyrochlores as promising nuclear waste forms. The dissolution mechanism was accessed by microscopic studies. In addition to grain boundary dissolution a dissolution of the grains was determined by VSI. In summary a refined mechanistic understanding of key properties of pyrochlore-related zirconates with respect to their application as a nuclear waste form could be obtained.

**Acknowledgements**

The authors are thankful to M. Stennett and N. Hyatt for helping with the TEM study; K. Holliday and T. Stumpf for helping with the TRLFS measurements and C. Fischer and A. Luettge for helping with the VSI dissolution studies. S.F. wants to thank N. Marks for engaging discussions of the order/disorder transition of pyrochlore type oxides.

NRG is gratefully acknowledged for the possibility to fabricate the plutonium pyrochlores in their laboratories in Petten (NL).

This work was supported by the Ministerium für Innovation, Wissenschaft, Forschung und Technologie (MIWFT) des Landes Nordrhein-Westfalen; AZ: 323-005-0911-0129.

## Literature


[1] Hamilton, L.H.; Scowcroft, B.; Ayers, M.H.; Bailey, V.A.; Carnesale, A.; Domenici, P.; Eisenhower, S.; Hagel, C.; Lash, J.; Macfarlane, A.M.; Meserve, R.A.; Moniz, E.J.; Peterson, P.; Rowe, J.; Sharp, P. Blue Ribbon Commission on America's Nuclear Future - report to the secretary of energy; Blue Ribbon Commission on America's Nuclear Future; **2012**.

[2] World Nuclear News UK government increases control of civil plutonium. http://www.world-nuclear-news.org/WR-UK-government-increases-control-of-civil-plutonium-03071401.html (accessed 03.09.2014).

[3] Lumpkin, G.R. Ceramic waste forms for actinides. Elements **2006**, 2 (6), 365-372.

[4] Donald, I.W.; Metcalfe, B.L.; Taylor, R.N.J. The immobilization of high level radioactive wastes using ceramics and glasses. J. Mater. Sci. **1997**, 32, 5851-5887.

[5] Lian, J.; Chen, J.; Wang, L.M.; Ewing, R.C.; Farmer, J.M.; Boatner, L.A.; Helean, K.B. Radiation-induced amorphization of rare-earth titanate pyrochlores. Phys. Rev. B **2003**, 68 (13), 134107.

[6] Wang, S.X.; Wang, L.M.; Ewing, R.C.; Kutty, K.V.G. Ion irradiation effects for two pyrochlore compositions: $Gd_2Ti_2O_7$ and $Gd_2Zr_2O_7$. Mater. Res. Soc. Symp. Proc. **1999**, 540, 355-360.

[7] Ewing, R.C.; Weber, W.J.; Lian, J. Nuclear waste disposal-pyrochlore ($A_2B_2O_7$): nuclear waste form for the immobilization of plutonium and "minor" actinides. J. Appl. Phys. **2004**, 95, 5949-5971.

[8] Finkeldei, S. Pyrochlore as nuclear waste form: actinide uptake and chemical stability. RWTH Aachen, Jülich, **2015**.

[9] Buenzli, J.-C.G., Lanthanide probes in life, chemical and earth sciences : theory and practice. Elsevier: Amsterdam, **1989**; p 219-293.

[10] Holliday, K.; Finkeldei, S.; Neumeier, S.; Walther, C.; Bosbach, D.; Stumpf, T. TRLFS of $Eu^{3+}$ and $Cm^{3+}$ doped $La_2Zr_2O_7$: a comparison of defect fluorite to pyrochlore structures. J. Nucl. Mater. **2013**, 433, 479-485.

[11] Finkeldei, S.; Brandt, F.; Rozov, K.; Bukaemskiy, A.A.; Neumeier, S.; Bosbach, D. Dissolution of $ZrO_2$ based pyrochlores in the acid pH range: a macroscopic and electron microscopy study. Appl. Geochem. **2014**, 49, 31-41.

## 5.8. Synthesis and Characterization of Geopolymers as Nuclear Waste Forms for the Safe Disposal of Fission Products Cs-137 and Sr-90

S. Weigelt, H. Schlenz, D. Bosbach

Corresponding author: h.schlenz@fz-juelich.de

**Abstract**

This project focuses on the application of a relatively new class of inorganic binders (matrices) and materials known as “inorganic polymers”, “geopolymer matrices” or simply “geopolymers” in the nuclear industry. The ecological character, variability in structure and composition, as well as the stability and safety of geopolymers altogether provide important potential for the use of these materials. The main application of these geopolymers within the nuclear industry is as competitive materials which can advantageously substitute or complement concretes made from OPC (ordinary Portland cement). Main objectives of the project are the development of geopolymer materials for capturing and containing radionuclides in solid waste forms. These objectives will be realized by developing and characterizing sophisticated geopolymer matrices which are optimized for the safe retention of selected radionuclides such as Cs-137 and Sr-90, respectively, for time periods and conditions required by individual national legislations.

**Introduction**

This project is related to the utilization of geopolymer matrices (and their derived composites) in order to realize the principal and potential advantages of these materials for a range of challenges faced in the nuclear industry. These materials offer opportunities for custom tailored design of waste immobilization matrices for highly problematic radioisotopes such as Cs-137, with ion-specific entrapment properties and high leaching resistance. The application of advanced geopolymer and inorganic matrices introduces extensive research and development challenges that cross several technical disciplines. This transdisciplinary approach to develop geopolymer and inorganic materials must not only include the classical chemical preparations of new materials, but also advanced characterization methods under conditions applicable to the nuclear industry. Care must be taken to characterize the materials in terms of both nuclear chemistry and physics, as well as applicability to construction.

The potential of the geopolymer materials to increase overall safety in the nuclear industry arises from principal structural differences between the geopolymers and OPC concretes. In contrast to OPC concretes, based on hydrated calcium silicate (C3S and C2S) products, the geopolymer matrices represent mainly amorphous aluminosilicate structures linked into three-dimensional networks via aluminate species. The structural differences partly explain the higher chemical and thermal stabilities of geopolymer materials, the differences are also supposed to play an important role for the retention of radionuclides and other elements in geopolymer matrices and are closely related to the potential applications in nuclear industry, namely the replacement of OPC concretes exposed to high temperature and/or radiation field by geopolymer materials. The stability of OPC concrete depends on the capability to retain hydration water, but this can be lost by increasing temperature above 300-500°C or by high

irradiation doses (>1010 Gy). As geopolymers are resistant to temperatures exceeding 1000°C, it can be anticipated that their resistance to radiation damages will be adequately increased as well. Another benefit arising from the presence of aluminate species in the geopolymer matrices is that it could be used for effective capturing and containment of radionuclides. The negative charges of the anionic $[AlO_4]^-$ units are preferably compensated by alkaline or alkaline earth cations and radionuclides such as Cs-137 or Sr-90, which can thus be effectively immobilized in the geopolymer matrix. The performance of the resulting product is anticipated to increase safety of radioactive waste disposal, and one could even think about the conditioning of intermediate level waste using geopolymers. Overall stability of the amorphous 3D network structure and the absence of C3S hydrates in the geopolymer matrix ensure higher stability of matrices to thermal cycling and to chemical corrosion by acids or sulphates. This increased stability of the matrices could be utilized for construction of waste containers. Structures of the geopolymer matrices could incorporate B and Li atoms that are known as absorbers of slow neutrons, and the natural content of protons in the coordinating water sphere of the cations act as retardant of fast neutrons. Geopolymer matrices could be filled with powdered heavy elements, such as Pb or W, or by $BaSO_4$ in order to improve gamma irradiation shielding capacity. Such modified matrices and composite geopolymer materials in form of painted layers or cast construction elements enable the preparation of effective and stable materials for neutron and gamma shielding purposes.

**Materials and Methods**

The main objective of this project are new geopolymers for the immobilization of selected radionuclides, including structural characterization of geopolymers of variable compositions containing the radionuclides Cs-137 and Sr-90 and their diffusivity, focusing on kaolin-based and metakaolin-based geopolymers. To this purpose it is intended to investigate the structure, chemical durability, mechanical properties, thermal stability, and irradiation resistance of such materials, with the main focus on structural features and their impact on material properties. The leaching behaviour of the radio-nuclides from the encapsulated radioactive waste materials is a crucial part of the immobilisation techniques that determine overall safety of a storage/disposal system. The outputs will provide robust modeling of the environmental impact of nuclear waste disposal including open and closed circuit (e.g. impact of pore water on the rate of migration properties of these two radionuclides). To this purpose it is proposed to set up experimental regimes that encompass the diffusivity of $Cs^+$ and $Sr^{2+}$ (both internal and external) of the polymeric matrix, comparison of the diffusivity rates with OPC/blast furnace slag formulations, and identification of any ion exchange processes taking place within the different matrices.

Challenges for the application of geopolymers as nuclear waste forms are: 1. β and γ radiation of Cs-137 and Sr-90 cause heat generation and radiolysis. 2. Possible contact with corrosive media in the repository. 3. Treatment of large amounts of nuclear waste necessary. This compares to the special properties of geopolymers: I. Heat and fire resistance up to 1000°C. II. The negative charge of the $[AlO_4]^-$ tetrahedra is balanced by alkaline or alkaline earth cations which in turn enables structural incorporation. III. High acidic and alkaline resistance. IV. High freeze-thaw resistance. V. Simple production even on a large scale. VI. Less $CO_2$ emissions during production compared to Ordinary Portland Cement (OPC).

For this project we decided to start with metakaolin-based geopolymers that show the following general composition:

$M_{2/z}O \cdot Al_2O_3 \cdot y\ SiO_2 \cdot w\ H_2O$,
with $M^{z+}$ = $Na^+$, $K^+$, $Rb^+$, $Cs^+$, $Ca^{2+}$, $Sr^{2+}$ ($y$ = 2-35; $w$ = 5-20).
The basic building units are corner-linked [$AlO_4$] – [$SiO_4$] tetrahedra that form the base for larger three-dimensional networks (see Fig. 50):

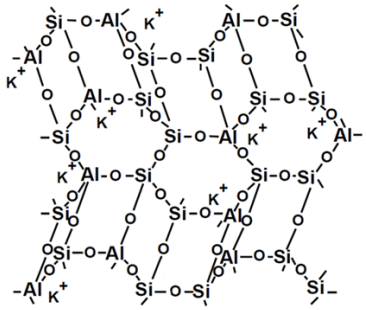

**Fig. 50: Structure model of a metakaolin-based geopolymer [12].**

The following chemical compositions are currently subject of our investigations:
$(K_{1-x}Cs_x)_2O \cdot Al_2O_3 \cdot 5\ SiO_2 \cdot 11\ H_2O$
$(Ca_{1-x}Sr_x)O \cdot Al_2O_3 \cdot 5\ SiO_2 \cdot 11\ H_2O$
The crucial question is whether Cs and Sr can be incorporated permanently on regular structural positions or if they favor interstitial sites within channels and cavities. In order to answer this question several different compositions were synthesized under variable conditions, and the obtained samples were subsequently structurally investigated using different analytical techniques such as powder X-ray diffraction, Raman- and IR-spectroscopy, SEM and MAS-NMR, respectively.


**Fig. 51: A Varian 600/54 MHz premium shielded high resolution spectrometer (14.1 Tesla; Magic angle 54.7°) used for the MAS-NMR measurements shown in the next section.**

The MAS-NMR (Fig. 51) investigations are conducted in tight cooperation with the group of H. Heise (Institute ICS-6 of Research Center Jülich).

**Preliminary Results**

In the following some selected preliminary results are presented. Fig. 52 shows the Raman spectra

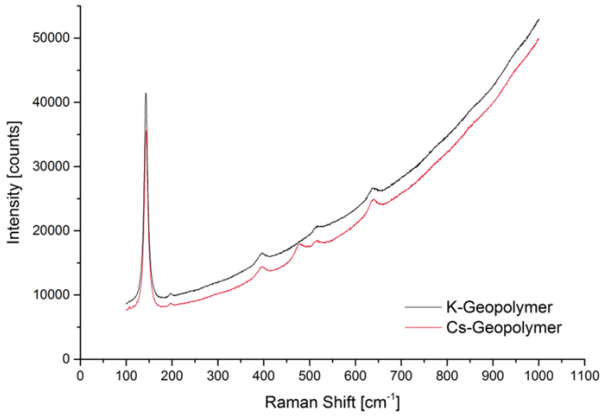


**Fig. 52: Raman spectra of two different geopolymers.**

of two different geopolymers, a pure K-geopolymer and a pure Cs-Geopolymer, respectively. Both samples show strong fluorescence and only weak signals originated by the geopolymer structure can be observed. This hampers the structural characterization of the short-range order of these mainly amorphous materials. The strong peak at low frequencies results from $TiO_2$ impurities of the educts and doesn't deliver usable structural information.

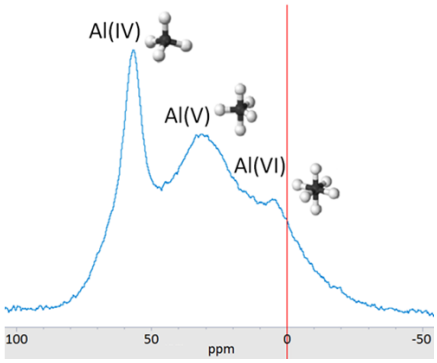


**Fig. 53: Al-27 MAS-NMR spectrum of a geopolymer containing 60 % K + 40 % Cs. Three different Al-O coordinations can be identified. The red line indicates zero chemical shift.**

The ideal geopolymer structure would exclusively comprise four-fold coordinated Al (see Fig. 50), but as can be easily seen from Fig. 53, also five-fold coordinated and even six-fold coordinated Al is part of the structure. The two latter Al-O coordinations are currently supposed to be artefacts of the educts that were used for synthesis, especially the six-fold coordination found within the crystal structure of Kaolin.

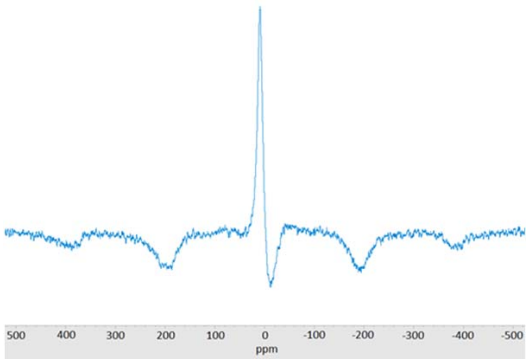


**Fig. 54: Cs-133 MAS-NMR spectrum of the identical geopolymer as shown in Fig. 53.**

The result of a Cs-133 MAS-NMR inversion recovery experiment (two pulses with different time in between) is shown in Figure 5. Rotation frequency of the sample was equal 15 kHz. This spectrum shows two different Cs-species: a stronger signal with spinning sidebands indicating an immobile species and a narrow less intense signal indicating a more mobile species. Additionally, Si-29 MAS-NMR experiments were performed (not shown here for reasons of space) that support the results of the Al-27 MAS-NMR experiments.

**Conclusions**

Powder X-ray diffraction is not applicable as it doesn't supply enough structural information because of the missing long range order in the geopolymer structure. Because of strong fluorescence the structural characterization by means of Raman spectroscopy is also strongly limited. Solid state MAS-NMR spectroscopy seems to be a good method to investigate the geopolymers' short range order.

The chemical composition of the educts has a significant impact on the structure of the received geopolymer.

Further structural characterization as well as investigations of geopolymers' properties will include (e.g. thermal analysis): 1. Investigation of the influence of different synthesis parameters, as well as irradiation, heat and pressure. 2. The syntheses of ($Na_{1-x}Cs_x$)- and ($Rb_{1-x}Cs_x$)-geopolymers and their respective characterization by means of MAS NMR.

Another option will be *in situ* HT-XRD experiments using Synchrotron radiation, in order to enable the calculation of radial distribution functions (RDF). This way the determination of interatomic distances and coordination numbers will be possible. More sophisticated structure models will be constructed via Reverse-Monte-Carlo simulations (RMC). In addition leaching experiments and irradiation experiments will be performed.

An important observation is the identification of two different Cs-species, with a dominating immobile species and only a minor amount of mobile Cs. As a preliminary result, most of the Cs can be found and immobilized on regular structural sites.

**References**

[1] N. Nakicenovic. Supportive measures and policies for developing countries: a paradigm shift. Background Paper for World Economic and Social Survey 2009 of the UN. 2009.

[2] Bundesamt für Strahlenschutz. url: http://www.bfs.de/de/endlager/abfaelle/abfallverursacher.html.

[3] W.J. Weber et al. »Materials Science of High-Level NuclearWaste Immobilization«. In: MRS Bulletin (2009).

[4] Bundesamt für Strahlenschutz. url: http://www.bfs.de/de/endlager/abfaelle/abfallarten.html.
[5] D.S. Perera et al. »Geopolymers for the immobilization of radioactive waste«. In: Scientific Basis for Nuclear Waste Management XXVIII. 2004.
[6] T. Hanzlicek, M. Steinerova, and P. Straka. »Radioactive Metal Isotopes Stabilized in a Geopolymer Matrix: Determination of a Leaching Extract by a Radiotracer Method«. In: Journal of the American Ceramic Society 89.11 (2006), S. 3541–3543.
[7] A.D. Chervonnyi, N.A. Chervonnaya. »Geopolymeric agent for immobilization of radioactive ashes after biomass burning«. In: Radiochemistry 45.2 (2003), S. 182–188.
[8] J. Magill et al. Karlsruher Nuklidkarte. 8. Aufl. Nucleonica, 2012.
[9] Live Chart of Nuclides: nuclear structure and decay data. International Atomic Energy Agency. https://www-nds.iaea.org/relnsd/vcharthtml/VChartHTML.html.
[10] Geopolymer Institute. url: http://www.geopolymer.org/science/introduction.
[11] J. Davidovits. »Geopolymers and geopolymeric materials«. In: Journal of Thermal Analysis (1989).
[12] J. Davidovits. »Geopolymers: Man-Made Rock Geosynthesis and the Resulting Development of Very Early High Strength Cement«. In: Journal of Materials Education 16(2&3) (1994), S. 91–139.
[13] V.F.F. Barbosa, K.J.D. MacKenzie, and Clelio Thaumaturgo. »Synthesis and characterization of materials based on inorganic polymers of alumina and silica: sodium polysialate polymers«. In: International Journal of Inorganic Materials 2.4 (2000), S. 309 –317.
[14] Geopolymer Institute. url: http://www.geopolymer.org/science/about-geopolymerization.
[15] Peigang He et al. »Effect of cesium substitution on the thermal evolution and ceramics formation of potassium-based geopolymer«. In: Ceramics International 36.8 (2010), S. 2395 –2400.
[16] S.L. Flegler, J.W. Heckma, and K.L. Klomparens. Elektronenmikroskopie: Grundlagen – Methoden – Anwendungen. Heidelberg, Berlin, Oxford: Spektrum, Akademischer Verlag, 1995.
[17] L. Reimer and G. Pfefferkorn. Raster-Elektronenmikroskopie. Berlin, Heidelberg, New York: Springer-Verlag Berlin Heidelberg, 1973.
[18] C. Colliex. Elektronenmikroskopie: Eine anwendungsbezogene Einführung. Stuttgart: Wissenschaftliche Verlagsgesellschaft mbH, 2008. isbn: 9783804723993.
[19] R.L. Frost, T.H. Tran, and J. Kristof. »The structure of an intercalated ordered kaolinite – a Raman microscopy study«. In: Clay Minerals 32 (1997), S. 587–596.

## 5.10. Complex chemistry of thorium in oxo-molybdate and oxo-tungstates systems

Bin Xiao[†,‡], Thorsten M. Gesing[§], Philip Kegler[†], and Evgeny V. Alekseev[†,‡,*]

†Institute for Energy and Climate Research (IEK-6), Forschungszentrum Jülich GmbH, 52428 Jülich, Germany

‡Institut für Kristallographie, RWTH Aachen University, 52066 Aachen, Germany

§Chemische Kristallographie fester Stoffe, Institut für Anorganische Chemie, Universität Bremen, Leobener Straße, D-28359 Bremen, Germany

**Introduction**

In the past two years (2013-2014), the group "Solid state chemistry of actinides" has been focused on the phase exploration and characterization with U and Th as modelling elements for actinides in high and low valence states. This work mainly focuses on the synthesis and physicochemical properties characterization of the novel actinide compounds (U and Th) composed from oxo-salts based on tri-, four-, five- and hexavalent elements (B, P, As, S, Se, Te, Mo and W). The structural information is the basis and the most important prerequisite for all physiochemical properties. Our aim is to understand and try to establish a structure-properties relationship in order to collect enough information for better understanding the coordination behavior of actinide compounds. Based on this, we have already obtained more than 50 new phases for the thorium molybdates and tungstates.[1-4] In our lab, we mainly use four kinds of methods, that is, room-temperature slow evaporation method, mild-hydrothermal method, high-temperature solid-state synthesis method and high-temperature and high-pressure method to synthesize the actinide compounds. Actinide compounds including hexavalent cations such as Se, Cr and Mo have attracted considerable attentions because they play a significant role in nuclear waste management and safety assessment (ENREF2). The chemical reaction between these fission products and actinide elements may lead to the formation of complex compounds, which can cause the deformation of the fuel and in turn to affect the fuel behavior.

Remarkable achievement on synthesis and structural characterization of actinides containing hexavalent cations have been gained over the past few decades, especially in the field of uranium (VI) chemistry for both minerals and synthetic phases. On the contrary, sparse studies have been conducted on low-valent actinides such as Th(IV), Np(IV) and Pu(IV) within the compounds containing hexavalent cations. In is clear that their chemical properties are very differently from those of U(VI) counterparts. These actinide compounds are interesting due to their diverse and complex structural features, which are influenced by a number of factors including a rich topological geometry, the diverse combinations and many possible ways of oxo-polyhedral linkages. Based on this, using high-temperature solid-state and hydrothermal synthetic methods, we have obtained and systematically investigated a large family of novel inorganic thorium compounds containing hexavalent cations (Se, Cr, Te, W, Mo). The structural dimensionality among these compounds ranges from finite clusters through chains and sheets to framework. All these hexavalent cations are typically coordinated with four O atoms, creating a $\boldsymbol{T}O_4$ tetrahedral (T = Se, Cr, Te, W, Mo) configuration. The $\boldsymbol{T}O_4$ tetrahedra can further connect through corner-, edge-, or face-sharing manners with actinide polyhedra to create clusters, one-dimensional (1D) chains, two-

dimensional (2D) sheets and three-dimensional (3D) framework structures. In the following we briefly presented the main achievement in two oxo-salt families with Th(IV) and these are thorium molybdates and tungstates.

**I. Thorium molybdates family**

Our efforts to exploir the new phases and their properties in the thorium molybdate family resulted in a previously unknown low-temperature $ThMo_2O_8$ polymorph a monoclinic-$ThMo_2O_8$. Its crystal structure can be viewed as a 3-dimensional (3D) framework constructed from $ThO_8$ antiprisms and $MoO_4$ tetrahedra (Fig. 55).

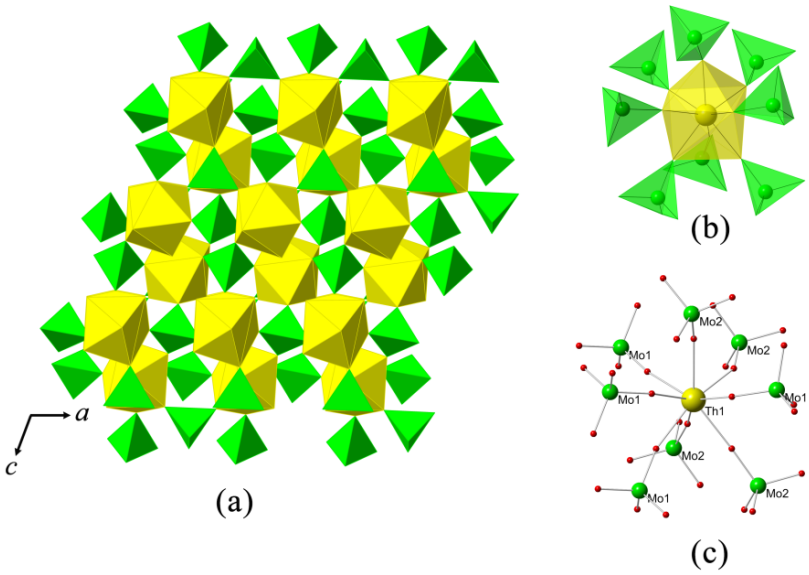


**Fig. 55: (a) View of the structure of monoclinic-$ThMo_2O_8$. (b, c) The local coordination environment around Th site. Th is shown in yellow, molybdenum in green and oxygen atoms are in red.**

This is a third $ThMo_2O_8$ polymorphic modification obtained under ambient condition. $ThMo_2O_8$ was first reported by *Freundlich* and *Pagès* in 1969 as the orthorhombic phase ($\alpha$-$ThMo_2O_8$).[5] The single crystal research of this phase was performed by *Thoret*[6], and further structural studies were carried out by *Cremers et al*[7]. The orthorhombic-$ThMo_2O_8$ is isostructural to $\gamma$-$UMo_2O_8$ and $PuMo_2O_8$ where the Th atoms are coordinated to eight oxygen atoms belonging to $MoO_4$ tetrahedra[8]. Later, *Larson et al* reported the structure of trigonal $ThMo_2O_8$ ($\beta$-$ThMo_2O_8$).[9] Following on this, very recently, *Orlandi et al.* have discovered the first two natural thorium molybdate hydrates, $Th(MoO_4)_2{\cdot}3H_2O$ (ichnusaite) and $Th(MoO_4)_2{\cdot}H_2O$ (Nuragheite), respectively.[10,11] Unlike the orthorhombic-$ThMo_2O_8$ which involves Th only in an eightfold square antiprismatic coordination, the Th atoms occur in both six- and nine-coordination in hexagonal-$ThMo_2O_8$. The monoclinic to orthorhombic and hexagonal to orthorhombic phase transitions happen at very similar temperature around 840 K (Fig. 56).

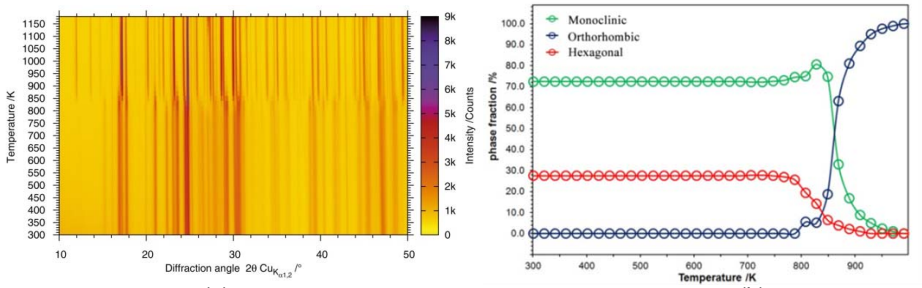


**Fig. 56: (a) Temperature-dependent X-ray powder pattern given as 2D-plot and showing monoclinic and hexagonal phases transformation to the orthorhombic one. (b) phases conversion as a function of temperature**

Using high-temperature/high-temperature method (P at around 3.5 GPa), we obtained a another HT/HP-orhtorhombic $ThMo_2O_8$ polymorph with crucial change in its density and structure. The density is around 5 g/cm$^3$ for the ambient pressure $ThMo_2O_8$ polymorphs. It, however, increases to nearly 5.9 g/cm$^3$ at high pressure condition. The nearly 20% of increase in density from ambient to high-temperature high pressure polymorphs is obviously associated with the change of atomic coordination and its connections, which is illustrated in Fig. 57 All the Th polyhedra are separated from each other among three ambient polymorphs. They are, however, connected together via face-sharing at high-pressure condition. As a result, the Th-Th bond distance for HT/HP-orthorhombic-$ThMo_2O_8$ is quite short, only 4 Å compared with that of the ambient polymorphs (6 Å). Similarly, for Mo polyhedra, instead of being isolated with each other in the ambient condition, they form a corner-sharing chain with much short Mo-Mo distance in the high-pressure status. Because of such huge structural changes, the HT/HP polymorph is stable after pressure release to ambient conditions.

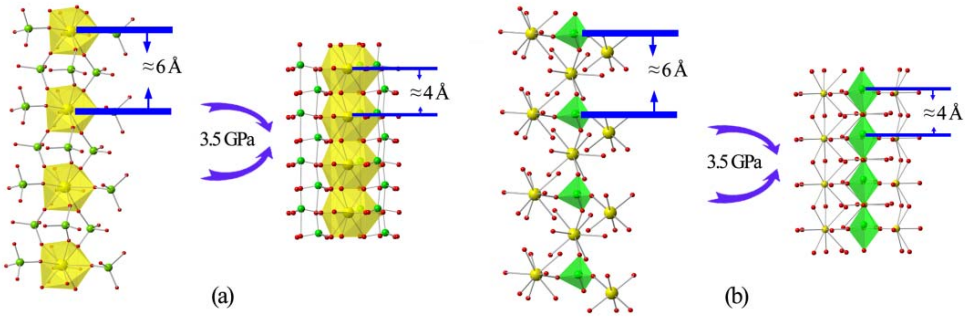


**Fig. 57: The nature of high-temperature/high-pressure induced phase transition. (a, b) Th and Mo polyhedral geometries change among the ambient and high-pressure (3.5 GPa) condition. Th is shown in yellow, molybdenum in green and oxygen atoms are in red.**

It is also noteworthy that there is a close structural resemblance between newly obtained $Nd_2Th_3(MoO_4)_9$ and hexagonal-$ThMo_2O_8$. Both compounds have similar unit-cell parameters. The *a* and *b* parameters of $Nd_2Th_3(MoO_4)_9$ is shorter than those of hexagonal-$ThMo_2O_8$ and this shortening can be explained by including smaller size of $Nd^{3+}$ cations compared to $Th^{4+}$.

Fig. 58 show polyhedral representations of both compounds. The similarity is best shown by projecting $Nd_2Th_3(MoO_4)_9$ and hexagonal-$ThMo_2O_8$ along each crystallographic *c*-axis. However, the further structural analysis reveals that all the six-coordinated sites ($NdO_6$ octahedra) in $Nd_2Th_3(MoO_4)_9$ are connected together through face-sharing manner while the corresponding sites ($ThO_6$ octehedra) observed in hexagonal-$ThMo_2O_8$ are completely separated. (Fig. 58 (c) and (d) respectively). Because of this, the associated Nd-Nd bond distance in $Nd_2Th_3(MoO_4)_9$ is remarkably short, only around 3.1 Å. The fact that $Nd_2Th_3(MoO_4)_9$ and hexagonal-$ThMo_2O_8$ are based on similar structural framework while containing different cations indicates the $Th^{4+}$ cations can be partially substituted by other trivalent ions while keeping the same structural skeleton. This means such framework has the ability to host diverse cations of various radii as well as valence without considerable geometric parameters change. The case of the $Nd_2Th_3(MoO_4)_9$ demonstrates a potential possibility of An(III) ($Am^{3+}$, $Cm^{3+}$ and etc.) inclusion in to structures of An(IV) molybdates.

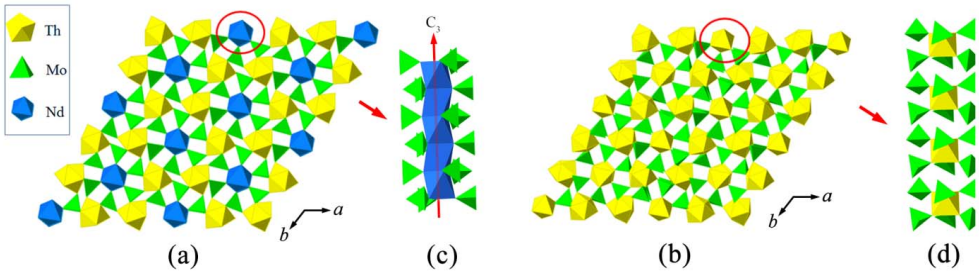


**Fig. 58: Comparison of structures observed in $Nd_2Th_3(MoO_4)_9$ and hexagonal-$ThMo_2O_8$, respectively. (a and b) The polyhedral representations in $Nd_2Th_3(MoO_4)_9$ and hexagonal-$ThMo_2O_8$, respectively. (c) face-sharing Nd-Nd chain in $Nd_2Th_3(MoO_4)_9$. (d) Isolated $ThO_6$ octahedra in hexagonal-$ThMo_2O_8$.**

We also studied the effects of alkali and alkali-earth elements presence in the systems with Th and molybdenum. As a result, we obtained and characterized several series of novel Th based phases. As an example, four thorium rubidium molybdates, that are, $Rb_8Th(MoO_4)_6$, $Rb_2Th(MoO_4)_3$, $Rb_4Th(MoO_4)_4$ and $Rb_4Th_5(MoO_4)_{12}$ were obtained via high-temperature solid-state reactions. All of them are constructed from $MoO_4$ tetrahedra and $ThO_8$ square anti-prisms. However, these compounds adopt the whole range of possible structure dimensionalities from 0D to 3D: finite clusters, chains, sheets and frameworks, given in Fig. 59. $Rb_8Th(MoO_4)_6$ crystallizes in zero-dimension containing clusters of $[Th(MoO_4)_6]^{8-}$. $Rb_2Th(MoO_4)_3$ is formed based upon one-dimensional chains with configuration units $[Th(MoO_4)_3]^{2-}$. Two-dimensional sheets occur in compound $Rb_4Th(MoO_4)_4$ and three-dimensional framework with channels formed by thorium and molybdate polyhedra are observed in $Rb_4Th_5(MoO_4)_{12}$. Besides, three cesium thorium molybdates $Cs_2Th(MoO_4)_3$, $Cs_2Th_3(MoO_4)_7$ and $Cs_4Th(MoO_4)_4$ were also synthesized *via* the high-temperature solid-state method. The thorium-molybdate $[Th(MoO_4)_3]^{2-}$ chains in $Cs_2Th(MoO_4)_3$ are topologically related to those in $K_2Th(MoO_4)_3$, an example of a scheelite related $CaWO_4$ structure which is a well-known structure type accommodated by a wide range of inorganic compounds.

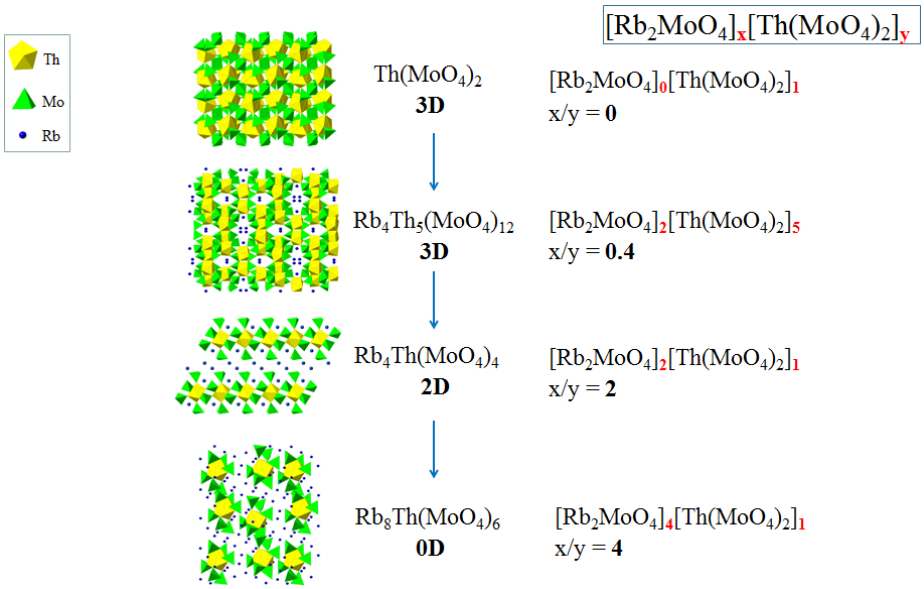


**Fig. 59: Dimensionality reduction in Rb thorium molybdates.**

Compound $Cs_2Th_3(MoO_4)_7$, with 3 different Th polyhedral environments $ThO_7$, $ThO_8$ and $ThO_9$, is indeed an unique case in the chemistry of thorium. The channels existing in $Cs_2Th_3(MoO_4)_7$ compound depicted in terms of tubular building units can be topologically transformed by regular honeycomb-shaped hexagons.

**II. Thorium tungstates family**

New families of the thorium compounds – tungstates were studied. We selected $A_6Th_6(WO_4)_{14}O$ (A = K and Rb) as an example of its complexity. The structures of the phases are shown in Fig. 60. They are based on a rare dinuclear confacial bioctahedral $[W_2O_9]^{6+}$ core, encapsulated by $[Th_6W_7O_{45}(W_2O_9)]^{32-}$ cage with cross-section similar to the six-leafed lily. Typically, the $WO_x$ polydedra can be aggregated though corner- and edge-sharing connectivity to construct condensed oxotungstates but rarely crystallize in face-sharing structures, since the electrostatic repulsion between these highly charged metal centers keep them from moving close to each other. According to Pauling's rule, the presence of face sharing will lead to strong repulsive forces between the central cations of the polyhedra, therefore the more flexible configurations such as vertex- and edge-sharing become the overwhelming connections in the crystal chemistry of W(VI). It is a high likelihood that the special coordination geometries about the $[Th_6W_7O_{46}(W_2O_9)]^{32-}$ cage stabilize such uncommon $[W_2O_9]^{6-}$ bioctehedral polyhedra. Due to the extraordinary complex structures the studied family has unusual thermal behavior which was studied with high temperature X-ray diffraction. Generally, we demonstrated that the chemistry of thorium tungstates is more complex and diverse compare to the chemistry and structural the properties of their molybdenum analogues.

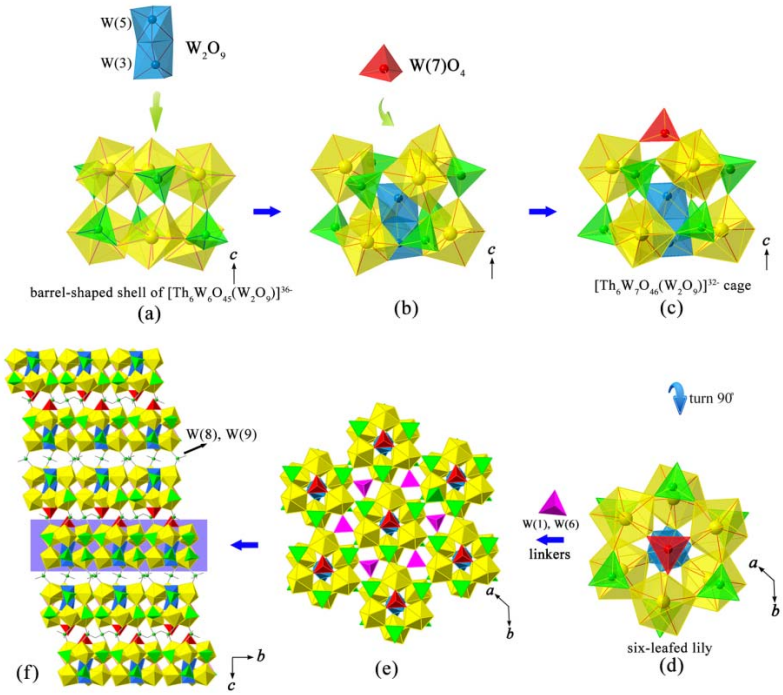


**Fig. 60: A schematic representation of fragments hierarchy in $K_6Th_6(WO_4)_{14}O$. $ThO_8$ antiprisms are represented in yellow, $WO_4$ tetrahedra in the barrel-shaped shell are in green, $W(7)O_4$ apexes are coloured in red and $WO_4$ linkers are in purple. The $[W_2O_9]^{6-}$ confacial cores are in light blue.**

## References


[1] Xiao, B.; Dellen, J.; Schlenz, H.; Bosbach, D.; Suleimanov, E. V.; Alekseev, E. V., *Cryst. Growth Des.* **2014,** *14*, 2677-2684.

[2] Xiao, B.; Gesing, T. M.; Kegler, P.; Modolo, G.; Bosbach, D.; Schlenz, H.; Suleimanov, E. V.; Alekseev, E. V., *Inorg. Chem.* **2014,** *53*, 3088-3098.

[3] Xiao, B.; Gesing, T. M.; Robben, L.; Bosbach, D.; Alekseev, E. V., *Chem. Eur. J.* **2015**, (accepted, doi:*10.1002/chem.201500500*).

[4] Xiao, B.; Langer, E.; Dellen, J.; Schlenz, H.; Bosbach, D.; Suleimanov, E. V.; Alekseev, E. V., *Inorg. Chem.* **2015,** *54*, 3022-3030.

[5] Freundlich, W. a. P., M *C. R. Acad. Sci.* **1969,** *269*.

[6] Thoret, J., *Rev. Chim. Minér.* **1974,** *11*.

[7] Cremers, T. L.; Eller, P. G.; Penneman, R. A., *Acta Crystallographica Section C* **1983,** *39*, 1165-1167.

[8] Krivovichev, S. V.; Burns, P. C., *Doklady Akad. Nauk* **2004,** *49*, 76-77.

[9] Larson, E. M.; Eller, P. G.; Cremers, T. L.; Penneman, R. A.; Herrick, C. C., *Acta Crystallographica Section C* **1989,** *45*, 1669-1672.

[10] Orlandi, P.; Biagioni, C.; Bindi, L.; Merlino, S., *Am. Mineral.* **2015,** *100*, 267-273.

[11] Orlandi, P.; Biagioni, C.; Bindi, L.; Nestola, F., *Am. Mineral.* **2014,** *99*, 2089-2094.

## 5.11. Predicting properties of ceramic waste forms from first principles

Piotr M. Kowalski, George Beridze, Yan Li and Yaqi Ji
Corresponding author: p.kowalski@fz-juelich.de

**Abstract**
Monazite- and pyrochlore-type ceramics are considered as potential host matrices for the immobilization of radionuclides inside a deep-geological disposal site. There is actively ongoing research efforts aimed into characterization of these materials and understanding their behavior under disposal conditions. However, experimental methods have limitations, for instance because of activities of the samples, and are often restricted to the specific laboratory conditions which may not always resemble the ones expected in a repository. We thus complement the experimental research by investigation of various properties of ceramic waste forms using modern computational resources and methods of applied computational chemistry and materials science. Among simulated materials properties are the structural parameters, the excess enthalpies of mixing, the heat capacities, the atoms threshold displacement energies and the energetics of defects formation. The obtained results are important for the assessment of the thermodynamical stability and radiation damage resistance of novel nuclear waste forms.

**Introduction**
Over the last two decades the computational methods of quantum chemistry have been successfully applied in various research fields in order to study the properties of minerals and fluids of chemically complex compositions. They are also used for investigation of materials considered for nuclear waste management [1]. Here we discuss applications of atomistic modeling to investigation of novel nuclear waste forms, namely the monazite- and pyrochlore-type ceramics. First, we discuss the correct ab initio approach which is fundamental for reliable atomistic modeling of these f-materials. Having established a good computational methodology we have then simulated various properties of the ceramics, including the excess properties of mixing, the heat capacities, the threshold displacement energies and the energetics of defect formation. All these properties are important for characterization of the nuclear waste forms and some of the information is only accessible by atomistic simulations.

**Materials and Methods**
Because of its feasibility allowing for computation of chemically complex systems containing hundreds of atoms, Density Functional Theory (DFT) is the most common ab initio method used in computational materials science [2]. However, the applicability of standard DFT to actinide-bearing materials is often questionable.

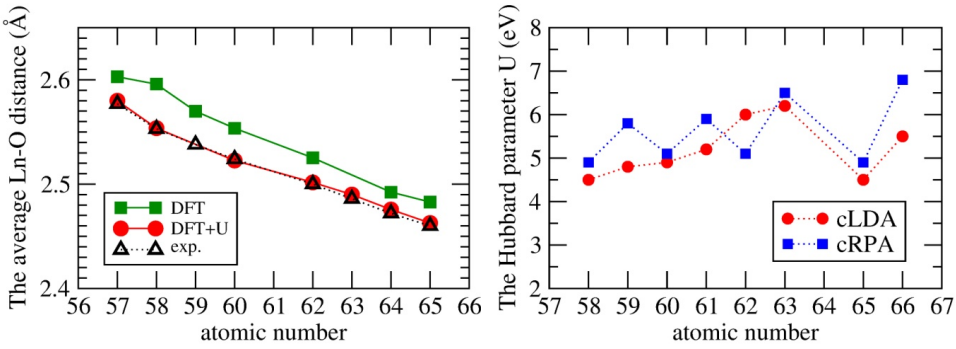


**Fig. 61. Average *Ln*-O distance predicted by DFT (PBE) [27], DFT+*U* with the Hubbard U parameter derived using the linear response method of [10], and measured experimentally. Right: the Hubbard U parameter computed with the linear response (constrained local density approximation, cLDA) and cRPA methods for $Ln_2O_3$.**

For instance, the $AnO_2$ solids (*An*=U, Np and Pu) are predicted to be metals, while these materials are insulators [3]. The enthalpies of reactions involving actinide-bearing molecular complexes are often highly overestimated [4]. Therefore, more accurate hybrid-functionals DFT or post Hartree-Fock methods such as MP2, CCDT or CI [5] are often suggested as an alternative computational method. However, due to their computational intensity, these methods cannot be currently applied to systems larger than a few tens of atoms. This would prohibit ab initio atomistic simulations of materials of interest for nuclear waste management. Recently, we found that the DFT+*U* method, which is a simple modification of DFT that accounts for electronic correlations, with the Hubbard *U* parameter derived *ab initio* results in good description of structures and energetics of uranium-bearing molecular compounds and solids [6], and monazite- and pyrochlore-type ceramics [7,8]. In Fig. 57 we show the excellent performance of DFT+*U* method for Ln-O distances. In these calculations we used PBEsol exchange-correlation functional [9] and the Hubbard *U* parameters were derived using the linear response method [10]. This excellent result was obtained by considering variation of the Hubbard U parameter along the lanthanide-series, which is illustrated in Fig. 61. Recently, we computed these parameters with a different method, the constrained random phase approximation (cRPA) [11], and obtained values that are consistent with the linear response calculations, which is shown in Fig. 61. The studies of ceramic materials revealed that DFT calculations performed using pseudopotentials with f-electrons frozen in the core can results in better agreement with DFT+*U* method than DFT when f-electrons are treated explicitly [7]. Since such an approach is computationally very stable we used it in subsequent calculations of some materials properties.

The *ab initio* calculations were performed with quantum-espresso DFT plane wave code (www.quantum-espresso.org), which uses ultrasoft pseudopotentials to represent core electrons [12]. The energy cutoff was set at 50 Ry. In these studies, along with the standard generalized gradient approximation (GGA) functionals, such as the PBE [13] and PBEsol [9], we used the DFT+*U* method, which utilizes a Hubbard model to account for a strong on-site coulomb repulsion between *f*-electrons [10]. The Hubbard *U* parameter was determined self-consistently for each specific compound using the linear response [10] or cRPA methods [11].

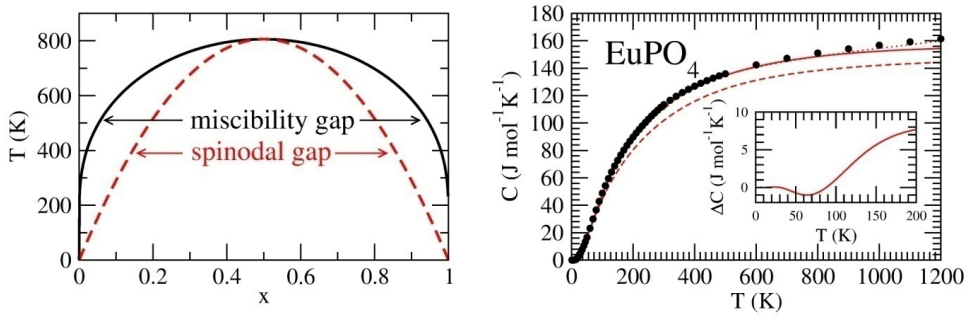


**Fig. 62: Left: The miscibility and spinodal gaps predicted for $La_{(1-x)}Eu_xPO_4$ solid solution. Right: Heat capacities of $LaPO_4$ and $EuPO_4$ monazites. The lines represent the calculations using quasiharmonic approximation (solid), contribution from the lattice vibrations only (dashed) and results corrected for anharmonic effects (dotted). Points represent the experimental data. All the data are taken from [7] and references cited in that paper. The insert shows the low temperature difference between heat capacities of $EuPO_4$ and $LaPO_4$.**

## Results and Discussion

### Excess thermodynamic properties of monazite-type solid solutions

One important aspect of a nuclear waste form material is its ability to form a stable solid solution with radionuclides. The Margules interaction parameter, W, is an important indicator of the thermodynamical stability of a solid solution [14]. In case of regular solid solution, such as monazite-type solid solutions, the enthalpy of mixing is given as $H^E = Wx(1-x)$ [15]. The miscibility gap, indicating demixing, forms if $W > 2RT$, where $R$ is the gas constant and T is the temperature [14]. Recently we have computed the interaction parameters for a series of $La_{(1-x)}(Ln,An)_xPO_4$ solid solutions and concluded that $W$ [kJ/mol] = 0.618 ($\Delta V$ [$cm^3$/mol])$^2$, where ΔV is the difference in volumes of the solution endmembers [16]. We found that this relationship holds for both lanthanide and actinide substituting cations, which also indicates that lanthanides are good surrogates for investigation of the properties of actinide-bearing monazites. Our results indicate that only certain solid solutions, including $La_{(1-x)}Pu_xPO_4$ are stable at ambient conditions. For most of the compositions a miscibility gap forms even at higher temperatures. One example is the $La_{(1-x)}Eu_xPO_4$ solid solution. For this case we got W = 13.5 kJ/mol, which indicates demixing at relatively high temperature. The miscibility gap for this solid solution is illustrated in Fig. 62. Below T~800 K a wide miscibility gap forms, with broad region of definitive instability indicated by the spinodal gap. Since accurate values of the interaction parameters are extremely difficult to obtain by experimental techniques (see [15]), only atomistic modeling simulations can provide this useful information that is needed for the assessment of novel waste forms stability.

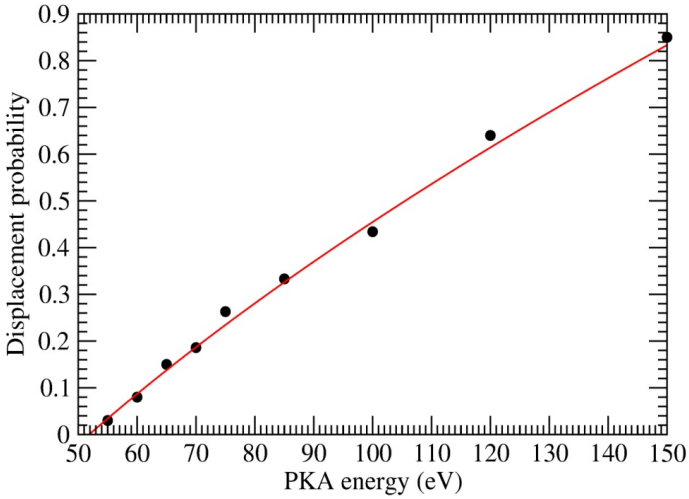


**Fig. 63: The probability of *Ln* in $LaPO_4$ for La PKA. The solid line is the fit using Eq. (3).**

**Heat capacities of monazite-type ceramics**

Another thermodynamic parameter important in the assessment of the stability of a nuclear waste form is the heat capacity. Recently, we have computed heat capacities of a series of lanthanide- and actinide- monazites [17]. Comparison of computed and measured heat capacities of $EuPO_4$ is given in Fig. 62. We obtained an excellent match to the experiment for $LnPO_4$ monazites which allowed us to conclude that two major contributions to the heat capacity of the monazite-type ceramics are the lattice vibrations and the thermal excitation of the f-electrons given by the Schottky contribution [18]. With atomistic modeling we have been able to explain the experimentally seen variation of the heat capacities along the lanthanide series as well as the subtle low temperature difference in the heat capacities of $LaPO_4$ and $EuPO_4$, which has been recently observed experimentally [19].

**Simulation of radiation damage**

The threshold displacement energy, $E_d$, is an important parameter that describes the radiation damage in a material. It describes the minimal energy required to dislocate an atom from its original position inside the crystalline net. The $E_d$ values are used to simulate the extent of radiation damage of materials with codes such as SRIM [20]. The $E_d$ of primary knock-out atom (PKA) depends on the local structure of a material. We performed simulations of $E_d$ of La cation in $LaPO_4$ monazite by applying initial velocities to PKA lanthanum atom in 100-400 randomly chosen directions. Considering such simulations are computationally very intensive for ab initio methods, we fitted a set of force-fields describing interatomic interactions in a way that they reproduce ab initio structures and energetics of monazites. Then we performed NVE molecular dynamics simulation runs using classical molecular dynamics LAMMPS code [21] for 5 ps. The initial and final positions of PKA atoms were compared in order to derive the probability of a displacement as a function of initial energy. The results of such simulations are illustrated in Fig. 63. When the energy was smaller than 50 eV no displacements were observed indicating that this energy is too low to dislocate a La cation. On the other hand, for energies larger than

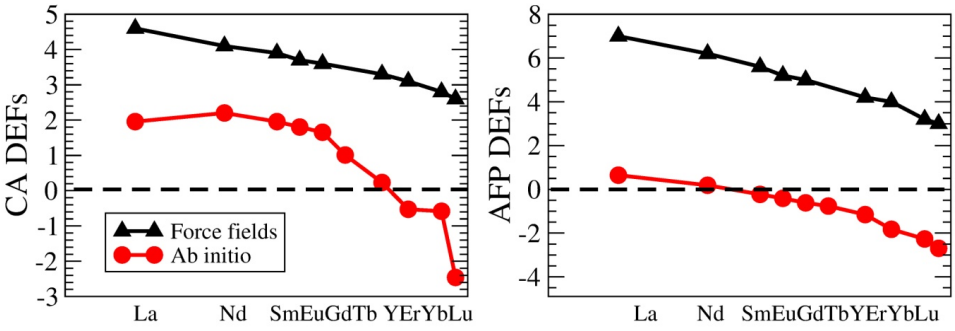


**Fig. 64: The force field [25,26] and *ab initio* prediction of the cation antisite (CA) and anion Frenkel pair (AFP) defect formation energies (DFEs) in $Ln_2Zr_2O_7$ pyrochlores.**

100 eV most of the events resulted in dislocations. The observed probabilities are described by a simple function [22]:

$$P = \frac{1}{\beta}(E^{\alpha} - E_d^{\alpha})$$

The obtained values of $E_d$, α, β are 51.85 eV, 9.48 and 0.57, respectively. Our results thus show that $E_d$ of lanthanum in La-monazite is ~52 eV, which is a relatively high value. It is comparable to $E_d$ of Ti in rutile [23].

**Defect formation energies in $Ln_2Zr_2O_7$ pyrochlores**

Certain pyrochlores under irradiation transfer to a disordered fluorite, which is a solid phase, rather than becoming amorphous. This makes them interesting materials for immobilization of radionuclides [24]. However, the origin of this order-disorder transition of selected pyrochlores is not well understood. The determination of the energetics of simple defects formation in pyrochlore is a first step in a quest to understand the process. We thus performed *ab initio* calculations of cation-antisite and anion Frenkel pair defect formation energies in pyrochlores [8]. The results for $Ln_2Zr_2O_7$series are provided in Fig. 64 together with the results of previous force-field-based atomistic modeling [25,26]. As evident from Fig. 64, the previous calculations highly overestimated the defect formation energies by up to 6 eV. Also on the qualitative level, *ab initio* calculations reveal different trends along the lanthanide series. In general, the obtained defect formation energies correlate well with the stability field of pyrochlores. We found that the compositions that form disordered fluorite have negative anion Frenkel pair defect formation energies. This indicates that the diffusion of oxygen atoms is one of the factors leading to the disordering of selected pyrochlores and their subsequent transition to the disordered fluorite phase. More information on these studies is provided in [8].

**Conclusions**

Here we have presented an overview of our recent results of atomistic modeling of the monazite- and pyrochlore-type ceramics. We have shown that with an appropriate choice of the computational method the structural and thermodynamic properties of these materials

can be computed with computationally feasible DFT-based methods, especially with DFT+*U* method which performs very well for structures and energetics of monazites. We derived Margules interaction parameters for monazite-type solid solutions which allows for estimation of the thermodynamical stability of these ceramic waste forms. Modeling of heat capacities of the monazites allowed for identification of the two main processes contributing to the variation of the heat capacity along the lanthanide series as the lattice vibrations and the thermal excitation of *f*-electrons. Investigation of the energetics of defect formation in pyrochlore revealed that the compounds that form defective fluorite have negative anion Frenkel pair defect formation energies which suggest that easiness of oxygen diffusion is one of the factors responsible for transformation of pyrochlore of selected composition to disordered fluorite. The above examples show the importance of atomistic modeling as a complementary tool for investigation of properties of nuclear materials.

**Acknowledgments**

We acknowledge the computing time on RWTH Aachen cluster awarded through Jülich-Aachen research alliance (JARA-HPC).

**References**

[1] A. Chrones, M. J. D. Rushton, C. Jiang & L. H. Tsoukalas, Nuclear Wasteform Materials: Atomistic Simulation Case Studies. *J. Nucl. Mater.*, 441 (**2013**), 29-39.

[2] S. Jahn & P. M. Kowalski, Theoretical Approaches to Structure and Spectroscopy of Earth Materials. *Rev. Mineral. Geochem.*, 78 (**2014**), 691-743.

[3] X. D. Wen, R. L. Martin, T. M. Henderson & G. E. Scuseria, Density functional theory studies of the electronic structure of solid state actinide oxides: *Chem. Rev.*, 113 (**2013**), 1063.

[4] G. A. Shamov, G. Schreckenbach & T. N. Vo, A Comparative Relativistic DFT and ab Initio Study on the Structure and Thermodynamics of the Oxofluorides of Uranium(IV), (V) and (VI), *Chem. Eur. J.*, 13 (**2007**), 4932-4947.

[5] Ch. Hattig, „Beyond Hartree-Fock: MP2 and Coupled-Cluster Methods for Large SystemsComputational Nanoscience: Do It Yourself!", J. Grotendorst, S. Bluegel, D. Marx (Eds.), John von Neumann Institute for Computing, Julich, *NIC Series*, Vol. 31, (**2006**), 245-278.

[6] G. Beridze & P. M. Kowalski, Benchmarking the DFT+U Method for Thermochemical Calculations of Uranium Molecular Compounds and Solids. *J. Phys. Chem. A*, 118 (**2014**), 11797-11810.

[7] A. Blanca-Romero, P. M. Kowalski, G. Beridze, H. Schlenz & D. Bosbach, Performance of DFT+U Method for Prediction of Structural and Thermodynamic Parameters of Monazite-type Ceramics. *J. Comput. Chem.*, 35 (**2014**), 1339-1346.

[8] Y. Li, P. M. Kowalski, G. Beridze, A. Birnie, S. Finkeldei & D. Bosbach, Defect Formation Energies in $A_2B_2O_7$ Pyrochlores. *Scr. Mater.*, (**2015**). doi:10.1016/j.scriptamat.2015.05.010.

[9] J. P. Perdew, A. Ruzsinszky, G. I. Csonka, O. A. Vydrov, G. E. Scuseria, L. A. Constantin, X. Zhou & K. Burke, Restoring the Density-Gradient Expansion for Exchange in Solids and Surfaces, *Phys. Rev. Lett.*, 100 (**2008**), 136406.

[10] M. Cococcioni & S. de Gironcoli, Linear response approach to the calculation of the effective interaction parameters in the LDA+U method, *Phys. Rev. B*, 71 (2005), 035105.

[11] F. Aryasetiawan, K. Karlsson, O. Jepsen & U. Schönberger, Calculations of Hubbard U from first-principles. *Phys. Rev. B*, 74 (**2006**), 125106.

[12] D. Vanderbilt, Soft self-consistent pseudopotentials in a generalized eigenvalue formalism, *Phys. Rev. B*, 41 (**1990**), 7892.

[13] J. P. Perdew, K. Burke & M. Ernzerhof, Generalized Gradient Approximation Made Simple, *Phys. Rev. Lett.*, 77, (**1996**), 3865.

[14] P. Glynn. Solid-Solution Solubilities and Thermodynamics: Sulfates, Carbonates and Halides. *Rev. Mineral. Geochem.*, 40 (**2000**), 481–511.

[15] K. Popa, R. J .M. Konings & T. Geisler, High-temperature calorimetry of $(La_{1-x}Ln_x)PO_4$ solid solutions, *J. Chem. Thermodyn.*, 39 (**2007**), 236–239.

[16] Y. Li, P. M. Kowalski, A. Blanca-Romero, V. Vinograd & D. Bosbach, Ab Initio Calculation of Excess Properties of Solid Solutions. *J. Solid State Chem.*, 220 (**2014**), 137-141.

[17] P. M. Kowalski, G. Beridze, V. Vinograd & D. Bosbach, Heat Capacity of Lanthanide and Actinide Monazite-type Ceramics. J. Nucl. Mater., 464 (**2015**), 147-154.

[18] E. F. Jr. Westrum, Schottky Contributions in Chemical Thermodynamics. *J. Therm. Anal. Calorim.*, 30 (**1985**), 1209–1215.

[19] A. Thust, Y. Arinicheva, Y. E. Haussuehl, L. Bayarjagal, S. C. Vogel, S. Neumeier & B. Winkler, *J. Am. Ceram. Soc*., (**2015**), (accepted).
[20] RIM The Stoping and Range of Ions in Matter (http://www.srim.org).
[21] S. Plimpton, Fast Parallel Algorithms for Short-Range Molecular Dynamics, *J. Comput. Phys*.,117 (**1995**), 1-19, http://lammps.sandia.gov.
[22] M. Robinson, N. A. Marks & G. R. Lumpkin, Structural dependence of threshold displacement energies in rutile, anatase and brookite $TiO_2$. *Mater. Chem. Phys*., 147 (**2014**), 311-318.
[23] M. Robinson, N. A. Marks, K. R. Whittle & G. R. Lumpkin, Systematic Calculaiton of threshold displacement energies: Case Study in Rutile. *Phys. Rev. B*, 85 (**2012**), 104105-104115.
[24] R. C. Ewing, J. W. Weber & J. Lian, Nuclear Waste Disposal—Pyrochlore Nuclear Waste Form for the Immobilization of Plutonium and “Minor” Actinides. *J. Appl. Phys*., 95 (**2004**), 5949.
[25] K. E. Sickafus, L. Minervini, R. W. Grimes, J. A. Valdez, M. Ishimaru, F. Li, K. J. McClellan & T. Hartmann, Radiation Tolerance of Complex Oxides. *Science*, 289 (**2000**), 748–751.
[26] L. Minervini, R. W. Grimes & K. E. Sickafus, Disorder in Pyrochlore Oxides. *J. Am. Ceram. Soc*., 83 (**2000**), 1873–1878.
[27] J. R. Rustad, Density Functional Calculations of the Enthalpies of Formation of Rare-earth Orthophosphates. *Am. Mineral*., 97 (**2012**), 791–799.

# 5.12. Thermal neutron die-away times in large samples irradiated at the MEDINA facility

Frank Mildenberger, Eric Mauerhofer
Corresponding author: e.mauerhofer@fz-juelich.de

**Abstract**
In order to measure delayed gamma-rays without appreciable interferences of prompt gamma-rays, the specific thermal neutron-die-away times in large samples at the MEDINA facility are studied. The thermal neutron die-away times range between 2 and 5 ms according to the irradiated materials.

**Introduction**
In a previous paper [1] we reported on the development of an analytical facility called MEDINA (Multi Element Determination based on Instrumental Neutron Activation) for the determination of non-radioactive elements in 200-l radioactive waste drums by Prompt- and Delayed-Gamma-Neutron-Activation-Analysis (P&DGNAA) using a 14 MeV neutron generator. Additional information about the waste composition could be derived measuring delayed gamma-rays from short-lived fast and thermal neutron activation products (e.g. $^{16}$N, $^{24m}$Na, $^{27}$Mg, $^{28}$Al, $^{52}$V, $^{207m}$Pb). The sensitive detection of these delayed gamma-rays requires that thermal neutrons have almost vanished. Therefore the thermal neutron die-away time has to be known in order to achieve an optimal discrimination between prompt and delayed gamma-ray spectra acquisition and thus a good signal to background ratio for the measurement of delayed gamma-rays. It is a fundamental parameter in the application of activation techniques with pulsed neutron sources such as the Differential Die-away Analysis for the assay of fissile materials in nuclear waste or in cargo [2,3,4]. In this work, thermal neutron die-away times are investigated by measuring the prompt gamma-ray spectra for different large samples.

**Measurements**
Further information on the MEDINA facility including the nuclear electronics used for the treatment of the detector signals and the acquisition of the gamma-ray spectra are given in [1]. The thermal neutron die-away times are determined by measuring (1) the gamma-ray spectra for the empty chamber, (2) for an empty 200-l steel drum, (3) for a 200-l steel drum filled with concrete and (4) filled with polyethylene. The concrete and polyethylene drum is composed of 76 cylindrical bodies (height: 20 cm, diameter: 11 cm) of each material placed concentrically in a 200-l steel drum. The weight of concrete and polyethylene is 195.5 kg and 120.8 kg respectively. The weight of the steel drum is 52.2 kg. Due to the voids the apparent density of the concrete matrix is 1.02 g cm$^{-3}$ and this of the polyethylene matrix 0.61 g cm$^{-3}$.
The neutron generator is operated in pulse mode with an acceleration voltage of 85 kV and a current of 40 µA corresponding to a neutron emission of about 8 $10^7$ ns$^{-1}$. The length of the neutron pulses is set to 250 µs. The repetition period of the neutron pulses is set to 5 ms. The counting time between the neutron pulses is set to $t_c$ = 500 µs while the waiting period $t_d$ between the end of the neutron pulses and the start of the counting is varied from 0 to 4500 µs for the empty chamber, the empty drum and the drum filled with concrete by steps of 500 µs. For the drum filled with PE the counting is varied from 0 to 3000 µs by steps of 250 µs for the first 1 ms and afterwards with steps of 500 µs.

The prompt gamma-rays of $^{1}$H (2223.2 keV), $^{10}$B (477.6 keV), $^{12}$C (3683.9 and 4945.3 keV), $^{28}$Si (3538.9 keV), $^{35}$Cl (1164.8 keV), $^{40}$Ca (1942.6 keV) and $^{56}$Fe (352.3, 691.9 and 7631.5 keV) emitted from different parts of the facility [1], from the empty drum and from the drum filled with concrete or polyethylene are considered for the determination of the thermal neutron die-away times.

**Results and Discussion**

The resulting values of the die-away times of the different measurements are given in Tab. 2. The time dependence of the count rate of the gamma-rays is shown in Fig. 65 for the drum filled with concrete and the drum filled with polyethylene.

**Tab. 2: Thermal neutron die-away times $\Lambda$ for the empty chamber, empty drum and the drum filled with concrete or polyethylene (PE).**

| Isotope | Eγ (keV) | Empty chamber | Empty drum | Drum filled with concrete | Drum filled with PE |
|---|---|---|---|---|---|
| | | $\Lambda$ (ms) | $\Lambda$ (ms) | $\Lambda$ (ms) | $\Lambda$ (ms) |
| $^{1}$H | 2223.2 | - | - | - | 0.59 ± 0.04 |
| | | 3.16 ± 0.16 | 2.59 ± 0.11 | 2.34 ± 0.05 | 2.32 ± 0.07 |
| $^{10}$B | 477.6 | 4.56 ± 0.20 | 3.56 ± 0.25 | 2.37 ± 0.04 | 2.72 ± 0.19 |
| $^{12}$C | 3683.9 | 5.30 ± 0.22 | 3.55 ± 0.10 | 2.83 ± 0.07 | 3.16 ± 0.06 |
| | 4945.3 | 5.25 ± 0.28 | 3.43 ± 0.09 | 2.77 ± 0.08 | 3.21 ± 0.05 |
| $^{28}$Si | 3538.9 | 2.71 ± 0.10 | - | 2.00 ± 0.02 | - |
| $^{35}$Cl | 1164.8 | 4.28 ± 0.13 | 3.54 ± 0.16 | 2.63 ± 0.06 | 2.92 ± 0.13 |
| $^{40}$Ca | 1942.6 | 3.26 ± 0.17 | 3.32 ± 0.22 | 2.21 ± 0.03 | 2.42 ± 0.06 |
| $^{56}$Fe | 352.3 | - | 3.28 ± 0.16 | 2.32 ± 0.05 | 2.46 ± 0.05 |
| | 691.9 | - | 3.39 ± 0.21 | 2.33 ± 0.06 | 2.36 ± 0.05 |
| | 7645.5 | 2.48 ± 0.09 | 3.25 ± 0.10 | 2.31 ± 0.06 | 2.44 ± 0.06 |
| Detector count rate | | 0.37 ± 0.06 | 0.32 ± 0.06 | 0.39 ± 0.03 | 0.38 ± 0.01 |
| | | 4.20 ± 0.09 | 3.07 ± 0.03 | 2.70 ± 0.04 | 2.72 ± 0.04 |

In the case of the empty chamber and the empty drum the count rate is decaying exponentially with a single constant for all gamma-rays over the entire range of time studied. The highest value 5.30 ms is obtained from the gamma-rays of $^{12}$C and is associated to the low absorption and high scattering of thermal neutrons in graphite. The gamma-rays of $^{1}$H lead to a lower die-away time of 3.16 ms which is representative for the behavior of the thermal neutrons in the CFRP-components containing a fairly amount of hydrogen (3%). The gamma-rays of $^{35}$Cl and $^{10}$B provide similar die-away times lying between those obtained for graphite and CFRP as they originate from the two materials. The lowest value of the die-away time 2.48 ms is obtained from the high energy gamma-ray of $^{56}$Fe for the steel housing of the neutron generator and is related to the high thermal neutron absorption of iron. The die-away times obtained from the gamma-rays of $^{28}$Si and $^{40}$Ca are difficult to interpret due to their different origins. However the fact that the values are about 50 % lower than the die-away time in graphite suggests a thermal neutron absorbing environment which could be the $^{6}$LiF detector shielding for silicon and the concrete ground floor for calcium. The presence of the steel drum in the empty chamber induces a homogeneous decay of the thermal neutron flux in the whole system with a mean die-away time of 3.32 ms, similar to that determined from the gamma-rays of $^{56}$Fe for the steel drum, 3.31 ms.

In the case of the drum filled with concrete two groups of gamma-rays with different behavior of the count rate time dependence are observed. The first group consists of the gamma-rays of $^{1}$H, $^{10}$B, $^{28}$Si and $^{40}$Ca mainly emitted from the concrete matrix whose count rates are

decaying exponentially with similar die-away times over the entire range of time studied. These data lead to a mean die-away time of 2.23 ms for concrete. The second group consisting of the $^{12}C$, $^{35}Cl$ and $^{56}Fe$ gamma-rays emitted from the facility and the steel drum shows first an increase of the count rate until 1 ms explained by due the perturbation of the thermal neutron energy distribution through the presence of the concrete matrix and secondly a single exponential decay of the count rate after about 1 ms. The thermal neutron flux in the steel drum decays with a die-away time of 2.32 ms similar to that of concrete and is 30 % lower than that observed for the empty drum. A mean die-away time of 2.41 ms may be assigned to the whole system which is 27 % lower than the value deduced for system with the empty drum.

For the drum filled with polyethylene the count rate of the gamma-ray of $^{1}H$ is described by a double exponential decay with a fast die-away time of 0.59 ms attributed to the rapid thermalization of fast neutrons in polyethylene and a slow-die away time of 2.32 ms which is comparable to that obtained for concrete. The count rates of the gamma-rays emitted from the facility and the steel drum show the same trend as previously observed for concrete, an increase until 1 ms followed by a single exponential decay. The die-away times obtained here are slightly higher by 6 % to 16 % than that determined for concrete due to the high scattering of thermal neutrons by hydrogen. The mean die-away time for the whole system is 2.67 ms and is 20 % lower than the value determined for the system with the empty drum.

In all cases the detector count rate undergoes a double exponential decay and the resulting die-away times are given in Tab. 2. The fast die-away times ranging 0.32 and 0.39 ms are almost independent of the material inside the irradiation chamber and represent probably the decay of the fast neutrons in the HPGe-detector as the gamma-rays of $^{71m}Ge$ and $^{75m}Ge$ induced by (n,2n)-reactions are observed in the spectra [1]. However the slow die-away times reflect well the presence of material inside the chamber and agree well with the corresponding values obtained from the gamma-rays count rates.

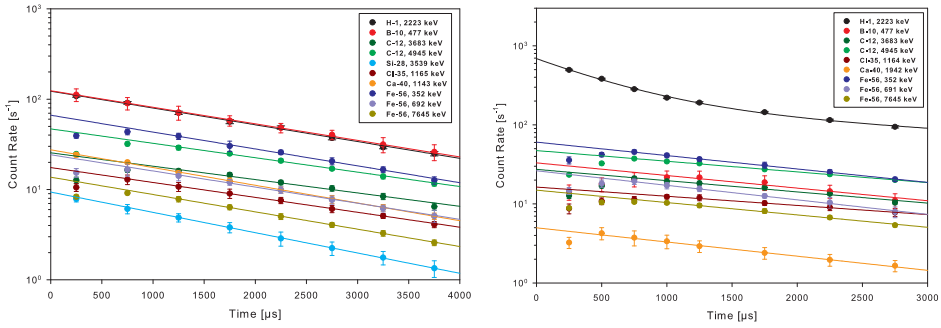


**Fig. 65: Time dependence of the count rate of the gamma-rays for the drum filled with concrete (left figure) and filled with polyethylene (right figure).**

## Conclusion

The chamber of the MEDINA facility ensures a long thermal neutron die-away time between 2 and 5 ms. Using in a conservative way the highest value of the die-away time measured for the system with the empty drum, 3.56 ms, the waiting time required to record the delayed gamma-ray spectra after the neutron pulses with a negligible prompt gamma-ray contribution is around 12 ms (about 97 % of the thermal neutrons have already vanished).

## References


[1] E. Mauerhofer, A. Havenith (2014) The MEDINA facility for the assay of the chemotoxic inventory of radioactive waste packages. J Radioanal. Nucl. Chem. DOI 10.1007/s10967-014-3210-2

[2] K.A. Jordan, T. Gozani, J. Vuljic (2008) Differential die-away analysis system response modeling and detector design. Nucl. Instr. and methods in physics research, DOI 10.1016/j.nima.2008.02.039

[3] K.A. Jordan, J. Vuljic, T. Gozani (2007) Remote thermal neutron die-away measurements to improve Differential Die-Away Analysis. Nucl. Instr. and methods in physics research, DOI 10.1016/j.nima.2007.04.089

[4] M. Yee Ryan, Shaw J. Timothy, Tsahi Gozani (2009) Thermal Neutron Die-Away Studies in a 14 MeV Neutron-Based Active Interrogation System. IEEE Transactions on Nuclear Science, DOI 10.1109/TNS.2009.2017373

## 5.13. Fast Neutron Radiography

Manuel Schumann[1], Eric Mauerhofer[1], G. Kemmerling[2], M. Willenbockel[2]

[1]Institute of Energy and Climate Research – Nuclear Waste Management and Reactor Safety, Forschungszentrum Jülich GmbH, 52425 Jülich, Germany
[2]Central Institute for Engineering, Electronics and Analytics – Electronics Systems, Forschungszentrum Jülich GmbH, 52425 Jülich, Germany

Corresponding author: e.mauerhofer@fz-juelich.de

**Introduction**

The accurate determination of the isotope specific activity content of radioactive waste drums by gamma-scanning requires knowledge of the waste matrix composition including the spatial distribution of internal shielding structures of unknown design. A correction for a non-uniform material density distribution may be achieved by using gamma-ray imaging with external $^{60}$Co or $^{152}$Eu transmission sources (state of the art) [1]. However $^{60}$Co or $^{152}$Eu may be present in the waste drums to be assayed rending difficult or impossible the determination of the gamma-ray attenuation properties of the waste matrix. Moreover $^{60}$Co and $^{152}$Eu emit low energy gamma-rays (< 1.5 MeV) which are largely absorbed by high density materials. Fast (14 MeV) neutron imaging may be an alternative to gamma-ray imaging due to the high penetration range of fast neutrons in thick and dense objects [2].
In this work we investigated the performance of a compact fast neutron radiography system using a 14 MeV neutron generator and an amorphous silicon flat panel linked to a plastic converter as imaging detector. The developed test facility for fast neutron imaging and the results obtained from the measurements of various materials are presented.

**Test facility for fast neutron imaging**

The experimental setup of the fast neutron radiography test facility is shown in Fig. 66. Fast neutrons with an energy of 14 MeV are produced by a deuterium-tritium fusion neutron generator (GENIE 16GT, Sodern) which is operated in continuous wave mode at a neutron emission of about $8.5 \cdot 10^7$ n s$^{-1}$. For radioprotection reasons the neutron generator is embedded in a 10 to 20 cm thick polyethylene-housing with a square aperture (l = 25.5 cm, h = 27 cm) at the tritium target location. Fast neutrons are indirectly detected with a $41 \times 41$ cm$^2$ amorphous silicon (aSi) photodiode flat-panel detector (XRD 1642 CP0, PerkinElmer) originally designed for X-ray radiography. The active detector area consists of $1024 \times 1024$ pixels with a pitch of 400 $\mu$m. For our purpose the original scintillator for X-ray radiography is replaced by a 3 mm thick polyvinyltoluene based plastic scintillator of type EJ-260 (Eljen Technology) covering the active detector area. EJ-260 emits green light (wavelength of maximum emission: 490 nm) and thus matches well the wavelength absorption range of aSi. The careful mounting of the plastic scintillator on the aSi was performed by the PerkinElmer company. The flat panel detector is positioned at a distance of 42 cm from the neutron source i.e. tritium target of the neutron generator. Objects for imaging are placed on a lift table. Neutron radiography is performed for 900 s corresponding to the acquisition of 450 frames at 2 s. After shutdown of the neutron generator an offset image is recorded during 200 s (100 frames at 2 s) for background correction.

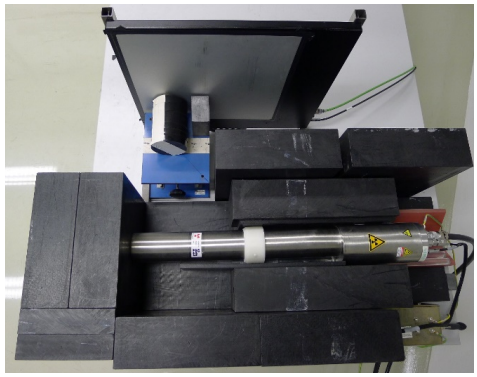

**Fig. 66: Experimental setup for neutron radiography with test samples of lead and PE. The upper part of the PE shielding is removed to show the neutron generator.**

**Fast Neutron Flux**

For simulation studies the fast neutron emission has to be known. The fast neutron flux is evaluated irradiating foils of aluminum (99.99 % Al, weight: 101 mg, area: 1.22×1.22 $cm^2$, thickness: 250 μm) and gold (99.95 % Au, weight: 135 mg, area = 1.18×1.18 $cm^2$, thickness: 50 μm). The foils are placed 30 cm in front of the neutron source and the irradiation time is 2 h. The activity of the radionuclides $^{24}Na$ ($T_{½}$ = 14.96 h) and $^{196}Au$ ($T_{½}$ = 6.318 d) induced by the fast neutron reactions $^{27}Al(n,\alpha)^{24}Na$ ($\sigma$ = 0.122 b) and $^{197}Au(n,2n)^{196}Au$ ($\sigma$ = 2.172 b) is determined by gamma-ray spectrometry with an HPGe-detector operated in a lead chamber as low level counting system. The distance between foils and HPGe-detector is 4 cm and the counting time 24 h. The detection efficiency of the counting geometry is derived from the measurement of a filter paper of same dimension as the foils on which a $^{152}Eu$ standard solution is dropped. The activities of $^{24}Na$ and $^{196}Au$ calculated from the counts of their respective gamma-rays at 1368.6 keV ($I\gamma$ = 100 %) and 355.7 keV ($I\gamma$ = 87 %) are 0.38 ± 0.06 Bq and 0.10 ± 0.02 Bq. The resulting mean value of the fast neutron flux is (1.4 ± 0.3) × $10^4$ n $s^{-1}$ $cm^{-2}$ and corresponds to a value of the neutron emission of (1.6 ± 0.3) × $10^8$ n $s^{-1}$ which is of the same order of magnitude than the value given by the supplier of the neutron generator.

**Neutron Radiography**

Fast neutron radiograph of a polyethylene cylinder and a lead block placed 1cm away from each other (Fig. 66) is shown in Fig. 67a. The polyethylene cylinder has a diameter of 10.5 cm and a length of 14.5 cm and lies horizontally on the lift table. The lead block has a height of 10 cm, a width of 5 cm and a length of 8 cm. The distance between the items and the flat panel is 0.5 cm. The lift table is adjusted so that the middle of the space between the items is aligned with the tritium target of the neutron generator. Both items are visible together with the plate of the lift table and a part of the polyethylene shielding of the neutron generator (upper and right part of the image). In order to obtain a better image of the items by eliminating in particularly the shadow image produced by the lift table a second radiograph is performed without the items and shown in Fig. 67b. This radiograph is subtracted from the previous one providing an image where the two items are clearly visualized (Fig. 67c).

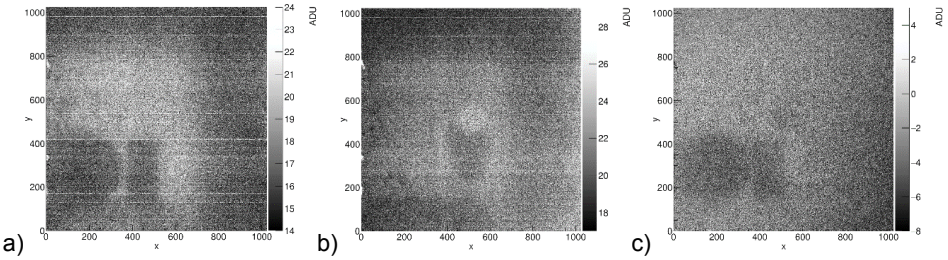


**Fig. 67: Neutron radiographs a) with PE cylinder and lead block, b) without PE cylinder and lead block and c) subtraction of both radiographs.**

The image reveals nearly the same contrast for the polyethylene cylinder and the lead block. This is in agreement with the fast neutron attenuation calculated from the item length and the macroscopic absorption cross section (0.111 $cm^{-1}$ for polyethylene and 0.172 $cm^{-1}$ for lead): 20 % for the polyethylene cylinder and 25 % for the lead block. The left part of the image obtained for the polyethylene cylinder shows a blurring due to the neutron beam divergence and the eccentric positioning of this item relative to the tritium target.
The neutron radiograph of a steel eye bolt M52 lying on two aluminium blocks is shown in Fig. 68a. The different thicknesses of the eye bolt as well as the difference in the fast neutron attenuation between aluminium and steel are clearly visible.

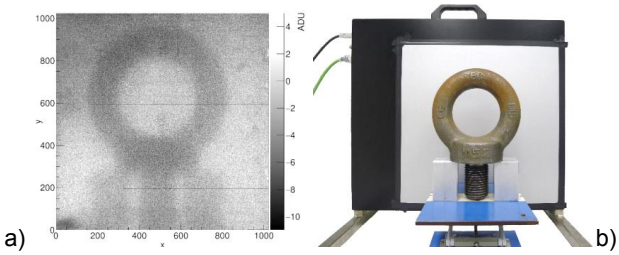


**Fig. 68: a) Neutron radiographs of an eye bolt M52 lying on two aluminium bricks. b) Measurement configuration.**

**Reference Measurements**

For detector calibration reference measurements with bricks ($5 \times 8 \times 10\ cm^3$) of various materials (Al, C, Fe, Pb, W, concrete and PE) were carried out. Neutron radiographs were recorded for different thicknesses of each material and for different combinations of two materials positioned one behind the other and vice versa corresponding to a total sample thickness of 10 cm. In order to determine fast neutron attenuation values the recorded images were analysed with a homemade algorithm based on a Gaussian filter including profile correction. As shown in Fig. 69 the measured attenuation (MA) may be express in function of the macroscopic absorption cross section for fast neutron section $\Sigma_{mac}$ ($cm^{-1}$) [3] and the sample thickness d (cm) though the following linear relation $MA = p_0 + [1 - \exp(-\Sigma_{mac} \cdot d)] \cdot p_1$ which may be used to determine the neutron absorption of unknown samples.

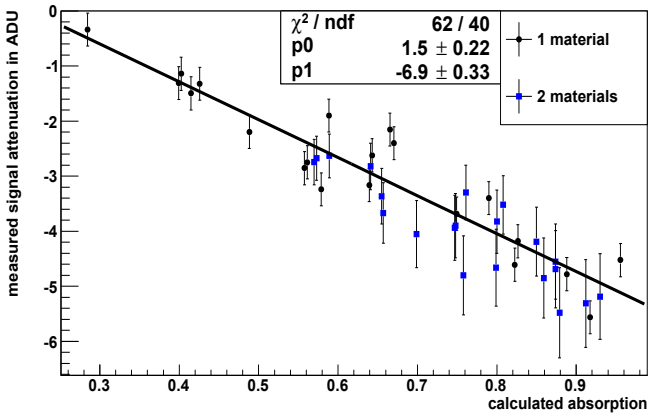


**Fig. 69: Linear relation between measured and calculated neutron attenuation.**

## Conclusion

Despite the low neutron flux and low detector efficiency neutron radiography of various materials was successfully performed. In order to improve the fast neutron detection sensitivity as well as the resolution a new scintillator composed of stacked scintillating fibres is under development.


## Acknowledgements

Financial support for this research was provided by the German Federal Ministry of Education and Research (Contract No. 0S9022B).


## References


[1] E. Mauerhofer, R. Odoj, Messmethoden zur Charakterisierung radioaktiver Abfälle und zur Freimessung von Reststoffen aus der Stilllegung kerntechnischer Anlagen (MESRAB), Lehrstuhl für Werkstoffchemie, RWTH,(2006)

[2] Jacob G Fantidis, Bandekas V Dimitrios, Potolias Constantinos and Vordos Nick, Fast and Thermal neutron radiographies based on a compact neutron generator, Journal of Theoretical and Applied Physics 6 (2012) 20

[3] M.B. Chadwick, M. Herman, P. Obložinský, M.E. Dunn, Y. Danon, et al., ENDF/B-VII.1: Nuclear Data for Science and Technology: Cross Sections, Covariances, Fission Product Yields and Decay Data, Nuclear Data Sheets 112 (2011) 2887

## 5.14. TransActinide Nuclear Data Evaluation and Measurement (TANDEM) for PGAA of inelastic scattering reactions from fission neutrons at MLZ, Garching

M. Rossbach*, C.Genreith, E. Mauerhofer

* Corresponding author: m.rossbach@fz-juelich.de

**Abstract**

The need for accurate nuclear reaction data of actinides is well documented and several initiatives from international Organizations for improvement have been initiated in the past. This need, particularly in view of method development for non-destructive analysis of nuclear waste, has generated a joint effort to use prompt and delayed Neutron Activation Techniques to enhance nuclear capture data of some long lived actinides such as $^{237}$Np, $^{242}$Pu and Am-241 in the frame of a multilateral cooperation. This research initiative tends to explore possibilities for the development of non-destructive active neutron interrogation techniques to quantify actinides in mixed waste and residues from decommissioning of nuclear installations for safe treatment and storage of such materials.

**Introduction**

The International Atomic Energy Agency (IAEA) and the Nuclear Energy Agency (NEA) of the OECD have pointed out at various opportunities that actinide nuclear data are scarce and sometimes rather uncertain [1-3]. Initiatives by the EU have been launched to enhance international cooperation for improvement of actinide nuclear data such as TALISMAN (Transnational Access to large Infrastructure for a Safe Management of Actinides) [4], ERINDA (European Research Infrastructures for Nuclear Data Applications) or CHANDA (Solving Challenges in Nuclear Data for the Safety of European Nuclear Facilities) [5]. The benefit of these programs rests largely in providing access to necessary infrastructures, however, cooperative research in the field of method development and actinide characterization is strongly dependent on individual initiatives. Hence, the three groups working on PGAA at the FZJ, the FRM II and the BNC agreed to sign a Memorandum of Understanding (MoU) and initiated TANDEM to explore and develop Prompt Gamma Activation Analysis (PGAA) for improving nuclear reaction data of actinides with a focus on nuclear waste and related issues. At a later stage the LBNL and LLNL joined the group as research interests coincided and actinides of interest could be made available for joint experiments at the neutron beam facilities in Budapest and in Garching. Furthermore, a well shielded gamma spectrometer has been installed at the fission neutron beam line SR10 of the FRM II to investigate gamma emission from inelastic neutron scattering reactions of elements and actinides. Three years of successful cooperation have generated various results and plans to enhance the focus of TANDEM into the investigation of long lived fission products are being pursued.

**Materials and Methods**

Prompt Gamma Activation Analysis (PGAA) using thermal or cold neutron beams at high-flux research reactors like Forschungsneutronenquelle Heinz Maier-Leibnitz, FRM II in Garching, Germany, is an ideal tool for basic nuclear prompt and decay investigations as it provides

well-defined neutron energy, sample irradiation conditions in a low background environment, and sensitive and versatile detector and counting conditions. The major constraint experienced at FRM II is limited availability of beam time as worldwide there are only a few PGAA facilities offering high enough neutron fluxes. For our experiments we could also use the Budapest reactor PGAA system offering a lower thermal equivalent neutron flux intensity of 7 x $10^7$ n $cm^{-2}$ $s^{-1}$ compared to FRM II with 2 x $10^{10}$ n $cm^{-2}$ $s^{-1}$ . Both experimental facilities are described in more detail in [6, 7].

Sample preparation techniques for actinides have been developed at the Institute IEK-6 of the Research Centre Jülich [8, 9]. 4 x 4 cm Suprasil© quartz sheets (0.2 ± 0.02 mm thick) have been purchased from Heraeus Quarzschmelze Hanau, Germany. $^{237}$Np and $^{242}$Pu were obtained from Oak Ridge via TUM as oxides and pressed into small 3 mm diam. pallets. The samples were encased between the quartz sheets and sealed with epoxy. $^{241}$Am activity (185 MBq) was obtained from Eckert & Ziegler, Nuclitec, Braunschweig and delivered to PTB in Braunschweig, the German National Metrology Institute, for accurate preparation and calibration of the sources. A drop of the $^{241}$Am solution was dried on the center of one of the quartz sheets and afterwards covered with another sheet. Two samples have been prepared by drying the droplet on top of small circular gold foils (3 mm diam., 0.003 mm thick), serving as neutron flux monitors. These were also sealed between quartz sheets using epoxy. The activity of the $^{241}$Am in the samples was determined with an uncertainty of 0.75 %, hence the mass of $^{241}$Am could be calculated with similar accuracy.

The gamma-ray peaks in the obtained gamma ray spectra were evaluated using Hypermet-PC [10]. This program was especially developed for the evaluation of complex prompt-gamma spectra in the energy range from 20 keV to 12 MeV. As the resolution of HPGe detectors degrades rapidly at higher energies it is imperative to use software with accurate energy and efficiency calibration as well as correct background subtraction over the entire range of energies and peak shapes encountered. The influence of neutron and gamma attenuation in the samples and casing material was accounted for by careful MCNP and GEANT 4 simulations. Both irradiation and counting facilities for PGAA measurements were simulated for optimization and background reduction prior to the measurements.

DICEBOX [11], a Monte-Carlo computer code originally developed at Řež, Czech Republic, generates simulated neutron-capture decay schemes based on nuclear level density and photon-strength function models. The simulated intensities of transitions populating low-lying levels can be normalized to the experimental cross sections de-exciting those levels in order to determine the unobserved cross section feeding the ground state. Combined with the observed cross section feeding the ground state this gives the total radiative thermal neutron-capture cross section $\sigma_0$ [12]. This program was applied at LBNL to simulate unobserved transitions in level schemes for $^{242}$Pu successfully and will also be used to investigate $^{241}$Am and $^{237}$Np data.

The TANDEM collaboration developed a new instrument using fission neutrons for PGAA investigations and applied it to investigate inelastic scattering reactions of actinides and other elements. This instrument is composed of a well-shielded HPGe detector with associated electronics at the fast neutron beam at the SR10 beam line of the FRM II reactor. In contrast to cold neutron PGAA monitoring neutron capture (n,$\gamma$) reactions, this device will provide information on inelastic scattering (n,n'$\gamma$) reactions of the originally exposed isotopes. Decay measurements of the irradiated samples can provide information on other reaction channels, such as (n,p), (n,$\alpha$) or (n,2n) resulting from the high energy neutron irradiation. However, for

the development of a possible analytical method based on neutron activation using neutron generators this (n,n'$\gamma$) reaction is of particular interest.

**Results**

Appropriate sample preparation techniques for PGAA investigations of radioactive samples were developed at the Research Centre in Jülich. The samples have been irradiated at the PGAA stations in Budapest and Garching and the spectra were evaluated at the FZJ. Thermal capture cross sections were calculated after neutron flux determination from a co-irradiated Au foil (0.05 mm thick). Results for $^{237}$Np, $^{242}$Pu and $^{241}$Am compare very well with literature values as can be seen from Fig. 70, Fig. 71, Fig. 72 [9, 13-14].

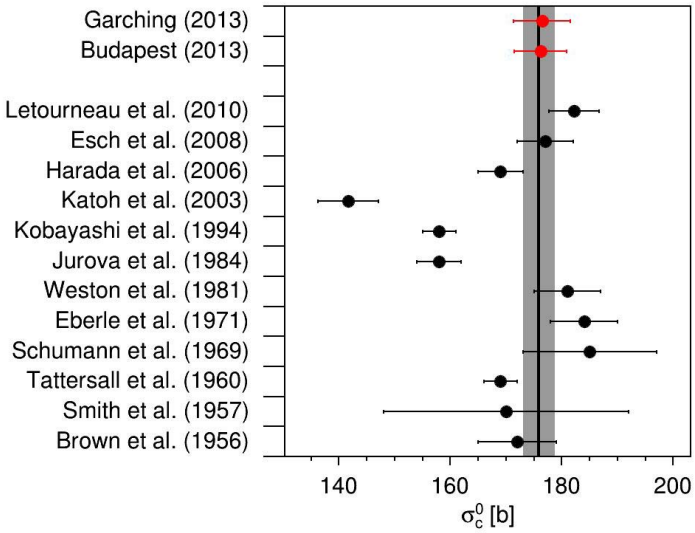


**Fig. 70: Neutron capture cross section values for $^{237}$Np compared to literature values. The vertical line represents the ENDF value.**

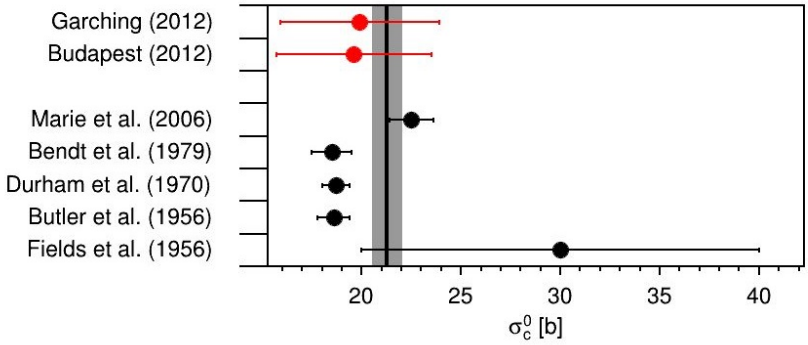


**Fig. 71: Neutron capture cross section values for $^{242}$Pu compared to literature values. The vertical line represents the ENDF value.**

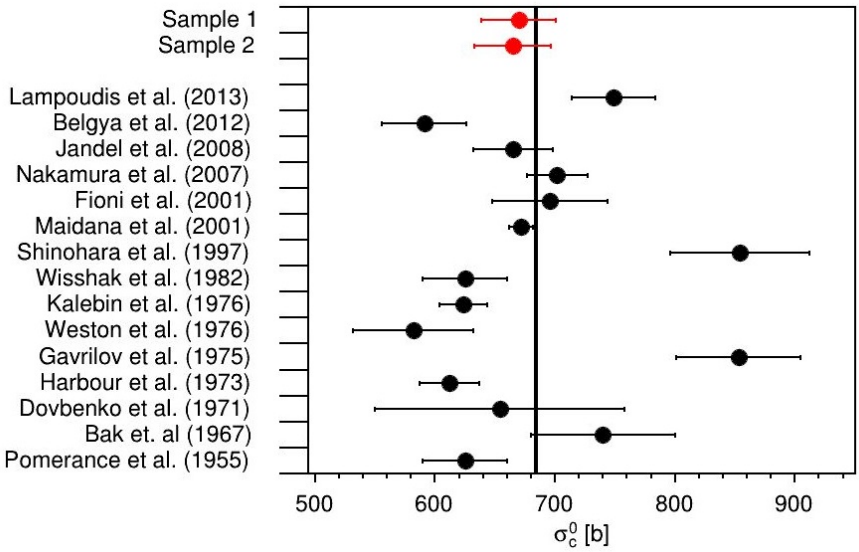


**Fig. 72: Neutron capture cross sections values for $^{241}$Am compared to literature values. The vertical line represents the ENDF value.**

As the uncertainties of the experimentally determined cross section for $^{242}$Pu were comparatively large, this nuclide was investigated using DICEBOX at the LBNL, Berkeley. One of the coworkers from Jülich (C.G.) had the opportunity to spend a two-month scientific visit there to be introduced in using this Monte-Carlo code and evaluated the decay transitions from the continuum, in addition to the experimentally-determined prompt gamma lines. This evaluation is independent from tabulated emission probabilities which are associated with large uncertainties propagating to the experimentally-determined values (see Fig. 73). The result for the capture cross section of $^{242}$Pu (n,$\gamma$) $^{243}$Pu obtained from the simulation is 21.9 ± 1.5 barn, a considerably smaller uncertainty compared to the mean experimental value of 19.8 ± 4 barn. Similar evaluations for $^{237}$Np and $^{241}$Am are in progress.

With respect to development of PGAA based analysis of actinides the absolute detection limits for $^{237}$Np, $^{241}$Am and $^{242}$Pu under FRM II irradiation conditions are (using low-energy gamma lines up to 300 keV) 0.06, 0.02 and 0.2 µg respectively, and 1.4, 0.6 and 10 µg for high energy gamma rays. These values seem to suffice for the analysis of small samples, such as safeguards swipe samples, and look rather promising for the further development of methods for actinide analysis in debris from decommissioning or low and medium activity nuclear waste forms. Development of innovative fuel and storage matrices for actinides can also profit from a sensitive neutron interrogation technique.

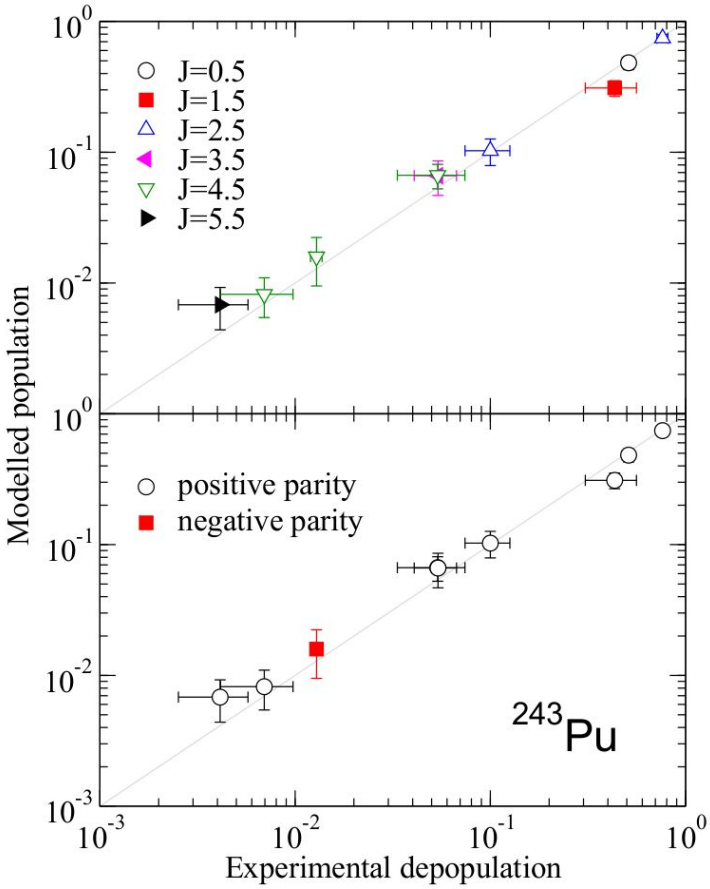


**Fig. 73: Comparison between experimental and simulated results for $^{243}$Pu using DICEBOX [15].**

**The new Fast Neutron Gamma Spectroscopy System FaNGaS**

The development and installation of a Fast Neutron Prompt Gamma instrument at the SR10 beam line of the FRM II (Fig. 74) is a major achievement of the successful collaboration with the TANDEM cooperation. 106 to 108 fission neutrons from a 95 % enriched $^{235}$U converter are extracted in the S10 channel and directed into a bunker for medical and radiographic purposes. A specially designed pair of collimators reduces the beam size to 5 cm diameter, which helps to reduce the detector background. An electrically cooled 50 % eff. n-type HPGe detector (Ametec) connected to a DSPEC (digital spectroscopy system) is heavily shielded against fast and thermal neutrons and gamma radiation by 15 cm lead, 1 cm B4C and 30 cm of PE (from the detector to the outside). In front of the 5 cm diameter collimator the samples are mounted in a Teflon frame for exposure to the neutron beam. Scattered and hence thermalized neutrons can be shielded from the sample by thin $^{6}$Li-glas to cover the sample at the irradiation position. Careful neutron flux characterization using the threshold reaction technique is in progress. After checking the feasibility under the actual background

conditions a set of stable elements have been irradiated and results are being compared with the hitherto only comprehensive compilation of inelastic scattering reactions of 1978 [16]. Once the new instrument has demonstrated its suitability and sensitivity our existing actinide samples will be investigated in detail to extract further information for the development of analytical tools for characterization of nuclear materials.


**Fig. 74: FaNGaS, the Fast Neutron Gamma Spectroscopy instrument at the SR10 beam line of the FRM II Research Reactor in Garching.**

**Discussion and Conclusion**

Bringing together a competent team of experts under a common heading, formalized at least to some extent, releases substantial synergies provided a spirit of team work and collaboration prevails. In our case there was substantial exchange of basic knowledge as the individual partners came from different backgrounds; some were more familiar with generation of nuclear data, some were experts in applying the PGAA technique and others could provide experience in sample preparation and/or MCNP simulations. This combination of a suite of capabilities rendered the TANDEM cooperation highly productive and innovative. The MoU on PGAA development will be renewed for another three years and new partners will be incorporated in the TANDEM cooperation. The focus of our collaboration will be extended to include also long lived fission products such as $^{93}$Zr, $^{135}$Cs, $^{107}$Pd or $^{129}$I to the scope of our investigations. Furthermore, it is also a major intent of the collaboration to contribute to preservation of nuclear basic knowledge by, e.g., training PhD students and introducing postdocs into the fields of PGAA and nuclear data generation. The long-range target, however, remains the development of analytical techniques based on neutron active interrogation and gamma spectrometry for the non-destructive (possibly also remote) characterization of nuclear waste and debris from decommissioning activities. These activities will strongly increase in the near future (especially in Germany) and our initiative is particularly motivated to address the need for safe disposal of hazardous materials.

**Acknowledgement**

Many individuals have actively contributed to the success of this collaboration. We would like to sincerely thank them all without mentioning all of them. Special thanks are going to the workshop team of Ayhan Egmen of the FZJ and the team of the FRM II, radiation safety and security. We are particularly thankful for generous financial support to the BMBF under grant 02S9052 and to Dr. M. Weigl from the Projektträger Karlsruhe as the competent and always helpful administrator of the project. Financial support for our irradiations at the Budapest research reactor was generously provided by the ERINDA EU project.

**References**

[1] D.L. Smith, N. Otuka (2012): Experimental Nuclear Reaction Data Uncertainties: Basic concepts and documentation. Nucl. Data Sheets113 3006-3053
[2] A.L. Nichols: Nuclear data requirements for decay heat calculations. Workshop on nuclear reaction data and nuclear Reactors: Physics Desighn and Safety, Trieste 25.02.-28.03.2002, IAEA Vienna, LNS520003
[3] H. Harada, A. Plompen: Meeting Nuclear Data Needs for Advanced Reactor Systems, Report by the Working Party on International Data Evaluation Co-operation of the NEA Nuclear Science Committee, OECD 2014, NEA/NSC/WPEC/DOC(2014)446
[4] www.talisman-project.eu
[5] www.chanda-nd.eu
[6] P. Kudejova et al. (2008): J. Radioanal. Nucl. Chem. 278, 691-695.
[7] Z. Rvay, T. Belgya, G. Molnár (2005): J. of Radioanal. Nucl. Chem. 265, 261-26.
[8] C. Genreith, M. Rossbach, E. Mauerhofer, T. Belgya, G. Caspary (2012): Nukleonika 57, 443-44.
[9] C. Genreith, M. Rossbach, E. Mauerhofer, T. Belgya, G. Caspary (2013): J. Radioanal. Nucl. Chem. 296(2), 699-703 DOI 10.1007/s10967-012-2080-8
[10] Z. Révay, T. Belgya, G. Molnár (2005): J. Radioanal. Nucl. Chem. 265, 261-265.
[11] F. Běcvář (1998): Nucl. Instr. Meth. A 417, 434.
[12] R.B. Firestone, K. Abusaleem, M.S. Basunia, F. Bečvář, T. Belgya, L.A. Bernstein, H. Choi, J.E. Escher, A.M. Hurst, M.M. KrtičKa, Zs. Revay, A.M. Rogers, M. Rossbach, S. Siem, B. Sleaford, N.C. Summers, L. Szentmiklosi, K. van Bibber, M. Wiedeking (2014): EGAF: measurement and Analysis of Gamma-ray Cross Sections. Proc. of Int. Conf. Nucl.Data Sci. Technol. March 4-8, 2013 New York, USA. Nucl. Data Sheets 119, 79-87.
[13] C. Genreith, M. Rossbach, Zs. Revay, P. Kudejova (2014): Determination of (n, γ) Cross Sections of $^{241}$Am by PGAA, Proc. of Int. Conf. Nucl.Data Sci. Technol. March 4-8, 2013 New York, USA. Nucl. Data Sheets 119, 69-71
[14] M. Rossbach, C. Genreith (2014): $^{241}$Am: a difficult actinide for (n,γ) cross section measurement In: Proceedings of the ERINDA Workshop, CERN, Geneva, Switzerland, 1-3 October 2013, edited by Enrico Chiaveri, CERN-Proceedings-2014-002 (CERN, Geneva, 2014) 157-163
[15] C. Genreith (2014): Partial Neutron Capture Cross Sections of Actinides using Cold Neutron Prompt Gamma Activation Analysis. PhD Thesis, Rheinisch Westfäliche Technische Hochschule RWTH Aachen
[16] M.R. Ahmed, S. Al-Najjar, M.A. Al-Amili, N. Al-Assafi, N. Rammo, A.M. Demidov, L.I. Govor, Yu.K. Cherepantsev (1978): Atlas of Gamma-Ray Spectra from the Inelastic Scattering of Reactor Fast Neutrons. Moscow Atomizdat

## 5.15. The release of $^{3}H$ and $^{14}C$ from irradiated nuclear graphite

L. Kuhne, C. Rizzato, E. Petrova, K. Baginski, N. Shcherbina

Corresponding author: n.shcherbina@fz-juelich.de

**Abstract**

The release of $^{3}H$ and $^{14}C$ from irradiated nuclear graphite from AVR (Arbeitsgemeinschaft Versuchsreaktor Juelich), was investigated under different repository relevant conditions. In particular, the speciation of $^{14}C$ and $^{3}H$ in the released fractions was studied. Examined by chemical analysis and chromatographic techniques, the radiocarbon fraction was shown to consist of $^{14}CO$, $^{14}CO_2$ as well as $^{14}C$-bearing organic compounds, e.g. alkanes and formic acid. Release of tritium in form of HT, HTO and C-T organic compounds was demonstrated. Annual release rates of $^{14}C$ and $^{3}H$ at ambient temperature and pressure comprised 1.48 % and 0.01 % respectively. An increase in release rates up to 7.10 % and 0.14 % correspondingly was observed during the storage at 70 °C. These findings are consistent with earlier studies on irradiated graphite conditioning at high temperature, which indicate $^{3}H$ to be strongly retained in graphite. This information is important for developing measures for graphite waste minimization (decontamination) or final disposal.

**Introduction**

Worldwide over 250 000 tons of neutron irradiated graphite from nuclear reactors are temporarily retained in interim storage facilities [1], as management concepts for the contaminated graphite waste remain an open issue. In Germany it is anticipated that a major part of contaminated graphite will be disposed of in an underground repository (i.e. KONRAD), which requires radioactive wastes to be accordingly specified. The major part of the radioactive contamination in nuclear graphite comprises longer-lived activation products. Among them are $^{14}C$ and $^{3}H$, which are mobile under environmental conditions and show a potential threat for bio-incorporation after release [1]. Their release rates are mainly controlled by the chemical state of $^{14}C$ and $^{3}H$ in irradiated graphite and will also influence their transport in the near-field of the final disposal. Therefore the release rates and composition of released fractions is the information required for the risk assessment of repository on the short-terms. During the operational phase of a final repository there is a danger of $^{14}C$ bio-incorporation unless it is retained in the corresponding waste packages. For instance, frequently used cemented waste form due to its higher water content and basic pH, can surely retain species $CO_2$, there will be, however, no retention of CO, HT, HTO or volatile organic forms [2].

The complex character of $^{14}C$ speciation in the released fractions was indicated in earlier studies [3-5]. Leaching studies on moderator and reflector graphite from reactor samples, performed to simulate the effect of water infiltration into the waste packages, have demonstrated that a fraction of about 0.1% of the total disposed $^{14}C$-inventory was released within three years, with 80% of the released $^{14}C$ in organic form. However, no additional information on the organic speciation was reported [3]. The importance of the speciation of mobilized $^{14}C$ and $^{3}H$ was already stressed a decade ago as information required for development of models for the long-term behavior of graphitic wastes. Up to now, most studies give no precise or incomplete information and no quantitative or qualitative analysis of released carbon compounds [4,5]. In this work the release behavior of $^{14}C$ from irradiated graphite from the Jülich experimental high-temperature pebble-bed reactor (AVR) under

repository relevant conditions was investigated. Two cases of $^{14}C$ release were under consideration: (1) release into the gaseous phase, relevant for the operational phase of the repository, and (2) release into aqueous solutions, relevant for the post-closure phase. Along with the determination of $^{14}C$ release rates, the speciation of released organic and inorganic $^{14}C$-compounds was performed.

**Experimental**

To study $^{14}C$ and $^{3}H$ release into the gaseous phase 1.5 g of AVR graphite-powder were weighed in 25 mL glass vials. 100 µL of deionized water (MQ) were added to simulated humid repository conditions (RH 100 %). The glass vials were stored at different temperatures (20, 50 and 70 °C) under ambient conditions for a year. By the end of storage time the gas over the graphite sample was analyzed using a sequence of washing-bottles, shown in Fig. 75. This sequential procedure is designed to differentiate among CO, $CO_2$, $H_2$, $H_2O$ and organic species when being present in the gas flow. The washing-bottle pairs 3 and 5, filled with 0.1 M $HNO_3$ and 2 M NaOH respectively, retain $^{3}H$ (in form of HTO) and $^{14}CO_2$. If any CO, $H_2$, or organics are present in the gas phase, they will be completely oxidized in the oven-tube at 800 °C supplied with $CuO_2$. The corresponding fractions of HTO and $^{14}CO_2$ will be retained in washing-bottle pairs 9 and 11. After 4 h the oxidation and absorption of $^{14}C$ and $^{3}H$ was considered to be complete, and solutions from the washing-bottle pairs were analyzed by Liquid Scintillation Counting (LSC). For that 3 mL of solution were mixed with 17 mL of multipurpose LSC-cocktail (FA Meridian) and analyzed by TriCarb (FA Perkin Elmer). Gas-chromatography (GC-R, RAGA, FA Raytest) coupled to a radioactivity flow detector and a mass-spectrometer was used for detailed speciation of organic compounds in the gas phase.

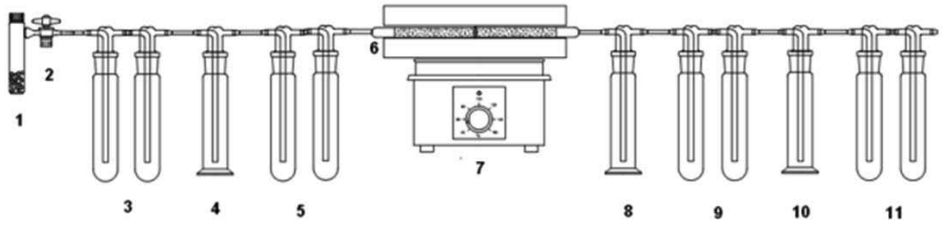


**Fig. 75: The scheme of the order of washing-bottles for $^{3}H$ and $^{14}C$ sequential analysis: 1: A glass-vial with a graphite sample; 2: glass-valve; 3 and 9: washing-bottles filled with 0.1 M $HNO_3$; 4, 8 and 10: protection-bottle; 5: two washing-bottles filled with 2 M NaOH; 6: tube filled with CuO; 7: tubular oven.**

To study the leaching of $^{14}C$ and $^{3}H$ from irradiated graphite, 1.5 g of AVR-graphite sample (powder) was contacted with 2 mL of MQ-water. Leaching was carried out under ambient atmosphere and pressure at 70 °C. After 7 days of leaching, 1 mL of solution was sampled and analyzed by HPLC coupled to UV/vis-IR spectrophotometer (FA Knauer).

Prior to the sequential chemical analysis of the $^{14}C$ and $^{3}H$ release, the graphite samples were characterized by Scanning Electron Microscopy. The specific surface area was determined by $N_2$ adsorption at 70 K using the BET equation.

## Results and discussion

### The release of $^{14}C$

A model experiment on $^{14}C$ release from the nuclear graphite powder was performed in order to estimate the volatility of $^{14}C$ under conditions relevant to final disposal. Although disposal of contaminated graphite is anticipated in blocks or as cemented waste form, the powder is commonly used in our work to facilitate the release (due to the high surface are) and to provide a measurable amount of $^{14}C$. Humid conditions were used to simulate conditions relevant for final disposal. The diagrams in Fig. 76A show the distribution of $^{14}C$ between gas and solid phase found after one year of sample conditioning at room temperature. Under ambient conditions an annual fractional $^{14}C$-release of 1.4% was measured. Consistent to earlier works [3-5], different chemical forms of $^{14}C$ were observed in the gas phase. Among them are $CO_2$, CO and $^{14}C$-bearing organic substances. For the samples conditioned at 50 °C no significant difference in $^{14}C$ release and speciation was found. Conditioning of the graphite powder at 70 °C, resulted in the annual $^{14}C$ release of 7.1%, mostly due to an increase in CO and the organic fraction (Fig. 76B). At the same time, the release in form of $CO_2$ did not change significantly. Additionally, in every case (i.e. 20-70°C) water soluble organics, like formic acid, were detected, which was consistent with HPLC analysis of aqueous solutions from leaching tests with AVR graphite. It is important to keep in mind that the current sequential analysis does not allow distinguishing among fractions of CO and organic substances: both are not retained by the washing-bottle pair 5, and are retained only after complete oxidation with $CuO_2$, in washing-bottle pair 11 as $CO_2$. Therefore complimentary analysis of the gas phase over the graphite samples were performed with GC-MS, which allows for a more detailed speciation of aliphatic molecules and organic acids. The results of the GC-MS measurements (Fig. 77)) show the signals of small volatile aliphatic moieties, like n-heptane, n-hexane and n-pentane. In other words, the gaseous fraction of $^{14}C$ released during the conditioning of graphite powder at 70 °C reveals a rather complex composition, containing substances from CO and $CO_2$ to aliphatic and carboxylic moieties. In order to understand how exactly these complex $^{14}C$-species are released, the formation of these$^{14}C$-bearing species must be understood.

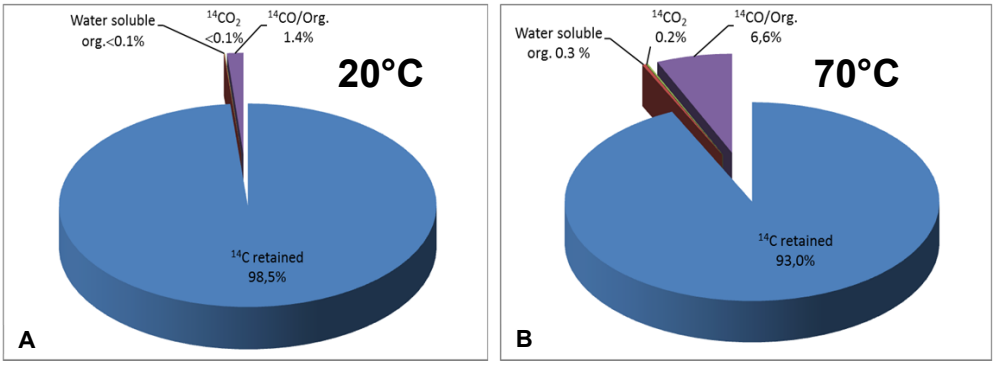


**Fig. 76: Speciation of $^{14}C$ in the gas fraction released at 20°C (A) and 70°C (B).**

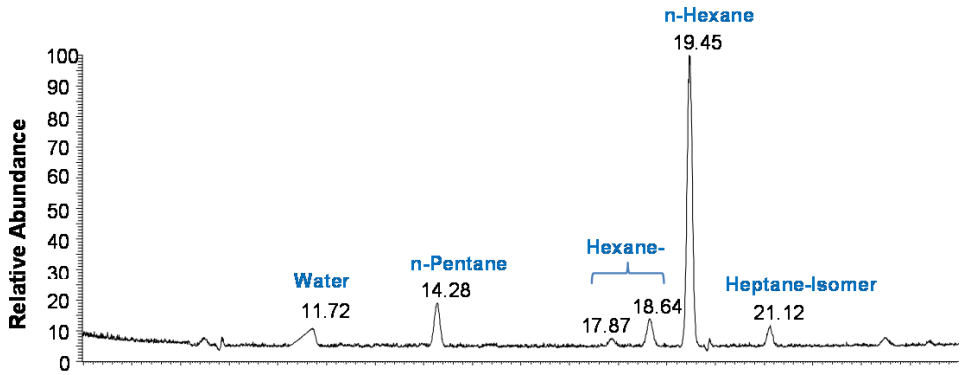


**Fig. 77: A Chromatogram of the gas phase over the AVR graphite powder conditioned at 70 °C in humid air atmosphere.**

The occurrence of oxidized and long-chained organics species is attributed to the irradiation-induced processes in nuclear graphite during reactor operation. In particular, $^{14}C$ originates from the neutron activation of $^{14}N$, $^{13}C$ and $^{17}O$, which are either present as an impurity of pitch binder, or are adsorbed in the pores (see Fig. 78). Typically, the production of $^{14}C$ is accompanied by a multiple recoil of the activated atom, which is accompanied by disorder of the graphite structure, formation of isolated defects and finally amorphisation of graphite. Besides that, both neutron- and gamma-irradiation is capable of displacing the C-atoms: threshold displacement energy ranges between 25.0 and 44.5 eV [6,7]. According to recent theoretical simulations, the recoil cascade evolves within ps, creating up to 900 displaced atoms, depending on the type and energy of irradiation [8]. The key observation is that the displaced C-atoms prevalently remain in between the graphene layers with unsaturated bonds and, similar to C atoms at the graphene plane edges, are considered to have noticeably greater reactivity compared to C atoms in the basal planes [9-11]. Thus building up the carbon chains is not unprobable, if interstitial $^{14}C$ atom serves as an active site of graphene. Then, depending on the redox conditions during reactor decommissioning these carbon chains may evolve. As contact with water and air cannot be ruled out, further redox processes may take place. According to recent theoretical simulations, the process of water interaction with defects in the graphite structure has exothermal character leading to the chemisorption of H and OH [12]. The products of water radiolysis, i.e. $HO^{\bullet}$ and $H^{\bullet}$ radicals, as well may attack the interstitial $^{14}C$ atoms, resulting either in carbon oxidation or polymerization process. The relevance of radiation effects to graphite corrosion has been emphasized elsewhere [13]. The studies of irradiated graphite by X-ray Photoelectron Spectroscopy revealed that the fraction of C-O groups may reach ≈ 27 % of all species occurring on the graphite surface due to irradiation-induced oxidation. The effect is, certainly, dependent on the irradiation and storage conditions, however, these findings demonstrate that severe corrosion of irradiated graphite may occur in the long-term if subjected to oxidizing conditions (e.g. humid air).

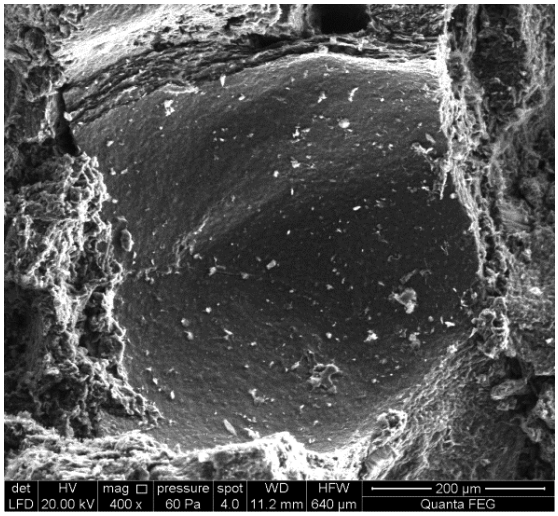


**Fig. 78: SEM image of an irradiated graphite sample, demonstrating the inhomogeneous structure of nuclear graphite: $^{14}N$, the main precursor of $^{14}C$, is typically accommodated in amorphous regions and pores.**

**The release of $^{3}H$**

In contrast to $^{14}C$, the release rate of $^{3}H$ was found to be remarkably low, 0.01% at 20 °C, showing no clear dependence on the conditioning temperature. The $^{3}H$ in the released fraction was distributed between HTO, HT and $^{3}H$-bearing organic species. As the conditioning temperature of 70 °C is rather low for breaking the C-$^{3}H$ bonds, the organic fraction is considered to be weakly bound to the graphite surface, e.g. adsorbed. A similar speciation was also suggested in earlier work, where high temperature treatment was applied for investigating the mechanism of $^{3}H$ release from irradiated graphite [11]. It was assumed that the release of $^{3}H$ is controlled by diffusion out of the grain boundaries [6,11]. Remarkably, a significant release was reported only above 870 °C (≈5 %) and attributed to the release of HTO and HT. However, in this temperature range the pyrolysis of aliphatic fragments starts to play an important role in the release. The thermodynamics of alkanes cracking suggest a low probability of H abstraction from the aliphatic chain compared to the abstraction of the $C_1$-$C_2$ fragments, indicating that $^{3}H$ releases are most likely in form of R-C-$^{3}H$ fragments [14]. Release of HT or HTO does not require breaking the covalent bonds, therefore they are more probable to be release at lower temperatures. The release process will be retarded if HT or HTO are located in closed porosity, then the diffusion to the grain boundaries will be the release rate limiting step. The contribution of diffusion of $^{3}H$-bearing species to the $^{3}H$ release remains unclear yet [11]. The key finding demonstrates that only a small $^{3}H$ fraction of 0.01 %, i.e. the weakly bond fraction, can be released under ambient conditions, whereas the remainder is strongly retained in the graphite. In terms of graphite disposal this means that most of the $^{3}H$ will be strongly retained in the graphite lattice and is unlikely to be released during the operational phase of a final repository.

## Conclusion

In our work the release behavior of $^{14}C$ and $^{3}H$ from irradiated nuclear graphite from AVR under different disposal relevant conditions was investigated. The annual fractional release of $^{14}C$ and $^{3}H$ from the powdered graphite sample at ambient temperature (i.e. 20 °C) was 1.48 % and 0.01 % respectively. Increasing the storage temperature, e.g. to 70 °C, results in a significant increase of $^{14}C$ release rates up to 7.1 % per year; the release rate for $^{3}H$ may rise by an order of magnitude, i.e. up to 0.14 % per year. The study of $^{14}C$ and $^{3}H$ speciation revealed that besides $^{14}CO_2$, HTO and HT, a significant amount of $^{14}CO$, $^{14}C$- and $^{3}H$-bearing organics (i.e. n-heptane, n-hexane and n-pentane) is released into the gaseous phase. These substances are of high concern for the safety assessment of repository due to their low retention in the cementatious environment. These findings are important for the development of a strategy for the management of nuclear graphite wastes, which remains the actual problem worldwide; e.g. a proper waste form for encapsulation of contaminated graphite has to be developed to prevent the release of easily volatile $^{14}C$- and $^{3}H$-fractions in the short-term. Alternatively, the weakly bound fractions could be removed, e.g. by thermal treatment, before graphite disposal.

## References


[1] EPRI. Graphite decommissioning. Options for graphite treatment, recycling, or disposal, including a discussion of safety-related issues. Technical report (2006).

[2] Johnson, L.H., Schwyn, B. Behavior of $^{14}C$ in the safety assessment of a repository for spent fuel, high-level waste and Long-lived Intermediate Level Waste in Opalinus Clay. Nagra, Internal report 04-03 (2004) 1–7.

[3] Isobe, M., Yamamoto, T., Takahashi, R., Sasoh, M., Nakane, Y., Sakai, H. Chemical form of organic C-14 leaching from irradiated graphite in Tokai plant. Atomic Energy Society of Japan, Autumn Meeting, L28 (2008).

[4] Eurajoki, T. Behaviour of carbon-14 released from activated steel in repository conditions – a key issue in the long-term safety of decommissioningwaste. NKS Seminar on Decommissioning of Nuclear Facilities, September, (2010) 14–16.

[5] Magnusson, Å. Measurement of the distribution of organic and inorganic $^{14}C$ in a graphite reflector from a Swedish nuclear reactor. Department of Physics, Lund University, Sweden, Report 01/02, LUNFD6/(NFFR-5016)/1-60/(2002).

[6] Fachinger, J. Graphite. In: Comprehensive nuclear materials. Elsevier (2012) 539-561.

[7] Hehr, B.D., Hawari, A.I., Gillette, V.H. Molecular dynamics simulations of graphite at high temperatures. Nucl Technol. 160(2) (2007) 251–256.

[8] Christie, H.J., Robinson, M., Roach, D.L., Ross, D.K., Suarez-Martinez, I. Simulating radiation damage cascades in graphite. Carbon 81 (2015) 105-114.

[9] Zhu, Z. H., Finnerty, J., Lu, G.Q., Wilson, M.A., Yang, R.T. Molecular orbital theory oft he $H_2O$-Carbon reaction. Energy & Fuels, 16 (2002) 847-854.

[10] Kim, C., Choi, Y.S., Lee, S.M., Park, J.T., Kim, B., Lee, Y.H. The effect of gas adsorption on the field emission mechanism of carbon nanotubes. J. Am. Chem. Soc., 124 (2002) 9906-9911.

[11] Vulpius, D., Baginski, K., Fischer, C., Thomauske, B. Localisation and chemical bond of radionuclides in neutron-irradiated nuclear graphite. J. Nucl. Mat. 438 (2013) 163-177.

[12] Cabrera-Sanfelix, P., Darling, G.R. Dissociative adsorption of water at vacancy defects in graphite. J. Phys. Chem. C, 111 (2007) 18258-18263.

[13] LaBrier, D., Dunyik-Gougar, M.L. Identification and location of $^{14}C$-bearing species in thermally treated neutron irradiated graphites NBG-18 and NBG-25: pre- and post-thermal treatment. J. Nucl. Mat. 460 (2015) 174-183.

[14] Doue, F., Guiochon, G. The mechanism of pyrolysis of some normal and branched $C_6$ to $C_9$ alkanes. Composition of their pyrolysis products. J. Phys. Chem. 73(9) (1969) 2804-2809.

## 5.16. Research and Development in Safeguards Analytical Techniques and Measurements

M. Dürr, A. Knott, R. Middendorp

Corresponding author: ma.duerr@fz-juelich.de

### Introduction

The application of safeguards by the IAEA involves analytical measurements of samples taken during inspections. The development and advancement of analytical techniques with support from the Member States contributes to strengthened and more efficient verification of compliance with non-proliferation obligations. Since recently, a cooperation agreement was established between Forschungszentrum Jülich and the IAEA in the field of analytical services. The current working areas of the Forschungszentrum with IAEA's Office of Analytical Services (SGAS) are: (i) Analysis of impurities in nuclear material samples, (ii) Production of synthetic micro-particles as calibration standard and reference material for particle analysis, and (iii) qualification of the Forschungszentrum Jülich as a member of the IAEA network of analytical laboratories for safeguards (NWAL).
Concerning impurity analysis of uranium-oxide samples, analysis of trace elements in solid uranium samples is performed using existing capabilities in inductively coupled mass spectrometry. With respect to the synthesis of particles, a dedicated setup for the production of uranium particles is being developed, which addresses the urgent need for material tailored for its use in quality assurance measures for particle analysis of environmental swipe samples. Furthermore, Forschungszentrum Jülich was nominated as a candidate laboratory for membership in the NWAL network. To this end, analytical capabilities at Forschungszentrum Jülich have been joined to form an analytical service within a dedicated quality management system.

### R & D for International Safeguards at Forschungszentrum Jülich

In the development of methods and techniques for its safeguards mission, the IAEA relies on support from member states. In the analytical regime support may be provided in form of in-kind donations, analytical services or through consultancy and delegation of experts. The strengthening measures for Safeguards have led to an increasing degree of sophistication of analytical techniques and procedures used nowadays, which are not only applied for the purpose of verifying declared nuclear material flows and inventories, but also for acquisition of information, e.g. from environmental samples. The scope extension of analytical measurements as part of strengthened safeguards leads to a plurality of techniques and methods and an increased complexity 0. Research institutions can provide support in the development and adaptation of techniques towards application in Safeguards.

The IAEA performs the analysis of safeguards samples 'in-house' via SGAS, but also relies on the Network of Analytical Laboratories (NWAL), i.e. laboratories that have qualified to conduct analysis tasks for the Agency. The German Support Programme to the IAEA contributes to the development and advancement of safeguards and has become increasingly engaged in providing support in the area of analytical measurements. In a joint

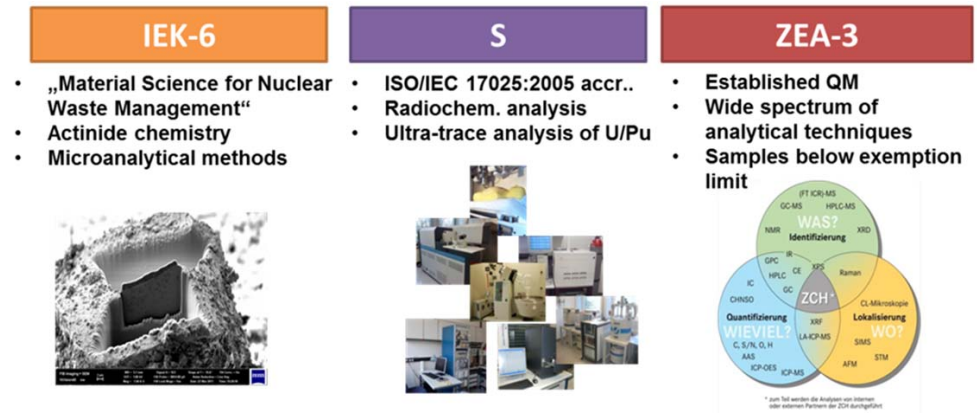


**Fig. 79: Three departments of Forschungszentrum Jülich - IEK-6, S, and ZEA-3 - contribute to the advancement of safeguards analytical techniques and measurements.**

initiative, three departments of Forschungszentrum Jülich, IEK-6 (Institute for Nuclear Waste Management and Reactor Safety), S (Department of Safety and Radiation Protection), ZEA-3 (Central Institute for Analytics), joined their analytical capabilities to provide support to IAEA safeguards. In mutual visits between representatives from Forschungszentrum Jülich and the IAEA areas of collaboration could be identified.

The three organizational units offer their combined capabilities (see overview in Fig. 79), where IEK-6 brings in expertise in chemistry and material science with actinide bearing materials. This expertise is complemented by a series of analytical techniques, in particular micro-analytical methods like scanning electron microscopy, focussed ion-beam but also Raman-spectroscopy and X-ray diffraction. Furthermore, IEK-6 is licensed to handle bulk amounts of uranium and small amounts of plutonium. The department of Safety and Radiation Protection (S) is an accredited laboratory for radiochemical analyses according to ISO/IEC 17025:2005 with competency in ultra-trace analysis of U/Pu isotopes. The Central Institute for Analytics (ZEA-3) is a central department offering a wide range of analytical techniques in support of all research institutes within Forschungszentrum Jülich, but also to external customers. ZEA-3 provides analysis of non-active samples, i.e. such with radioactivity levels below the exemption limit.

Furthermore, a cooperation agreement was signed between Forschungszentrum Jülich (lead taken by IEK-6) and IAEA SGAS as a framework for cooperation in the area of analytical measurements for safeguards.

As a result of the arrangements described above, following activities of the Forschungszentrum Jülich in the area of analytical measurements for safeguards have emerged:

- Analysis of impurities in nuclear material samples,
- Production of micro-particles as reference material,
- Qualification for membership in the Network of Analytical Laboratories (NWAL).

These activities are outlined in further detail in the following sections.

**Analysis of Impurities in Nuclear Material Samples**

The aforementioned three organizational units established a process to address the analysis of nuclear material samples. In general, samples are dissolved and diluted and, if required, spiked at the radiochemistry laboratory of IEK-6. The diluted samples can be transferred to further analysis to the laboratories of the other departments for further analysis. For quantitative determination of uranium and impurity contents, ICP-MS is used for mass-spectrometry of samples taking advantage of stringent quality control routines established in the respective laboratories of S and ZEA-3.

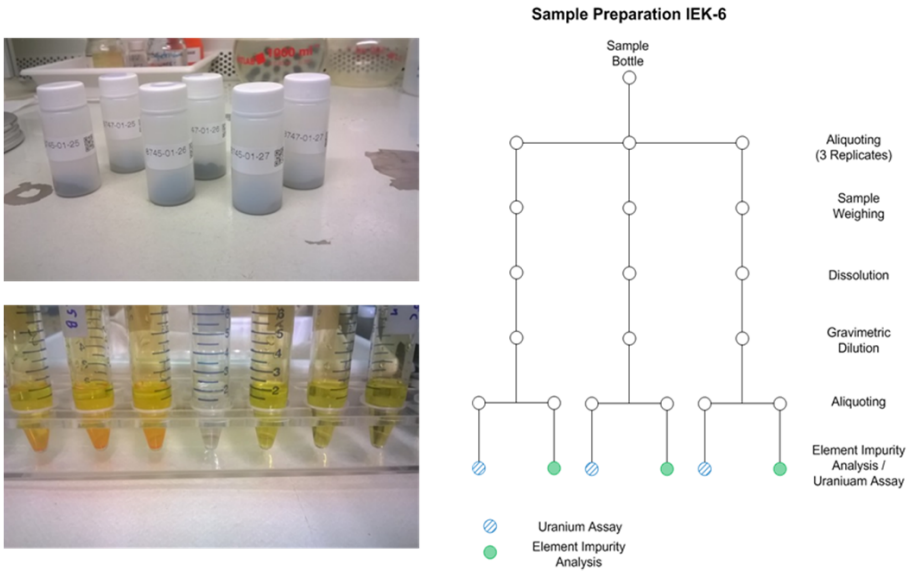


**Fig. 80: Sample bottles with uranium oxide received for determination of elemental impurities (top left) and a subsample under dissolution (bottom left). Sample preparation scheme for uranium oxide samples (right).**

The analysis of nuclear material samples is formalized in a procedure description, including the share of responsibilities and the work flow between the three involved departments. In principle, the procedure may be included under the quality management system of the ISO/IEC 17025:2005 accredited laboratory of the Department for Safety and Radiation Protection S.

In 2014, the consortium of the three institutes IEK-6, ZEA-3 and S was invited to participate in an interlaboratory comparison for the analysis of elemental impurities in uranium oxide samples. Three replicate samples representing two different types of impurity content where analysed for elemental impurity content. The analysis scheme involves tasks for all three departments involved in the effort (see Fig. 80). In total the weight content of 64 elements was determined with mass spectrometric measurements. Special attention was given to possible contaminants introduced during sample preparation. The performance results of the comparison will be disclosed in the second half of 2015.

**Production of Micro-Particles as Reference Material**

In analytical measurements reference materials are needed for calibration of instruments, validation of methods and for quality control. In particular since the introduction of highly sensitive Large Geometry SIMS analysis and the routine analysis of the uranium minor isotopes, there is a need for customized reference material for particle analysis of environmental samples.

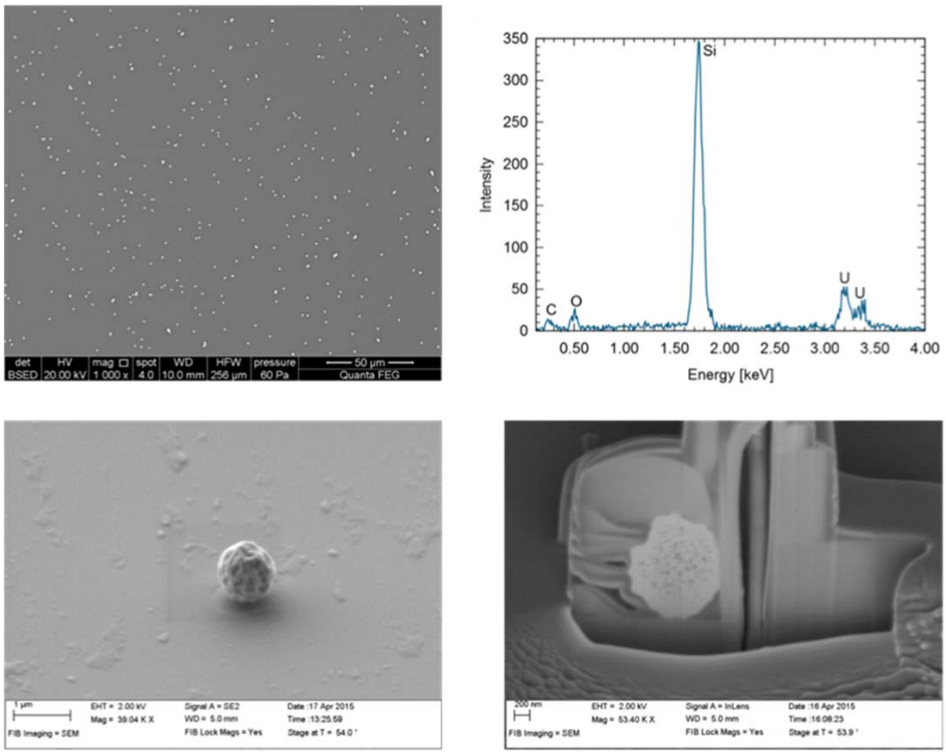


**Fig. 81: SEM (left) and EDX (right-top) of produced microparticles deposited on a Si wafer and a cross-section prepared by FIB milling (right-bottom).**

In the past, several approaches were made for production of particles to be used as a reference standard in particle analysis. Preferably, all particles would be uniform in the characteristics relevant to the analytical application. Generally this means that the particles should be identical in physical and chemical properties. In a joint project between the Forschungszentrum Jülich and the IAEA, an approach to particle production was chosen which allows the synthesis of uranium particles with a determined amount per particle and isotopic composition[2]. This approach is based on the generation of an aerosol from a liquid feed composed of uranium solution diluted in water-ethanol mixture. The aerosol is generated by a vibrating orifice aerosol generator which under certain operating conditions creates mono-disperse droplets, i.e. the droplets all have a uniform diameter. After evaporation, the droplets form a solid uranium-compound from the non-volatile component of the aerosol. The particles are transported via a carrier air-stream to a heating zone, where

particles are heated to a temperature of up to 1000 °C and are therefore oxidized. This way, particles are sufficiently stabilized and can be collected on a suitable carrier.
The production process in principle allows determination of the amount of uranium amount per particle by adjusting the U-concentration of the feed accordingly. The isotopic composition of the particles is determined by that of the feed solution. The chemical form of the particles depends on various parameters of the production process, e.g. temperature and dwell times of particles in the various stages of the process. For particles produced in Jülich, a collaborative effort with the IAEA and the JRC-IRMM of the European Commission is planned to verify the isotopic content and the uranium amount per particle.

The characterization of particles is performed at IEK-6 using particle search routines of a scanning electron microscope (SEM) in order to characterize size, morphology and elemental composition of the produced particles. For SEM characterization uranium particles are readily identified in the backscatter-electron imaging mode. A particle search was conducted and EDX elemental analysis has confirmed that the particles consist of uranium. Under optimal conditions the particles are spherical and mono-disperse. In previous work undertaken to characterize particles produced using the VOAG, it was reported that some voids may be present [3]. Under the currently optimized production parameters (500°C heating temperature), produced particles had been selected for preparation using a Focused Ion Beam (FIB) apparatus (Zeiss Nvision 40 Cross Beam Workstation). The FIB apparatus features high-resolution SEM such that the shape and surface of particles can be studied with high detail (Fig. 81 – bottom left). The FIB technique allows for surface modification with an ion-beam thus serving as a ‘milling machine’ on the nano- and micro- scale and is ideally suited to study the internal morphology of particles (Fig. 81 – bottom right). A random selection of six uranium particles from a production run (heat treatment temperature 500 °C) was sliced to study the internal of produced particles. All particles on the sample were spherical and free of voids. Some porosity is observed in the centre of the particles, with higher density at the perimeter.

As certification of particle properties requires extensive analytical effort and therefore careful attention is required to properly determine the suitable form. Each option chosen for packaging the particles brings certain advantages and disadvantages in consideration of their use as material or use in quality control or reference material. Among the options that are currently being considered is direct impaction of particles onto a substrate or transfer of particles into a suspension. However, open questions remain concerning stability of particles within the suspension, which are currently being addressed by systematically studying processes like dissolution and isotope exchange on particles produced with the setup with the technique installed in Jülich.

**Qualification as Member of NWAL**

Forschungszentrum Jülich was nominated as a candidate for membership in NWAL early 2013, with the initial scope of nuclear material analysis. So far the efforts at Forschungszentrum Jülich focused on quality management and qualification of analytical methods for analysis of safeguards samples. Due to a recent shift of priorities, technical discussions are ongoing on the involvement of Forschungszentrum Jülich as a laboratory for provision of particle reference materials. This would require a fully controlled production process and specified user requirements on particle characteristics.

## Conclusion and Outlook

In the past few years, Forschungszentrum Jülich has become engaged in the area of analytical techniques in the domain of International Safeguards. Analytical measurements and techniques for safeguards applications benefit from involvement of scientific research institutions. In particular with the high degree of sophistication of methods and instrumentation used in laboratories for safeguards, research and development of techniques and methods provides valuable support to the advancement and improvement of safeguards. The collaboration between IAEA SGAS and Forschungszentrum Jülich has materialized in the production of particles for quality control. The goal in the future is qualification of the joint laboratories of IEK-6, S and ZEA-3 for membership in NWAL as a provider of particles for quality assurance purposes. The existing capabilities of the consortium were applied in elemental impurity analysis of uranium oxide material as part of an interlaboratory comparison organized by the IAEA.

## Acknowledgements

This work was supported by German Support Program to the IAEA under task C.43/A1960 and task C.45/A1961 and the Federal Ministry for Economic Affairs and Energy (FKZ 02W6263).

## References

[1] Safeguards Techniques and Equipment: 2011 Edition, International Nuclear Verification Series No. 1 (Rev. 2), International Atomic Energy Agency, Vienna, 2011

[2] Knott, A. and Dürr, M., Production of monodisperse uranium particles for nuclear safeguards applications. ESARDA Bulletin, 49, 2013, 40.

[3] Kraiem, M., Richter, S., Erdmann, N., Kühn, H., Hedberg, M., Aregbe, Y., Characterizing uranium oxide reference particles for isotopic abundances and uranium mass by single particle isotope dilution mass spectrometry. Anal. Chim. Acta, 748, 2012, 37.

## 5.17. Formalizing Acquisition Path Analysis

C. Listner, I. Niemeyer, M. J. Canty*, A. Rezniczek#, G. Stein§

Corresponding author: c.listner@fz-juelich.de

* Consultant, Jülich
# UBA Unternehmensberatung GmbH, Herzogenrath
§ Consultant, Bonn

### Introduction

Since the first ideas for supervising nuclear material, the verification system has evolved constantly. After gaining first experiences with item-specific safeguards according to the commitments in INFCIRC/66, the system of international safeguards was established by the signature and ratification of the Non-proliferation Treaty (NPT) in 1970. The treaty implementation has mainly been governed by comprehensive safeguards agreements (CSA) and later the additional protocol (AP) with Integrated Safeguards.
In order to verify the State's compliance to these provisions, the International Atomic Energy Agency (IAEA) has been carried out a mechanistic, check-list approach to safeguards with limited success. This method has been superseded over the past years by a holistic approach called the State-level concept (SLC). The SLC's main idea is to move away from material centric approaches to a system analysis view of nuclear proliferation which clearly identifies the actors, their possibilities and their safeguards significance. Due to its general and comprehensive nature, the SLC has great potential to replace voluntary offer agreements (VOA) in nuclear weapon States (NWS) and to be used in other fields of treaty verification.
Underneath the new paradigmatic view to nuclear verification, the State-level concept essentially consists of three processes which help to develop State-level safeguards approaches (SLA) [1]:

1. Identification of plausible acquisition paths.
2. Specification and prioritization of State-specific technical objectives (TO).
3. Identification of safeguards measures to address the technical objectives.

This paper concentrates on the first step of this process which is also known as acquisition path analysis (APA). APA is defined as the analysis of all plausible sequences of activities which a State could consider to acquire weapons usable material [2]. The purpose of the APA is to determine whether a proposed set of safeguards measures is sufficient. Therefore, some overlap to the second step, the definition of technical objectives, is obvious.
The approach to acquisition path analysis used in this paper has advanced over the past years [3-7]. Motivated from the fact that the SLC tries to come up with adaptive safeguards approaches, the main idea of this approach to APA is to account for differentiation without discrimination. In order to accomplish this, the available safeguards-relevant information is processed in an objective, transparent, reproducible, standardized and well-documented way in contrast to reasoning-with-words or black-box-approaches.
Besides the methodology and its progress, the new verification paradigm has to be compatible with the existing approach to nuclear material accounting, a major element of traditional safeguards. Therefore, it will be shown how performance targets can be derived from a risk assessment of the State's as well as the IAEA's strategic options.

Moreover, the determination of the model parameters has turned out to be a non-trivial task [5]. Especially, when it comes to detection probabilities that can be reasonably claimed within a technical objective, the user needs to consider the detection of proliferation activities in declared facilities as well as in potential undeclared installations. This paper proposes four concepts how to overcome this issue.

In the following, the methodology and its recent enhancements will be presented. Then, a discussion on the relationship between game theory and performance targets will be carried out. Afterwards, a case study focusing on the strategic assessment part of the method will be shown. Next, some considerations will be given to the determination of model parameters, especially the quantification of detection probabilities. Finally, conclusions of the paper and an outlook on future work will be presented.


**Fig. 82: Three step approach to acquisition path analysis.**

### Materials and Methods

The given approach to acquisition path analysis consists of three general steps: First, the potential acquisition network is modeled based on the IAEA's physical model and experts' evaluations. Second, using this model all plausible acquisition paths are extracted automatically. Third, the State's and the inspectorate's options are assessed strategically. The workflow is depicted in Fig. 82. In the following, a description of the three stages will be given. A more in depth discussion can be found in Listner et al. [8].

During the first step of the process, also known as network modeling, a State-specific acquisition model is set up. Mathematically, such a network can be seen as a directed graph with material forms represented by nodes and processes represented by edges. The IAEA's physical model [9] serves as a starting point, where all proliferation relevant materials and processes are formally described in a general acquisition model for nuclear weapons usable material.[1] Based on the IAEA's physical model, a mathematical model has been derived that encodes all the potential materials and activities in a single directed graph (see Figure 2).

There are four categories of processes in this model: diversion from existing facilities (div), undeclared import (imp), misuse of existing facilities (mis), processing in clandestine facilities (cland). When assessing a State's options for acquiring nuclear weapons usable material, specific processes of these four types are included in or excluded from the model. E.g. if a State does not have an enrichment facility on its ground, all edges of type misuse in

[1] In principle, also the weaponization step itself could be modeled using a graph theoretic approach. However, due to the definition of acquisition path analysis given in International Atomic Energy Agency (IAEA) [2], this paper's approach ends at weapons usable material.

connection with enrichment will be removed from the model. On the other hand, there will be always the option for enriching in clandestine facilities and hence these processes will remain in every State's case.

Besides the mere presence of edges in the model, these edges will be assessed in terms of attractiveness for the particular State. Three dimensions of attractiveness are used which originate from the GIF methodology [10]: Technical difficulty (TD), proliferation time (PT) and proliferation cost (PC).[2] For each process, the three dimensions are graded based on expert judgment. The grades range from $0$ meaning a very attractive option to $3$ being very unattractive. Using the arithmetic mean for each edge $e$, a single edge weight $w_e$ is calculated from these figures.

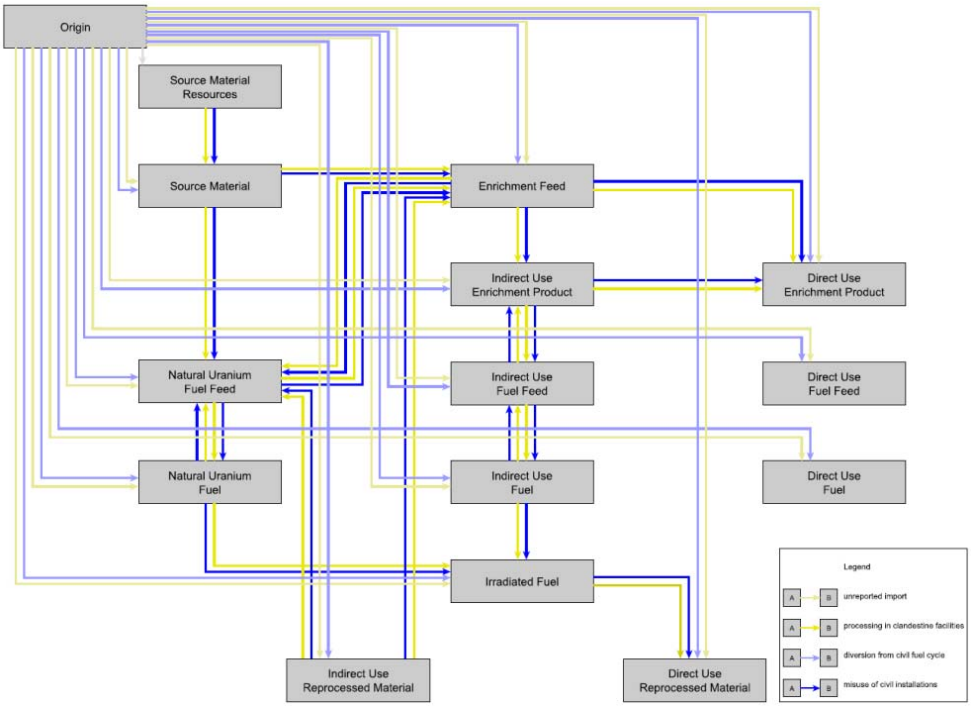


**Fig. 83: Generic Phyiscal Model.**

After having specified the edge weights, it is necessary to model the inspectorate's side i.e. the possible technical objectives $t$ with their respective non-detection probability $\beta_e^{(t)}$ on a specific edge $e$. Also the inspectorate costs $c_t$ generated by technical objective $t$ have to be quantified. Although no specific safeguards measures have been determined at this point, an expert can estimate the costs for attaining a given detection probability based on experience and knowledge about the State's capabilities, fuel cycle as well as existing safeguards approaches. While these figures can be specified for the edges related to the declared fuel cycle, i.e. misuse and diversion, deriving this information for the undeclared processes, i.e.

[2] These dimensions only represent technical aspects of proliferation as if no inspectorate was present. The interplay of State and inspectorate will be considered separately in the third stage of the process.

undeclared import and clandestine processing, is yet an unsolved task. However, the given approach assumes that such quantification can in principle be done for all types of processes, no matter whether they take place in declared facilities or elsewhere in the State.
As a result of the first step, a directed multi-graph is produced that represents the State's options for acquiring weapons usable material including their attractiveness in terms of time, cost and technical difficulty. Furthermore, also the inspectorate's options to control the activities are given, including the costs and non-detection probabilities in specific areas of the State's acquisition network.

**Tab. 3: Game Theoretic Payoffs**

| | No Alarm | Alarm |
|---|---|---|
| Compliant Behavior | $(0, 0)$ | $(-f, -e)$ |
| Non-compliant Behavior along path $p_i$ | $(di, -c)$ | $(-b, -a)$ |

This directed multi-graph is now analyzed in terms of all technically plausible acquisition paths. In order to accomplish this, a fully automated software extracts all paths from node 'Origin' to any node representing weapons usable material by applying the Depth-First-Search (DFS) algorithm [11, pp. 540-549]. For each path $p_i$, the overall attractiveness is calculated by the sum of the weights of the constituting edges $E(p_i)$, i.e.

$$l_i = \sum_{e \in E(p_i)} w_e. \qquad (1)$$

The list of paths is then reordered by attractiveness and all paths are visualized. It has to be emphasized that not only the shortest path but all technically plausible paths are considered. Therefore, this approach is comprehensive and avoids ignoring technically less attractive paths which could be strategically interesting.
Using the results of the first and second step, especially the list of paths with their respective attractiveness as well as the non-detection probabilities of technical objectives, the third step assesses the strategies of both parties, i.e. the State and the inspectorate. On the one hand, all acquisition paths and the option of compliant behavior are considered to be the State's strategy set. On the other hand, the strategies of the IAEA are all combinations of technical objectives (TOC) that have been defined in the first part of the process. The overall non-detection probability of $TOC_j$ for a given path $p_i$ can be calculated using the product rule for probabilities by

$$\beta_{ij} = \prod_{e \in E(p_i), t \in TOC_j} \beta_e^{(t)}. \qquad (2)$$

For each strategy combination a pair of payoff values for State and Inspectorate $(H_1, H_2)$ can be defined (see Table 1). For the IAEA, the strategic outcomes in increasing order of preference are undetected non-compliance $(-c)$, detected non-compliance $(-a)$, false alarm $(-e)$ and compliance without alarm $(0)$. These parameters can be selected freely as long as the ordering is kept.
Regarding the State, the strategic outcomes ordered increasingly by preference are detected non-compliance $(-b)$, false alarm $(-f\ )$, compliance without alarm $(0)$ and successful

acquisition along path $p_i$ ($d_i$). The path length $l_i$ calculated in step two is used to obtain the payoff values for successful acquisition by

$$d_i = \frac{l_1}{l_i}. \qquad (3)$$

The decision whether an alarm is raised by the inspectorate depends on the non-detection probabilities. Hence, for each strategy combination an expected outcome for both players can be calculated. In case the State decides to follow an acquisition path $i$ and the IAEA has $TOC_j$ in place, this payoff for the State is given by the expected benefit from a successful acquisition plus the risk of getting caught red-handed, i.e.

$$H_1^{(i)} = d_i\beta_{ij} - b\big(1 - \beta_{ij}\big). \qquad (4)$$

For the IAEA, the expected payoff can be derived from the sum of the risks of detected and undetected non-compliance, i.e.

$$H_2^{(i)} = -c\beta_{ij} - a\big(1 - \beta_{ij}\big). \qquad (5)$$

In case the State behaves in compliance with its given commitments, the outcome for both sides is only determined by the false alarm risk with false alarm probability $\alpha_j$, i.e.

$$H_1^{(compliant)} = -f\alpha_j \qquad (6)$$

for the State and

$$H_2^{(compliant)} = -e\alpha_j \qquad (7)$$

for the IAEA.

Based on these considerations, a stable strategy combination $(H_1^*, H_2^*)$ known as the Nash equilibrium can be calculated using the Lemke-Howson-algorithm [12]. The Nash equilibrium is characterized by the fact that it is impossible for either of the two actors to deviate unilaterally from the equilibrium strategy and increase its expected payoff. Hence, it seems rational for both players not to deviate and pursue the equilibrium strategy. This very limited definition of rationality only means that the actors care for the risks and benefits they are facing.

Using the equilibrium payoff value for the IAEA and scaling the IAEA's payoff parameters to $c = 1$, it is possible to define effectiveness as

$$E = 100\% + H_2^*. \qquad (8)$$

In case of $0\%$ effectiveness, the equilibrium ends in non-compliance with no possibility of detection. For $100\%$ effectiveness, compliance with no false alarm is achieved almost surely. As the ultimate goal of acquisition path analysis is the selection of a TOC inducing compliant behavior (expressed by the term sufficient in the APA definition), this paper proposes to use a TOC leading to a high effectiveness value in the Nash equilibrium.

Moreover, in cases where compliant behavior can be induced in the Nash equilibrium, it is also possible and reasonable to gain an increase in efficiency. By iterating over a cost threshold $W$ and calculating the Nash equilibrium for this range of values, a strategy with a given level of effectiveness at minimum costs can be selected.

Strategic Assessment using Performance Targets and Game Theory

In the previous section, it has been shown how a game theoretic, highly quantitative approach to technical objectives determination could look like. Alternatively, a more qualitative approach based on the idea of performance targets [13] can be used, whichallocates more flexibility to the analyst. This section will show that the philosophy behind these two different approaches to APA can be considered to be equivalent.

A performance target on the path level can be defined as the minimum detection probability that is needed in order to deter a State from pursuing this path. This means that if performance targets are properly defined for a given set of acquisition paths, these paths can be considered to be adequately covered by safeguards measures. Hence, the State is likely to act in compliance with its given commitments.

More formally, one can say that for given acquisition path $p_i$ and technical objectives combination $TOC_j$, path coverage is achieved if the risk for the State to get caught along the path is higher than the benefit of a successful acquisition[3], i.e.

$$d_i\beta_{ij} - b(1-\beta_{ij}) \leq 0. \qquad (9)$$

In the past, the IAEA has considered it to be sufficient to obtain a detection probability of $90\%$ in nuclear facilities with high potential to be used in nuclear weapons programmes. Transferring this to the idea of acquisition path analysis, for the most attractive path a performance target of $90\%$ should be reached. As shown in Avenhaus and Canty [14], this directly influences the choice of the payoff values in Equation 9, i.e.

$$0 \geq d_1 \cdot 0.1 - b \cdot 0.9,$$
$$9 \geq {}^{d_1}/_{b}.$$

Because the payoff values are ranging from $0$ to $1$ (see Equation 3) with $d_1 = 1$, the State's payoff for a successful acquisition is $b = 1/9$.

Using these parameter values derived for the most attractive path, one can reinsert them into Equation 9 which leads to

$$\beta_{ij} \leq \frac{b}{d_i+b} = \frac{1}{9\frac{l_1}{l_i}+1}. \qquad (10)$$

This gives a rationale to define the path performance targets for the detection probability based on its attractiveness as

$$PT_i = DP_i^{(\min)} = 1 - \beta_{ij}^{(max)} = \frac{l_1}{l_1+l_i b}. \qquad (11)$$

[3] For reasons of simplicity, false alarm risks are ignored in this paper. A similar argument can be made, if false alarm risks are included in the model.

This calculation of performance targets can be used within the methodology of Budlong Sylvester et al. [15] in order to specify the appropriate technical objectives. If all performance targets are fulfilled, it is guaranteed under the assumptions of the model that the State will chose to behave in compliance with its commitments.
While the methodology in Budlong Sylvester et al. [15] leaves the decision up to the analyst which technical objectives to choose, the methodology in Section 2 uses an optimization technique to determine them. From the standpoint of the underlying philosophy however, both methods are equivalent.

## Conclusions and Outlook

This paper shows how acquisition path analysis can be carried out using a comprehensive methodology which is yet compatible with the principles defined in Cooley [1]. Furthermore, two possibilities for determining technical objectives were proposed. The first more quantitative approach delivers a set of technical objectives with optimal effectiveness under the assumptions of a game theoretic model. Besides the high degree of automation, this approach also allows for an inherent randomization of technical objectives. However, the analyst has to specify a set of parameters in this approach. Therefore a good understanding of the model is necessary, as the influence of the parameters on the model's outcome is very complex.
The alternative approach overcomes these drawbacks by a higher degree of interaction with the analyst. Moreover, it allows for re-prioritization of paths based on possible indications. On the other hand, this flexibility leads to less reproducibility of the results when transferring the task to a different analyst.
In summary, both methodologies have their advantages and disadvantages. However, it also has been shown that the underlying philosophy of both approaches is the same.
In the future, the outcomes sensitivity on the selected parameters in both approaches will be investigated. Furthermore, the applicability of the presented ideas to other applications in the area arms control and disarmament will be investigated. Finally, the methodology will be iteratively improved with the help of experts at the IAEA.

## References


[1] J. N. Cooley. "Progress in Evolving the State-level Concept". In: *Seventh INMM/ESARDA Joint Workshop Future Directions for Nuclear Safeguards and Verification*. **2011**.
[2] International Atomic Energy Agency (IAEA). "IAEA Safeguards Glossary". In: *International Nuclear Verification Series No. 3* (**2001**).
[3] C. Listner et al. "A Concept for Handling Acquisition Path Analysis in the Framework of IAEA's State-level Approach". In: *Proceedings of the 53rd INMM Annual Meeting*. INMM. **2012**.
[4] C. Listner et al. "Approaching acquisition path analysis formally - experiences so far". In: *Proceedings of the 54th INMM Annual Meeting*. INMM. **2013**.
[5] C. Listner et al. "Approaching acquisition path analysis formally - a comparison between AP and non-AP States". In: *Proceedings of the 35th ESARDA Annual Meeting*. **2013**.
[6] C. Listner et al. "Evolution of Safeguards - What Can Formal Acquisition Path Analysis Contribute?" In: Institute of Nuclear Materials Management 55th Annual Meeting, Atlanta(USA), 07/20/2014 - 07/24/2014. **2014**.
[7] C. Listner et al. "Quantifying Detection Probabilities for Proliferation Activities in Undeclared Facilities". In: Symposium on International Safeguards: Linking Strategy, Implementation and People, Vienna(Austria), 10/20/2014 - 10/24/2014. **2014**, p. 28.
[8] C. Listner et al. *A Concept for Handling Acquisition Path Analysis in the Framework of IAEA's State-level Approach*. Tech. rep. JOPAG/04.13-PRG-400. **2013**.
[9] International Atomic Energy Agency (IAEA). "The Physical Model". STR-314. **1999**.
[10] GEN IV International Forum. *Evaluation Methodology for Proliferation Resistance and Physical Protection of Generation IV Nuclear Energy Systems*. **2006**.
[11] T.H. Cormen et al. *Introduction to Algorithms*. 2nd. Cambridge, MA, USA: MIT Press, **2001**.

[12] M. J. Canty. *Resolving conflicts with Mathematica: algorithms for two-person games*. AP, **2003**.
[13] C.L. Murphy et al. “Evolution of Safeguards - An Information-driven Approach to Acquisition Path Analysis”. In: *Proceedings of the 55th INMM Annual Meeting*. INMM. **2014**.
[14] R. Avenhaus and M.J. Canty. “Formal Models of Verification”. In: *Verifying Treaty Compliance*. Ed. by R. Avenhaus et al. Springer, **2006**, pp. 295–319.
[15] K. W. Budlong Sylvester et al. “The Use of Performance Targets in the State-Level Concept”. In: *Proceedings of the 55th INMM Annual Meeting*. INMM. **2014**.

## 5.18. Non-nuclear applications

### Non-Nuclear Applications of Prompt and Delayed Gamma Neutron Activation Analysis

Prompt and Delayed Gamma Neutron Activation Analysis (P&DGNAA) based on neutron generator or isotopic neutron sources is a versatile and powerful non-destructive analytical technique which may found applications in relevant fields such as safeguards (specific detection of nuclear materials), home-land security (detection of dangerous substances like chemicals or explosive), primary natural resources prospection (in situ borehole-logging, analysis of drilling core) and secondary natural resources assay (analysis of baring material, urban-mining, sludge, characterization of Waste Electrical and Electronic Equipment (WEEE) for recycling). Furthermore P&DGNAA may be implemented in industrial processes for parameter optimization and for quality control of products and also to determine the toxicity level of residues.

The MEDINA technology [1,2] based on P&DGNAA and developed for the characterization of radioactive waste has attracted quite some interest in recycling industry. The performance of MEDINA to determine the elemental composition of various large samples such as catalytic converters (Umicore AG & Co. KG, Belgium), CRT-glass (3S International, USA), Fluorescent powder (BLUBOX Company, Switzerland) and material from remedial activities (Eberhard Recycling AG, Switzerland) were investigated. In cooperation with RWE Power AG application of P&DGNAA for online elemental analysis of brown coal for firing optimization is also investigated.

#### References


[1] E. Mauerhofer, A. Havenith, The MEDINA facility for the assay of chemotoxic inventory of radioactive waste packages J Radioanal Nucl Chem (**2014**) 302:483-488

[2] Patent AU2011282018; Forschungszentrum Jülich GmbH, E. Mauerhofer, J. Kettler


### Application of safeguards methods and techniques in the context of BWC verification

Many of the technologies and methodologies originally developed for verifying safeguards agreements in the context of the Nuclear Non-proliferation Treaty (NPT) could also be used for other verification regimes. In this regard, IEK-6 started to collaborate with the Research Group for Biological Arms Control at Carl Friedrich von Weizsäcker-Centre for Science and Peace Research (ZNF), University of Hamburg, on new strategies and concepts for the lacking verification system of the Biological Weapons Convention (BWC). The main focus has been on remote sensing and satellite imagery processing for off-site inspection of potential production facilities as well as mathematical models to analyse all potential paths by which a State could acquire biological warfare agents.

**Rare earth element separation by solvent extraction**

During the last decades the demand for rare earth elements (REE) increases as a result of rising technology applications (e.g. hybrid cars, wind turbines, industrial catalyst, etc.). China has, beside Australia and the United States, the largest rare earth deposits and has a global monopoly on rare earths mining [1]. Since last years, caused by a Chinese export restriction, a significant increase in rare earth prices was observed. Expecting a rising demand for rare earth metals a shortage of rare earths is upcoming. The separation of rare earth elements, the last step of rare earth mineral beneficiation, is the most value creating procedure. The most challenging separation is the separation of two directly neighboring rare earth elements [2]. There have been major developments in the technology for the separation of high purity rare earths. One advantageous technique for rare earth purification involves hydrometallurgical processes, such as those developed at IEK-6 for actinide(III) partitioning [3]. Both families of f-elements have very similar physical and chemical properties. Many extraction systems with relatively low rare earth separation factors were described in the literature. Neighboring rare earth, being chemically similar, show in Satos report separation factors from 1.03-2.58 [4]. Satos data were reproduced and for heavier rare earth elements (e.g. Er, Yb) a higher extraction at lower concentrations can be observed. In collaboration with an industrial partner, the IEK-6 will use its expertise to develop more efficient extraction systems for the mutual lanthanide separation.

**References**


[1] Kynicky, J., Smith, M. P., Xu, C., Elements 2012, 8, 361-367.
[2] Gupta, C. K., Krishnamurthy, N., Extractive metallurgy of rare earths, CRC Press, Boca Raton, Florida, 2005.
[3] Modolo, G., Odoj, R., J. Alloy. Compd. 1998, 271-273, 248-251.
[4] Sato, T., Hydrometallurgy 1989, 22, 121-140.

# 6 Education and training activities

Education in nuclear safety research in particular with RWTH Aachen University is supported by IEK-6. Prof. Dirk Bosbach holds the chair for the disposal of nuclear waste. Further, an accredited Master Curriculum "Nuclear Safety Engineering" was established at RWTH Aachen University in 2010 and in the meantime several students participated this two years programme. A practical course on nuclear measuring techniques in the radiochemistry laboratories of IEK-6 as well as the lecture "Introduction to Nuclear Chemistry" was launched in 2010 and has attracted students from nuclear safety engineering, chemistry, computational engineering science and nuclear technology at RWTH Aachen University. Lectures are also given at the Aachen University of Applied Science by IEK-6 staff.
In the framework of the JARA cooperation Prof. Dr. Evgeny Alekseev and PD Dr. Hartmut Schlenz are teaching at the Institute of Crystallography / RWTH Aachen University and at the Faculty of Mathematics and Natural Sciences / University of Bonn respectively. Additionally PD Dr. Giuseppe Modolo habilitated at RWTH Aachen University.

The IEK-6 also participates in the new graduate school Energy and Climate HITEC, which was founded in 2011 in Jülich. The IEK-6 supports HITEC Theme Days “Nuclear waste disposal and reactor safety” held at RWTH Aachen University, HITEC Methods Days “Application of X-ray diffraction methods in energy research” as well as HITEC Labs “Synthesis methods for immobilizing radioactive elements in ceramic host phases” and “Structural characterization of ceramics by spectroscopic and diffraction methods”, which are hands-on practical training lasting two to three days for small groups of PhD students from various HITEC fields. Furthermore, biannual Orientation Days (in March and October) are organized for new HITEC participates. Second-year PhD students organize a three-day retreat; where they present their projects and the scientific methods employed and discuss them with their fellow PhD students.

## 6.1. Courses taught at universities by IEK-6 staff

**Prof. Dr. D. Bosbach**

RWTH Aachen University
Faculty of Georesources and Materials Engineering
Topic: Grundlagen der Kernchemie, Hours: 2 SWS, since WS 2010
Topic: Langzeitsicherheit der Endlagerung, Hours: 2 SWS, WS 2012/2013 2013/2014
Topic: Kerntechnisches Messpraktikum, 1 week, since WS 2010

**Prof. Dr. B. Thomauske**

RWTH Aachen University
Faculty of Georesources and Materials Engineering
Topic: Endlagerung radioaktiver Abfälle und Sicherheitsanalysen, Hours: 2 SWS, WS 2013/2014
Topic: Nuklearer Brennstoffkreislauf I, Hours: 2 SWS, since WS 2010
Topic: Produkte und Märkte der Rohstoffindustrie, Hours: 2 SWS, since WS 2010
Topic: Rohstoffe und Energieversorgung, Hours: 2 SWS, since WS 2010

**Prof. Dr. E. Alekseev**

RWTH Aachen University
Faculty of Georesources and Materials Engineering
Topic: Some aspects of solid state and coordination chemistry of actinides, Hours: 4 SWS, SS 2014
Topic: Single-crystal diffraction on actinide compounds, Hours: 4 SWS, SS 2014
Topic: Grundzüge der Kristallographie, Hours: 4 SWS, Since WS 2012

**PD Dr. H. Schlenz**

University of Bonn
Faculty of Mathematics and Natural Sciences
Topics: Crystallography and Applied Mineralogy, Hours: 2 SWS

**PD Dr. G. Modolo**

Aachen University of Applied Science, Fachbereich Chemie und Biotechnologie
European Master of Science in Nuclear Applications
Topic: Nuclear Fuel Cycle, Hours: 2 SWS since 2010

RWTH Aachen University
Faculty of Georesources and Materials Engineering
Topic: Brennstoffe, Wiederaufbereitung und Konditionierung, Hours: 2 SWS, since 2011
Topic: Sicherheit in der Wiederaufarbeitung, Hours: 3 SWS, since 2011

**Dr. I. Niemeyer**

RWTH Aachen University
Faculty of Georesources and Materials Engineering
Topic: Nuclear Safeguards and Non-Proliferation, Hours: 2 SWS, SS 2013, SS 2014

**Dr. H. Tietze-Jaensch**

Aachen University of Applied Science
Nuclear Chemistry Seminar
Topic: Safety Assessment and Comparing Safety Records of Various Energy Carriers, 2 h lecture, May 2014

University of South China, Hengyang, China
Inst. of Physics and Nuclear Technology
Topic: Nuclear Energy Production & Safety Prospects, 18 h lecture, Oct. 2014

Seminar European Spallation Source (ESS), Lund, Sweden
Inst. of Physics and Nuclear Technology
Topic: Safe Nuclear Waste Disposal, Characterization, Quality Control and Numerical Assessment of Radioactive Waste Properties, 2 h lecture, May 2014

6th International Summer School: Operational Issues in Radioactive Waste Management and Nuclear Decommissioning, Joint Research Centre Ispra, Italy
Inst. of Physics and Nuclear Technology
Topic: Nuclear Waste Characterization and Quality Control, 3 h lecture, Sep. 2014

7th International School on Nuclear Power, Warsaw, Poland
Inst. of Physics and Nuclear Technology
Topic: Experience from Preparing a Nuclear Waste Repository in Germany, 2 h lecture, Nov. 2014

## 6.2. Habilitation

**Dr. Giuseppe Modolo** defended successfully his Habilitation "Untersuchungen zur Abtrennung, Konversion und Transmutation von langlebigen Radionukliden - Ein Beitrag zur fortschrittlichen Entsorgung von hochradioaktiven Abfällen" at the RWTH Aachen university, faculty 5 – Georesources and Materials Engineering and obtained the permission to teach in the subject area of Chemistry and Technology of Nuclear Disposal.

## 6.3. Graduates

18 PhD students are currently (Dec. 2014) working on research projects related to the safe management of nuclear waste in Jülich. 7 PhD candidates had successfully defended their theses during the last 2 years. Furthermore, 13 diploma, bachelor, and master theses were finished in 2013 / 2014. Currently, 4 students are working on their theses. 6 students passed an internship at IEK-6 during the last 2 years.

### *6.3.1 Bachelor, Diploma, Master Thesis*

**Barth, A.:** Management safeguards-relevanter Informationen aus Fernerkundungsdaten mit Hilfe von Geoinformations-Technologien, Diploma Thesis, TU Bergakademie Freiberg, 99 p., 2013.

**Dellen, J.**: Synthesis and Characterization of Kosnarite-type Ceramics as Potential Actinide Waste Forms, Bachelor Thesis, Hogeschool Zuyd Heerlen, Netherlands, 54 p., 2013.

**Göbbels, C.:** A numerical method for the gamma spectrometry of bulk samples, Master Thesis, FH Aachen, 59 p., 2014.

**Königs, U.:** Synthese von lamellaren Doppelhydroxidverbindungen mit unterschiedlichen Zwischenschichtanionen und strukturelle / thermodynamische Beschreibung, Bachelor, FH Aachen,111 p., 2014.

**Langer, E.:** New U and Th Selenate and Selenite Compounds: Synthesis, Structural and Spectroscopic Investigation, Master Thesis, RWTH Aachen, 93 p., 2014.

**Lange, S.:** Selective extraction of trivalent Americium from PUREX raffinate by the use of $CyMe_4BTPhen$ and TEDGA, Master Thesis, FH Aachen, 80p., 2014.

**Lichte, E.:** The dissolution behavior of magnesium oxide based inert matrix fuel for the transmutation of plutonium and minor actinides, Master Thesis, FH Aachen, 73 p., 2013.

**Middendorp, R.:** Preparation and characterization of U/Nd oxide microspheres synthesized by the week-acid resin process, Master Thesis, FH Aachen, 89 p., 2013.

**Mildenberger, F.:** Konzeptionierung einer Neutronenabschirmung für die MEDINA-Testeinrichtung, Master Thesis, RWTH Aachen University, 188 p., 2013.

**Poll, A.**: Charakterisierung von Präcursor Lösungen für die Partikelherstelluzng mittels Inerter Gelierung, Bachelor Thesis, 2014

**Schmidt, H.:** Selektive Am(III) Extraktion aus PUREX-Raffinaten unter Einsatz von Dithiophosphinsäuren; Master Thesis, RWTH Aachen University, 100 p., 2014.

**Schreinemachers, C.:** Preparation and characterization of U / Nd microspheres synthesized by internal gelation, Master Thesis, FH Aachen, 102 p., 2013.

**Weber, J.:** Uptake of radium and solid solution formation in the ternary system of (Ba,Ra Sr,)$SO_4$, Master Thesis, Rheinische Friedrich-Wilhelms-Universität Bonn, 95 p., 2013.

**Velten, C.**: Experimente zur Validierung der Bestimmung von thermischen Wirkungsquerschnitten für Neutroneneinfang mittels PGAA, Bachelor Thesis, RWTH Aachen University, 52 p., 2013

### *6.3.2 Doctoral Thesis*

**Finkeldei, S.:** Pyrochlore as nuclear waste form: actinide uptake and chemical stability, Schriften des Forschungszentrums Jülich Reihe Energie & Umwelt / Energy & Environment 276, 153 p. (2014) RWTH Aachen University

**Havenith, A.:** Stoffliche Charakterisierung radioaktiver Abfallprodukte durch ein Multi-Element-Analyseverfahren basieren auf der instrumentellen Neutronen-aktivierungs-Analyse – MEDINA- (2014) RWTH Aachen University

**Krings, T.:** SGSreco – Radiologische Charakterisierung von Abfallfässern durch Segmentierte y-Scan Messungen; Schriften des Forschungszentrums Jülich Reihe Energie & Umwelt / Energy & Environment 208, ix, 181, XI Seiten (2014) RWTH Aachen University

**Labs, S.:** Secondary Phases of Spent Nuclear Fuel - Coffinite, $USiO_4$, and Studtite, $UO_4$*$4H_2O$ - Synthesis, Characterization and Investigations Regarding Phase Stability, Schriften des Forschungszentrums Jülich Reihe Energie & Umwelt / Energy & Environment 267, 195 p. (2014) RWTH Aachen University

**Listner, C.:** Änderungsdetektion digitaler Fernerkundungsdaten mittels objekt-basierter Bildanalyse; Schriften des Forschungszentrums Jülich Reihe Energie & Umwelt / Energy & Environment 242, 176 p. (2014), TU Bergakademie Freiberg

**Schneider, St.:** Numerische Simulation von Abfallgebinden aus der Wiederaufbereitung von Kernbrennstoffen, RWTH Aachen University

**Sypula, M.:** Innovative SANEX process for trivalent actinides separation from PUREX raffinate; Schriften des Forschungszentrums Jülich Reihe Energie & Umwelt / Energy & Environment 200, 220 p. (2014) RWTH Aachen University

## 6.4. Vocational training

Forschungszentrum Jülich offers different vocational training programs. The 3 years lasting education is supported by IEK-6 in nuclear- / radio-chemistry. In 2013/14 three laboratory assistants were trained in the laboratories of IEK-6. One of them finished their education successfully in 2014 and received a certificate of apprenticeship.

## 6.5. Further education and information events

IEK-6 is committed to support the education of young people including schoolchildren in nuclear safety research. Forschungszentrum Jülich participates in the nationwide **"Girls Day".** Girls from $5^{th}$ to $13^{th}$ class have the opportunity to become familiar with different professions such as chemist, physicist, or firewoman as well as the working conditions at laboratories, garages and offices. At IEK-6, the topic "No fear of radioactive materials" was presented. Basics about radioactivity in the environment and radioactive decay as well as different measuring techniques were explained. Measurements of different sample were carried out by the girls themselves to get a feeling for radioactivity and attract children's interest in science.

An **excursion** of IEK-6 Ph.D. students, technical and scientific staff to the **German repository project sites Asse II, Gorleben, and "Schacht Konrad"** was organized. The three sites are located in close proximity to each other in the federal state of Lower Saxony.
At all sites the facilities above ground were visited and an underground visit was organized, too. After the technical visits discussions with on-site staff and members of the site operators were held.
The Gorleben salt dome was under investigation as a site for the disposal of heat-generating waste, but the project is currently stopped and no waste packages have been disposed of here. Asse II is a former salt mine and was later used for investigating the storage of low and intermediate level radioactive waste. However, as water is penetrating into the mine, the safe retrieval of the waste packages is currently investigated. At both sites the mines and especially different places which were recently discussed in the public were visited. For example, the inclusion of organic material in the Gorleben salt, and points where water penetrates into the Asse II mine were shown.
At the Gorleben site the "Pilot-Konditionierungsanlage", a pilot plant for the conditioning of spent fuel into disposal casks, was visited, too.
The former iron ore mine "Schacht Konrad" in Salzgitter is currently reconstructed to become the German final repository for non-heat-generating waste. The construction sites of some storage cabins were visited underground.

**Fig. 84: Group photo at the Gorleben site (Bundesamt für Strahlenschutz, DBE).**

Within the framework of the german joint research project “Fundamental studies on conditioning of long-lived radionuclides in ceramic waste forms” (funded by Federal Ministry of Education and Research (BMBF, grant no.: 02NUK021)) IEK-6 organized in July 2014 the „**8th European Summer School** on supramolecular, intermolecular, interaggregate interactions and separation chemistry“. Approximately 60 participants from France, Russia and Germany joined the summer school; 18 lectures and 37 posters were presented addressing topics of international relevance with respect to Nuclear Waste Management and mobility of radionuclides in the environment as well as state-of-the art analytical methods.

**Fig. 85: Prof. Dr. Evgeny Alekseev (IEK-6) was giving a lecture (right) on solid state chemisty of actinides to the participants (left) of the European summer school.**

## 6.6. Institute Seminar

The IEK-6 organizes an institute seminar with internal talks and invited speakers, to present the recent research activities. Further information on www.fz-juelich.de/iek/iek-6.

### *6.6.1 Internal talks 2013*

27.02.2013 **H. Curtius, E. Alekseev, P. Kowalski, S. Neumeier, G. Modolo, I. Niemeyer, D. Vulpius, H. Tietze-Jaensch, H.J. Steinmetz:** Vorträge der Gruppenleiter, „Ergebnisse aus 2012 und Ausblick 2013“

06.03.2013 **S. Lab:** Coffinite, $USiO_4$, and Studtite, $UO_4*4H_2O$ - relevant phases in a final repository for spent nuclear fuel?

13.03.2013 **S. Omanovic:** Selective separation of rare earth metals by organophosphorus extractants

**M. Dürr:** Die Kooperation FZ Jülich - IAEO im Bereich der Analytik für Internationale Kontrollen

20.03.2013 **C. Listner:** Einschätzung von Proliferationsrisiken anhand mathematischer Modelle

**E. Ebert:** Dissolution behavior of MgO and Mo based ADS inert matrix fuel

10.04.2013: **Y. Arinicheva:** Studies on structure and stability of monazite-type ceramics for the conditioning of minor actinides

**A. Knott:** Aufbau und Implementierung einer Apparatur zur Herstellung monodisperser Partikel zur Verwendung als Standard in der Partikelanalyse

24.05.2013: **G. Beridze:** Computing actinide-bearing materials

**K. Baginski:** Thermische Behandlung von radioaktivem Graphit

15.05.2013: **C. Schreinemachers:** Preparation and characterization of U / Nd microspheres synthesized by internal gelation

**J. Assenmacher:** Fundamental Investigations of the Complexation of Aromatic Dithiophosphinic Acids with Actinides(III) and Europium(III) using Solvent Extraction and TRLFS

22.05.2013 **T. Krings:** SGSreco: A computer code for the precise and reliable reconstruction of activities in radioactive waste drums by Segmented Gamma-Scanning

**C. Rizzato:** Thermal Treatments of Nuclear Graphite: results and interpretation

05.06.2013: **L. Kuhne:** DIDO-Rückbauprojekt Radiochemische Analysen

**K. Rozov:** Preparation, structure and thermodynamics of Fe(II)-, Co(II)-, Ni(II)- and Zr(IV)-containing layered double hydroxides (LDHs)

19.06.2013: **P. Kaufholz:** Trivalent Actinide separation by an innovative SANEX process

**G. Deißmann:** Endlagerung radioaktiver Abfälle in den Niederlanden: Der OPERA safety case

26.06.2013: **J. Heuser:** Investigations of Lanthanide-Phosphates - potential host matrices for radionuclides

**A. Bukaemskiy:** Stability of Pyrochlore phase for zirconia based ceramics. Experimental and modeling study

03.07.2013: **C. Genreith:** Prompt Gamma Aktivierungsanalyse von $^{237}$NP, $^{242}$Pu und $^{241}$Am

29.10.2013 **R. Middendorp**: Preparation and characterization of U/Nd microspheres synthesized by the weak-acid resin process

20.11.2013 **G. Deißmann:** Long-term performance of potential plutonium wasteforms under conditions relevant to geological disposal in the UK

**M. Dürr:** Safeguards für die nukleare Entsorgung im Zeichen der 'Energiewende'

27.11.2013 **P. Kegler:** Chemistry under extreme conditions: the new high pressure - high temperature facility at IEK-6

**C. Murphy:** Los Alamos National Laboratory and the International Safeguards System

04.12.2013 **A. Blanca Romero:** Atomistic modelling of Monazite-type ceramic

**A. Knott:** Monodisperse Partikel für Safeguards-Anwendungen

19.12.2013 **E. Lichte:** The dissolution behavior of magnesium oxide based inert matrix fuel for the transmutation of plutonium and minor actinides

### *6.6.2 Internal talks 2014*

23.01.2014 **H. Schmidt:** Selektive Am(III)-Extraktion aus PUREX-Raffinaten unter Einsatz von Dithiophosphinsäuren

29.01.2014 **J. Dellen:** Synthesis and Characterization of Kosnarite-type Ceramics

**F. Brandt:** Uptake of Ra during recrystallization of barite: experiments and thermodynamic modelling

12.02.2014 **A. Wilden:** Modified Diglycolamides for actinide separation: Solvent Extraction and Time-Resolved Laser Fluorescence Spepctroscopy: Complexation Studies

**N. Yu:** New thorium arsenates family $A_2Th(AsO_4)_2$ (A = Li, Na, K, Rb, Cs): formation, structures and properties

19.02.2014 **M. Klinkenberg:** Uptake of Radium by barite under repository relevant conditions

**B. Xiao:** New aspects of Th solid-state chemistry in oxo-molybdate systems

12.03.2014 **S. Neumeier:** BMBF Projekt “Conditioning”

**J. Weber:** Ra uptake and solid solution formation in the ternary system of $(Ba,Ra,Sr)SO_4$

19.03.2014 **E. Petrova:** Irradiated reactor graphite study in the MEPHI

26.03.2014 **A. Havenith:** Berücksichtigung wassergefährdender Stoffe im Endlagerverfahren Konrad

**M. Schumann:** Aufbau und Test einer Anlage zur Radiographie mit schnellen Neutronen

02.04.2013 **Zs. Revay:** In-beam activation analysis at the high-flux PGAA facility at FRM II, Garching

**C. Genreith:** Radiative capture cross sections of actinides using PGAA with cold neutrons

07.05.2013 **V. Vinograd:** The Oklo phenomenon

14.05.2014 **S. Omanovic:** Rare Earth Separation by Sovent Extraction

**J. Heuser:** Investigations of Sm-based monazite-type ceramics

23.06.2014 **E. Langer:** New U and Th Selenate and Selenite Compounds: Synthesis, Structural and Spectroscopic Investigation

25.06.2014 **I. Fast:** Bestimmung der Unsicherheiten des nuklearen Inventars von abgebrannten Brennelementen durch sekundären Reaktorparameter

17.07.2014 **S. Lange:** Selective extraction of trivalent Americium from PUREX raffinate by the use of CyMe4BTPhen and TEDGA

03.09.2014 **P. Kaufholz:** Americium selective extraction using hydrophilic complexing abents

17.09.2014 **K. Rozov:** Estimation of thermodynamic properties of layered double hydroxides (LDHs) by using a calorimetric method

**P. Heath** (University of Sheffield): The characterisation of heterogeneous wasteforms from ion exchange materials

22.10.2014 **H. Schmidt:** Radiation stability of nitrogen donor ligands

**S. Labs:** Newly made discoveries in the Th_xB_(1-x)SiO_4, (B=Zr,Hf) solid solution systems

05.11.2014 **A. Fichtner:** Gas release from spent nuclear fuel during prolonged interim storage

**Y. Li:** Molecular modeling of pyrochlore

12.11.2014 **R. Middendorp:** Uranium Oxide Microspheres as (Certified) Reference Material for Nuclear Safeguard Particle Analysis

**A. Neumann:** Laboratory Powder X-ray Diffraction at non-ambient conditions

19.11.2014 **D. Bosbach:** Endlagerforschung

**G. Deissmann:** Aspekte zur Standortauswahl und zum Langzeit-sicherheitsnachweis (Safety Case) für ein Endlager für wärmegenerierende hochradioaktive Abfälle

26.11.2014 **P. Kowalski:** Nuclear waste management on supercomputers or: How I learned to stop worrying and love the actinides

**J. Weber:** Radium up take into Barite

### *6.6.3 Invited talks 2013*

26.02.2013 **Prof. Dr. K.-J. Röhlig:** Endlagerung radioaktiver Abfälle: Konzepte und Projekte
Institut für Endlagerforschung, TH Clausthal

05.04.2013 **Prof. Dr. Ch. Poinssot:** The recycling of the actinides, a cornerstone for sustainable fuel cycles. Insight on the French CEA/DRCP programs
Chef du Département RadioChimie et Procédés, Commissariat à l'Energie Atomique et aux Energies Alternatives, CEA Marcoule, France

09.04.2013 **Dr. Schartmann:** Firmenporträt Brenk Systemplanung
Brenk Systemplanung GmbH, Aachen

23.04.2013 **Dr. Geiger:** Garnet Solid Solutions: Microscopic Structural - Macroscopic Thermodynamic Relationships
Materialforschung & Physik, Section Mineralogy, Universität Salzburg, Salzburg, Austria

21.05.2013 **Dr. N. Shcherbina:** Marie Curie fellowship: A proposal for collaborative work PSI-FZJ
Paul-Scherrer-Institut, Villingen, Switzerland

03.06.2013 **Prof. Dr. A. Lüttge:** Driving Dissolution Studies in a New Direction
Geowissenschaften, University Bremen

27.06.2013 **Dr. J. Mönig:** Development of the „smart Kd“ approach for long-term safety analysis
Gesellschaft für Anlagen- und Reaktorsicherheit mbH (GRS), Köln

17.07.2013 **Prof. Dr. R. Ewing**: Plutonium: Nuclear vs. Geologic Solutions
Department of Earth & Environmental Sciences, University of Michigan

06.08.2013: **Prof. Dr. B.J. Kennedy:** From Disorder comes Order: Studies of the Fluorite-Pyrochlore Transformation
President of the Australian Institute of Nuclear Science and Engineering

05.09.2013: **Dr. G. Lumpkin:** Atomistic modelling and experimental studies of nuclear fuel cycle materials at ANSTO
Australian Nuclear Science and Technology Organization (ANSTO), Institute of Materials Engineering

### *6.6.4 Invited talks 2014*

04.02.2014 **Prof. A. Abdelouas:** Research and Development activities on nuclear waste management at SUBATECH
SUBATECH, Nantes, France

06.02.2014 **Dr. C. Hennig:** Polynuclear complexes of tetravalent actinides and lanthanides with simple carboxyl ligands
HZDR-ROBL

25.03.2014 **Dr. J.P. Icenhower:** Determining glass dissolution rates using interferometry and the role of uncertainties associated with surface area
Lawrence Berkeley National Laboratory, CF, USA

04.06.2014 **Dr. U. Breuer:** Neue Atomsonde am Forschungszentrum Jülich - Grundlagen und erste Ergebnisse
Central Institute of Engineering, Electronics and Analytics, ZEA-3 Analytics

01.07.2014 **G. Gluschke:** IT/Cyber Security and Nuclear Security Education
Institute for Security and Safety (ISS) at the Brandenburg University of Applied Sciences

08.09.2014 **Prof. A. Navrotsky:** Thermochemical studies of Actinide Materials
University of California at Davis, USA

12.09.2014 **Prof. Dr. W.J. Weber:** Radiation Effects in Ceramics used for the Conditioning of Actinides
University of Tennessee, USA

09.10.2014 **Dr. G. Thorogood:** Current Activities of the Institute of Materials Engineering at ANSTO
ANSTO (Australian Nuclear Science and Technology Organisation)

18.11.2014 **Prof. A. Chmielewski:** INCT program in radio- and radiation chemistry beneficial for health, environment and energy
Polytechnische Universität Warschau, ICNT

20.11.2014 **Dr. T. Schäfer:** Überblick der hydrogeochemischen Arbeiten des INE und zukünftige Schwerpunkte
INE, KIT, Karlsruhe

24.11.2014 **Dr. V.V. Rondinella:** Post irradiation examination of nuclear fuel under extreme conditions
Joint Research Centre Institute for Transuranium Elements (ITU), Karlsruhe

18.12.2014 **PD Dr. C. Degueldre:** Post irradiation examination of nuclear fuel: The advantage of combining advanced analytical techniques
Paul Scherrer Institut Schweiz

## 6.7. Visiting Scientists / Research Visits

**Visiting Scientists**

**Marcin Brykalla** 25.11.2013 – 20.12.2013
Institute of Nuclear Chemistry and Technology, Warsaw, Poland

**Marcin Rogowski** 25.11.2013 – 20.12.2013
Institute of Nuclear Chemistry and Technology, Warsaw, Poland

**Chantell Murphy** 01.10.2013 - 31.12.2013
University of New Mexico, New Mexico, USA

**Michael Gray** 14.10.2013 - 16.12.2013
University of Carlifornia Irvine, Irvine, CA, USA

**Vladislav Klepov** 01.10.2013 – 31.07.2014
Samara State University, Samara, RU

**Sergei Novikov** 01.11.2013 – 30.08.2014
Samara State University, Samara, RU

**Andreas Neumann** 2013/2014
RWTH Aachen University, Aachen, Germany

**Florent Tocino** 10.03.2014 – 21.03.2014
Laboratoire des Interfaces de Matériaux en Evolution (LIME)**;** Institut de Chimie Séparative de Marcoule (ICSM), France

**Paul Heath** 23.07.2014 – 02.10.2014
Sheffield University, Sheffield, UK

**April Birnie** 09.06.2014 – 29.08.2014
Smith College, Northampton, MA, USA

**Tangi Nicol** 01.10.2014 – 31.09.2015
CEA-Cadarache, France

**Maxim Lelet** 08.12.2014 – 20.12.2014
Lobachevsky State University of Nizhni Novgorod, RU

**Research visits of IEK-6 staff**

| | |
|---|---|
| **Yulia Arinicheva** | 07.07.2013 - 19.07.2013 |
| Institut de Chimie Séparative de Marcoule (ICSM), France | 15.09.2013 - 11.10.2013 |
| **Christoph Genreith** | 01.08.2013 - 31.09.2013 |
| Lawrence Berkeley National Laboratory (LBNL) in Berkeley, CA, USA | |
| **Sabrina Labs** | 04.11.2013 - 10.11.2013 |
| Lujan Center at Los Alamos neutron Science Center, Los Alamos, NM, USA | |
| University of California, Davis, CA, USA | 10.11.2013 - 18.11.2013 |
| | 14.11.2014 - 29.11.2014 |

# 7 Awards

**Ivan Fast** received the Roy G. Post Foundation Scholarship at the international Waste Management (WM) conference 2013 in Phoenix, US as financial support to his PhD thesis in the subject area of nuclear waste management.

**Andreas Havenith** was awarded with the Karl-Wirtz-Prise at the annual meeting of the „Kerntechnische Gesellschaft e.V. (KTG)“ in Mai 2014 in Berlin, Germany for his outstanding scientific contribution in the subject of nuclear applications.

**Yulia Arinicheva** won the 1st Juelich Science Slam of the Helmholtz graduate school “Helmholtz Interdisciplinary Doctoral Training in Energy and Climate (HITEC)” with a popular scientific presentation of her PhD thesis “Monazites – a potential waste form for nuclear waste disposal”.

**Fig. 86: Yulia Arinicheva is the winner of the 1st Jülich Science Slam.**

**Sarah Finkeldei** received for her presentation on „Pyrochlore as Nuclear Waste Form: Actinide Uptake and Chemical Stability“ at the annual symposium of the Helmholtz Interdisciplinary Doctoral Training in Energy and Climate (HITEC) graduate school the HITEC Communicator Award.

## 7.1. Poster Awards

**Christoph Genreith** was awarded with the best poster prize at the 525. WE-Heraeus-Sminar on "Nuclear Physics Data for the Transmutation of Nuclear Waste" in Bad Honnef for his poster "Neutron Capture Cross Sections of $^{237}$Np and $^{242}$Pu from Prompt Gamma Radiation".

At Symposium E “Scientific basis of the nuclear fuel cycle” of the E-MRS Spring Meeting 2013 in Strassbourg **Christian Schreinemachers** and **Julia Heuser** were awarded with the best poster prizes for their contribution on "Characterization of U/Nd microspheres synthesized by internal gelation” and “Raman and IR spectroscopy of Monazite-type Ceramics used for Nuclear Waste Conditioning”, respectively.

**Sarah Finkeldei** was awarded with the best poster prize at the international conference Acitinides 2013 in Karlsruhe, Germany for her contributoion on "Pyrochlore – a promising host phase for actinide immobilisation".

At the Joint international conference on “Supercomputing in Nuclear Applications & Monte Carlo (SNA + MC 2013)” in Paris, France **Manuel Schumann** was awarded with a poster prize for his contribution on "Monte-Carlo Applications for Nondestructive Nuclear Waste Analysis".

At the international "22$^{nd}$ Annual Conference of the German Crystallographic Society (DGK)“ 2014 in Berlin, Germany **Na Yu** received a poster award for her contribution on "Thorium Arsenates from High Temperature Solid State Reactions".

**Elena Ebert** was awarded with a poster prize for her contribution on "Dissolution behavior of MgO based Inert Matrix Fuel for the transmutation of plutonium and minor actinides” at the international "17$^{th}$ Radiochemical Conference, RadChem 2014“, Marianske Lazne, Czeck Republic.

## 7.2. Scholarships

**Yulia Arinicheva** was granted by the international Advisory Board of the Helmholtz Interdisciplinary Doctoral Training in Energy and Climate (HITEC) graduate school for a 3-years fellowship to support her PhD thesis at Forschungszentrum Jülich.

**April Birnie**, Smith College, Northampton, Massachusettes, US received a 3-months fellowship of the DAAD-Rise (Research Internships in Science and Engineering) foundation to perform atomistic simulations in the Young Investigator Group of **Dr. Piotr Kowalski** (IEK-6).

# 8 Selected R&D projects

## 8.1. EU projects

**ASGARD** - Advanced fuelS for Generation IV reActors: Reprocessing and Dissolution, 10/2011 – 10/2015, Work package leader: Dr. G. Modolo, FZJ

**Carbowaste** - Treatment and Disposal of Irradiated Graphite and Other Carbonaceous Waste, 04/2008 – 03/2013, Coordination: FZJ

**FIRST-Nuclides** - Determination of the first radionuclide release fraction, 01/2012 – 12/2014

**SACSESS** - Safety of Actinide Separation Processes, 03/2013 – 02/2016, Work package leader: Dr. G. Modolo, FZJ

**SKIN** - Slow Processes in Close-to-Equilibrium Conditions for Radionuclides in Water/Solid Systems of Relevance to Nuclear Waste Management, 01/2011 – 12/2013; Work package leader: Prof. D. Bosbach, FZJ

**G-SEXTANT** – Geospatial Intelligence Services in Support of EU External Action; 01/2013 – 03/2015; Work package leader: Dr. I. Niemeyer

## 8.2. More projects

**ImmoRad** - Grundlegende Untersuchungen zur Immobilisierung langlebiger Radionuklide durch die Wechselwirkung mit endlagerrelevanten Sekundärphasen; 02/2012 – 01/2015, Bundesministerium für Bildung und Forschung (BMBF)

**VESPA** - Verhalten langlebiger Spalt- und Aktivierungsprodukte im Nahfeld eines Endlagers und Möglichkeiten ihrer Rückhaltung (07/2010 – 06/2013)
Bundesministerium für Wirtschaft und Technologie (BMWi)

Radiographie mittels schneller Neutronen zur Charakterisierung radioaktiver Abfälle (**Neutronen Imaging**); 05/2012 - 04/2015
Bundesministerium für Bildung und Forschung (BMBF)

Untersuchungen zum grundlegenden Verständnis der selektiven Komplexierung von f-Elementen (**f-KOM**); 07/2012 - 06/2015
Bundesministerium für Bildung und Forschung (BMBF)

**Conditioning** - Grundlegende Untersuchungen zur Immobilisierung langlebiger Radionuklide mittels Einbau in endlagerrelevante Keramiken; 10/2012-03/2016

Bundesministerium für Bildung und Forschung (BMBF)
Coordination: FZJ

Bestimmung und Validierung nuklearer Daten von Actiniden zur Zerstörungsfreien Spaltstoffanalyse in Abfallproben durch prompt Gamma Neutronenaktivierungsanalyse (**PGAA-Actinide**); 08/2012 – 07/2015
Bundesministerium für Bildung und Forschung (BMBF)

Synthese und Charakterisierung keramischer Samarium-Phosphat- und Samarium-Phosphosilicat-Phasen zur Immobilisierung von Actinoiden; 04/2012 – 06/2015
Deutsche Forschungsgemeinschaft DFG

# 9 Committee work

**Prof. Dr. Dirk Bosbach:**

- Speaker of the Helmholtz research program "Nuclear Waste Management, Safety and Radiation Research"
- Member of the advisory board of the Nuclear chemistry division of the German Chemical Society (GDCh)
- Member of the scientific advisory boards of the TALISMAN network
- Member of the scientific advisory board of the ENTRIA Research Platform
- Member of the NEA TDB Iron II expert group
- Representative of FZJ in the German Alliance for Competence in Nuclear Technology
- Representative of FZJ in the Impelementation of Geological Disposal - Technology Plattform (IGD-TP)
- Representative of FZJ in the Sustainable Nuclear Energy - Technology Platform (SNETP) incl. the NUGENIA network

**Dr. Martin Dürr**

- Institute of Nuclear Materials Management (INMM): Member International Safeguards Division (ISD)
- European Safeguards Research and Development Association (ESARDA):,Member WG Techniques and Standards for Destructive Analysis (DA)
- Representative of FZ Jülich in the German Safeguards Coordination Committee (AG Kernmaterialüberwachung, AKÜ)

**Clemens Listner**

- European Safeguards Research and Development Association (ESARDA): Member WG Verification Technologies and Methodologies (VTM)
- Institute of Nuclear Materials Management (INMM): Member International Safeguards Division (ISD), Associate Editor of the Journal of Nuclear Materials Management (JNMM)

**Dr. Eric Mauerhofer**

- Member of Executive Committee for the valorization of neutron activation analysis in the field of recycling and quality control at Forschungszentrum Jülich GmbH

- Member of Steering Committee of European Network of Testing facilities for the quality checking of Radioactive waste Packages (ENTRAP) and Leader of Working Group Non-Destructive Assay
- Scientific Consultant for RWE Power AG in the field on online coal-analytics
- Scientific and organization Committee of 25th Seminar on Activation Analysis and Gamma Spectroscopy, Aachen, Germany (2015)
- Member of the Scientific Committee and Session organizer ANIMMA 2015, Lisbon, Portugal.
- Reviewer for Journal of Radioanalytical and Nuclear Chemistry

**Dr. Giuseppe Modolo:**

- Technical Programm Committee of the international Solvent extraction Conference: ISEC 2014
- Technical Programm Committee of the First SACSESS International Workshop 2015
- International Global 2013 conference, Technical Conference Committee
- E-MRS 2013, Symposium E: Scientific basis of the nuclear fuel cycle, Scientific Committee
- Editorial Board of the Journal Solvent Extraction and Ion Exchange
- Distinguished reviewers board of the Journal of Radioanalytical and Nuclear Chemisty

**Dr. Irmgard Niemeyer:**

- Standing Advisory Group on Safeguards Implementation (SAGSI): German member
- European Safeguards Research and Development Association (ESARDA): Designated Vice President 2015/16, Representative of FZ Jülich in the Steering Committee, Chair Symposium 2015 Committee, Member Symposium 2013 Committee, Chair WG Verification Technologies and Methodologies (VTM), Member WG Training and Knowledge Management (KTM)
- Institute of Nuclear Materials Management (INMM): Member International Safeguards Division (ISD), Vice-Chair WG Open-source and Geospatial Information
- Representative of FZ Jülich in the German Safeguards Coordination Committee (AG Kernmaterialüberwachung, AKÜ)
- Member of the Working Group “Fissile Material Cut-off Treaty” (FMCT) of the Foreign Federal Office
- International Society for Photogrammetry and Remote Sensing (ISPRS): Appointed member of the International Policy Advisory Committee (IPAC)
- IEEE Geophysics and Remote Sensing Society (IEEE): Reviewer

**Dr. Bernd Richter (2013):**

- Institute of Nuclear Materials Management (INMM): Member International Safeguards Division (ISD), Associate Editor
- European Safeguards Research and Development Association (ESARDA): Member Editorial Committee, Member WG Containment/Surveillance (C/S)
- Member of the German Safeguards Coordination Committee (AG Kernmaterialüberwachung, AKÜ)

**Dr. Matthias Rossbach:**

- International Committee on Activation Analysis
- International Scientific Advisory Committee for the Budapest Neutron Centre, Hungarian Academy of Sciences
- Review Panel Imaging, Analysis, Nuclear and Particle Physics for Beam-time at all Instruments hosted at FRM II Research Reactor, Garching
- Scientific Committee of the 14$^{th}$ International Conference on Modern Trends in Activation Analysis, MTAA14
- Scientific Advisory Committee of the 2016 Int. Conf. on Nuclear Data for Science and Technology, Bruges, Belgium
- WPEC sub-group SG-41: Improving nuclear data accuracy of 241Am and 237Np capture cross sections

**Priv.-Doz. Dr. Hartmut Schlenz:**

- Nuclear Energy Agency of the OECD: TDB-Fe2 (2011-2015)

**Dr. Holger Tietze-Jaensch:**

- AK-HAW: Arbeitskreis HAW-Produkte des BMFT and BMWi
- Labonet: akkreditierter deutscher Vertreter im EU-Netzwerk Labonet
- IAEA: akkreditierter deutscher Vertreter beim IAEA Arbeitskreis zur Characterization of Radioactive Waste
- Entrap-SC: Member of the Steering Committee of the EU-Arbeitskreises ENTRAP (European Network of Testing facilities for the quality checking of Radioactive waste Packages)
- Pol.Reg.EnergyComm: akkreditiertes Mitglied in der Kommission für Energieeffizienz der polnischen Regierung, Berater insbeondere für nukleare Energie

- iPAC & PAC -WM: Member of the International Advisory Committee (IPAC) and of the Program Advisory Committee (PAC) of Waste Management, Phoenix, AZ, USA

**Dr. Steinmetz:**

- International Program Advisory Committee (IPAC) of the Annual Arizona Waste Management Conference
- Session Co-Chair and Lead Organisator "Russian Session WM 15"
- Expert called by the German Office of Radiation Protection (BfS) as well as the Highest Authorities and Ministries of the German Federal States.

**Katharina Aymanns:**

- European Safeguards Research and Development Association (ESARDA): Member WG Containment & Surveillance (C&S)
- Deputy chairperson in the DIN Standards Committee Materials Testing

# 10 Patents

**W. von Lensa, C. Rizzato, D. Vulpius, and C. Fischer:** Verfahren zur Dekontamination von Radionukliden aus neutronenbestrahlten Kohlenstoff- und/oder Graphitwerkstoffen. Deutsche Patentanmeldung 10 2013 003 847.2 vom 07.03.2013

# 11 Publications

The scientific and technical results of the work carried out at IEK-6 are published in relevant journals and presented to interested specialist audience at national and international conferences on the subject.

**Tab. 4: Publications 2013/2014**

| Year | | 2013 | 2014 |
|---|---|---|---|
| **Publications** | Peer-reviewed journals | 37 | 44 |
| | Books | 1 | 1 |
| | Proceedings | 20 | 29 |
| **Conferences** | Presentations | 44 | 59 |
| | Poster | 34 | 48 |

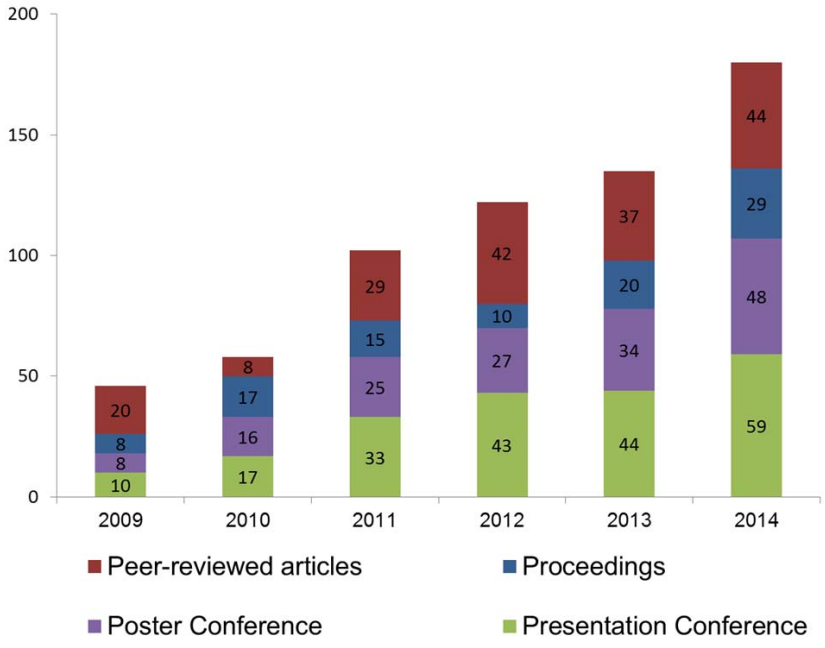


**Fig. 87: Publications 2009 - 2014.**

## 11.1. Publications 2013

### *11.1.1 Journal papers*

Peer-reviewed journals


Aksyutina, Y., Aumann, T., Fynbo, H. O. U., Geissel, H., Ickert, G., Johansson, H. T., Jonson, B., Kulessa, R., Langer, C., LeBleis, T., Mahata, K., Münzenberg, G., Boretzky, K., Nilsson, T., Nyman, G., Palit, R., Paschalis, S., Prokopowicz, W., Reifarth, R., Rossi, D., Richter, A., Riisager, K., Schrieder, G., Borge, M. J. G., Simon, H., Sümmerer, K., Tengblad, O., Weick, H., Zhukov, M. V., Caesar, C., Chatillon, A., Chulkov, L. V., Cortina-Gil, D., Datta Pramanik, U., Emling, H., Momentum profile analysis in one-neutron knockout from Borromean nuclei: Physics letters / B, v. 718, no. 4-5, p. 1309 - 1313.

Alekseev, E., Felbinger, O., Pokrovsky, L. D., Pugachev, A. M., Surovtsev, N. V., Atuchin, V. V., Wu, S., Malcherek, T., Depmeier, W., Modolo, G., Gesing, T. M., Krivovichev, S. V., Suleimanov, E. V., Gavrilova, T. A., $K[AsW_2O_9]$, the first member of the arsenate–tungsten bronze family: Synthesis, structure, spectroscopic and non-linear optical properties: Journal of solid state chemistry, v. 204, p. 59 - 63.

Banik, N. L., Denecke, M. A., Geist, A., Modolo, G., Panak, P. J., Rothe, J., 2,6-Bis(5,6-dipropyl-1,2,4-triazin-3-yl)-pyridine: Structures of An(III) and Ln(III) 1:3 complexes and selectivity: Inorganic chemistry communications, v. 29, p. 172 - 174.

Cross, J. N., Duncan, P. M., Villa, E. M., Polinski, M. J., Babo, J.-M., Alekseev, E., Booth, C. H., Albrecht-Schmitt, T. E., From Yellow to Black: Dramatic Changes between Cerium(IV) and Plutonium(IV) Molybdates: Journal of the American Chemical Society, v. 135, no. 7, p. 2769 - 2775.

Curtius, H., Kaiser, G., Rozov, K., Neumann, A., Dardenne, K., Bosbach, D., Preparation and characterization of Fe-, Co-, and Ni-containing Mg-Al-Layered double hydroxides: Clays and clay minerals, v. 61, no. 5, p. 425-440.

Genreith, C., Rossbach, M., Mauerhofer, E., Belgya, T., Caspary, G., Measurement of thermal neutron capture cross sections of $^{237}Np$ and $^{242}Pu$ using prompt gamma neutron activation: Journal of radioanalytical and nuclear chemistry, v. 296, no. 2, p. 699-703.

Kaufhold, S., Klinkenberg, M., Dohrmann, Comparison of the dry densities of highly compacted bentonites: Clay minerals, v. 48, no. 1, p. 105 - 115.

Kaufhold, S., Plötze, M., Klinkenberg, M., Dohrmann, R., Siegesmund, S., Density and porosity of bentonites: Journal of porous materials, v. 20, p. 191-208.

Kettler, J., Mauerhofer, E., Steinbusch, M., Detection of unexploded ordnance by PGNAA based borehole-logging: Journal of radioanalytical and nuclear chemistry, v. 295, issue 3, p. 2071-2075.

Knott, A., and Dürr, M., Production of monodisperse uranium particles for nuclear safeguards applications: ESARDA bulletin, v. 49, p. 40-45.

Kowalski, P., Wunder, B., Jahn, S., Ab initio prediction of equilibrium boron isotope fractionation between minerals and aqueous fluids at high P and T: Geochimica et cosmochimica acta, v. 101, p. 285 - 301.

Krings, T., Genreith, C., Mauerhofer, E., Rossbach, M., A numerical method to improve the reconstruction of the activity content in homogeneous radioactive waste drums: Nuclear instruments & methods in physics research / A, v. 701, p. 262-267.

Lelet, M. I., Ogurtsova, O. V., Suleimanov, E. V., Geiger, C. A., Depmeier, W., Alekseev, E. V., A Calorimetric and Thermodynamic Investigation of Potassium Uranyl Tungstate $K_2[(UO_2)(W_2O_8)]$: The journal of chemical thermodynamics, v. 57, p. 430 – 435.

MacGregor, J., Grew, E. S., De Hoog, J. C. M., Harley, S. L., Kowalski, P., Yates, M. G., Carson, C. J., Boron isotopic composition of tourmaline, prismatine, and grandidierite from granulite facies paragneisses in the Larsemann Hills, Prydz Bay, East Antarctica: Evidence for a non-marine evaporite source: Geochimica et cosmochimica acta, v. 123, p. 261 - 283.

Magnusson, D., Geist, A., Wilden, A., Modolo, G., Direct Selective Extraction of Actinides (III) from PUREX Raffinate using a Mixture of CyMe4-BTBP and TODGA as 1-cycle SANEX Solvent Part II: Flow-sheet Design for a Counter-Current Centrifugal Contactor Demonstration Process: Solvent extraction and ion exchange, v. 31, no. 1, p. 1-11.

Modolo, G., Wilden, A., Daniels, H., Geist, A., Magnusson, D., Malmbeck, R., Development and demonstration of a new SANEX Partitioning Process for selective actinide(III)/lanthanide(III) separation using a mixture of CyMe 4 BTBP and TODGA: Radiochimica acta, v. 101, no. 3, p. 155 - 162.

Nelson, A.-G. D., Alekseev, E., Albrecht-Schmitt, T. E., Ewing, R. C., Uranium diphosphonates templated by interlayer organic amines: Journal of solid state chemistry, v. 198, p. 270 - 278.

Nussbaum, S., Tueshaus, J., Niemeyer, I., Images Objects vs. Pixels: A Comparison of New Methods From Both Domains: ESARDA bulletin, v. 49, p. 66-74.

Polinski, M. J., Alekseev, E., Darling, V. R., Cross, J. N., Depmeier, W., Albrecht-Schmitt, T. E., A New Family of Lanthanide Borate Halides with Unusual Coordination and a New Neodymium-Containing Cationic Framework: Inorganic chemistry, v. 52, no. 4, p. 1965 - 1975.

Polinski, M. J., Alekseev, E., Depmeier, W., Albrecht-Schmitt, T. E., Recent advances in trivalent f-element borate chemistry: Zeitschrift für Kristallographie / Crystalline materials, v. 228, no. 10, p. 489–498.

Polinski, M. J., Cross, J. N., Villa, E. M., Lin, J., Alekseev, E., Depmeier, W., Albrecht-Schmitt, T. E., Synthesis of Divalent Europium Borate via in Situ Reductive Techniques: Inorganic chemistry, v. 52, no. 14, p. 8099 - 8105.

Rozov, K., Curtius, H., Neumann, A., Bosbach, D., Synthesis, characterization and stability properties of Cl-bearing hydrotalcite-pyroaurite solids: Radiochimica acta: international journal for chemical aspects of nuclear science and technology, v. 101, no. 2, p. 101-110.

Schlenz, H., Heuser, J., Neumann, A., Schmitz, S., Bosbach, D., Monazite as a suitable actinide waste form: Zeitschrift für Kristallographie / Crystalline materials, v. 228, no. 3, p. 113-123.

Schmidt, M., Heck, S., Bosbach, D., Ganschow, S., Walther, C., Stumpf, T., Characterization of powellite-based solid solutions by site-selective time resolved laser fluorescence spectroscopy: Dalton transactions, v. 42, no. 23, p. 8387-8393.

Schucknecht, A., Ersami, S., Niemeyer, I., Matschullat, J., Assessing vegetation variability and trends in north-eastern Brazil using AVHRR and MODIS NDVI time series: European journal of remote sensing, v. 46, p. 40 - 59.

Spiekermann, G., Steele-MacInnis, M., Kowalski, P., Schmidt, C., Jahn, S., Vibrational properties of silica species in $MgO$-$SiO_2$ glasses obtained from ab initio molecular dynamics: Chemical geology, v. 346, p. 22 - 33.

Villa, E. M., Alekseev, E., Depmeier, W., Albrecht-Schmitt, T. E., Syntheses, Structures, and Comparisons of Thallium Uranium Phosphites, Mixed Phosphate-Phosphites, and Phosphate: Crystal growth & design, v. 13, no. 4, p. 1721 - 1729.

Villa, E. M., Diwu, J., Alekseev, E., Depmeier, W., Albrecht-Schmitt, T. E., Structural changes within the alkaline earth uranyl phosphites: Dalton transactions, v. 42, no. 26, p. 9637 -.

Villa, E. M., Marr, C. J., Diwu, J., Alekseev, E., Depmeier, W., Albrecht-Schmitt, T. E., From Order to Disorder and Back Again: In Situ Hydrothermal Redox Reactions of Uranium Phosphites and Phosphates: Inorganic chemistry, v. 52, no. 2, p. 965 - 973.

Vinograd, V. L., Brandt, F., Rozov, K., Klinkenberg, M., Refson, K., Winkler, B., Bosbach, D., Solid–aqueous equilibrium in the $BaSO_4$–$RaSO_4$–$H_2O$ system: First-principles calculations and a thermodynamic assessment: Geochimica et cosmochimica acta, v. 122, p. 398 - 417.

Vulpius, D., Baginski, K., Fischer, C., Thomauske, B., Location and chemical bond of radionuclides in neutron-irradiated nuclear graphite: Journal of nuclear materials, v. 438, no. 1-3, p. 163 - 177.

Vulpius, D., Baginski, K., Kraus, B., Thomauske, B., Thermal treatment of neutron-irradiated nuclear graphite: Nuclear engineering and design, v. 265, p. 294 - 309.

Wilden, A., Modolo, G., Bosbach, D., Lange, S., Sadowski, F., Beele, B. B., Skerencak-Frech, A., Panak, P. J., Iqbal, M., Verboom, W., Geist, A., Modified Diglycolamides for the An(III) + Ln(III) co-separation: Evaluation by Solvent Extraction and Time-Resolved Laser Fluorescence Spectroscopy: Solvent extraction and ion exchange, v. 31, no. 7, p.

Wilden, A., Modolo, G., Hudson, M. J., Schreinemachers, C., Sadowski, F., Lange, S., Sypula, M., Magnusson, D., Geist, A., Lewis, F. W., Harwood, L. M., Direct Selective Extraction of Actinides (III) from PUREX Raffinate using a Mixture of CyMe4BTBP and TODGA as 1-cycle SANEX Solvent Part III: Demonstration of a Laboratory-Scale Counter-Current Centrifugal Contactor Process: Solvent extraction and ion exchange, v. 31, no. 5, p. 519-537.

Wu, S., Polinski, M. J., Malcherek, T., Bismayer, U., Klinkenberg, M., Modolo, G., Bosbach, D., Depmeier, W., Albrecht-Schmitt, T. E., Alekseev, E., Novel Fundamental Building Blocks and Site Dependent Isomorphism in the First Actinide Borophosphates: Inorganic chemistry, v. 52, no. 14, p. 7881 - 7888.

Wu, S., Wang, S., Alekseev, E., Polinski, M., Beermann, O., Kegler, P., Malcherek, T., Holzheid, A., Depmeier, W., Bosbach, D., Albrecht-Schmitt, T. E., High Structural Complexity of Potassium Uranyl Borates Derived from High-Temperature/High-Pressure Reactions: Inorganic chemistry, v. 52, no. 9, p. 5110 - 5118.

Wu, S., Wang, S., Polinski, M. J., Depmeier, W., Albrecht-Schmitt, T. E., Alekseev, E., A new low temperature route to uranyl borates with structural variations: Zeitschrift für Kristallographie / Crystalline materials, v. 228, p. 429–435.

### *11.1.2 Proceedings/Books*

Proceedings


Aneheim, E., Ekberg, C., Modolo, G., Wilden, A., Single centrifugal contactor test of a proposed group actinide extraction process for partitioning and transmutation purposes, APSORC'13 - 5th Asia-Pacific Symposium on Radiochemistry: Kanazawa, Japan, p. 11 p.

Brandt, F., Klinkenberg, M., Rozov, K., Breuer, U., Bosbach, D., Recrystallization of barite in the presence of radium, in Proceedings 2nd annual workshop, 7th EC FP - SKIN, Volume 4364, Forschungszentrum Jülich.

Catalán, S., Carrasco, J. M., Tremblay, P.-E., Jordi, C., Napiwotzki, R., Luri, X., Robin, A. C., Kowalski, P., Reylé, C., White Dwarfs as Seen by Gaia, 18th European White Dwarf Workshop, EUROWD12: Krakow, Poland, p. 245-248.

Curtius, H., Müller, E., Müskes, H. W., Klinkenberg, M., Bosbach, D., Selection and Characterisation of HTR Fuel, 1st Annual Workshop of the Collaborative Project "FAST/INSTANT release of Safety Relevant Radionuclides from Spent Nuclear Fuel: Budapest, Ungarn, p. 12.

Dürr, M., Niemeyer, I., Richter, B., Stein, G., Trautwein, W., Rezniczek, Considering Integrated Safeguards and the State-Level Concept in the Development of Equipment and Techniques for Safeguards, 54th INMM Annual Meeting 2013: Palm Desert, Germany, p. 1-10.

Geist, A., Modolo, G., Wilden, A., Kaufholz, P., Minor Actinide Separation: Simplification of the DIAMEX-SANEX Strategy by Means of Novel SANEX Processes, GLOBAL2013: International Nuclear Fuel Cycle Conference: Salt Lake City, USA, p. 1054-1059.

Genreith, C., and Rossbach, M., $^{241}$Am: a difficult actinide for (n,gamma) cross section measurement, ERINDA Workshop 2013: CERN, Geneva, Swizerland, p. 7.

Jussofie, A., Graf, W., van Bevern, K., Niemeyer, I., Rezniczek, A., Trautwein, W., Schoop, K., Ahaus remote data transmission (RDT) field test – from the operators' point of view., ESARDA Symposium: Bruges, Belgium, p. 1-5.

Kempl, J., Frost, D., Vroon, P., Kowalski, P., van Westrenen, W., Silicon Isotope Fractionation Between Metal and Silicate at High Pressure and High Temperature — Implications for Earth's Core, 44th Lunar and Planetary Science Conference: The Woodlands, Texas, USA, p. 1891.

Knott, A., and Dürr, M., Production of monodisperse uranium particles for nuclear safeguards applications, ESARDA Symposium: Bruges, Belgium, p. 8.

Kowalski, P., Saumon, D., Holberg, J., Leggett, S., Towards an Understanding of the Atmospheres of Cool White Dwarfs, 18th european White Dwarf Workshop, Astronomical Soc. of the Pacific, p. 173-178.

Listner, C., Canty, M., Rezniczek, A., Stein, G., Niemeyer, I., Approaching acquisition path analysis formally - a comparison between AP and non-AP States, ESARDA Symposium: Bruges, Belgium, p. 10.

Listner, C., Canty, M., Rezniczek, A., Stein, G., Niemeyer, I., Approaching acquisition path analysis formally - experiences so far, 54th INMM Annual Meeting: Palm Desert, USA, p. 1-10.

Mauerhofer, E., Carasco, C., Payan, E., Kettler, J., Havenith, A., Perrot, B., Ma, J. L., Quantitative Comparison Bettween PGNAA Measurements and MCNP calculations in view of the Characterization of Radioactive Wastes in Germany and France, Advancements in Nuclear Instrumentation Measurement Methods and their Applications: Marseille, France, p. 49.

Mauerhofer, E., Havenith, A., Carasco, C., Payan, E., Kettler, J., Ma, J. L., Perot, B., Quantitative comparison between PGNAA measurements and MCNP calculations in view of the characterization of radioactive wastes in Germany and France, Application of accelerators in research and industry: Twenty-Second International Conference, Volume 1525: Ft. Worth, TX, p. 432-435.

Niemeyer, I., Dürr, M., Richter, B., Trautwein, W., The German Support Programme to the IAEA: 35 Years of Technical Developments and Further Improvement of IAEA Safeguards, 54th INMM Annual Meeting: Palm Desert, USA, p. 1-10.

Niemeyer, I., Listner, C., Martens, S., Monitoring Uranium Mining and Processing Sites Under Decommissioning Using Hyperspectral Imagery, ESARDA Symposium: Bruges, Belgium, p. 9.

Niemeyer, I., Nussbaum, S., Tueshaus, J., Listner, C., Advances in detecting changes at nuclear facilities using very high-resolution optical satellite imagery, 54th INMM Annual Meeting: Palm Desert, USA, p. 1-9.

Nussbaum, S., Tueshaus, J., Niemeyer, I., Image Objects vs. Pixels: A comparison of new methods from both domains, ESARDA Symposium: Bruges, Belgium, p. 10 p.

Wilden, A., Modolo, G., Bosbach, D., Lange, S., Sadowski, F., Beele, B. B., Skerencak-Frech, A., Panak, P. J., Geist, A., Iqbal, M., Verboom, W., Modified Diglycolamides for Actinide Separation: Solvent Extraction and Time Resolved Laser Fluorescence Spectroscopy Complexation Studies, GLOBAL2013: Salt Lake City, USA, p. 907-911.

Books

Beele, B. B., Bremer, A., Geist, A., Magnusson, D., Malmbeck, R., Modolo, G., Müllich, U., Panak, P. J., Ruff, C., Wilden, A., Separation of long-lived minor actinides, Jahresbericht KIT-INE: Karlsruhe, Karlsruhe Institute of Technology, p. 4 p.

### *11.1.3 Internal reports*


Bukaemskiy, A., Ebert, E., Lichte, E., Modolo, G., Neumeier, S., Sadowski, F., Schreinemachers, C., Partner interim Report No. 3.

Bukaemskiy, A., Ebert, E., Modolo, G., Neumeier, S., Sadowski, F., Schreinemachers, C., Wegener, T., Wilden, A., Partner interim Report No. 2.

Rossbach, M., Genreith, C., Revay, Z., Kudejova, P., Determination of the thermal neutron cross section of trans-uranium actinides.

Wilden, A., and Modolo, G., 1. Halbjahresbericht zum BMBF Forschungsvorhabens „Verbundprojekt f-Kom: Untersuchungen zum grundlegenden Verständnis der selektiven Komplexierung von f-Elementen“, Förderzeichen 02NUK020E.

Wilden, A., and Modolo, G., 2. Halbjahresbericht zum BMBF Forschungsvorhabens „Verbundprojekt f-Kom: Untersuchungen zum grundlegenden Verständnis der selektiven Komplexierung von f-Elementen“, Förderzeichen 02NUK020E.


### *11.1.4 Poster*


Aneheim, E., Ekberg, C., Modolo, G., Wilden, A., Single centrifugal contactor test of a proposed group actinide extraction process for partitioning and transmutation purposes, APSORC’13 - 5$^{th}$ Asia-Pacific Symposium on Radiochemistry: Kanazawa, Japan.

Arinicheva, Y., Neumeier, S., Bukaemskiy, A., Brandt, F., Modolo, G., Bosbach, D., Immobilisation of long-lived radionuclides by means of structural incorporation in monazite-type phosphates, HITEC Fellow Candidates Week: Juelich, Germany.

Baginski, K., Vulpius, D., Rizzato, C., Fischer, C., von Lensa, W., Partial Decontamination of Radioactive Graphite obtained by Thermal Treatment, ICEM 2013, 15$^{th}$ International Conference on Environmental Remediation and Radioactive Waste Management: Brussels, Belgium.

Baginski, K., Vulpius, D., von Lensa, W., Möglichkeiten der Teildekontamination von radioaktivem Graphit durch thermische Behandlung, KONTEC 2013, „Internationales Symposium „Konditionierung radioaktiver Betriebs- und Stilllegungsabfälle": Dresden, Germany.

Beele, B. B., Wilden, A., Skerencak-Frech, A., Lange, S., Sadowski, F., Modolo, G., Geist, A., Panak, P. J., TRLFS Study on the Complexation of Cm(III) and Eu(III) with methyl-substituted Diglycolamides, Actinides 2013: Karlsruhe, Germany.

Blanca Romero, A., Beridze, G., Kowalski, P., Computational Science in Nuclear Waste Management: ab Initio Investigation of F-Elements Bearing Monazite, Goldschmidt 2013 conference: Florence, Italy.

Brandt, F., Klinkenberg, M., Breuer, U., Rozov, K., Bosbach, D., Uptake of Radium during barite recrystallization, EURADWASTE ’13, 8$^{th}$ EC Conference on the Management of Radioactive Waste Community Policy and Research on Disposal: Vilnius, Lithuania.

Bukaemskiy, A., Brandt, F., Finkeldei, S., Neumeier, S., Modolo, G., Bosbach, D., Phase stability of Zirconia based Pyrochlore ceramics, E-MRS Spring Meeting: Strasbourg, France.

Bukaemskiy, A., Finkeldei, S., Brandt, F., Neumeier, S., Modolo, G., Bosbach, D., Phase stability of Zirconia based Pyrochlore ceramics, CALPHAD XLII: San Sebastian, Spain.

Deissmann, G., Filby, A., Haneke, K., Wiegers, R., Bosbach, D., Scoping calculations for the near-field evolution in a geological repository for high-level radioactive waste in Boom Clay in the Netherlands, MRS 2013 Scientific Basis for Nuclear Waste Disposal: Barcelona, Spain.

Deissmann, G., Neumeier, S., Brandt, F., Modolo, G., Bosbach, D., Elicitation of dissolution rate data for potential wasteform types for plutonium under repository conditions, Migration 2013: Brighton, UK.

Ebert, E., Bukaemskiy, A., Neumeier, S., Modolo, G., Bosbach, D., Dissolution behavior of MgO and Mo based ADS inert matrix fuel, E-MRS Spring Meeting: Strasbourg, France.

Ebert, E., Lichte, E., Cheng, M., Steppert, M., Walther, C., Bukaemskiy, A., Sadowski, F., Neumeier, S., Modolo, G., Bosbach, D., Auflösungsverhalten von Mo- und MgO-basierten ADS Inertmatrixbrennstoffen, GDCh Wissenschaftsforum Chemie 2013: Darmstadt, Germany.

Engels, R., Furletov, S., Neike, D., Rossbach, M., Schitthelm, O., Vasques, R., Schumann, M., Carasco, C., Payan, E., Perot, B., Ma, J.-L., Furletova, J., Frank, M., Genreith, C., Havenith, A., Kemmerling, G., Kettler, J., Krings, T., Mauerhofer, E., Monte-Carlo Applications for Nondestructive Nuclear Waste Analysis, Joint International Conference on Supercomputing in Nuclear Applications + Monte Carlo: Paris, Frankreich.

Finkeldei, S., Brandt, F., Bukaemskiy, A. A., Neumeier, S., Modolo, G., Bosbach, D., Pyrochlore Ceramics as Potential Nuclear Waste Forms, 50 Jahrfeier IEK-6: Jülich & Aachen, Germany.

Finkeldei, S., Holliday, K., de Visser-Týnová, E., Bruin, J., Brandt, F., Neumeier, S., Modolo, G., Stumpf, T., Bosbach, D., Pyrochlore – a promising host phase for actinide immobilization, Actinides 2013: Karlsruhe, Germany.

Genreith, C., and Rossbach, M., Neutron Capture Cross Sections of $^{237}$Np and $^{242}$Pu from Prompt Gamma Radiation, 525. WE-Heraeus-Seminar on Nuclear Physics Data for the Transmutation of Nuclear Waste: Bad Honnef, Germany.

Heuser, J., Bukaemskiy, A., Neumeier, S., Brandt, F., Schlenz, H., Dacheux, N., Calvier, N., Neumann, A., Hirsch, A., Bosbach, D., Raman and IR spectroscopy of Monazite-type Ceramics used for Nuclear Waste Conditioning, Goldschmidt Conference 2013: Firenze, Italy.

Heuser, J., Bukaemskiy, A., Neumeier, S., Neumann, A., Bosbach, D., Raman and IR spectroscopy of Monazite-type Ceramics used for Nuclear Waste Conditioning, EMRS Spring Meeting 2013: Strasbourg, France.

Klinkenberg, M., Brandt, F., Breuer, U., Bosbach, D., Recrystallization of barite in the presence of Radium – a microscopic and spectroscopic study, Migration 2013: Brighton, UK.

Kuhne, L., Stauch, B., von Lensa, W., Charakterisierung von Radionukliden in Reaktorbauteilen, VKTA Dresden, 7 Workshop RCA mit dem Schwerpunktthema „ Hürden und Fallstricke bei der Charakterisierung von Abfall-Gebinden“: Dresden, Germany.

Labs, S., Bauer, J. D., Winkler, B., Bayarjargal, Curtius, H., Bosbach, D., High-pressure behaviour of studtite, $UO_4{\cdot}4H_2O$, and metastudtite, $UO_4{\cdot}2H_2O$ - a Raman investigation, EMRS Spring Meeting: Strasbourg, France.

Labs, S., Weiss, S., Hennig, C., Curtius, H., Bosbach, D., Structural Investigation of Solid Solutions in the System $USiO_4$ – $ThSiO_4$, Migration Conference: Brighton, GB.

Labs, S., Weiss, S., Hennig, C., Hübner, R., Curtius, H., Bosbach, D., Synthesis and structure investigation of $USiO_4$ - comparison between local structure and bulk, EMRS Spring Meeting: Strasbourg, France.

Li, Y., Kowalski, P., Romero, A. B., Beridze, G., Efficient ab-initio methods for computation of actinide- and lanthanide-bearring materials relevant for nuclear waste management, Wissenschaftsforum Chemie 2013: Darmstadt, Germany.

Neumann, A., Curtius, H., Klinkenberg, M., Bosbach, D., Kaiser, G., Formation and characterisation of Lesukite, 21st Annual Conference of the German Crystallographic Society DGK: Freiberg, Germany.

Neumeier, S., Modolo, G., Bosbach, D., German Joint Research Project "Conditioning of long-lived Radionuclides in Ceramic Waste Forms", Actinides 2013: Karlsruhe, Germany.

Rizzato, C., von Lensa, W., Banford, A. W., Bradbury, D., Goodwin, J., Grambow, B., Grave, M. J., Jones, A. N., Pina, G., Vulpius, D., CARBOWASTE: Treatment and Disposal of Irradiated Nuclear Graphite and Other Carbonaceous Waste, EURADWASTE ´13, 8th EC Conference on the Management of Radioactive Waste Community Policy and Research on Disposal: Vilnius, Lithuania.

Schreinemachers, C., Bukaemskiy, A., Neumeier, S., Modolo, G., Bosbach, D., Characterization of U/Nd microspheres synthesized by internal gelation, E-MRS Spring Meeting: Strasbourg, France.

Schumann, M., Engels, R., Mauerhofer, E., Neike, D., Rossbach, M., Schitthelm, o., Varques, R., Carasco, C., Payan, E., Perot, B., Ma, J.-L., Frank, M., Furletov, S., Furletova, J., Genreith, C., Havenith, A., Kemmerling, G., Krings, T., Kettler, J., Zerstörungsfreie Charakterisierung Radioaktiver Abfälle, 7. VKTA Workshop on Radiochemical Analysis: Dresden, Deutschland.

Torapava, N., Neumeier, S., Modolo, G., Heuser, J., Bukaemskiy, A., Dellen, J., Walther, C., Immobilization of long-lived iodine after incorporation into apatite matrice, First Russian Nordic Symposium on Radiochemistry (RNSR): Moscow, Russia.

Torapava, N., Neumeier, S., Modolo, G., Heuser, J., Bukaemskiy, A., Dellen, J., Walther, C., Immobilization of long-lived iodine after incorporation into apatite matrice, Goldschmidt Conference: Florence, Italy.

Wilden, A., Kaufholz, P., Modolo, G., Partitioning – Chemische Abtrennung der langlebigen radiotoxischen Elemente, Tag der Neugier: Jülich, Germany.

Wilden, A., and Modolo, G., Partitioning – Chemical separation of the Long-lived Radiotoxic Elements, 50-Jahr’s Feier IEK-6: Aachen/Jülich, Germany.

### *11.1.5 Presentations*

Conferences:

Arinicheva, Y., Bukaemskiy, A. A., Neumeier, S., Modolo, G., Roth, G., Bosbach, D., Studies on thermal and mechanical properties of monazite-type ceramics for the conditioning of minor actinides, E-MRS Spring Meeting: Strasbourg, France.

Arinicheva, Y., Neumeier, S., Bukaemskiy, A., Brandt, F., Modolo, G., Bosbach, D., Synthesis, microstructure and physical - mechanical properties of monazite - type ceramics for the conditioning of minor actinides, First Russian Nordic Symposium on Radiochemistry (RNSR): Moscow, Russia.

Baginski, K., Vulpius, D., Rizzato, C., von Lensa, W., Kraus, B., Fischer, C., Untersuchung für die Graphitentsorgung – Thermische Behantlung, VKTA, 7th Workshop RCA mit dem Schwerpunktthema „ Hürden und Fallstricke bei der Charakterisierung von Abfall-Gebinden“: Dresden, Germany.

Brandt, F., Klinkenberg, M., Vinograd, V., Rozov, K., Bosbach, D., Radium solubility in the presence of barite: sorption experiments and atomistic modeling, Migration 2013: Brighton, Great Britain.

Brandt, F., Klinkenberg, M., Vinograd, V., Rozov, K., Bosbach, D., Solid solution formation and uptake of Radium in the presence of barite, Goldschmidt Conference 2013: Firenze, Italy.

Bukaemskiy, A., Finkeldei, S., Arinicheva, Y., Brandt, F., Neumeier, S., Modolo, G., Bosbach, D., Evolution of phase compositions and crystallization behavior of different ceramics for nuclear applications, Euromat2013 Conference: Sevilla, Spain.

Deissmann, G., Brandt, F., Neumeier, S., Modolo, G., Bosbach, D., Evaluation of the corrosion behaviour of potential plutonium wasteforms under conditions relevant for geological disposal, Goldschmidt Conference 2013: Florence, Italy.

Deissmann, G., Neumeier, S., Brandt, F., Modolo, G., Bosbach, D., Evaluation of the long-term behaviour of potential plutonium wasteforms in a geological repository, MRS 2013 Scientific Basis for Nuclear Waste Disposal: Barcelona, Spain.

Dürr, M., Knott, A., Niemeyer, I., Bosbach, D., Beiträge des FZ Jülich im Bereich der Analytik für internationale Kontrollen der Kernenergie, 6. Symposium Nukleare und radiologische Bedrohungen: Euskirchen, Germany.

Dürr, M., Niemeyer, I., Richter, B., Stein, G., Trautwein, W., Rezniczek, A., Considering Integrated Safeguards and the State-Level Concept in the Development of Equipment and Techniques for Safeguards, 54th INMM Annual Meeting 2013: Palm Desert, USA.

Finkeldei, S., Brandt, F., Bukaemskiy, A., Holliday, K. S., de Visser-Týnova, E., Bruin, J., Neumeier, S., Modolo, G., Bosbach, D., Zirconia based Nuclear Waste Forms for Actinides: Synthesis and dissolution Kinetics, GDCh Wissenschaftsforum Chemie 2013: Darmstadt, Germany.

Finkeldei, S., Brandt, F., Bukaemskiy, A., Neumeier, S., Modolo, G., Bosbach, D., Dissolution kinetics of $ZrO_2$ based ceramics, E-MRS Spring Meeting: Strasbourg, Germany.

Finkeldei, S., Brandt, F., Bukaemskiy, A., Neumeier, S., Modolo, G., Bosbach, D., Dissolution kinetics of $ZrO_2$ based innovative waste forms, Goldschmidt Conference: Florence, Italy.

Heuser, J., Schlenz, H., Babelot, C., Schmitz, S., Schuppik, T., Bosbach, D., Raman spectroscopic Investigations of Monazite-type Ceramics used for Nuclear Waste Conditioning, Deutsche Gesellschaft für Kristallographie: Freiberg, Germany.

Jussofie, A., Graf, W., van Bevern, K., Niemeyer, I., Rezniczek, A., Trautwein, W., Schoop, K., Ahaus remote data transmission (RDT) field test – from the operators' point of view., ESARDA Symposium: Bruges, Belgium.

Klinkenberg, M., Brandt, F., Breuer, U., Bosbach, D., A Microscopic and ToF-SIMS Study on the Ra Uptatke by barite, Goldschmidt 2013: Firenze, Italy.

Knott, A., and Dürr, M., Production of monodisperse uranium particles for nuclear safeguards applications, ESARDA Symposium: Bruges, Belgium.

Labs, S., Baking yellow cake, Hemdsärmelkolloquien 2013: Freiburg, Germany.

Labs, S., Hartl, M., Daemen, L., Neumann, A., Curtius, H., Bosbach, D., Structure investigation of metastudtite, $UO_4$ *$2H_2O$, EUROMAT 2013 Conference: Sevilla, Spain.

Listner, C., Canty, M., Rezniczek, A., Stein, G., Can State-level Safeguards be applied in Nuclear Weapon States?, 77. Jahrestagung der DPG und DPG-Frühjahrstagung: Dresden, Germany.

Listner, C., Canty, M., Rezniczek, A., Stein, G., Niemeyer, I., Acquisition Pathway Analysis, ESARDA Joint meeting on "IAEA State Level Conept": Ispra, Italy.

Listner, C., Canty, M., Rezniczek, A., Stein, G., Niemeyer, I., Approaching acquisition path analysis formally - a comparison between AP and non-AP States, ESARDA Symposium: Bruges, Belgium.

Listner, C., Canty, M., Rezniczek, A., Stein, G., Niemeyer, I., Approaching acquisition path analysis formally - experiences so far, 54$^{th}$ INMM Annual Meeting: Palm Desert, USA.

Listner, C., Canty, M., Rezniczek, A., Stein, G., Niemeyer, I., Risikobewertung im Rahmen des staatenspezifischen Kontrollansatzes als Modell für nukleare Verifikation, 6. Symposium Nukleare und radiologische Bedrohungen: Euskirchen, Germany.

Modolo, G., Wilden, A., Bosbach, D., Geist, A., Development and demonstration of innovative partitioning processes (i-SANEX and 1-cycle SANEX) for actinide partitioning, E-MRS 2013 Spring Meeting: Strasbourg, France.

Neumann, A., Zaddach, J., Heuser, J., Schlenz, H., Peters, L., Bosbach, D., Roth, G., Synthesis of monazite-type Sm(Ca,Ce)$PO_4$ solid solutions, EMRS Spring Meeting 2013: Strasbourg, France.

Neumeier, S., Brandt, F., Arinicheva, Y., Bukaemskiy, A., Schlenz, H., Modolo, G., Bosbach, D., Conditioning of Minor Actinides in La-Monazite Ceramics, E-MRS Spring Meeting: Strasbourg, France.

Neumeier, S., Bukaemskiy, A., Brandt, F., Finkeldei, S., Arinicheva, Y., Modolo, G., Bosbach, D., Ceramic waste forms for the conditioning of minor actinides, First Russian Nordic Symposium on Radiochemistry (RNSR): Moscow, Russia.

Neumeier, S., Finkeldei, S., Arinicheva, Y., Bukaemskiy, A., Brandt, F., Modolo, G., Bosbach, D., Mechanical properties and dissolution behaviour of Monazite- and Pyrochlore-type ceramics for the immobilization of Minor Actinides, Euromat2013 Conference: Sevilla, Spain.

Niemeyer, I., Hinterlassenschaften des Uranerzbergbaus: Monitoring mittels der Hyperspektralfernerkundung, 14. Geokinematischer Tag: Freiberg, Germany.

Niemeyer, I., Remote sensing and geoinformation technologies in support of nuclear non-proliferation and arms control verification regimes, Jahrestagung der Deutschen Physikalischen Gesellschaft: Dresden, Germany.

Niemeyer, I., ISPRS IPAC Round Table “Earth Observation Data in the Internet Age”, ISPRS Conference on „Serving Society with Geoinformatics“: Antalya, Turkey.

Niemeyer, I., Dürr, M., Richter, B., The German Support Programme to the IAEA: 35 Years of Technical Developments and Further Improvement of IAEA Safeguards, 54th INMM Annual Meeting: Palm Desert, USA.

Niemeyer, I., Listner, C., Martens, S., Monitoring Uranium Mining and Processing Sites Under Decommissioning Using Hyperspectral Imagery, ESARDA Symposium: Bruges, Belgium.

Niemeyer, I., Nussbaum, S., Tueshaus, J., Listner, C., Advances in detecting changes at nuclear facilities using very high-resolution optical satellite imagery, 54th INMM Annual Meeting: Palm Desert, USA.

Nussbaum, S., Tueshaus, J., Niemeyer, I., Image Objects vs. Pixels: A comparison of new methods from both domains, ESARDA Symposium: Bruges, Belgium.

Rizzato, C., von Lensa, W., Vulpius, D., Baginski, K., Fischer, C., Thermal Treatments of Irradiated Graphite, CARBOWASTE & IAEA Coordinated Research Project: Treatment of Irradiated Graphite to meet Acceptance Criteria for Waste Disposal, Joint Workshop IAEA: Vilnius, Lithuania.

Rossbach, M., Genreith, C., Revay, Z., Belgya, T., Randriamalala, T., Do we need $k_0$ values for actinides?, 6th International $k_0$-Users' Workshop: Budapest, Hungary.

Rossbach, M., Genreith, C., Scholten, B., Nukleare Daten als Grundlagen für Forschung und Technologie, 24. Seminar "Aktivierungsanalyse und Gammaspektroskopie": Garching, Germany.

Rossbach, M., Genreith, C., Belgya, T., Revay, Z., Sleaford, B. W., Escher, J. E., Determination of thermal (n,g) cross sections of $^{241}$Am by PGAA, International Conference on Nuclear Data for Science and Technology: New York, USA.

von Lensa, W., Rizzato, C., Banford, A. W., Bradbury, D., Goodwin, J., Grambow, B., Grave, M. J., Jones, A. N., Pina, G., Vulpius, D., CARBOWASTE: Treatment and Disposal of Irradiated Nuclear Graphite and Other Carbonaceous Waste, EURADWASTE ´13, 8th EC Conference on the Management of Radioactive Waste Community Policy and Research on Disposal: Vilnius, Lithuania.

Wilden, A., Modolo, G., Bosbach, D., Lange, S., Sadowski, F., Beele, B. B., Skerencak-Frech, A., Panak, P. J., Geist, A., Iqbal, M., Verboom, W., Modified Diglycolamides for actinide separation: Solvent Extraction and Time-Resolved Laser Fluorescence

Spectroscopy Complexation Studies, GLOBAL2013: International Nuclear Fuel Cycle Conference: Salt Lake City, USA.

Wilden, A., Modolo, G., Bosbach, D., Lange, S., Sadowski, F., Beele, B. B., Skerencak-Frech, A., Panak, P. J., Iqbal, M., Verboom, W., Geist, A., Modifizierte Diglycolamide für die Actinidenabtrennung: Untersuchungen zur Komplexierung durch Flüssig-Flüssig-Extraktion und zeitaufgelöste Laserfluoreszenzspektroskopie, GDCh-Wissenschaftsforum Chemie 2013: Darmstadt, Germany.

Wilden, A., Modolo, G., Kaufholz, P., Geist, A., Magnusson, D., Sypula, M., Bosbach, D., Development and laboratory-scale innovative-SANEX process demonstration for minor actinide partitioning using annular centrifugal contactors, Actinides 2013: Karlsruhe, Germany.

Invited Talks

Bauer, J., Labs, S., Weiss, S., Bayarjagal, L., Curtius, H., Morgenroth, W., Bosbach, D., Hennig, C., Winkler, B., Raman Spectroscopy and Powder Diffraction Study of Synthetic Coffinite ($USiO_4$) at High Pressures, Goldschmidt Conference 2013: Firenze, Italy.

Bosbach, D., Brandt, F., Klinkenberg, M., Rozov, K., Vinograd, V., Radium solubility control in the $BaSO_4$ – $RaSO_4$ solid-solution aqueous solution system, GDCh-Wissenschaftsforum Chemie 2013: Darmstadt, Germany.

Kowalski, P., Actinide Compounds from DFT, The joint DMG and BMBF-IMMORAD Verbundprojekt workshop "From atomistic calculations to thermodynamic modelling": Frankfurt, Germany.

Kowalski, P., and Jahn, S., Fractionation of Si Isotopes during Core Formation from First Principles Calculations, Goldschmidt 2013 Conference: Florence, Italy.

Modolo, G., Wilden, A., Geist, A., Challenges during the Hydrometallurgical Separation of Minor Actinides from Used Fuel, IAEA Technical Meeting on Advanced Actinide Recycle Technologies: Vienna, Austria.

Neumeier, S., Grundlegende Untersuchungen zur Immobilisierung langlebiger Radionuklide mittels Einbau in endlagerrelevante Keramiken (Conditioning), 1. Projektstatusgespräch zur BMBF-geförderten Nuklearen Sicherheitsforschung: Karlsruhe, Germany.

Neumeier, S., Bukaemskiy, A., Brandt, F., Wilden, A., Finkeldei, S., Arinicheva, Y., Heuser, J., Schreinemachers, C., Modolo, G., Bosbach, D., The role of ceramic materials in innovative nuclear waste management strategies, Seminar im Institut für Radioökologie und Strahlenschutz: Leibniz Universität Hannover, Germany.

Niemeyer, I., and Listner, C., Der staatsspezifische Kontrollansatz im Rahmen der IAEO-Safeguardsüberwachung und seine mögliche Anwendung in weiteren Verifikationsregimen, IFSH/ZNF-Kolloquium "Frieden und Sicherheit": Hamburg, Germany.

Niemeyer, I., and Listner, C., Satellitenfernerkundung zur Unterstützung der Rüstungskontrolle und Nichtverbreitung, Amaldi-Workshop "Eine Welt ohne Nuklearwaffen? Aufgaben der Wissenschaft": Hamburg, Germany.

Niemeyer, I., EO Supporting Nuclear Non-Proliferation, Arms Control and Disarmament, ISPRS Conference on „Serving Society with Geoinformatics“: Antalya, Turkey.

Suzuki-Muresan, T., Grambow, B., Duro, L., Bosbach, D., Brandt, F., Kulik, D., SKIN: "Investigation of slow processes in close-to-equilibrium conditions in water/solid systems and their impact on the mobility of radionuclides from radioactive waste geologica lrepositories", EURADWASTE '13, 8th EC Conference on the Management of Radioactive Waste Community Policy and Research on Disposal: Vilnius, Lithuania.

Tietze-Jaensch, H., Aksyutina, Y., Weidenfeld, M., Fast, I., Schneider, S., Produktkontrolle radioaktiver Abfälle aus Wiederaufarbeitungsanlagen Glaskokillen, Kompaktgebinde und Simulation, GRS Bereichsseminar: Braunschweig, Germany.

von Lensa, W., Rizzato, C., Banford, A. W., Bradbury, D., Goodwin, J., Grambow, B., Grave, M. J., Jones, A. N., Pina, G., Vulpius, D., Assessment/development of technologies and management options for irradiated-graphite and carbonaceous waste, EURADWASTE '13, 8th EC Conference on the Management of Radioactive Waste Community Policy and Research on Disposal: Vilnius, Lithuania.

Wilden, A., Deutsch-Französische Kooperation in der Entsorgungsforschung, Forschungszentrum Jülich – IEK-6, 1. Projektstatusgespräch zur BMBF-geförderten Nuklearen Sicherheitsforschung: Karlsruhe, Germany.

Additional/Internal Talks

Arinicheva, Y., Bukaemskiy, A., Neumeier, S., Studies on structure and stability of monazite-type ceramics for the conditioning of minor actinides, BMBF-Meeting Verbundprojekt "Conditioning", Hanover, Germany.

Arinicheva, Y., Bukaemskiy, A., Neumeier, S., Synthesis and mechanical properties of monazite-type ceramics for the conditioning of minor actinides, Kick-off meeting, BMBF-Meeting Verbundprojekt "Conditioning": Aachen, Germany.

Arinicheva, Y., Finkeldei, S., Neumeier, S., Brandt, F., Bukaemskiy, A., Deissmann, G., Filby, A., Dissolution behaviour and radiation damages, BMBF-Meeting Verbundprojekt "Conditioning": Aachen, Germany.

Arinicheva, Y., Neumeier, S., Bukaemskiy, A., Synthesis, microstructure and physical and mechanical properties of monazite-type ceramics for the conditioning of minor actinides, Microsymposium IGEM RAS: Moscow, Russia.

Arinicheva, Y., Neumeier, S., Clavier, N., Dacheux, N., Synthesis and microstructure of phosphate ceramics with monazite structure, Presentation within the 'HITEC Go'-Student exchange Program: Marcoule, France.

Brandt, F., and Finkeldei, S., Conditioning of Minor Actinides in $ZrO_2$ based Pyrochlore-type Ceramics, Cooperation meeting - The University of Sheffield: Sheffield, United Kingdom.

Curtius, H., Institute of Energy and Climate Research- IEK-6: Nuclear Waste Management and reactor safety, HITEC Woche.

Curtius, H., Spent fuel corrosion, Bilaterales Treffen mit PSI.

Curtius, H., VESPA-I and VESPA-II: Behaviour of long-lived fission and activation products and possibilities of their retention in the near-field, Projekttreffen VESPA-I: Jülich, Germany.

Curtius, H., Müskes, H.-W., Güngör, M., Lieck, N., Bosbach, D., Instant radionuclide release fraction of high burn-up spent nuclear fuel, 2nd annual project meeting „First Nuclides": Antwerpen, Belgium.

Ebert, E., Modolo, G., Neumeier, S., Bukaemskiy, A., Schreinemachers, C., Wilden, A., Progress report of beneficiary No. 2: Jülich within WP 2.1 of Domain 2, Inert Matrix Fuels, ASGARD 2nd Project Meeting: Alkmaar, Netherlands.

Finkeldei, S., Brandt, F., Bukaemskiy, A., Neumeier, S., Modolo, G., Bosbach, D., Dissolution kinetics of $ZrO_2$ based ceramics, BMBF-Meeting Verbundprojekt "Conditioning", Hanover, Germany.

Genreith, C., and Rossbach, M., Thermal Capture Cross Section determination of $^{241}Am$ using the FRM-II Cold Neutron Beam: Geel, Belgium.

Heuser, J., Bukaemskiy, A., Neumeier, S., Bosbach, D., Investigations of Lanthanide-Phosphates - potential host matrices for radionuclides -,,BMBF-Meeting Verbundprojekt "Conditioning": Hanover, Germany.

Klinkenberg, M., Brandt, F., Breuer, U., Bosbach, D., Uptake of Radium by barite under repository relevant conditons, Final SKIN Workshop: Barcelona, Spain.

Labs, S., $USiO_4$, $ThSiO_4$ and their Solid Solutions – Comparison of bulk and local structure, Trilaterales Meeting: Dresden/Rossendorf, Germany.

Li, Y., Ab initio calculations in nuclear waste management, The project meeting BMBF Verbundproject 'Conditioning': Hanover, Germany.

Listner, C., Satellite imagery change detection in support of nuclear non-proliferation and international safeguards, HITEC Symposium: Jülich, Germany.

Neumann, A., and Jung, C., Synthesis and Characterisation of $La(Ce,Sr)PO_4$ solid solutions, BMBF-Verbundprojekttreffen "coniditioning": Hannover, Germany.

Neumeier, S., Background of the Joint Research Project „Conditioning", BMBF-Meeting Verbundprojekt "Conditioning": Aachen, Germany.

Neumeier, S., Brandt, F., Bukaemskiy, A., Finkeldei, S., Arinicheva, Y., Modolo, G., Bosbach, D., Ceramic Materials for Nuclear Waste Management – Status at IEK-6 (FZJ), Microsymposium IGEM RAS: Moscow, Russia.

Neumeier, S., Finkeldei, S., Babelot, C., Holliday, K., Stumpf, T., TRLFS @ KIT, BMBF-Meeting Verbundprojekt "Conditioning": Aachen, Germany.

Schreinemachers, C., Bukaemskiy, A., Neumeier, S., Modolo, G., Ebert, E., Wilden, A., Progress report of beneficiary No. 2: Jülich within WP 2.3.1 of Domain 2, Conversion from solution to oxide pre-cursors, ASGARD 2nd Project Meeting: Alkmaar, Netherlands.

Schreinemachers, C., Bukaemskiy, A., Neumeier, S., Modolo, G., Ebert, E., Wilden, A., Progress report of beneficiary No. 3: Jülich within WP 2.3.1 of Domain 2, Conversion from solution to oxide pre-cursors, ASGARD 3rd Project Meeting: Warsaw, Poland.

Wilden, A., Lange, S., Sadowski, F., Bosbach, D., FZJ – IEK-6 progress report 01.06.2013-19.11.2013, 3. Halbjahrestreffen, BMBF Projekt f-Kom 02NUK020E: Karlsruhe, Germany.

## 11.2. Publications 2014

### *11.2.1 Journal papers*

Peer-reviewed Journals


Arinicheva, Y., Bukaemskiy, A., Neumeier, S., Modolo, G., Bosbach, D., 2014. Studies on thermal and mechanical properties of monazite-type ceramics for the conditioning of minor actinides: Progress in nuclear energy, 72: 144-148.

Bauer, J.D., Labs, S., Winkler, B., Weiss, S., Bayarjargal, L., Morgenroth, W., Milman, V., Perlov, A., Curtius, H., Bosbach, D., Zänker, H., 2014. High-Pressure Phase Transition of Coffinite, $USiO_4$. The journal of physical chemistry / C, 118(43): 25141 – 25149.

Belle, C.J., Wesch, G.E., Neumeier, S., Lozano-Rodríguez, M.J., Scheinost, A.C., Simon, U., 2014. Volume-doped cobalt titanates for ethanol sensing: An impedance and X-ray absorption spectroscopy study. Sensors and actuators / B, 192: 60 - 69.

Beridze, G. and Kowalski, P., 2014. Benchmarking the DFT+ U Method for Thermochemical Calculations of Uranium Molecular Compounds and Solids. The journal of physical chemistry / A, 118(50): 11797–11810.

Blanca Romero, A., Kowalski, P., Beridze, G., Schlenz, H., Bosbach, D., 2014. Performance of DFT+ U method for prediction of structural and thermodynamic parameters of monazite-type ceramics. Journal of computational chemistry, 35(18): 1339 - 1346.

Brandt, F., Neumeier, S., Schuppik, T., Arinicheva, Y., Bukaemskiy, A., Modolo, G., Bosbach, D., 2014. Conditioning of minor actinides in lanthanum monazite ceramics: A surrogate study with Europium. Progress in nuclear energy, 72: 140–143.

Brykala, M., Deptula, A., Rogowski, M., Lada, W., Olczak, T., Wawszczak, D., Smolinski, T., Wojtowicz, P., Modolo, G., 2014. Synthesis of microspheres of triuranium octaoxide by simultaneous water and nitrate extraction from ascorbate-uranyl sols. Journal of radioanalytical and nuclear chemistry, 299(1): 651-655.

Carrasco, J.M., Catalán, S., Jordi, C., Tremblay, P.-E., Napiwotzki, R., Luri, X., Robin, A.C., Kowalski, P., 2014. Gaia photometry for white dwarfs. Astronomy and astrophysics, 565: A11

Carrott, M., Bell, K., Müllich, U., Sarsfield, M., Wilden, A., Taylor, R., Brown, J., Geist, A., Gregson, C., Hères, X., Maher, C., Malmbeck, R., Mason, C., Modolo, G., 2014. Development of a New Flowsheet for Co-Separating the Transuranic Actinides: The "EURO-GANEX" Process. Solvent extraction and ion exchange, 32(5): 447 - 467.

Degueldre, C., Grimes, R., Rondinella, V., Poinssot, C., Bosbach, D., 2013. The Scientific Basis of the Nuclear Fuel Cycle. Progress in nuclear energy, 72: 3-4.

Deissmann, G., Neumeier, S., Brandt, F., Modolo, G., Bosbach, D., 2014. Evaluation of the long-term behavior of potential plutonium waste forms in a geological repository. MRS online proceedings library, 1665: nw37-s24.

Finkeldei, S., Brandt, F., Bukaemskiy, A., Neumeier, S., Modolo, G., Bosbach, D., 2014. Synthesis and dissolution kinetics of zirconia based ceramics: Progress in nuclear energy, 72: 130-133.

Finkeldei, S., Brandt, F., Rozov, K., Bukaemskiy, A., Neumeier, S., Bosbach, D., 2014. Dissolution of $ZrO_2$ based pyrochlores in the acid pH range: A macroscopic and electron microscopy study. Applied geochemistry, 49: 31-41.

Genreith, C., Rossbach, M., Revay, Z., Kudejova, P., 2014. Determination of (n,γ) Cross Sections of $^{241}$Am by PGAA. Int. Conf. Nucl.Data Sci. Technol., 119: 69-71.

Heberling, F., Bosbach, D., Pust, C., Schäfer, T., Stelling, J., Ukrainczyk, M., Vinograd, V., Vučak, M., Winkler, B., Eckhardt, J.-D., Fischer, U., Glowacky, J., Haist, M., Kramar, U., Loos, S., Müller, H.S., Neumann, T., 2014. Reactivity of the calcite–water-interface, from molecular scale processes to geochemical engineering. Applied geochemistry, 45: 158 - 190.

Heberling, F., Vinograd, V., Polly, R., Gale, J.D., Heck, S., Rothe, J., Bosbach, D., Geckeis, H., Winkler, B., 2014. A thermodynamic adsorption/entrapment model for selenium(IV) coprecipitation with calcite. Geochimica et cosmochimica acta, 134: 16 - 38.

Held, P., Kegler, P., Schrottke, K., 2014. Influence of suspended particulate matter on salinity measurements. Continental shelf research, 85: 1-8.

Heuser, J., Bukaemskiy, A., Neumeier, S., Neumann, A., Bosbach, D., 2014. Raman and infrared spectroscopy of monazite-type ceramics used for nuclear waste conditioning. Progress in nuclear energy, 72: 149 - 155.

Jahn, S. and Kowalski, P., 2014. Theoretical Approaches to Structure and Spectroscopy of Earth Materials. Reviews in mineralogy & geochemistry, 78(1): 691-743.

Kaufhold, S., Grissemann, C., Dohrmann, R., Klinkenberg, M., Decher, A., 2014. Comparison of three small-scale devices for the investigation of the electrical conductivity/resistivity of swelling and other clay. Clays and clay minerals, 62(1): 1-12.

Klinkenberg, M., Brandt, F., Breuer, U., Bosbach, D., 2014. Uptake of Ra during the recrystallization of barite: a microscopic and ToF-SIMS study. Environmental science & technology, 48(12): 6620–6627.

Klinkenberg, M., Neumann, A., Curtius, H., Kaiser, G., Bosbach, D., 2014. Research reactor fuel element corrosion under repository relevant conditions: separation, identification, and quantification of secondary alteration phases of $UAl_x$-Al in $MgCl_2$-rich brine. Radiochimica acta, 102(4): 311–324.

Kowalski, P., 2014. Infrared absorption of dense helium and its importance in the atmospheres of cool white dwarfs. Astronomy and astrophysics, 566: L8

Labs, S., Hennig, C., Weiss, S., Curtius, H., Zänker, H., Bosbach, D., 2014. Synthesis of coffinite, $USiO_4$, and structural investigations of the $U_xTh_{(1-x)}SiO_4$ solid solutions: Environmental science & technology, 48 (1): 854-860.

Lelet, M.I., Suleimanov, E.V., Golubev, A.V., Geiger, C.A., Depmeier, W., Bosbach, D., Alekseev, E., 2014. Thermodynamic properties and behaviour of $A_2[(UO_2)(MoO_4)_2]$ compounds with A=Li, Na, K, Rb, and Cs. The journal of chemical thermodynamics, 79: 205 - 214.

Li, Y., Kowalski, P., Blanca Romero, A., Vinograd, V., Bosbach, D., 2014. Ab initio calculation of excess properties of $La_{1-x}Ln_xPO_4$ solid solutions. Journal of solid state chemistry, 220: 137 - 141.

Mauerhofer, E., Göbbels, C., Krings, T., 2014. On the applicability of $LaBr_3$ detectors in the non-destructive characterization of radioactive waste drums. Journal of radioanalytical and nuclear chemistry, 304: 7.

Mauerhofer, E. and Havenith, A., 2014. The MEDINA facility for the assay of the chemotoxic inventory of radioactive waste packages. Journal of radioanalytical and nuclear chemistry, 1: 1-15.

Modolo, G., Wilden, A., Kaufholz, P., Bosbach, D., Geist, A., 2014. Development and demonstration of innovative partitioning processes (i-SANEX and 1-cycle SANEX) for actinide partitioning. Progress in nuclear energy, 72: 107-114.

Polinski, M.J., Pace, K.A., Stritzinger, J.T., Lin, J., Cross, J.N., Cary, S.K., Cleve, S.M.V., Alekseev, E., Albrecht-Schmitt, T.E., 2014. Chirality and Polarity in the f-Block Borates $M_4[B_{16}O_{26}(OH)_4\ (H_2O)_3\ Cl_4\ ]$ (M=Sm, Eu, Gd, Pu, Am, Cm, and Cf). Chemistry - a European journal, 20(32): 9892 - 9896.

Retegan, T., Drew, M., Ekberg, C., Engdahl, E.L., Hudson, M.J., Fermvik, A., Foreman, M.R.S., Modolo, G., Geist, A., 2014. Synthesis and Screening of t-Bu-$CyMe_4$-BTBP, and Comparison with $CyMe_4$-BTBP. Solvent extraction and ion exchange, N/A: 1 - 17.

Saumon, D., Holberg, J.B., Kowalski, P., 2014. NEAR-UV ABSORPTION IN VERY COOL DA WHITE DWARFS. The astrophysical journal / 1, 790(1): 50

Schreinemachers, C., Bukaemskiy, A., Klinkenberg, M., Neumeier, S., Modolo, G., Bosbach, D., Characterization of uranium neodymium oxide microspheres synthesized by internal gelation: Progress in nuclear energy, v. 72, p. 17-21.

Stritzinger, J.T., Alekseev, E., Polinski, M.J., Cross, J.N., Eaton, T.M., Albrecht-Schmitt, T.E., 2014. Further Evidence for the Stabilization of U(V) within a Tetraoxo Core. Inorganic chemistry, 53(10): 5294 - 5299.

Wilden, A., Modolo, G., Bosbach, D., Lange, S., Sadowski, F., Beele, B.B., Skerencak-Frech, A., Panak, P.J., Iqbal, M., Verboom, W., Geist, A., 2014. Modified Diglycolamides for the An(III) + Ln(III) co-separation: Evaluation by Solvent Extraction and Time-Resolved Laser Fluorescence Spectroscopy. Solvent extraction and ion exchange, 32(2): 119-137.

Wu, S., Kowalski, P., Yu, N., Malcherek, T., Depmeier, W., Bosbach, D., Wang, S., Suleimanov, E.V., Albrecht-Schmitt, T.E., Alekseev, E., 2014. Highly Distorted Uranyl Ion Coordination and One/Two-Dimensional Structural Relationship in the $Ba_2[UO_2(TO_4)_2]$ (T = P, As) System: An Experimental and Computational Study. Inorganic chemistry, 53(14): 7650 - 7660.

Xiao, B., Dellen, J., Schlenz, H., Bosbach, D., Suleimanov, E.V., Alekseev, E., 2014. Unexpected Structural Complexity in Cesium Thorium Molybdates. Crystal growth & design, 14(5): 2677 - 2684.

Xiao, B., Gesing, T.M., Kegler, P., Modolo, G., Bosbach, D., Schlenz, H., Suleimanov, E.V., Alekseev, E., 2014. High-Temperature Phase Transitions, Spectroscopic Properties, and Dimensionality Reduction in Rubidium Thorium Molybdate Family. Inorganic chemistry, 53(6): 3088 - 3098.

Yu, N., Klepov, V., Villa, E.M., Bosbach, D., Suleimanov, E.V., Depmeier, W., Albrecht-Schmitt, T.E., Alekseev, E., 2014. Topologically identical, but geometrically isomeric layers in hydrous α-, β-Rb[$UO_2(AsO_3OH)(AsO_2(OH)_2]$•H2O and anhydrous $Rb[UO_2(AsO_3OH)(AsO_2(OH)_2)]$. Journal of solid state chemistry, 215: 152 - 159.

Yu, N., Klepov, V.V., Kegler, P., Bosbach, D., Albrecht-Schmitt, T.E., Alekseev, E., 2014. $Th(As^{III}_4As^{V}_4O_{18})$: a Mixed-Valent Oxoarsenic(III)/arsenic(V) Actinide Compound Obtained under Extreme Conditions. Inorganic chemistry, 53(16): 8194 - 8196.

Yu, N., Klepov, V.V., Modolo, G., Bosbach, D., Suleimanov, E.V., Gesing, T.M., Robben, L., Alekseev, E., 2014. Morphotropy and Temperature-Driven Polymorphism in $A_2Th(AsO_4)_2$ (A = Li, Na, K, Rb, Cs) Series. Inorganic chemistry, 53(20): 11231 - 11241.

Zhao, P., Murshed, M.M., Alekseev, E., Atuchin, V.V., Pugachev, A.M., Gesing, T.M., 2014. Synthesis, structure and properties of $Na[AsW_2O_9]$. Materials research bulletin, 60: 258 - 263.

### *11.2.2 Proceedings/Books*

Proceedings

Brandt, F., Klinkenberg, M., Breuer, U., Rozov, K., Bosbach, D., 2014. SKIN – Uptake of Radium during Barite Recrystallisation, 8th EC Conference on the Management of Radioactive Waste Community Policy and Research on Disposal. European Union, Vilnius, Lithuania, pp. 487-490.

Curtius, H., Müskes, H.W., Güngör, M., Lieck, N., Bosbach, D., 2014. First results on instant radionuclide release fraction from spent $UO_2$ TRISO coated particles, 2nd Annual Workshop Proccedings of the collaborative project „Fast/Insatnt release of safety relevant radionuclides from spent fuel. KIT Scientific Publ., Karlsruhe, pp. 97-103.

d'Angelo, P., Rossi, C., Minet, C., Eineder, M., Flory, M., Niemeyer, I., 2014. High Resolution 3D Earth Observation Data Analysis for Safeguards Activities, Symposium on International Safeguards: Linking Strategy, Implementation and People, Vienna, Austria, pp. 8 p.

Dreicer, M., Listner, C., Chen, C., Stein, G., Niemeyer, I., 2014. Applying State-level Approaches to Arms Control Verification, Institute of Nuclear Materials Management 55th Annual Meeting, Atlanta, USA, pp. 1-6.

Dürr, M., Knott, A., Middendorp, R., Niemeyer, I., Küppers, S., Zoriy, M., Froning, M., Bosbach, D., 2014. Activities at Forschungszentrum Jülich in Safeguards AnalyticalTechniques and Measurements, Symposium on International Safeguards: Linking Strategy, Implementation and People, Conference ID: 46090 (CN-220), Vienna, Austria, pp. 5.

Gray, M., Zalupski, P., Modolo, G., Nilsson, M., 2014. Activity coefficients of di-(2-ethyl hexyl) phosphoric acid by vapor pressure osmometry and slope analysis, 20th International Solvent Extraction Conference 2014, Würzburg, Germany, pp. p. 772-777.

Haas, E., Chang, H.L., James, S., Phillips, J., Listner, C., 2014. Proliferation Resistance and Safeguards by Design – The Safeguardability Assessment Toolprovided by the INPRO

Collaborative Project “PROSA” (Proliferation Resistance andSafeguardability Assessment), Symposium on International Safeguards: Linking Strategy, Implementation and People, Vienna, Austria, pp. 8 p.

Jahn, S., Haigis, V., Kowalski, P., Künzel, D., Spiekermann, G., Wagner, J., 2014. First-Principles View on Element and Isotope Cycles in the Earth's Interior, NIC Symposium 2014, Jülich, Germany, pp. 317-324.

Kaufholz, P., Wilden, A., Modolo, G., Sadowski, F., Lange, S., Bosbach, D., Harwood, L.M., Smith, A.W., 2014. Development of a TODGA-based liquid-liquid extraction system for the separation of Am(III) using hydrophilic complexing agents, 20th International Solvent Extraction Conference 2014, Würzburg, Germany, pp. p. 1163.

Kienzler, B., Metz, V., Zumbiehl, A.F., Curti, E., Lemmens, K., Vandenborre, J., Pablo, J.d., Casas, I., Clarens, F., Hózer, Z., Roth, O., González-Robles, E., Duro, L., Valls, A., Wegen, D., Carbol, P., Serrano-Purroy, D., Curtius, H., Günther-Leopold, I., 2014. FIRST-Nuclides: “Fast / Instant Release of Safety Relevant Radionuclides from Spent Nuclear Fuel”, 8th EC Conference on the Management of Radioactive Waste Community Policy and Research on Disposal. European Union, Vilnius, Lithuania, pp. 221-228.

Knott, A., Dürr, M., Niemeyer, I., Bosbach, D., 2014. Towards Production of Monodisperse Reference Particles for Nuclear Safeguards Applications, Institute of Nuclear Materials Management 55th Annual Meeting, Atlanta, USA, pp. 1-8.

Knott, A., Vogt, S., Wegrzynek, D., Chinea-Cano, E., Dürr, M., 2014. Production and Characterization of Monodisperse Reference Particles, Symposium on International Safeguards: Linking Strategy, Implementation and People, Vienna, Austria, pp. 1-7.

Listner, C., Canty, M., Stein, G., Rezniczek, A., Niemeyer, I., 2014. Quantifying Detection Probabilities for Proliferation Activities in Undeclared Facilities, Symposium on International Safeguards: Linking Strategy, Implementation and People, Vienna, Austria, pp. 28.

Listner, C., Murphy, C., Canty, M., Stein, G., Rezniczek, A.U.G., Niemeyer, I., 2014. Evolution of Safeguards - What Can Formal Acquisition Path Analysis Contribute?, Institute of Nuclear Materials Management 55th Annual Meeting, Atlanta, USA, pp. 1-10.

Malmbeck, R., Carrott, M., Christiansen, B., Geist, A., Hérès, X., Magnusson, D., Modolo, G., Sorel, C., Taylor, R., Wilden, A., 2014. EURO-GANEX, a Process for the Co-separation of TRU, Sustainable Nuclear Energy Conference, Manchester, England, pp. 7 p.

Malmbeck, R., Carrott, M., Geist, A., Hérès, X., Magnusson, D., Modolo, G., Sorel, C., Taylor, R,. Wilden, A., 2014. The Hydrometallurgical Co-separation of Neptunium, Plutonium, Americium and Curium by the EURO-GANEX Process, 20th International Solvent Extraction Conference 2014, Würzburg, Germany, pp. 39-44 p.

Murphy, C., Listner, C., Boyer, B., Budlong Sylvester, K., 2014. Evolution of Safeguards - An Expert-driven Approach to Acquisition Path Analysis, Institute of Nuclear Materials Management 55th Annual Meeting, Atlanta, USA, pp. 1-9.

Niemeyer, I., Altmann, J., Filbert, W., Kaiser, S., Uchtmann, S., Trautwein, W., 2014. Safeguarding Geological Repositories – R&D Contributions from the German Support Programme, Symposium on International Safeguards: Linking Strategy, Implementation and People, Vienna, Austria, pp. 12 p.

Niemeyer, I., Listner, C., Canty, M., Wolfart, E., Lagrange, J.-M., 2014. Integrated Analysis of Satellite Imagery for Nuclear Monitoring - Results from G-SEXTANT, Institute of Nuclear Materials Management 55th Annual Meeting, Atlanta, USA, pp. 1-10.

Omanovic, S., Modolo, G., Sadowski, F., Bosbach, D., 2014. Solvent Extraction studies for the Separation of rare earth elements using neutral and acidic organophosphorus extractants, 20th International Solvent Extraction Conference 2014, Würzburg, Germany, pp. p. 898.

Rossbach, M. and Genreith, C., 2014. $^{241}$Am: a difficult actinide for (n,γ) cross section measurement, ERINDA Workshop, Geneva, Switzerland, pp. 157-163.

Sevini, F., Niemeyer, I., Vincze, A., van der Meer, K., 2014. ESARDA Contributions to IAEA State-level Concept, Institute of Nuclear Materials Management 55th Annual Meeting, Atlanta, USA, pp. 1-10.

Stein, G., Rezniczek, A., Niemeyer, I., Listner, C., Trautwein, W., 2014. The Evolution of International Safeguards - A View from Germany, Institute of Nuclear Materials Management 55th Annual Meeting, Atlanta, USA, pp. 1-7.

Suzuki-Muresan, T., Grambow, B., Hedström, H., Torapava, N., Bosbach, D., Brandt, F., Klinkenberg, M., Stumpf, T., Evans, N., Hinchliff, J., Curti, E., Kulik, D., Montavon, G., Thien, B., Cui, D., Spahiu, K., Liu, C., Prieto, M., Ribet, S., Borre, J.v.d., Duro, L., Grive, M., Valls, A., Colas, E., Ekberg, C., 2014. SKIN: Slow Processes in Close-to-equilibrium Conditions for Radionuclides in Water/solid Systems of Relevance to Nuclear Waste Management, 8th EC Conference on the Management of Radioactive Waste Community Policy and Research on Disposal. European Union, Vilnius, Lithuania, pp. 249-257.

von Lensa, W., Rizzato, C., Banford, A.W., Bradbury, D., Goodwin, J., Grambow, B., Grave, M.J., Jones, A.N., Pina, G., Vulpius, D., 2014. CARBOWASTE: Assessment/development of Technologies and Management Options for Irradiated-graphite and Carbonaceous Waste, 8th EC Conference on the Management of Radioactive Waste Community Policy and Research on Disposal. European Union, Vilnius, Lithuania, pp. 229-238.

Wilden, A., Modolo, G., Kaufholz, P., Sadowski, F., Lange, S., Sypula, M., Magnusson, D., Müllich, U., Geist, A., Bosbach, D., 2014. Spiked Laboratory-scale Continuous Counter-Current Centrifugal Contactor Demonstration of a Novel innovative-SANEX Process, Sustainable Nuclear Energy Conference, Manchester, England, pp. 10 p.

Wilden, A., Modolo, G., Kaufholz, P., Sadowski, F., Lange, S., Sypula, M., Magnusson, D., Müllich, U., Geist, A., Bosbach, D., 2014. Spiked Laboratory-scale Continuous Counter-Current Centrifugal Contactor Demonstration of a Novel innovative-SANEX Process, 20th International Solvent Extraction Conference 2014, Würzburg, Germany, pp. 130-135 p.

Wilden, A., Modolo, G., Sadowski, F., Lange, S., Bremer, A., Panak, P.J., Geist, A., 2014. Process development studies and demonstration of an r-SANEX process using C5-BPP – selective separation of trivalent actinides from lanthanides, 20th International Solvent Extraction Conference 2014, Würzburg, Germany, pp. 144-149 p.

Wilden, A., Modolo, G., Sadowski, F., Lange, S., Bremer, A., Panak, P.J., Geist, A., 2014. Process development studies towards an r-SANEX process using C5-BPP – selective separation of trivalent actinides from lanthanides, Sustainable Nuclear Energy Conference, Manchester, England, pp. 8 p.

Books

Becker, M., Bollingerfehr, W., Gompper, K., Hannstein, V., Havenith, A., Kettler, J., Maschek, W., Merk, B., Modolo, G., Mönig, J., Müller, G., Neumeier, S., Buhmann, D., Puente-Espel, F., Renn, O., Rineiski, A., Ruddat, M., Salvatores, M., Sanchez-Espinoza, V.H., Schwenk-Ferrero, A., Seubert, A., Sonnenburg, H.-G., Velkov, K., Fazio, C., Vezzoni, B., Weiß, F.P., Wetzel, T., Wilden, A., Gabrielli, F., Gallego Carrera, D., Geckeis, H., Geist, A., Gerbert, G., Gmal, B., 2014. Partitionierung und Transmutation nuklearer Abfälle. Forschung - Entwicklung - Gesellschaftliche Implikationen (acatech STUDIE), Partitionierung und Transmutation nuklearer Abfälle. Forschung - Entwicklung - Gesellschaftliche Implikationen (acatech STUDIE). Herbert Utz Verlag, München, pp. 291.

### *11.2.3 Internal reports*

Bukaemskiy, A., Ebert, E., Lichte, E., Middendorp, R., Modolo, G., Neumeier, S., Sadowski, F., Schreinemachers, C., 2014. Partner interim Report No. 4.

Bukaemskiy, A., Ebert, E., Middendorp, R., Modolo, G., Neumeier, S., Sadowski, F., Schreinemachers, C., 2014. Partner interim Report No. 5.

Göbbels, C., 2014. Characterization of small samples at the MEDINA facility using prompt and delayed gamma-ray neutron activation analysis.

Modolo, G., 2013. EU-Projekt SACSESS, Work package activity summary report WP 1.4, WPASR N°1.

Modolo, G., 2014. EU-Projekt SACSESS, Work package activity summary report WP 1.4, WPASR N°2.

Modolo, G., 2014. EU-Projekt SACSESS, Work package activity summary report WP 1.4, WPASR N°3.

Modolo, G., Lange, S., Kaufholz, P., Sadowski, F., Schmidt, H., Wilden, A., 2014. EU-Projekt SACSESS, HYBAR 3 Half Yearly Beneficiary Activity Report No. 3.

Modolo, G., Wilden, A., Casnati, A., Harwood, L., Smith, A., Kaufholz, P., Marie, C., Miguirditchian, M., Wagner, C., Müllich, U., Munzel, D., Panak, P.J., Geist, A., 2014. EU-Projekt SACSESS, Deliverable D14.1, Report on the formulation of a set of Am(III) alone extraction systems.

Modolo, G., Wilden, A., Kaufholz, P., Sadowski, F., Lange, S., Hupert, M., Santiago-Schübel, B., 2014. EU-Projekt SACSESS, HYBAR 2 Half Yearly Beneficiary Activity Report No. 2.

Neumeier, S., Kegler, P., Bosbach, D., 2014. 8$^{th}$ European Summer School on Separation Chemistry and Conditioning as well as Supramolecular, Intermolecular, Interaggregate Interactions, Forschungszentrum Jülich GmbH Zentralbibliothek, Verlag, Jülich.

Verboom, W., Modolo, G., Wilden, A., Galan, H., Geist, A., 2014. EU-Projekt SACSESS (Contract Number: FP7-CP-2012-323282), Deliverable 12.1, State of the art concerning TODGA TWE-21 molecule based systems.

Verhoef, E.V., de Bruin, A.M.G., Wiegers, R.B., Neeft, E.A.C., Deissmann, G., 2014. Cementitious materials in OPERA disposal concept in Boom Clay, COVRA.

Wilden, A. and Modolo, G., 2014. 3. Halbjahresbericht zum BMBF Forschungsvorhabens „Verbundprojekt f-Kom: Untersuchungen zum grundlegenden Verständnis der selektiven Komplexierung von f-Elementen“, Förderzeichen 02NUK020E.

### *11.2.4 Poster*

Arinicheva, Y., Clavier, N., Neumeier, S., Bukaemskiy, A., Podor, R., Ravaux, J., Dacheux, N., Bosbach, D., 2014. Synthesis, characterisation, sintering behaviour and microstructure of lanthanum europium phosphates with monazite structure, Sintering 2014, Dresden, Germany.

Arinicheva, Y., Janeth Lozano-Rodriguez, M., Neumeier, S., Scheinost, A.C., Clavier, N., Bosbach, D., 2014. Structural studies on (La,Eu)$PO_4$ solid solutions by Infrared, Raman and X-ray Absorption Spectroscopy, Advanced Techniques in Actinide Spectroscopy 2014, Dresden, Germany.

Bauer, J.D., Labs, S., Bayarjargal, L., Winkler, B., 2014. Materials properties at high pressure in the diamond anvil cell, 8$^{th}$ European Summer School on Separation Chemistry and Conditioning as well as Supramolecular, Intermolecular, Interaggregate Interactions, Bonn/Bad Godesberg, Germany.

Beridze, G., Blanca Romero, A., Kowalski, P., 2014. Performance of DFT+U method for actinide- and lathanide-bearing materials relevant for nuclear waste management, CECAM workshop What anout U? Strong correlations from first principles, Lausanne, Switzerland.

Beridze, G., Blanca Romero, A., Li, Y., Kowalski, P., 2014. Ab initio calculations of f-element compounds and solids with DFT+U method, 78. Jahrestagung der DPG und DPG-Frühjahrstagung, Berlin, Germany.

Beridze, G. and Kowalski, P., 2014. DFT+U calculations of actinide- and lanthanide-bearing materials relevant for nuclear waste management, Dalton Discussion 14 – Advancing the chemistry of the f-elements,, Edinburgh, UK.

Beridze, G., Li, Y., Blanca Romero, A., Kowalski, P., 2014. Efficient ab-initio methods for computation of materials relevant for nuclear waste management, E-MRS 2014 FALL MEETING, Warsaw, Poland.

Beridze, G., Li, Y., Kowalski, P., 2014. Atomistic Modellnig for Nuclear Waste Management, BMBF and 8$^{th}$ European Summer School on Separation Chemistry and Conditioning as well as Supramolecular, Intermolecular, Interaggregate Interactions Summer School, Bonn Bad Godesberg, Germany.

Bourg, S., Geist, A., Gibilaro, M., Harisson, M., Flint, L., Biggs, S., Duplantier, B., Bell, K., Soucek, P., Rhodes, C., Taylor, R., Ekberg, C., Guilbaud, P., Modolo, G., Sharrad, C., Mendes, E., 2014. Recent achievements in the assessment of the safety of actinides Separation Projects in the European Project SACSESS, 13$^{th}$ Information Exchange

Meeting on Actinide and Fission Product Partitioning and Transmutation – IEMPT13, Seoul, Korea.

Brykala, M., Deptula, A., Rogowski, M., Schreinemachers, C., Modolo, G., 2014. Complex Sol-Gel Process (CSGP) as a method to preparation of various type of advanced nuclear fuels, 13th Information Exchange Meeting on Actinide and Fission Product Partitioning and Transmutation – IEMPT13, Seoul, Korea.

Bukaemskiy, A., Finkeldei, S., Brandt, F., Neumeier, S., Modolo, G., Bosbach, D., 2014. Stability of pyrochlore phase for zirconia based ceramics.Experimental and modeling study, 8th European Summer School on Separation Chemistry and Conditioning as well as Supramolecular, Intermolecular, Interaggregate Interactions, Bonn/Bad Godesberg, Germany.

Curtius, H., Lieck, N., Güngör, M., Kaiser, G., Klinkenberg, M., Bosbach, D., 2014. Leaching of spent $UO_2$TRISO coated particles - Instant radionuclide release fraction and microstructure evolution, Final workshop, FIRST NUCLIDES, Karlsruhe, Germany.

Ebert, E., Bukaemskiy, A., Sadowski, F., Brandt, F., Cheng, M., Steppert, M., Walther, C., Modolo, G., Bosbach, D., 2014. Dissolution behavior of MgO and Mo based Inert Matrix Fuel for the transmutation of plutonium and minor actinides, First joint workshop on f-element chemistry, Manchester, UK.

Ebert, E., Bukaemskiy, A., Sadowski, F., Brandt, F., Modolo, G., Bosbach, D., 2014. Dissolution behavior of MgO based Inert Matrix Fuel for the transmutation of plutonium and minor actinides, 17th Radiochemical Conference, Marianske Lazne, Czech Republic.

Ebert, E., Bukaemskiy, A., Sadowski, F., Brandt, F., Modolo, G., Bosbach, D., 2014. Dissolution studies on molybdenum-based inert matrix fuel targets for the transmutation of minor actinides, 17th Radiochemical Conference, Marianske Lazne, Czech Republic.

Ebert, E., Cheng, M., Steppert, M., Walther, C., Modolo, G., Bosbach, D., 2014. Electrospray Ionization Time-of-Flight Mass Spectrometry: Dissolution of Mo-based CERMET fuel, 8th European Summer School on Separation Chemistry and Conditioning as well as Supramolecular, Intermolecular, Interaggregate Interactions, Bonn, Germany.

Ebert, E., Modolo, G., Bukaemskiy, A., Brandt, F., Bosbach, D., Cheng, M., Steppert, M., Walther, C., 2014. Dissolution behaviour of MgO and Mo based inert Matrix fuel for the Transmutation of Plutonium and minor actinides, 13th Information Exchange Meeting on Actinide and Fission Product Partitioning and Transmutation – IEMPT13, Seoul, Korea.

Finkeldei, S., Brandt, F., Holliday, K., de Visser-Týnová, E., Neumeier, S., Bosbach, D., 2014. Synthesis and characterization of actinide zironia pyrochlores, MRS Fall Meeting 2014, Boston, USA, Boston, USA.

Finkeldei, S., Brandt, F., Neumeier, S., Bosbach, D., 2014. Dissolution Kinetics of Nuclear Waste Forms, 8th European Summer School on Separation Chemistry and Conditioning as well as Supramolecular, Intermolecular, Interaggregate Interactions, Bonn/ Bad Godesberg, Germany.

Gausse, C., Mesbah, A., Szenknect, S., Clavier, N., Dacheux, N., Neumeier, S., Bosbach, D., 2014. Solubility properties of the Ln-rhabdophane compounds:$LnPO_4{\cdot}nH_2O$ (Ln = La → Dy), precursor of the monazite phase, 8th European Summer School on Separation

Chemistry and Conditioning as well as Supramolecular, Intermolecular, Interaggregate Interactions, Bonn/Bad Godesberg, Germany.

Gausse, C., Szenknect, S., Mesbah, A., Clavier, N., Neumeier, S., Dacheux, N., 2014. Synthèse et solubilité de la rhabdophane $LnPO_4$, $0,67H_2O$ en tant que précurseur de la monazite (Synthesis and solubility of $LnPO_4$, $0.67H_2O$ rhabdophane as precursor of Monazite), Matériaux 2014, Montpellier, France.

Gray, M., Zalupski, P., Modolo, G., Nilsson, M., 2014. Activity coefficients of di-(2-ethyl hexyl) phophoric acid by vapor pressure osmometry and slope analysis, 20th International Solvent Extraction Conference 2014, Würzburg, Germany.

Heuser, J., Deissmann, G., Kowalski, P., Neumann, A., Bosbach, D., 2014. Experimental and computational simulation of radiation damages, 8th European Summer School on Separation Chemistry and Conditioning as well as Supramolecular, Intermolecular, Interaggregate Interactions, Bonn/Bad Godesberg, Germany.

Huittinen, N., Arinicheva, Y., Holthausen, J., Holliday, K.S., Neumeier, S., Stumpf, T., 2014. Site-selective TRLFS of Eu(III) doped rare earth phosphates for conditioning of radioactive wastes, Goldschmidt Conference, Sacramento, USA.

Huittinen, N., Arinicheva, Y., Holthausen, J., Neumeier, S., Baumann, N., Stumpf, T., 2014. Time-resolved laser-fluorescence spectroscopy (TRLFS)– A spectroscopic tool to investigate f-element interactions insolids and solutions on the molecular level, 8th European Summer School on Separation Chemistry and Conditioning as well as Supramolecular, Intermolecular, Interaggregate Interactions, Bonn/Bad Godesberg, Germany.

Kaufholz, P., Wilden, A., Modolo, G., Sadowski, F., Bosbach, D., Harwood, L.M., Lewis, F., Wagner, C., Geist, A., Panak, P., 2014. Development of a TODGA-based liquid-liquid extraction system for the separation of Am(III) using hydrophilic complexing agents, 20th International Solvent Extraction Conference 2014, Würzburg, Germany.

Klobes, B., Finkeldei, S., Bosbach, D., Hermann, R., 2014. A Local and General Perspective on Lattice Dynamics in Lanthanide Zirconate Pyrochlores for Nuclear Waste Management, Deutsche Tagung für Forschung mit Synchrotronstrahlung, Bonn, Germany.

Knott, A., Vogt, S., Wegrzynek, D., Chinea-Cano, E., 2014. Production and Characterization of Monodisperse Reference Particles, Symposium on International Safeguards: Linking Strategy, Implementation and People, Vienna, Austria.

Kowalski, P., Blanca Romero, A., Li, Y., Beridze, G., 2014. Ab initio modelling of f-electron materials relevant for nuclear waste management, NIC Symposium, Jülich, Germany.

Kowalski, P., Li, Y., Beridze, G., Blanca Romero, A., 2014. Computation of actinide- and lanthanide- bearding materials relevant for nuclear waste management, CECAM workshop on Molecular Simulations of Crystalization from Solution, Lugano, Switzerland.

Kowalski, P., Li, Y., Beridze, G., Blanca Romero, A., Heuser, J., 2014. Simulation of Ceramic Materials Relevant for Nuclear Waste Management, COSIRES – Computer Simulation of Radiation effects in Solids, Alicante, Spain.

Li, Y., Kowalski, P., Beridze, G., Blanca Romero, A., Heuser, J., 2014. Atomistic simulations of monazite-type ceramics, E-MRS 2014 FALL MEETING, Warsaw, Poland.

Middendorp, R., Knott, A., Dürr, M., 2014. Uniform Micro-Particles as Reference Material for Mass-Spectrometry, Advanced Techniques in Actinide Spectroscopy 2014, Dresden-Rossendorf, Germany.

Middendorp, R., Knott, A., Dürr, M., Niemeyer, I., Bosbach, D., 2014. Preparation of Microparticle Reference Materials for Nuclear Safeguards Particle Analysis, 8th European Summer School on Separation Chemistry and Conditioning as well as Supramolecular, Intermolecular, Interaggregate Interactions, Bonn, Germany.

Middendorp, R., Schreinemachers, C., Neumeier, S., Modolo, G., Bosbach, D., 2014. Investigations of the uranyl and neodymium(III) adsorption behavior on ion exchange resins for the weak-acid resin process, Radchem 2014 - 17th Radiochemical Conference, Marianske Lazne, Czech Republic.

Neumann, A., Hirsch, A., Heuser, J., Jung, P.C., Zaddach, J., Neumeier, S., Schlenz, H., Bosbach, D., Peters, L., Roth, G., 2014. (La, Sr, Ce) and (Sm, Ca, Ce) Monazite Solid Solutions, 22th Annual Meeting of the German Crystallographic Society, Berlin, Germany.

Neumann, A., Hirsch, A., Heuser, J., Jung, P.C., Zaddach, J., Neumeier, S., Schlenz, H., Bosbach, D., Peters, L., Roth, G., 2014. Phase relations of the Solid Solutions $Sm(Ca,Ce)PO_4$ and $La(Sr,Ce)PO_4$, Goldschmidt Conference, Sacramento, California, USA.

Omanovic, S., Modolo, G., Sadowski, F., Bosbach, D., 2014. Solvent Extraction studies for the Separation of rare earth elements using neutral and acidic organophosphorus extractants, 20th International Solvent Extraction Conference 2014, Würzburg, Germany.

Omanovic, S., Neumeier, S., Modolo, G., Bosbach, D., 2014. Non-nuclear applications – Separation of rare earth elements, 8th European Summer School on Separation Chemistry and Conditioning as well as Supramolecular, Intermolecular, Interaggregate Interactions, Bonn/Bad Godesberg, Germany.

Rozov, K., Curtius, H., Bosbach, D., 2014. Preparation and estimation of thermodynamic properties of Fe(II)-, Co(II)-, Ni(II)- and Zr(IV)-containing layered double hydroxides, DAEF2014 Key topics in deep geological disposal, Köln, Germany.

Schmidt, H., Wilden, A., Modolo, G., Bosbach, D., 2014. Radiation stability of partitioning relevant ligands for Minor Actinide separation, 8th European Summer School on Separation Chemistry and Conditioning as well as Supramolecular, Intermolecular, Interaggregate Interactions, Bonn - Bad Godesberg, Germany.

Schreinemachers, C., Middendorp, R., Bukaemskiy, A., Klinkenberg, M., Neumeier, S., Modolo, G., Bosbach, D., 2014. Fabrication of simulated minor actinide containing fuel particles and analytical characterization methods, 8th European Summer School on Separation Chemistry and Conditioning as well as Supramolecular, Intermolecular, Interaggregate Interactions, Bonn, Germany.

Thust, A., Arinicheva, Y., Haussühl, E., Neumeier, S., Bayarjargal, L., Winkler, B., 2014. Mechanical and physical properties of monazite-type ceramics $La_{(1-x)}Eu_{(x)}PO_4$, 22th Annual Meeting of the German Crystallographic Society, Berlin, Germany.

Thust, A., Haussühl, E., Arinicheva, Y., Neumeier, S., Winkler, B., 2014. Plane wave parallel plate ultrasound spectroscopy on ceramicpellets, 8th European Summer School on Separation Chemistry and Conditioning as well as Supramolecular, Intermolecular, Interaggregate Interactions, Bonn/Bad Godesberg, Germany.

Weber, J., Brandt, F., Klinkenberg, M., Savenko, A., Breuer, U., Bosbach, D., 2014. Combined chemical and structural investigations of $Ba_xRa_{1-x}SO_4$ on the atomic level by TEM and APT, 8th European Summer School on Separation Chemistry and Conditioning as well as Supramolecular, Intermolecular, Interaggregate Interactions, Bonn, Germany.

Weber, J., Breuer, U., Klinkenberg, M., Brandt, F., Savenko, A., Bosbach, D., 2014. Chemical and structural investigations of $Ba_xRa_{1-x}SO_4$ on the atomic level by TEM and APT, Atom Probe & Microscopy, Stuttgart, Germany.

Weber, J., Breuer, U., Savenko, A., Klinkenberg, M., Brandt, F., 2014. Ra uptake into barite - Method development for a characterization on the atomic level, 6th School on Atom Probe Tomography, Rouen, France.

Wilden, A., Modolo, G., Sadowski, F., Lange, S., Bremer, A., Munzel, D., Panak, P., Geist, A., 2014. Process development studies and demonstration of an r-SANEX process using C5-BPP – selective separation of trivalent actinides from lanthanides, Sustainable Nuclear Energy Conference, Manchester, England.

### *11.2.5 Presentations*

Conferences:

Alekseev, E., 2014. Solid state actinide chemistry and structural research in Jülich, 8th European Summer School on Separation Chemistry and Conditioning as well as Supramolecular, Intermolecular, Interaggregate Interactions, Bonn, Germany.

Alekseev, E., S, W., Kowalski, P., Depmeier, W., Albrecht-Schmidt, T.E., 2013. New Uranium Borates, Silicates and Germanates obtained under Extreme Conditions., EMRS 2013, Strassbourg, France.

Alekseev, E., Wu, S., Wang, S., M, P., Depmeier, W., Albrecht-Schmitt, T.E., 2013. Influence of extreme conditions on the formation and structures of uranyl borates., Actinides 2013, Karlsruhe, Germany.

d'Angelo, P., Rossi, C., Minet, C., Eineder, M., Flory, M., Niemeyer, I., 2014. High Resolution 3D Earth Observation Data Analysis for Safeguards Activities, Symposium on International Safeguards: Linking Strategy, Implementation and People, Vienna, Austria.

Brandt, F., Finkeldei, S., Fischer, C., Szenknect, S., Dacheux, N., Ravaux, J., Lüttge, A., Bosbach, D., 2014. Dissolution of $ZrO_2$ based pyrochlores and defect fluorites – from the macroscopic to the microscopic scale, IUMRS-ICA, Fukuoka, Japan.

Brandt, F., Klinkenberg, M., Vinograd, V., Rozov, K., Breuer, U., Bosbach, D., 2014. Radium solubility in the presence of barite: a combined experimental and atomistic modelling approach, 16th International Symposium on Solubility Phenomena and Related Equilibrium Processes, Karlsruhe, Germany.

Clavier, N., Arinicheva, Y., Bukaemskiy, A., Podor, R., Neumeier, S., Dacheux, N., 2014. Sintering of monazites: new insights from an in situ HT-ESEM approach, Materials Science & Technology, Pittsburgh, Pennsylvania, USA.

Curtius, H., Deissmann, G., Bosbach, D., 2014. Corrosion of spent fuels from research and prototype reactors under conditions relevant to geological disposal, Key topics in deep geological disposal (DAEF, Deutsche Arbeitsgemeinschaft Endlagerforschung), Köln, Germany.

Curtius, H., Lieck, N., Güngör, M., Kaiser, G., Klinkenberg, M., Bosbach, D., 2014. Leaching of spent $UO_2$TRISO coated particles - Instant radionuclide release fraction and microstructure evolution, Spent Fuel Workshop, Karlsruhe, Germany.

Dreicer, M., Listner, C., Chen, C., Stein, G., Niemeyer, I., 2014. Applying State-level Approaches to Arms Control Verification, Institute of Nuclear Materials Management 55th Annual Meeting, Atlanta, USA.

Dürr, M. and Knott, A., 2014. Auf Spurensuche: Die Herausforderungen der Mikroanalytik bei ihrem Einsatz in der nuklearen Verifikation, DPG Jahrestagung, Berlin, Germany.

Ebert, E., Cheng, M., Steppert, M., Walther, C., Modolo, G., Bosbach, D., 2014. Dissolution of Mo-based CerMet fuel: ESI-TOF MS speciation in nitric acid medium, 17th Radiochemical Conference, Marianske Lazne, Czech Republic.

Finkeldei, S., Holliday, K., Brandt, F., de Visser-Týnová, E., Bruin, J., Neumeier, S., Modolo, G., Bosbach, D., 2014. Structural Uptake of Actinides by Zirconia Based Pyrochlores, IUMRS-ICA, Fukuoka, Japan.

Hirsch, A., Neumann, A., Wätjen, A., Heuser, J., Thust, A., Peters, L., Roth, G., 2014. Synthesis and characterisation of (La,Pr) monazite solid solution series, 22nd Annual Meeting of the German Crystallographic Society, Berlin, Germany.

Huittinen, N., Arinicheva, Y., Holthausen, J., Neumeier, S., Stumpf, T., 2014. Site-selective TRLFS of Eu(III) doped rare earth phosphates for conditioning of radioactive wastes, Advanced Techniques in Actinide Spectroscopy 2014, Dresden, Germany.

Janeth Lozano-Rodriguez, M., Arinicheva, Y., Neumeier, S., Scheinost, A.C., 2014. Monazite as promising candidates for nuclear waste management: Structural characterization by X-ray Absorption, ACTINIDES XAS 2014, Bottstein, Swiss.

Kegler, P. and Alekseev, E., 2014. Actinide chemistry under extreme conditions: the new high pressure / high temperature facility at Jülich research center, 8th European Summer School on Separation Chemistry and Conditioning as well as Supramolecular, Intermolecular, Interaggregate Interactions, Bonn, Germany.

Kegler, P., Yu, N., Klepov, V.V., Xiao, B., Alekseev, E., 2014. Actinide chemistry under extreme conditions: The first example of a mixed valence As(III)/As(V) actinide compound, 92nd Annual Meeting of the German Mineralogical Society (DMG), Jena, Germany.

Kettler, J., Engels, R., Voß, D., Frank, M., Furletova, J., Havenith, A., Kemmerling, G., Mauerhofer, E., Schitthelm, O., Schumann, M., Vasques, R., 2014. Compact Neutron Imaging System for Radioactive-waste Analysis (NISRA), 10th World Conference on Neutron Radiography, Grindelwald, Schweiz.

Klepov, V., Yu, N., Alekseev, E., 2014. Single Crystal X-ray Diffraction and its Application in Actinide Studies, 8th European Summer School, Bonn, Germany.

Knott, A., Dürr, M., Niemeyer, I., Bosbach, D., 2014. Towards Production of Monodisperse Reference Particles for Nuclear Safeguards Applications, Institute of Nuclear Materials Management 55th Annual Meeting, Atlanta, USA.

Kowalski, P., 2014. Feasible and reliable approach to calculation of actinide- and lanthanide-bearing materials relevant for nuclear waste management, E-MRS 2014 Fall meeting: Symposium K - Computer modelling in nanoscience and nanotechnology: an atomic-scale perspective III, Warsaw, Poland.

Kowalski, P., 2014. Progress in computational modelling of ceramic materials, 4th Meeting BMBF Verbundprojekt: Fundamental studies on immobilization of long-lived radionuclides after incorporation into repository relevant ceramics (Conditioning), Bad Salzschlirf, Germany.

Kowalski, P., 2014. Progress in computational modelling of monazite, 3rd Meeting BMBF Verbundprojekt: Fundamental studies on immobilization of long-lived radionuclides after incorporation into repository relevant ceramics (Conditioning), Grenoble, France.

Listner, C., Murphy, C., Canty, M., Stein, G., Rezniczek, A.U.G., Niemeyer, I., 2014. Evolution of Safeguards - What Can Formal Acquisition Path Analysis Contribute?, Institute of Nuclear Materials Management 55th Annual Meeting, Atlanta, USA.

Listner, C., Stein, G., Niemeyer, I., Canty, M., Rezniczek, A.U.G., 2014. Information and Risk-driven Verfication - An Innovative Approach?, DPG Jahrestagung, Berlin, Germany.

Lozano-Rodriguez, J.M., Arinicheva, Y., Neumeier, S. and Scheinost, A.C., 2014. Monazite as promising candidates for nuclear waste management: Structural characterization by X-ray Absorption Spectroscopy, ACTINIDES XAS 2014, Bottstein, Swiss.

Malmbeck, R., Carrott, M., Christiansen, B., Geist, A., Hérès, X., Magnusson, D., Modolo, G., Sorel, C., Taylor, R., Wilden, A., 2014. EURO-GANEX, a Process for the Co-separation of TRU, Sustainable Nuclear Energy Conference, Manchester, England.

Malmbeck, R., Carrott, M., Geist, A., Hérès, X., Magnusson, D., Modolo, G., Sorel, C., Taylor, R., Wilden, A., 2014. The hydrometallurgical co-separation of neptunium, plutonium, americium, and curium by the EURO-GANEX process, 20th International Solvent Extraction Conference 2014, Würzburg, Germany.

Merk, B., Geist, A., Modolo, G., Knebel, J., 2014. The German P&T study - results and conclusions in the view of the contributing Helmholtz Research centres, 13th Information Exchange Meeting on Actinide and Fission Product Partitioning and Transmutation – IEMPT13, Seoul, Korea.

Mildenberger, F. and Mauerhofer, E., 2014. MEDINA facility - Influence of additional iron content in the matrix on the neutron flux calculation, European Network of Testing Facilities for the quality checking of RAdioactive waste Packages, Jülich, Germany.

Murphy, C., Listner, C., Boyer, B., Budlong Sylvester, K., 2014. Evolution of Safeguards - An Expert-driven Approach to Acquisition Path Analysis, Institute of Nuclear Materials Management 55th Annual Meeting, Atlanta, USA.

Neumeier, S., Arinicheva, Y., Bukaemskiy, A., Thust, A., Kowalski, P., Clavier, N., Modolo, G., Winkler, B., Dacheux, N., Bosbach, D., 2014. Physical properties of monazite-type ceramics ($La_{(1-x)}Eu_xPO_4$), IUMRS 2014, Fukuoka, Japan.

Neumeier, S., Arinicheva, Y., Huittinen, N., Bukaemskiy, A., Podor, R., Clavier, N., Dacheux, N., Stumpf , T., Bosbach, D., 2014. Advanced investigation on solid solution formation and on microstructure evolution during sintering of monazite-type ceramics, MRS Fall Meeting 2014, Boston, USA.

Neumeier, S., Finkeldei, S., Brandt, F., Bukaemskiy, A., Arinicheva, Y., Heuser, J., Modolo, G., Bosbach, D., 2014. Ceramic waste forms for the conditioning of Minor Actinides, 17th Radiochemical Conference, Marianske Lazne, Czech Republic.

Nicol, T., Carasco, Brackx, Mariani, Passard, Collot, Pérot, Mauerhofer, E., 2014. U235 and Pu239 characterization in radioactive waste using neutron-induced fission delayed gamma rays, IEE Nuclear Science Symposium & Medical Imaging Conference. IRE, Seattle, USA.

Nicol, T., Perot, B., Carasco, C., Brackx, E., Mariani, A., Passard, C., Mauerhofer, E., 2014. 235U AND 239Pu characterization in radioactive waste using neutron-induced fission delayed gamma rays, IEEE Nuclear science symposium & medical imaging conference, Seattle, USA.

Niemeyer, I., Altmann, J., Filbert, W., Kaiser, S., Uchtmann, S., Trautwein, W., 2014. Safeguarding Geological Repositories – R&D Contributions from the GER SP, Symposium on International Safeguards: Linking Strategy, Implementation and People, Vienna, Austria.

Niemeyer, I. and Listner, C., 2014. Geospatial Information and Technologies Supporting Non-proliferation, Arms Control, and Disarmament, DPG Jahrestagung, Berlin, Germany.

Niemeyer, I., Listner, C., Canty, M., 2014. Advances in the processing of VHR optical imagery in support of safeguards verification, Symposium on International Safeguards: Linking Strategy, Implementation and People, Vienna, Austria.

Niemeyer, I., Listner, C., Canty, M., Wolfart, E., Lagrange, J.-M., 2014. Integrated Analysis of Satellite Imagery for Nuclear Monitoring - Results from G-SEXTANT, Institute of Nuclear Materials Management 55th Annual Meeting, Atlanta, USA.

Pierce, R.A., Pak, D.J., Shehee, T.C., Fox, K.M., Imrich, K.J., Wilden, A., Modolo, G., 2014. Recovery of Uranium-Thorium from HTGR Fuel Using Salt-Based Graphite Digestion, International Meeting on Reduced Enrichment for Research and Test Reactors - RERTR-2014, Vienna, Austria.

Rossbach, M., Genreith, C., Scholten, B., 2013. Nukleare Daten als Grundlagen für Forschung und Technologie, 24. Seminar "Aktivierungsanalyse und Gammaspektroskopie" SAAGAS 2013, Garching, Germany.

Schreinemachers, C., Bukaemskiy, A., Klinkenberg, M., Neumeier, S., Modolo, G., Bosbach, D., 2014. Co-conversion of minor actinides in uranium based oxidic precursors by internal gelation, Radchem 2014 - 17th Radiochemical Conference, Marianske Lazne, Czech Republic.

Schumann, M., Engels, R., Furletova, J., Furletov, S., Kemmerling, G., Mauerhofer, E., 2014. Setup and test of a system for radiography with fast neutrons, ENTRAP Joint Working Group Meeting No.2, Jülich, Germany.

Schumann, M., Engels, R., Frank, M., Furletova, J., Havenith, A., Kemmerling, G., Kettler, J., Mauerhofer, E., Schitthelm, O., Vasques, R., 2014. Detector Development for Neutron Imaging System for Radioactive-Waste Analysis (NISRA) with 14 MeV Neutrons, 10th World Conference on Neutron Radiography, Grindelwald, Schweiz.

Sevini, F., Niemeyer, I., Vincze, A., van der Meer, K., 2014. ESARDA Contributions to IAEA State-level Concept, Institute of Nuclear Materials Management 55th Annual Meeting, Atlanta, USA.

Stein, G., Rezniczek, A., Niemeyer, I., Listner, C. and Trautwein, W., 2014. The Evolution of International Safeguards - A View from Germany, Institute of Nuclear Materials Management 55th Annual Meeting, Atlanta, USA.

Thust, A., Haussühl, E., Bayarjargal, L., Winkler, B., Arinicheva, Y., Neumeier, S., Bukaemskiy, A., 2014. Mechanical and Physical Properties of (La,Eu)$PO_4$ Ceramics - A Promising Waste form for Radioactive Waste, Materials Science & Engineering 2014, Darmstadt, Germany.

Wätjen, A., Schausten, C., Telle, R., Arinicheva, Y., Hirsch, A., 2014. Sintering and microstructure characterisation of monazite ($REPO_4$, with RE = La, Ce, Pr), Sintering 2014, Dresden, Germany.

Wätjen, A., Schausten, C., Telle, R., Arinicheva, Y., Neumeier, S., Hirsch, A., Roth, G., 2014. Sintering and microstructure characterisation of monazite ($REPO_4$, with RE = La, Ce, Pr), Materials Science & Engineering 2014, Darmstadt, Germany.

Weber, J., Breuer, U., Savenko, A., Klinkenberg, M., Brandt, F., Bosbach, D., 2014. Method development for the LEAP and TEM characterization of (Ba,Ra)$SO_4$ solid solution on the atomic level, DMG Annual Meeting, Jena, Germany.

Wilden, A., Modolo, G., Geist, A., 2014. Development and demonstration of innovative partitioning processes (i-SANEX and 1-cycle SANEX) for actinide partitioning, 13th Information Exchange Meeting on Actinide and Fission Product Partitioning and Transmutation – IEMPT13, Seoul, Korea.

Wilden, A., Modolo, G., Kaufholz, P., Sadowski, F., Lange, S., Sypula, M., Magnusson, D., Müllich, U., Geist, A., Bosbach, D., 2014. Spiked Laboratory-scale Continuous Counter-Current Centrifugal Contactor Demonstration of a Novel innovative-SANEX Process, Sustainable Nuclear Energy Conference, Manchester, England.

Wilden, A., Modolo, G., Kaufholz, P., Sadowski, F., Lange, S., Sypula, M., Magnusson, D., Müllich, U., Geist, A., Bosbach, D., 2014. Spiked Laboratory-scale Continuous Counter-Current Centrifugal Contactor Demonstration of a Novel innovative-SANEX Process, 20th International Solvent Extraction Conference 2014, Würzburg, Germany.

Wilden, A., Modolo, G., Sadowski, F., Lange, S., Bremer, A., Munzel, D., Panak, P.J., Geist, A., 2014. Process Development Studies towards an r-SANEX Process using C5-BPP – Selective Separation of Trivalent Actinides from Lanthanides, 20th International Solvent Extraction Conference 2014, Würzburg, Germany.

Xiao, B. and Alekseev, E., 2014. Synthesis and Crystal Structures of Thorium Compounds Mixed with Hexavalent Cations (W, Mo, Se, Te), Young Crystallographers of the German Crystallographic Society (DGK). Bremen, Germany.

Xiao, B., Alekseev, E., Gesin, T., 2014. High-Temperature Phase Transitions, Spectroscopic Properties, and Dimensionality Reduction in Rb-Th-Mo Family, 22nd Annual Conference of the German Crystallographic Society (DGK) 2014. Berlin, Berlin, Germany.

Yu, N., Klepov, V., Alekseev, E., 2014. Thorium Arsenates from High Temperature Solid State Reactions, 22nd Annual Conference of the German Crystallographic Society (DGK) 2014. Berlin, Berlin, Germany.

Invited Talks

Alekseev, E., 2014. New inside of crystal chemistry of Th molybdates and tungstates., International Actinide Coordination Chemistry Symposium., Suzhou, China.

Alekseev, E., 2014. New actinide materials from extreme conditions. Bremen, Bremen, Germany.

Alekseev, E., 2014. New aspects of structural and materials chemistry of Th molybdates and tungstates., Workshop "Radiation damage in structures", Hamburg, Germany.

Alekseev, E., 2014. New inside in crystal chemistry of Th molybdates and tungstates., Guangzhou, China.

Alekseev, E., 2014. Structural chemistry of actinide borates from normal and extreme conditions., 8th Belgian Crystallography Symposium., Brussels, Belgium.

Bosbach, D., Brandt, F., Klinkenberg, M., Vinograd, V., Rozov, K., Weber, J., Breuer, U., 2014. Radionuclide solubility control in solid solution –aqueous solutionsystems: Radium solubility in the presence of barite, 8th European Summer School on Separation Chemistry and Conditioning as well as Supramolecular, Intermolecular, Interaggregate Interactions, Bonn/Bad Godesberg, Germany.

Brandt, F., Finkeldei, S., Neumeier, S., Bosbach, D., 2014. Dissolution of nuclear waste forms: an introduction, 8th European Summer School on Separation Chemistry and Conditioning as well as Supramolecular, Intermolecular, Interaggregate Interactions, Bonn/ Bad Godesberg, Germany, Bonn, Germany.

Bukaemskiy, A., Finkeldei, S., Brandt, F., Neumeier, S., Modolo, G., Bosbach, D., 2014. Recent advances in ceramics for nuclear waste immobilization, CIMTEC, Montecatini Terme, Italy.

Kowalski, P., 2014. Nuclear Waste Management Related Research on Supercomputers, Seminar of Institute of Nuclear Chemistry and Technology: Centre for Radiochemistry and Nuclear Chemistry, Warsaw, Poland.

Kowalski, P., 2014. Nuclear waste management related research using modern computational techniques and resources, Körber-Stiftung: Forum für Impulse: Radiation damage in structures – relevance for nuclear waste disposal., Hamburg, Germany.

Li, Y., 2014. Nuclear waste management on supercomputers: Reliable modellingof f-elements-bearing ceramic materials, 8th European Summer School on Separation Chemistry and Conditioning as well as Supramolecular, Intermolecular, Interaggregate Interactions, Bonn/Bad Godesberg, Germany.

Listner, C., 2014. Bewertung der Risiken nuklearer Proliferation anhand mathematischer Modelle, Forschungsseminar Scientific Computing. TU Chemnitz, Chemnitz, Germany.

Modolo, G., 2014. Der Jülicher AVR Reaktor- Vollständiger Rückbau und Entsorgungsoptionen für den abgebrannten Brennstoff, Institutsseminar des Institut für Radioökologie und Strahlenschutz der Leibnitz Universität Hannover, Hannover, Germany.

Modolo, G., Wilden, A., Geist, A., Malmbeck, R., Taylor, R., 2014. Demonstration of innovative partitioning processes for minor actinide recycling from high active waste solutions, SESTEC 2014 conference, Mumbai, India.

Neumeier, S., Brandt, F., Bosbach, D., Bukaemskiy, A., Finkeldei, S., Heuser, J., Arinicheva, Y., Ebert, E., Schreinemachers, C., Wilden, A., Modolo, G., 2014. Ceramic materials for innovative nuclear waste management strategies, Seminar Institut für Ressourcenökologie, Helmholtz-Zentrum Dresden-Rossendorf, Dresden, Germany.

Neumeier, S., Brandt, F., Bosbach, D., Bukaemskiy, A., Finkeldei, S., Arinicheva, Y., Heuser, J., Ebert, E., Schreinemachers, C., Wilden, A., Modolo, G., 2014. Ceramic Waste Forms in Innovative Waste Management Strategies: Present Status and Perspectives, MRS Fall Meeting, Boston, USA.

Neumeier, S., Brandt, F., Bosbach, D., Bukaemskiy, A., Finkeldei, S., Arinicheva, Y., Heuser, J., Ebert, E., Schreinemachers, C., Wilden, A., Modolo, G., 2014. Ceramic Waste Forms: Present status and perspectives, International Conference and exposition on Advanced Ceramics and Composites, Daytona Beach, Florida, US.

Neumeier, S., Bukaemskiy, A., Brandt, F., Finkeldei, S., Arinicheva, Y., Modolo, G., Bosbach, D., 2014. Immobilization of long-lived radionuclides after incorporation into repository relevant ceramics (Conditioning), 8$^{th}$ European Summer School on Separation Chemistry and Conditioning as well as Supramolecular, Intermolecular, Interaggregate Interactions, Bonn/Bad Godesberg, Germany.

Neumeier, S., Kulriya, P.K., Arinicheva, Y., Huittinen, N., Lozano-Rodriguez, J., Deissmann, G., Bosbach, D., 2014. Structural in-situ investigations on (La,Eu)$PO_4$ and (La,Gd)$PO_4$ solid solution series under heavy ion irradiation, 57$^{th}$ Accelerator User Workshop, Delhi, India.

Niemeyer, I., 2014. Discussions during the Technical Meetings at the IAEA on the State-level Concept, 36$^{th}$ ESARDA Annual Meeting.

Niemeyer, I., 2014. Nuclear Verification from Space? Satellite Imagery in Support of Non-Proliferation and Arms Control, March Meeting 2014 of the American Physical Society, Denver, Colorado.

Niemeyer, I., 2014. Nuclear Verification from Space? Satellite Imagery Analysis in Support of Non-Proliferation, Arms Control and Disarmament, Physikalisches Kolloquium. TU Dortmund, Dortmund, Germany.

Niemeyer, I., 2014. Remote Sensing Imagery for Off-site inspections, Workshop “Open Source Tools for the Assessment of Compliance with the BWC”, Geneva, Switzerland.

Steppert, M., Cheng, M., Ebert, E., Chen, X., Walther, C., 2014. Ionic solution species of molybdenum in strongly acidic media characterized by means of electrospray ionization mass spectrometry, HZDR IRE Institutskolloquium.

Wilden, A., Modolo, G., Geist, A., Magnusson, D., Miguirditchian, M., Taylor, R., Malmbeck, R., 2014. Development & demonstration of Actinide separation processes in Europe, 8$^{th}$ European Summer School on Separation Chemistry and Conditioning as well as Supramolecular, Intermolecular, Interaggregate Interactions, Bonn - Bad Godesberg, Germany.

Wilden, A., Sypula, M., Malmbeck, R., Carpentier, C., Magnusson, D., Müllich, U., Geist, A., Miguirditchian, M., Sorel, C., Hérès, X., Sadowski, F., Lange, S., Modolo, G., Taylor, R.,

Carrott, M., Bell, K., McLachlan, F., Gregson, C., 2014. Development and demonstration of the EURO-GANEX process, TALISMAN First Plenary Meeting, Marcoule, France.

Additional Talks

Arinicheva, Y., 2014. Synthesis & MicrostructureandDissolution of(La,Eu)$PO_4$-Monazites, 4th Meeting BMBF Verbundprojekt "Conditioning", Bad Salzschlirf, Germany.

Arinicheva, Y., 2014. Synthesis, characterization and microstructure evolution during sinteringof monazite-type ceramics for the conditioning of minor actinides, 3rd Meeting BMBF Verbundprojekt "Conditioning", Grenoble, France.

Aymanns, K., 2014. Safeguards – Disposal of spent fuel in times of 'Energy Turnaround', 36th ESARDA Annual Meeting.

Bosbach, D., Brandt, F., Klinkenberg, M., Vinograd, V., Rozov, K., Weber, J., Breuer, U., 2014. Radionuclide solubility control in solid solution – aqueous solution systems: Radium solubility in the presence of barite, Workshop "Radiation damage in structures - Relevance for nuclear waste disposal" Körber-Stiftung, Forum für Impulse, Hamburg, Germany.

Brandt, F., Finkeldei, S., Fischer, C., Szenknect, S., Dacheux, N., Ravaux, J., Neumeier, S., Lüttge, A., Bosbach, D., 2014. Dissolution of $ZrO_2$ based pyrochlores anddefect fluorites – from the macroscopic to themicroscopic scale, 3rd Meeting BMBF Verbundprojekt "Conditioning", Grenoble, France.

Brandt, F., Klinkenberg, M., Vinograd, V., Rozov, K., Bosbach, D., 2014. Uptake of Ra in the presence of barite under near-to-equilibrium conditions, 2014 ImmoRad Project Meeting, Oviedo, Spain.

Bukaemskiy, A., 2014. Some aspects of Pyrochlore phase stability in thesystem $ZrO_2$-$Nd_2O_3$, 3rd Meeting BMBF Verbundprojekt "Conditioning", Grenoble, France.

Cheng, M., Ebert, E., Steppert, M., Walther, C., 2014. Investigations on $^{98}$Mo solution species by means of electrospray ionization mass spectrometry, ASGARD 4th Project Meeting, Stockholm, Sweden.

Curtius, H., 2014. Spent Fuel Investigations, Bilaterales Kooperationstreffen mit SCK.CEN, Mol, Belguim.

Ebert, E., Lichte, E., Schreinemachers, C., Modolo, G., Neumeier, S., Bukaemskiy, A., 2014. Progress report of Beneficiary No 2: Jülich, Domain 2: WP 2.1 Inert Matrix Fuels, ASGARD 4th Project Meeting, Stockholm, Sweden.

Ebert, E., Schreinemachers, C., Middendorp, R., Modolo, G., Neumeier, S., Bukaemskiy, A., 2014. Progress report of Beneficiary No 2: Jülich, Domain 2: WP 2.1 Inert Matrix Fuels, ASGARD 5th Project Meeting, Lancaster, UK.

Finkeldei, S., 2014. Pyrochlore as Nuclear Waste Form: Actinide Uptake and Chemical Stability, 2. HITEC Symposium in Energy and Climate Research.

Heuser, J., 2014. Sm-based Monazite-type Ceramicsused for Nuclear Waste Management, 3rd Meeting BMBF Verbundprojekt "Conditioning", Grenoble, France.

Kaufholz, P., 2014. Americium Selective Separation using Hydrophilic Complexing Agents, SACSESS Half-Yearly Meeting, Stenungsbaden, Sweden.

Kaufholz, P., Wilden, A., Sadowski, F., Lange, S., Modolo, G., 2014. JÜLICH contribution to SACSESS Domain 1 WP1.4: Safety of MA handling in the cycle, SACSESS First Annual Meeting, Toulouse, France.

Listner, C., Canty, M., Rezniczek, A.U.G., Stein, G., Niemeyer, I., 2014. Quantifying Detection Probabilities For Proliferation Activities Outside Declared Nuclear Facilities, 36th ESARDA Annual Meeting.

Lozano, J., Heuser, J., Arinicheva, Y., Scheinost, A., Neumeier, S., 2014. An EXAFS investigation of rare-earth local environment on phosphates solid solutions, 4th Meeting BMBF Verbundprojekt "Conditioning", Bad Salzschlirf, Germany.

Lozano, J., Scheinost, A., Arinicheva, Y., Heuser, J., Neumeier, S., 2014. Structural characterization of monazite, xenotimetypeby EXAFS, 3rd Meeting BMBF Verbundprojekt "Conditioning", Grenoble, France.

Mauerhofer, E., 2014. Characterization of radioactive waste, Joint meeting between FZ Juelich and SCK.CEN on radioactive waste and disposal, Mol, Belgium.

Middendorp, R., Schreinemachers, C., Ebert, E., Bukaemskiy, A., Neumeier, S., Modolo, G., 2014. Progress Report of Beneficiary No 5: Jülich. Domain2 ASGARD 5th Project Meeting, Lancaster, England.

Modolo, G., 2014. Herausforderungen bei der Rezyklierung von Seltenen Erden aus Sekundärrohstoffen, Habilitationsvortrag, Aachen, Germany.

Neumeier, S., 2014. Ceramic waste forms, Bilaterales Kooperationstreffen mit SCK.CEN, Mol, Belgien.

Neumeier, S. and Filby, A., 2014. Behaviour of phosphate ceramics in aqueous solutions – an experimental and modelling study, 4th Meeting BMBF Verbundprojekt "Conditioning", Bad Salzschlirf, Germany.

Schmidt, H., 2014. Radiation stability of nitrogen donor ligands, SACSESS Half-Yearly Meeting, Stenungsbaden, Sweden.

Schreinemachers, C., Middendorp, R., Bukaemskiy, A., Neumeier, S., Modolo, G., Ebert, E., Lichte, E., Wilden, A., 2014. Progress Report of Beneficiary No 4: Jülich; Domain2, WP 2.3: Conversion from solution to oxide pre-cursors, ASGARD 4th Project Meeting, Stockholm, Sweden.

Schreinemachers, C., Middendorp, R., Ebert, E., Bukaemskiy, A., Neumeier, S., Modolo, G., 2014. Progress Report of Beneficiary No 5: Jülich, ASGARD 5th Project Meeting, Lancaster, England.

Schumann, M., Engels, R., Kemmerling, G., Mauerhofer, E., 2014. Status Update Detector Tests & Flux-Determination.

Schumann, M., Engels, R., Kemmerling, G., Mauerhofer, E., 2014. Status Update: First Neutron-Radiography.

Schumann, M., Engels, R., Kemmerling, G., Mauerhofer, E., 2014. Status Update: First Neutron-Radiography.

Schumann, M., Engels, R., Kemmerling, G., Mauerhofer, E., 2014. Status Update: First Pictures.

Schumann, M., Engels, R., Kemmerling, G., Mauerhofer, E., 2014. Status Update: Reference Measurements.

Weber, J., Brandt, F., Klinkenberg, M., Vinograd, V., Rozov, K., Bosbach, D., 2014. The ternary system (Ba,Ra,Sr)$SO_4$, 2014 ImmoRad Project Meeting, Oviedo, Spain.

Wilden, A., Hupert, M., Santiago-Schübel, B., Lange, S., Modolo, G., 2014. JÜLICH contribution to SACSESS Domain 1 WP1.1: Safety of chemical systems, SACSESS First Annual Meeting, Toulouse, France.

Wilden, A., Kardhashi, D., Modolo, G., 2014. FZJ – IEK-6 progress report 10.07.2014-08.12.2014, 5. Halbjahrestreffen, BMBF Projekt f-Kom 02NUK020E, Karlsruhe, Germany.

Wilden, A., Lange, S., Modolo, G., 2014. FZJ – IEK-6 progress report 20.11.2013-09.07.2014, 4. Halbjahrestreffen, BMBF Projekt f-Kom 02NUK020E, Erlangen, Germany.

Wilden, A., Sadowski, F., Modolo, G., 2014. JÜLICH contribution to SACSESS Domain 1 WP1.2: Performance optimisation of chemical systems, SACSESS First Annual Meeting, Toulouse, France.

Wilden, A., Sypula, M., Malmbeck, R., Carpentier, C., Magnusson, D., Müllich, U., Geist, A., Hérès, X., Sadowski, F., Lange, S., Modolo, G., Taylor, R., Carrott, M., Bell, K., McLachlan, F., Gregson, C., 2014. A status on the EUROGANEX process developments, SACSESS First Annual Meeting, Toulouse, France.

Yu, N. and Alekseev, E., 2014. Thorium compounds containinggroup V elements (N, P, As), 4$^{th}$ Meeting BMBF Verbundprojekt "Conditioning", Bad Salzschlirf, Germany.

# 12 How to reach us

**By car**

**Coming from Cologne (Köln)** take the A 4 motorway (Cologne – Aachen), leave the motorway at the Düren exit, and then turn right towards Jülich (B 56). After about 10 km, turn off to the right onto the L 253, and follow the signs for "Forschungszentrum".

**Coming from Aachen** take the A 44 motorway (Aachen – Düsseldorf) and leave the motorway at the Jülich-West exit. At the first roundabout turn left towards Jülich, and at the second roundabout turn right towards Düren (B 56). After about 5 km, turn left onto the L 253 and follow the signs to "Forschungszentrum".

**Coming from Düsseldorf Airport** take the A 52 motorway (towards Düsseldorf/Mönchengladbach), followed by the A 57 (towards Cologne). Turn off at Neuss-West, and continue on the A 46 until you reach the crossroads "Kreuz Wanlo". Take the A 61 (towards Koblenz/Aachen) until you reach "Dreieck Jackerath" where you should take the A 44 (towards Aachen). Continue as described in "Coming from Düsseldorf".


**Fig. 88: Euregio Rheinland map**

**Coming from Düsseldorf** on the A44 motorway (Düsseldorf – Aachen) you have two options:

1. (Shorter route but more traffic) turn right at the Jülich-Ost exit onto the B 55n, which you should follow for approx. 500 m before turning right towards Jülich. After 200 m, before the radio masts, turn left and continue until you reach the "Merscher Höhe" roundabout. Turn left here, drive past the Solar Campus belonging to the University of Applied Sciences and continue straight along Brunnenstrasse. Cross the Römerstrasse junction, continue straight ahead onto Wiesenstrasse and then after the roundabout and the caravan dealers, turn left towards "Forschungszentrum" (signposted).
2. (Longer but quicker route) drive until you reach the "Jülich-West" exit. At the first roundabout turn left towards Jülich, and at the second roundabout turn right towards Düren (B 56). After about 5 km, turn left onto the L 253 and follow the signs to "Forschungszentrum".

### Navigation systems

In your navigation system, enter your destination as "Wilhelm-Johnen-Strasse". From there, it is only a few hundred metres to the main entrance – simply follow the signs. The Research Centre itself is not part of the network of public roads and is therefore not recognised by navigation systems.

### By train from Cologne Bonn Airport

From the railway station at the airport, take the S13 to Cologne main train station (Hauptbahnhof) and then continue with the regional express to Düren, or go to Köln-Ehrenfeld by regional express and then take the S12 to Düren. Continue from Düren as described in "By train".

### By train from Düsseldorf International Airport

From the railway station at the airport, travel to Cologne main train station and then continue on to Düren. Some trains go directly to Düren whereas other connections involve a change at Cologne main train station. Continue from Düren as described in "By train".


**Fig. 89: Forschungszentrum Jülich campus map**

### By train:

Take the train from Aachen or Cologne to the train station in Düren. From here, take the local train ("Rurtalbahn" [RTB]) for Jülich and get out at the "Forschungszentrum" stop. To make sure that the train stops at "Forschungszentrum" you should press the request stop button (Haltewunsch) in good time after the "Selgersdorf" stop. Bus number 11 leaves from this stop for the Research Centre (for bus timetables, see "Aachen - Jülich bus connections"). If you walk, it will take you approximately 20 minutes to reach the Research Centre's main entrance.

**By bus:**

**Aachen - Jülich bus connection**

The SB11 bus line connects the Research Centre to the local public transport system. Commuters from Aachen travelling to the Research Centre have 19 options every day of reaching their destination and 18 in the other direction to get back to Aachen.

**Institute:**

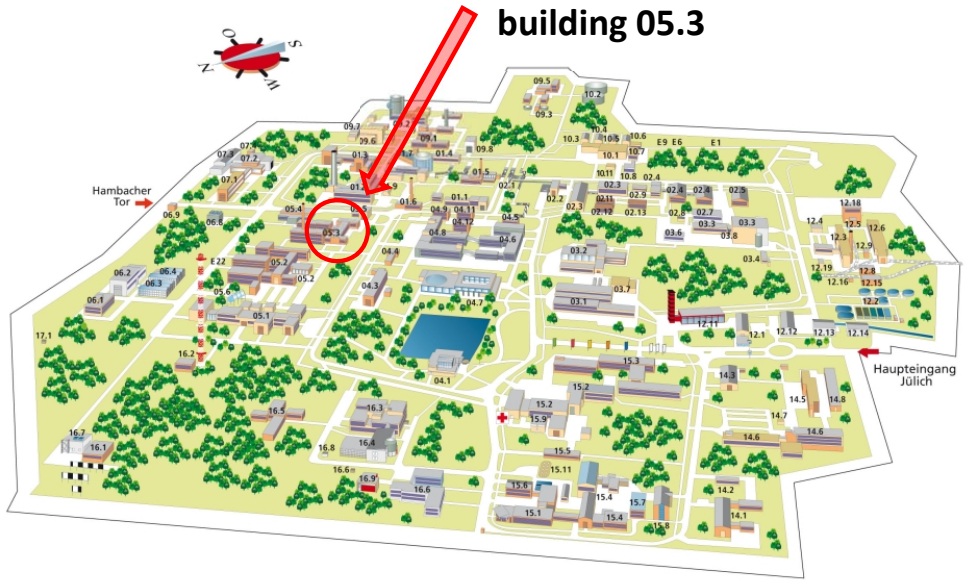


**Fig. 90: Map showing the Institute, Helmholtz-Ring H18, building no. 05.3.**

# 13 List of figures

# 14 List of tables

Band / Volume 314
**Entwicklung eines metallbasierten Substratkonzepts für energieeffiziente Gastrennmembranen**
J. A. Kot (2016), xi, 201 pp
ISBN: 978-3-95806-134-7

Band / Volume 315
**Langzeitbeobachtung der Dosisbelastung der Bevölkerung in radioaktiv kontaminierten Gebieten Weißrusslands – Korma-Studie II (1998 – 2015)**
P. Zoriy, H. Dederichs, J. Pillath, B. Heuel-Fabianek, P. Hill, R. Lennartz (2016), ca 104 pp
ISBN: 978-3-95806-137-8

Band / Volume 316
**Oxidation Mechanisms of Metallic Carrier Materials for Gas Separation Membranes**
M. Schiek (2016), 148 pp
ISBN: 978-3-95806-138-5

Band / Volume 317
**Thermoschockverhalten und temperaturabhängige Eigenschaften kohlenstoffarmer und -freier Feuerfestwerkstoffe**
A. Böhm (2016), VI, 153 pp
ISBN: 978-3-95806-139-2

Band / Volume 318
**Theoretical and experimental studies of runaway electrons in the TEXTOR tokamak**
S.S. Abdullaev, K.H. Finken, K. Wongrach, O. Willi (2016), X, 109 pp
ISBN: 978-3-95806-140-8

Band / Volume 319
**Modelling Thermodynamic Properties of Intercalation Compounds for Lithium Ion Batteries**
S. O. Dang (2016), x, 133 pp
ISBN: 978-3-95806-141-5

Band / Volume 320
**Atmospheric Mixing in a Lagrangian Framework**
M. Tao (2016), 146 pp
ISBN: 978-3-95806-142-2

Band / Volume 321
**Statistical analysis and combination of active and passive microwave remote sensing methods for soil moisture retrieval**
K. Rötzer (2016), XIV, 112 pp
ISBN: 978-3-95806-143-9

Band / Volume 322
**Langzeitstabilität der Polymerelektrolyt-Wasserelektrolyse bei reduziertem Iridiumgehalt**
C. G. Rakousky (2016), VIII, 199 pp
ISBN: 978-3-95806-147-7

Band / Volume 323
**Light induced water splitting using multijunction thin film silicon solar cells**
F. Urbain (2016), xi, 173, XLVI pp
ISBN: 978-3-95806-148-4

Band / Volume 324
**Properties of convective gravity waves derived by combining global modeling and satellite observations**
Q. T. Trinh (2016), III, 140 pp
ISBN: 978-3-95806-150-7

Band / Volume 325
**Feasible and Reliable Ab initio Atomistic Modeling for Nuclear Waste Management**
G. Beridze (2016), xix, 128 pp
ISBN: 978-3-95806-151-4

Band / Volume 326
**Sauerstoffspeicher für die oxidkeramische Batterie: Herstellung, Charakterisierung und Betriebsverhalten**
C. M. Berger (2016), XV, 128 pp
ISBN: 978-3-95806-154-5

Band / Volume 327
**Institute of Energy and Climate Research**
**IEK-6: Nuclear Waste Management – Report 2013 / 2014**
*Material Science for Nuclear Waste Management*
S. Neumeier, M. Klinkenberg, D. Bosbach (Eds.)
(2016), 219 pp
ISBN: 978-3-95806-155-2

Weitere ***Schriften des Verlags im Forschungszentrum Jülich*** unter
http://wwwzb1.fz-juelich.de/verlagextern1/index.asp

Energie & Umwelt /
Energy & Environment
Band / Volume 327
ISBN 978-3-95806-155-2